UNIVERSIDADE D
COIMBRA

Alireza Emami

State Estimation and Model Identification Methodologies for Applying to Electric Grids

Tese de Doutoramento em Engenharia Electrotécnica e de Computadores, ramo de Sistemas de Energia, orientada pelo Professor Doutor Rui Alexandre de Matos Araújo e apresentada ao Departamento de Engenharia Electrotécnica e de Computadores da Faculdade de Ciências e Tecnologia da Universidade de Coimbra.

April 2023

1 2  9 0

UNIVERSIDADE D
COIMBRA

Alireza Emami

State Estimation and Model Identification Methodologies for Applying to Electric Grids

Tese de Doutoramento em Engenharia Electrotécnica e de Computadores, ramo de Sistemas de Energia, orientada pelo Professor Doutor Rui Alexandre de Matos Araújo e apresentada ao Departamento de Engenharia Electrotécnica e de Computadores da Faculdade de Ciências e Tecnologia da Universidade de Coimbra.

April 2023

1 2  9 0

UNIVERSIDADE D
COIMBRA

Alireza Emami

Metodologias de Estimação de Estado e Identificação de Modelos para Aplicação em Redes Elétricas

Tese de Doutoramento em Engenharia Electrotécnica e de Computadores, ramo de Sistemas de Energia, orientada pelo Professor Doutor Rui Alexandre de Matos Araújo e apresentada ao Departamento de Engenharia Electrotécnica e de Computadores da Faculdade de Ciências e Tecnologia da Universidade de Coimbra.

Abril 2023

Acknowledgements

The development of this doctoral thesis would have been very difficult, or even impossible, without the contribution of people and institutions. First of all, I would like to thank God for the opportunities granted and for the strength in difficult times along this amazing and adventurous journey. I would like to thank my supervisor, Professor Dr. Rui Alexandre de Matos Araújo, for the trust he placed in my work, for the guidance and for the knowledge imparted. I would also like to thank the Institute of Systems and Robotics at the University of Coimbra (ISR-UC) for supporting this work.

I would like to thank the Fundação para a Ciência e a Tecnologia (FCT) which supported this thesis through the doctoral scholarship with the reference SFRH/BD/89186/2014. I would like to thank to the Project "Advances in Control Design Methodologies for Safety Critical Systems Applied to Robotics" (RELIABLE) with reference PTDC/EEI-AUT/3522/2020 financed by FCT. I would also like to thank to Project "Self-Learning Industrial Control Systems Through Process Data" (reference: SCIAD/2011/21531) co-financed by QREN, in the framework of the "Mais Centro - Regional Operational Program of the Centro", and by the European Union through the European Regional Development Fund (ERDF).

A deep thanks to my colleagues and friends at ISR-UC, especially Dr. Jérôme Mendes, Ricardo Maia, Dr. Francisco Souza, Dr. Saeid Rastegar, Dr. Symone Soares, Dr. Susana Freiria, Paula Fonseca, Nuno Quaresma and Edson Costa. I would like to express my gratitude to Professor Sérgio Cruz for preparing an experimental setup to test and evaluate the proposed methodologies.

I would like to thank my friends, to whom I often did not give the time and attention that were due to them, but even so, they were fundamental throughout this work. An eternal thanks to all my family. To my parents for their patience and unconditional love. To my dear sister, for her love and friendship at all times.

Thank you Afsoon for all the support, love, tranquility and security you have always provided.

Finally, I would like to thank everyone who in one way or another contributed to the realization of this thesis. To all my deep thanks.

Abstract

Monitoring, modeling, estimation, and control are important issues in nowadays electrical grids. However, because of the introduction of more recent concepts like smart grids, the existence of a large number of nonlinear and time-varying components, and the noticeable rising number of intermittent resources (like wind turbines and solar panels) and electric vehicles, addressing these issues is getting each time more challenging and difficult.

This is because, in smart grids, standards and phenomena may be created that have not existed and/or are not understood in conventional grids. For example in a conventional grid one house is always considered as a potential load even if it has some installed devices like solar panels that produce energy, but in a smart grid such a house could play a role as a source and feed its surplus electrical energy to the grid. Additionally, increasing the number of intermittent resources and electric cars makes electric networks' behavior more complex and unpredictable, particularly in terms of energy consumption and production. Further, there are a large number of nonlinear time-varying devices in electrical grids. Given the above facts, providing more accurate and reliable state variables to control and monitor electrical grids is a real challenge. In this context, three main research objectives and research directions are considered in this thesis.

The first objective is to design a distributed estimation approach, where simultaneous estimation of state variables and unknown inputs for large-scale discrete-time linear systems can be done. This method can function in the form of agent-based estimation in which each agent estimates the whole system states and unknown inputs associated with the whole system, by having access to only a subset of all measurements available locally for each agent. All agents try to reach consensus by exchanging their computed state variables with those of their neighboring agents. Sufficient conditions for stability and convergence of this distributed estimation method are

also discussed and provided using Lyapunov stability theory. It is worth mentioning that though this method is suitable for linear systems, it can be utilized for nonlinear systems if the linearized model of those nonlinear systems has the capability of being computed quite accurately.

The second objective is to develop a data-driven method to determine a global model of a real synchronous generator, a highly nonlinear and important component of power systems. In this approach, under several different planned conditions, the measurements obtained from the sensors and transducers installed at the inputs and outputs of a synchronous generator are stored and form several datasets. These datasets are used by fuzzy clustering, subspace identification, Takagi Sugeno (T-S) fuzzy modeling, and Particle swarm optimization (PSO) to create a global T-S fuzzy model. The resultant model of the proposed approach can provide accurate outputs under a wide range of mechanical power input values, even with noisy measurements.

The third and final objective is to design a robust and adaptive estimator that can do its main task, the estimation of system state variables, when model mismatches occur. Developing such a robust and reliable estimator is crucial for electrical networks because such networks are subject to a wide range of operating states, due to a variety of events such as loads, line switching, and source commitment, which can lead to some model mismatches. Towards this goal, an engineering approach is proposed that incorporates not only the estimation strategy but also the designer's knowledge and experience about the system's behavior.

The performance and effectiveness of the proposed methodologies are validated and demonstrated using available benchmarks like IEEE 5-generator 14-bus system, known models like 2nd-order and 4th-order nonlinear models of synchronous generators as well as real setup of a motor-generator set.

Keywords

Keywords: State Estimation, Model Identification, Power System, Electrical Grid, Kalman Filter, Robust Estimation, Synchronous Generator.

Resumo

Monitorização, modelação, estimação e controlo são questões importantes nas redes elétricas atuais. No entanto, devido à introdução de conceitos mais recentes como redes inteligentes, a existência de um grande número de componentes não lineares e variantes no tempo e o notável aumento do número de recursos intermitentes (como turbinas eólicas e painéis solares) e veículos elétricos, a abordagem destas questões está ficando cada vez mais desafiadora e difícil.

Isso porque, nas redes inteligentes, podem ser criados padrões e fenómenos que não existiam e/ou não são compreendidos nas redes convencionais. Por exemplo, numa rede convencional, uma casa é sempre considerada como uma carga potencial, mesmo que tenha alguns dispositivos instalados, como painéis solares que produzem energia, mas numa rede inteligente, essa casa pode desempenhar o papel de fonte e alimentar o seu excedente de energia elétrica à rede eléctrica. Adicionalmente, o aumento do número de recursos intermitentes e de carros elétricos torna o comportamento das redes elétricas mais complexo e imprevisível, nomeadamente ao nível do consumo e produção de energia. Além disso, há um grande número de dispositivos variantes no tempo e não lineares nas redes elétricas. Portanto, considerando os factos acima, fornecer métodos de estimativa e modelação para sistemas de controlo e monitorização, trabalhando em redes elétricas, com variáveis de estado mais precisas e confiáveis em redes elétricas é um verdadeiro desafio. Diante dos fatos acima, fornecer variáveis de estado mais precisas e confiáveis para controlar e monitorizar redes elétricas é um verdadeiro desafio. Neste contexto, três principais objetivos de pesquisa e direções de pesquisa são considerados nesta tese.

O primeiro objetivo é projectar uma abordagem de estimação distribuída, onde a estimativa simultânea de variáveis de estado e entradas desconhecidas para sistemas lineares de tempo discreto de grande escala podem ser feitas. Este método pode funcionar na forma de estimativa baseada em agente, na qual cada agente estima

todos os estados do sistema e as entradas desconhecidas associadas a todo o sistema, tendo acesso a apenas um subconjunto de todas as medições disponíveis localmente para cada agente. Todos os agentes tentam chegar a um consenso trocando as suas variáveis de estado computadas com aquelas dos seus agentes vizinhos. Condições suficientes para estabilidade e convergência deste método de estimação distribuído também são discutidas e fornecidas usando a teoria de estabilidade de Lyapunov. Vale ressaltar que embora este método seja adequado para sistemas lineares, ele pode ser utilizado para sistemas não lineares se o modelo linearizado desses sistemas não lineares tiver a capacidade de ser computado com bastante precisão.

O segundo objetivo é desenvolver um método baseado em dados para determinar um modelo global de um gerador síncrono real, um componente altamente não linear e importante dos sistemas de potência. Nesta abordagem, sob diversas condições planeadas, as medições obtidas dos sensores e transdutores instalados nas entradas e saídas de um gerador síncrono são armazenadas e formam diversos conjuntos de dados. Esses conjuntos de dados são usados por agrupamento difuso, identificação de sub-espaço, modelação difusa de Takagi-Sugeno (T-S) e optimização por enxame de partículas (PSO) para criar um modelo difuso T-S global. O modelo resultante da abordagem proposta pode fornecer saídas precisas sob uma ampla gama de valores de entrada de potência mecânica, mesmo com medições ruidosas.

O terceiro e último objetivo é projetar um estimador robusto e adaptativo que possa fazer a sua tarefa principal, a estimativa de variáveis de estado do sistema, quando ocorrem incompatibilidades de modelos. Desenvolver um estimador robusto e confiável é crucial para redes elétricas porque tais redes estão sujeitas a uma ampla gama de estados operacionais, devido a uma variedade de eventos, como cargas, comutação de linha e comprometimento de fonte, o que pode levar a algumas incompatibilidades de modelo. Para atingir esse objetivo, é proposta uma abordagem de engenharia que incorpora não apenas a estratégia de estimativa, mas também o conhecimento e a experiência do projetista sobre o comportamento do sistema.

O desempenho e a eficácia das metodologias propostas são validados e demonstrados usando benchmarks disponíveis como o sistema IEEE de 5 geradores e 14 barramentos, modelos conhecidos como modelos não lineares de 2.ª ordem e 4.ª ordem de geradores síncronos, bem como configuração real de um conjunto motor-gerador.

Palavras-Chave

Palavras-Chave: Estimação de Estado, Modelagem e Identificação, Sistema de Energia, Rede Elétrica, Filtro de Kalman, Estimação Robusta, Gerador Síncrono.

Abbreviations and Symbols

General Abbreviations

AI	Artificial Intelligence
ANN	Artificial Neural Network
BD	Bad Data
CKF	Cubature Kalman Filter
DAQ	Data Acquisition System
DC	Direct Current
DER	Distributed Energy Resource
DSE	Dynamic State Estimation
EKF	Extended Kalman Filter
EKF-UI	Extended Kalman Filter with Unknown Input
EPF	Extended Particle Filter
ERA	Eigensystem Realization Algorithm
FCM	Fuzzy C-Mean
FMLE	Fuzzy Maximum Likelihood Estimate
FNN	Forward Neural Network
GA	Genetic Algorithm
GM	Generalized Maximum Likelihood
GM-KKF	Generalized maximum-likelihood Koopman operator-based Kalman Filter
IEKF	Iterated Extended Kalman Filter
I/O	Input and Output
KF	Kalman Filter
LC	Linear Constraint

LS	Least-Square
MC	Monte Carlo
MP	Markov Parameter
MPC	Model Predictive Control
MSE	Mean Square Error
MVU	Minimum-Variance Unbiased
NERTSS	Nonlinear Extended Recursive Three-step Smoother
ORKID	Observer/Kalman Filter Identification
PED	Power Electronic Device
PER	Power Electronic based Resource
PF	Particle Filter
PMU	Phasor Measurement Unit
PnP	Plug and Play
POC	Power Operating Company
PSO	Particle Swarm Optimization
RCKF	Robust Cubature Kalman Filter
RMSE	Root Mean Square Error
SCADA	Supervisory Control and Data Acquisition
SCKF	Square-root Cubature Kalman Filter
SE	State Estimation
SER	Sustainable Energy Resource
SG	Synchronous Generator
SID	Subspace Identification
SIM	Subspace Identification Method
SOFTEKF	Second-Order Fault-Tolerant Extended Kalman Filter
SoSs	System of Systems
SRUKF-MM	Square Root Unscented Kalman Filter with Modified Measurement
SRWNN	Self-Recurrent Wavelet Neural Network
SVD	Singular Value Decomposition
T-S	Takagi Sugeno

UKF	Unscented Kalman Filter
WLS	Weighted Least Squares

General Symbols

$\delta_\Delta()$	Dirac delta function
Δ	Difference operator
$\mathbb{E}$	Expected value
$\mathbb{R}$	Field of real numbers
$\mathbb{R}^n$	n-dimensional Euclidean space
$\mathbf{y}$	Output vector
y	Output value
y_t	Output value of the t-th sample

Power System Modeling for Dynamic Studies (Chapter 2)

δ_i	Phase angle of generator i-th
ω	Angular frequency (in rad/s)
ω_0	Nominal frequency (in [rad/s])
e'_d	Direct transient axis voltage
e'_q	Quadratic transient axis voltage
E_{fd}	Field voltage
E_i	Voltage amplitude of generator i-th
$\mathbf{E}_N$	Voltage vector consists of generators' voltage
f	frequency (in [Hz])
f_0	Nominal frequency (in [Hz])
H	Inertia constant of synchronous generator
I_{Li}	Current of load at bus i-th
$\mathbf{I}$	Current vector consists of injected currents
$\mathbf{I}_N$	Current vector consists of all generators' currents
K^d	Damping factor
$P^g_{(i,t)}$	Active power of generator i-th at time t
P_{Li}	Active power at load bus i-th

$P^m_{(i,t)}$	Mechanical power of generator i-th at time t
$Q^g_{(i,t)}$	Reactive power of generator i-th at time t
Q_{Li}	Reactive power at load bus i-th
S_{Li}	Complex power at load bus i-th
t	t-th sample
T'_{do}	Direct transient open-circuit time constant
T'_{qo}	Quadratic transient open-circuit time constant
$V_{(i,t)}$	t-th sample of voltage value at bus i-th
$\mathbf{V}$	Voltage vector consists of generators' voltage and buses voltages
V_B	Bus voltage
V_{Li}	Voltage of load at bus i-th
$\mathbf{V}_S$	Voltage vector consists of voltage of buses
x'_d	Direct axis transient reactance
x_{di}	d-axis impedance of generator i-th
x_e	Transmission line reactance
x'_q	Quadratic axis transient reactance
$\bar{\mathbf{Y}}$	Reduced admittance matrix
$\mathbf{Y}_{SS}$	Admittance matrix

Overview of Dynamic State Estimation Methodologies Applied to the Power Systems (Chapter 3)

α	tuning parameter pertaining to UKF filter
β	tuning parameter pertaining to UKF filter
Δt	Sample interval
κ	Secondary scaling factor parameter pertaining to UKF filter
λ	Scaling factor parameter pertaining to UKF filter
$\theta_{(k)}$	k-th sample of a tuple consists of several parameters.
$\mathbf{A}$	Jacobian of $\mathbf{f}()$
$\mathbf{C}$	Jacobian of $\mathbf{h}()$
$\mathbb{E}$	Expected value
$\mathbf{f}()$	Nonlinear function vector corresponding to process model

$\mathbf{h}()$	Nonlinear function vector corresponding to measurement model
$\mathbf{I}$	Identity matrix
k	k-th sample
$\mathbf{K}_k$	Kalman filter gain corresponding to sample k-th
m	The number of inputs
n	The number of states
$\mathbf{P}_0$	Initial covariance matrix
$\mathbf{P}_k$	Covariance matrix of estimation error of $\hat{\mathbf{x}}_k$
$\mathbf{P}_k^-$	Covariance matrix of estimation error of $\hat{\mathbf{x}}_k^-$
q	The number of outputs
$\mathbf{Q}$	Covariance of noise vector corresponding to process model
$\mathbf{R}$	Covariance of noise vector corresponding to measurement model
T_{max}	Number of samples
t	t-th sample
$\mathbf{u}$	Input vector
$\mathbf{v}_c$	Gaussian noise vector corresponding to measurement model
$\mathbf{w}_c$	Gaussian noise vector corresponding to process model
$\mathbf{x}$	State vector
$\mathbf{x}_0$	Initial state vector
$\hat{\mathbf{x}}$	Estimate of state vector $\mathbf{x}$
$\hat{\mathbf{x}}_{k+1}^-$	A priori estimate of state vector $\mathbf{x}$
$\hat{\mathbf{x}}_0$	Initial estimate of state vector $\mathbf{x}$
$\mathbf{z}$	Measurement vector

Distributed Simultaneous Estimation of States and Unknown Inputs (Chapter 4)

$\boldsymbol{\delta}^l$	Constant coefficient vector
$\mathbf{A}$	Matrix pertaining to state equation
$\mathbf{C}$	Matrix pertaining to output equation
$\mathbf{B}$	Adjacency matrix of graph W
$\mathbf{d}$	Unknown input vector
$\hat{\mathbf{d}}$	Estimate of unknown input vector

$\mathbf{D}$	Degree matrix of graph W
$\mathbb{E}$	Expected value
E_w	Set of links inside the graph W
$\mathbf{I}$	Identity matrix
k	k-th sample
K	Number of samples
$\mathbf{L}$	Laplacian matrix of graph W
m	Number of unknown inputs
$\mathbf{M}^{\dagger}$	Moore-Penrose inverse of matrix $\mathbf{M}$
$\mathbf{M}^{T}$	Transpose of matrix $\mathbf{M}$
$\mathbf{M}_{d(k)}$	k-th sample of gain matrix pertaining to unknown input
$\mathbf{M}_{x(k)}$	k-th sample of gain matrix pertaining to state
n	Number of states
N	Number of nodes inside graph W
$\mathbf{N}_{x(k)}$	k-th sample of consensus gain
$\mathbf{P}_0$	Initial covariance matrix
$\mathbf{P}_k$	Covariance matrix of estimation error of $\hat{\mathbf{x}}_k$
$\mathbf{P}_k^-$	Covariance matrix of estimation error of $\hat{\mathbf{x}}_k^-$
q	Number of outputs
$\mathbf{Q}$	Covariance of noise corresponding to process model
$\mathbf{R}$	Covariance of noise corresponding to measurement model
$\mathbf{v}_{(k)}$	Gaussian noise vector corresponding to measurement model
$\mathbf{w}_{(k)}$	Gaussian noise vector corresponding to process model
W	Represent a graph
$\mathbf{x}$	State vector
$\mathbf{x}_0$	Initial state vector
$\hat{\mathbf{x}}$	Estimate of state vector $\mathbf{x}$
$\hat{\mathbf{x}}_{k+1}^-$	A priori estimate of state vector $\mathbf{x}$
$\hat{\mathbf{x}}_0$	Initial estimate of state vector $\mathbf{x}$
$\mathbf{y}_{(k)}$	k-th sample of output $\mathbf{y}$

A Systematic Approach to Modeling Synchronous Generator Using Markov Parameters and T-S Fuzzy Systems (Chapter 5)

δ^0	Initial phase angle of a generator
Δ	Difference operator
γ^i	Parameter of i-th fuzzy rule
ω	Angular frequency (in rad/s)
ω_0	Nominal frequency (in [rad/s])
σ_j^i	width of j-th Gaussian membership function corresponding to i-th rule
$\mu_{F_j^i}^i$	Membership function of the antecedent fuzzy set F_j^i corresponding to rule i
$\mathbf{A}^i$	Parameter of i-th sub-model
$\mathbf{B}^i$	Parameter of i-th sub-model
c	Number of clusters
$\mathbf{C}^i$	Parameter of i-th sub-model
$d_{(k)}^i$	Euclidean distance between the cluster centroid vector $\mathbf{v}_i$ and vector $\mathbf{z}_{(k)}$
$\mathbf{D}^i$	Parameter of i-th sub-model
$e_d^{'}$	Direct transient axis voltage
$e_q^{'}$	Quadratic transient axis voltage
E_{fd}	Field voltage
F_j^i	i-th fuzzy set of the j-th antecedent variable
h_k^i	k-th sample of activation degree of i-th fuzzy rule
H	Inertia constant of synchronous generator
$\mathbf{H}$	Hankel matrix
J_m	Objective function
k	sample time
K^d	Damping factor
l	Number of samples inside dataset S
l^i	Number of samples inside dataset S^i
L	Total number of samples
m	Number of input variables

n	Number of state variables
N	Number of data points
p	Number of antecedent variables
P	Active power of generator
P^m	Mechanical power
q	Number of output variables
Q	Reactive power of generator
R^i	i-th fuzzy inference rule
R	Number of rules
S	dataset
S^i	Portion of dataset S corresponding to i-th cluster
S_b^{sg}	Generator power base
T'_{do}	Direct transient open-circuit time constant
T'_{qo}	Quadratic transient open-circuit time constant
$\mathbf{u}_{(k)}$	k-th sample of input vector
$u_{(j,k)}$	j-th element of vector $\mathbf{u}_{(k)}$
$\mathbf{U}$	Membership matrix
V_t	Terminal voltage
V_B	Bus voltage
$\mathbf{V}$	Matrix of cluster centroid vectors
$\mathbf{v}_i$	i-th cluster centroid vector
x_d	Direct axis impedance of generator
x_e	Transmission line reactance
x_q	Quadratic axis impedance of generator
x'_d	Direct axis transient reactance
x'_q	Quadratic axis transient reactance
$\mathbf{x}^i_{(k)}$	k-th sample of state vector of i-th sub-model
$x^i_{(j,k)}$	j-th element of state vector $\mathbf{x}^i_{(k)}$
$\mathbf{y}^i_{(k)}$	k-th sample of output vector of i-th sub-model
$y^i_{(j,k)}$	j-th element of output vector $\mathbf{y}^i_{(k)}$

$z_{(j,k)}$	j-th element of vector $\mathbf{z}_{(k)}$
$\mathbf{z}_{(k)}$	k-th sample of vector of antecedent variables

Engineering Approach to Construct Robust Filter for Mismatched Nonlinear Dynamic Systems (Chapter 6)

$\boldsymbol{\alpha}_{(k)}$	k-th sample of attenuated adaptive coefficient
$\delta_{(i,k)}$	k-th sample of phase angle of generator i-th
ω	Angular frequency (in rad/s)
ω_0	Nominal frequency (in [rad/s])
$\mathbf{A}$	Jacobian matrix pertaining to state equation
$\mathbf{C}$	Jacobian matrix pertaining to measurements equation
$\mathbf{d}$	Compensation input vector
$\mathbf{g}_{(.)}$	Nonlinear function vector
$\mathbf{G}$	Compensation matrix
$\mathbf{h}_{(.)}$	Nonlinear function vector
$\mathbf{I}$	Identity matrix
k	k-th sample
K^d	Damping factor
K	Total number of samples
M	Total number of Monte Carlo simulations
m	Number of unknown inputs
$\mathbf{M}_{x(k)}$	k-th sample of gain matrix pertaining to state
$\mathbf{M}_{d(k)}$	k-th sample of gain matrix pertaining to unknown input
n	Number of states
$\mathbf{P}_0$	Initial covariance matrix
$\mathbf{P}_k$	Covariance matrix of estimation error of $\hat{\mathbf{x}}_k$
$\mathbf{P}_k^-$	Covariance matrix of estimation error of $\hat{\mathbf{x}}_k^-$
$P^g_{(i,t)}$	Active power of generator i-th at time t
$P^m_{(i,t)}$	Mechanical power of generator i-th at time t
q	Number of measurements

$\mathbf{Q}$	Covariance of noise vector corresponding to process model
$Q^g_{(i,t)}$	Reactive power of generator i-th at time t
$\mathbf{R}$	Covariance of noise vector corresponding to measurement model
$\mathbf{v}_{(k)}$	A bounded, unmeasured Gaussian noise vector corresponding to measurement model
$\mathbf{w}_{(k)}$	A bounded, unmeasured Gaussian noise vector corresponding to process model
$\mathbf{x}$	State vector
$\mathbf{x}_0$	Initial state vector
$\hat{\mathbf{x}}$	Estimate of state vector $\mathbf{x}$
$\hat{\mathbf{x}}^-_{k+1}$	A priori estimate of state vector $\mathbf{x}$
$\hat{\mathbf{x}}_0$	Initial estimate of state vector $\mathbf{x}$
$\mathbf{z}_{(k)}$	k-th sample of measurement vector $\mathbf{z}$

Contents

List of Figures

List of Tables

List of Algorithms

Chapter 1

Introduction

Contents

1.1 Main Motivation

Globally, power systems have long been important in providing energy sustainably and at large scales. Therefore, issues like their stability, control, and monitoring have been extensively investigated through many studies. This is because on one hand, a power system usually comprises a large number of nonlinear and time-varying elements, and on the other hand, the advent of various distributed energy resources (DERs) particularly ones producing energy intermittently, e.g. wind turbines, photovoltaic solar panels, and so on, requires smarter and more intelligent approaches and algorithms to guarantee one power system including a number of grids and microgrids can keep on working efficiently, stably and reliably. As a matter of fact, power system stability depends directly on the monitoring and control systems applied to power systems, and these systems depend directly on models' accuracy, and the availability and accuracy of state values.

Taking into account the above points, as well as the growing number of phasor measurement units (PMUs) that offer a higher rate and more accurate measurements, it is justified that developing on-line modeling, identification, as well as robust and/or distributed estimation methods would be very advantageous and promising for future electrical grids and microgrids.

Nevertheless, there are some challenges and issues to consider in this direction:

1. Power systems are often huge systems with many nonlinear time-varying components like motors, generators, etc, and because of this, they can be considered as a system of systems (SoSs).

2. Trying to combat climate change and strive for zero-emission carbon dioxide has led countries to use more sustainable energy resources (SERs) such as wind turbines and solar cells, but their intermittent nature makes power system design and behavior even more complex and variable.

3. Power systems are subject to a wide range of operating states due to a wide variety of events such as load changes, line switching, and source commitment.

4. As a result of some recent concepts like smart grids and microgrids as well as the possibility of components having varying roles, i.e., being sources or loads, rather than fixed roles, power systems are becoming even more complex.

5. Identifying and modeling the components that comprise power systems can enhance power system control and monitoring.

In light of the above points, this PhD thesis seeks to develop robust and/or distributed estimation approaches as well as on-line modeling and identification methodologies which can be applied to power systems (electrical networks).

1.2 State Estimation in Power System Motivation

Taking into account the points 1-5 mentioned in Section 1.1, achieving effective monitoring and control objectives is not a trivial task and is strongly dependent on having accurate instant state values. State estimation approaches can be considered as an effective way to attain precise state values, and as stated in point 1, power

systems can be considered as SoSs. Therefore, developing distributed methodologies for state estimation can significantly increase reliability and availability of state values in comparison with centralized methods, as distributed approaches are less prone to being limited when central processing is interrupted or when several measurements are missing [Cattivelli and Sayed, 2011]. In addition, the points 2, 3 and 4 suggest that power systems models are prone to experience more model changes during operation because of intermittent SERs, sudden load changes, line switching, etc. Therefore, developing robust estimation approaches, which are resilient and robust to these model variations and mismatches, can be a very efficient and promising solution.

1.3 Model Identification Motivation

In regard to point 5, one of the most promising approaches to improving the monitoring and control systems of a power system, and consequently improving its stability, is to obtain more accurate models of its components. In particular, synchronous generators have a significant effect on power system stability due to their nonlinear behavior and time-varying characteristics. As a result, studying and developing data-driven methodologies that can find their models when they are connected to the grid, without additional hardware other than some basic measurement devices and sensors, can be extremely useful and promising. By developing more accurate models of synchronous generators, it will be possible to achieve more reliable monitoring and control systems, estimators, as well as stability analysis, which are necessary for a power system to function sustainably. It is obvious that reaching more powerful methods for model identification of synchronous generators, which are considered as dynamic elements in power systems, can pave the way for improving the existing methodologies for other components of power systems such as power electronic based resources (PERs).

1.4 Thesis Contributions

Taking into account the above comments, this thesis makes a number of contributions. The main contributions of this thesis are:

1. *[Chapter 4], [Emami* et al.*, 2020]:* Design of a novel recursive distributed filter for linear discrete-time large-scale stochastic systems. The main contributions are: (1.1) its unbiasedness and minimum variance are examined; (1.2) the necessary and sufficient conditions for the stability and convergence of the proposed distributed filter are investigated and defined. Furthermore, the presented filter's performance is examined and verified using a numerical example;

2. *[Chapter 5], [Emami* et al.*, 2024]:* Design of a new method to find a global model for a synchronous generator from input and output measurement data using state-of-the-art methods in artificial intelligence (AI) such as fuzzy clustering, subspace identification, and Takagi Sugeno (T-S) fuzzy modeling. The main contributions are: (2.1) All steps, such as dataset construction, clustering, sub-model identification, and the training of a T-S fuzzy model to achieve the global model of a synchronous generator (SG), are chronologically explained; (2.2) Due to the choice of generator terminal voltage as an input, a connection to an infinite bus is not necessary, which is considered a benefit in comparison with the methods proposed e.g. in [Karrari and Malik, 2004; Ghahremani *et al.*, 2008; Dehghani and Nikravesh, 2008; Dehghani *et al.*, 2010; Grillo *et al.*, 2021]; (2.3) Micev *et al.* [2022] highlighted that most existing on-grid identification methods require additional equipment to inject extra signals for identification purposes, increasing the setup costs, while in this work, there is no need to do so; (2.4) The effectiveness of the proposed approach is illustrated by simulations on a known fourth-order SG nonlinear model as well as with real-world experimental results;

3. *[Chapter 6], [Emami* et al.*, -] (under-review):* Design of a novel approach to design a robust estimator that is able to keep its consistency in system state estimation when system process model mismatch occurs. The main contributions are: (3.1) A new adaptive methodology based on ensemble Kalman Filter (EKF) is proposed to tackle the model mismatch problem for nonlinear dynamic systems without imposing any linear constraints (refer to Section 6.3); (3.2) Providing a practical mechanism to incorporate and utilize the designer's knowledge and experience from the system's behavior in designing its corresponding filter; (3.3) Proposing an adaptive mechanism for adjusting the

coefficient of compensation input that seeks to improve the accuracy of results more effectively. (3.4) To assess the performance of the resulting estimator, which is obtained from the new proposed approach, its performance is compared with that of three well-known estimators, i.e., the unscented Kalman filter (UKF), the cubature Kalman filter (CKF), and the extended Kalman filter (EKF) on the IEEE 5-generator 14-bus system. The results indicate that the proposed method has led to an estimator outperforming its rivals under the presence of model errors.

1.5 Thesis Organization

The thesis is organized as follows:

- Chapter 2 provides an overview of a simple approach to modeling a classic power system. In addition, for one of the very key elements of many power systems, namely SGs, two well-known models, namely 2nd-order and fourth-order are illustrated;

- Chapter 3 provides an overview of estimation methods applied to dynamic state estimation (DSE) in power systems. The review focuses on methods, which are more robust to model mismatches or the inaccurate model of noise. Finally, the three well-known KF-based filters which are used for nonlinear systems, namely EKF, UKF and CKF are described in more procedural details.

- Chapter 4 describes the proposed methodology for distributed filter development. A list of the most recent, and state-of-the-art, distributed approaches to linear Kalman filters is presented. Furthermore, some main features of the resultant filter such as unbiasedness, minimum variance and stability conditions are discussed. Finally, an illustrative example is defined to evaluate the performance of the resulting distributed filter.

- Chapter 5 describes a novel approach to finding a global model for a synchronous generator from input and output measurement data using state-of-the-art methods in artificial intelligence (AI) such as fuzzy clustering, subspace identification, and Takagi Sugeno (T-S) fuzzy modeling. Results of simulation as well as experimental case studies are reported to evaluate, and demonstrate

the performance and effectiveness of the proposed data-driven approach over state-of-the-art approaches.

- Chapter 6 describes a novel approach to designing a robust adaptive estimator that is able to keep its consistency in system state estimation when system process model mismatch occurs. The performance of the resultant estimator is compared with that of three well-known estimators, i.e., the unscented Kalman filter (UKF), the cubature Kalman filter (CKF), and the extended Kalman filter (EKF) on the IEEE 5-generator 14-bus system.

- Chapter 7 presents concluding remarks. Future research suggestions are also outlined.

Chapter 2

Power System Modeling for Dynamic Studies

Contents

2.1 Introduction

This Chapter introduces the main components of an electric grid, their mathematical models, and how they can be taken together to create a complete mathematical model. Simulation software such as Simulink, DigSilent, and some others are available for effective electrical grid simulation, but many fundamental concepts and operations may be covered under the hood of these programs. For this reason, in this work, it was decided to use a mathematical-based approach rather than the intricate and mostly not free software, which has the potential of facilitating a better understanding of the underlying functions in an electric grid and microgrids.

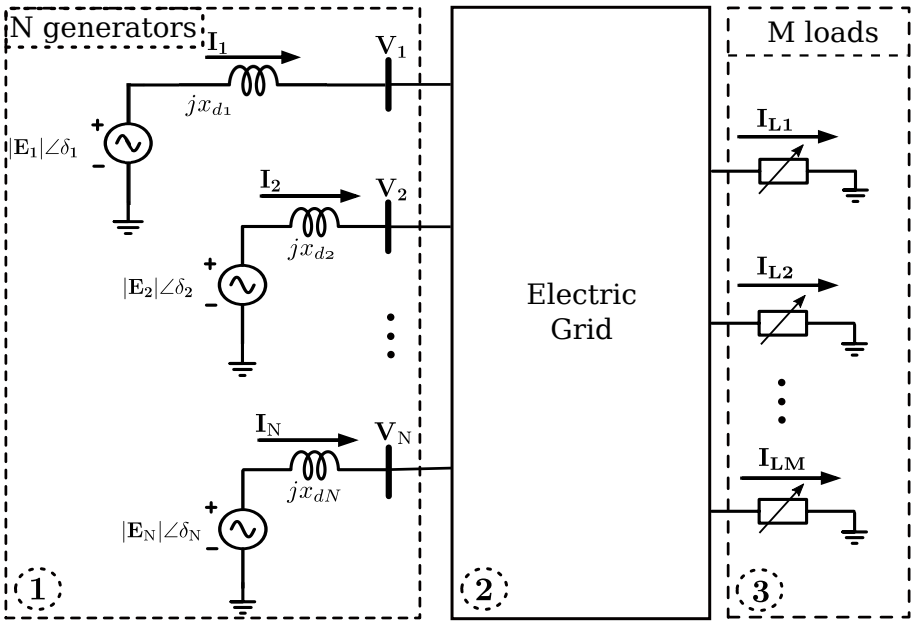

Figure 2.1: Electric network diagram.

Throughout this chapter, and throughout the thesis, the focus is more, but not exclusively, on synchronous generator models, since synchronous generators play such an important and crucial role in many power systems, and their dynamic behavior greatly affects the stability and reliability of power systems.

Section 2.2 describes the main components of a classical power system and how it is possible to model these components. Section 2.3 introduces two well-known and widely used models for synchronous generators. Finally, Section 2.4 gives brief conclusion remarks.

2.2 Power System Modeling

The classic schematic of a power system is illustrated in Figure 2.1, where three distinct parts can be observed. The first part, designated by the number 1, is the generating part. This is where the energy of the entire network is produced by N generators, which are linked through impedances (x_{di}) to the electric network. The second part, designated by the number 2, describes the topology of the electric grid and transmission lines, including their parameters. The third section, designated

by the number 3, describes the loads, including their parameters. Now that all the three main parts in Figure 2.1 are introduced, it is time to combine these three parts and make the whole model of the system. According to Figure 2.1, each generator is represented by a voltage source $|\mathrm{E}_i|\angle\delta_i$ in series with impedance $j\,x_{di}$, and for the sake of simplicity, it is assumed that each voltage source behind $j\,x_{di}$ has a constant amplitude between two consecutive simulation steps. There are two widely used models of synchronous generators that will be presented in Section 2.3. Based on these facts, the process to achieve the final model of a power system can be accomplished using the three steps below.

Step 1. In each electrical network, using Ohm's law along with some other crucial information, for instance knowing the topology of networks (how the buses and lines are arranged and connected), line impedances, etc, it is possible to obtain an admittance matrix which herein is named $\mathbf{Y}_{SS}$. The interested reader for further information could refer to e.g., [Grigsby, 2012].

Step 2. To integrate all loads on different buses into the electrical network, it is possible to convert the apparent power of each load into its equivalent shunt admittance and then update the $\mathbf{Y}_{SS}$ with these shunt admittances. With this regard, for example assuming that a load bus has a voltage $V_{L\,i}$ (it can be determined, e.g., from the power flow analysis [Grigsby, 2012]) and a complex power demand $S_{L\,i} = P_{L\,i} + j\,Q_{L\,i}$ then using $S_{L\,i} = V_{L\,i}\,I^*_{L\,i}$, one load can be converted into its equivalent shunt admittance at bus i as (2.1) [Wang, 2021]:

$$y_{Li} = \frac{I_{L\,i}}{V_{L\,i}} = \frac{S^*_{L\,i}}{|V_{L\,i}|^2} = \frac{P_{L\,i} - j\,Q_{L\,i}}{|V_{L\,i}|^{\,2}}. \tag{2.1}$$

Similarly, such an action can be repeated for all loads in one electric network to integrate them into the admittance matrix $\mathbf{Y}_{SS}$.

Step 3. The last step is to develop the model to include the N generators as well. Again according to Ohm's law, the relationship between the injected currents and bus voltages can be written in general form as (2.2) [Wang, 2021]:

$$\mathbf{I} = \mathbf{Y}_{bus}\,\mathbf{V}, \tag{2.2}$$

where the current vector $\mathbf{I}$ is obtained from the injected currents at each bus. As can be seen in Figure 2.1 , the injected currents just exist at buses connecting to

generators. Therefore, the injected current vector can be represented as (2.3):

$$\mathbf{I} = \begin{bmatrix} \mathbf{I}_N \\ \dots \\ \mathbf{0} \end{bmatrix}, \tag{2.3}$$

where $\mathbf{I}_N$ represents a vector consisting of the generators' currents. Also, matrix $\mathbf{Y}_{bus}$ and vector $\mathbf{V}$ in (2.2) can be defined as (2.4) [Wang, 2021]:

$$\mathbf{Y}_{bus} = \begin{bmatrix} \mathbf{Y}_{NN} & \vdots & \mathbf{Y}_{NS} \\ \dots & \dots & \dots \\ \mathbf{Y}_{SN} & \vdots & \mathbf{Y}_{SS} \end{bmatrix}, \quad \mathbf{V} = \begin{bmatrix} \mathbf{E}_N \\ \dots \\ \mathbf{V}_S \end{bmatrix}, \tag{2.4}$$

where $\mathbf{E}_N$ is a vector comprising the generators' internal voltages behind the corresponding $jx_{di}\,(i \in \{1, \dots, N\})$ and $\mathbf{V}_S$ is a vector consisting of the voltages of the buses. The subscript S represents the number of all nodes (buses), while the subscript N is used to represent the whole number of nodes (buses) connected directly to generators, and for the sake of simplicity, it is assumed that the first N buses of all buses are buses connected to given generators. $\mathbf{Y}_{NN} = \text{diag}([jx_{d1}, jx_{d2}, \dots, jx_{dN}])^{-1}$ is a diagonal matrix and $\mathbf{Y}_{NS} = \mathbf{Y}_{SN}^T$ is denoted as

$$\mathbf{Y}_{NS}[i][p] = \begin{cases} \frac{-1}{jx_{d\,i}}, & \text{if } g_i \text{ is connected to bus } p, \\ & i \in \{1, \dots, N\}, p \in \{1, \dots, S\}, \\ 0, & \text{otherwise,} \end{cases} \tag{2.5}$$

where g_i represents the i-th generator and S is the total number of the buses. Considering (2.2), (2.3), and (2.4), it is possible to calculate the injected currents vector of N generators, i.e. $\mathbf{I}_N$, as

$$\mathbf{I}_N = (\mathbf{Y}_{NN} - \mathbf{Y}_{NS}\,\mathbf{Y}_{SS}^{-1}\mathbf{Y}_{SN})\,\mathbf{E}_N = \bar{\mathbf{Y}}\mathbf{E}_N, \tag{2.6}$$

where $\bar{\mathbf{Y}} \in \mathbb{R}^{N\times N}$ is called the reduced admittance matrix [Wang, 2021]. Lastly, the active and reactive power of the generator i can be calculated by (2.7) and (2.8)

$$P^{g}_{(i,t)} = \mathrm{Re}(V_{(i,t)}\, I^{*}_{(i,t)}), \tag{2.7}$$

$$Q^{g}_{(i,t)} = \mathrm{Imag}(V_{(i,t)}\, I^{*}_{(i,t)}), \tag{2.8}$$

where $I_{(i,t)}$ is the i-th element of vector $\mathbf{I}_N$ and $V_{(i,t)}$ represents the voltage of the bus which is connected to the i-th generator and can be computed as (2.9):

$$V_{(i,t)} = E_{(i,t)} - jx_{d\,i}\, I_{(i,t)}, \tag{2.9}$$

where $E_{(i,t)}$ is the i-th element of vector $\mathbf{E}_N$, which can be defined more specifically as (2.10)-(2.11),

$$E_{(i,t)} = |E_{(i,t)}| \exp(j\,\delta_{(i,t)}) \tag{2.10}$$

$$\delta_{(i,t)} = \int_0^t \omega_0\, \Delta\bar{\omega}_{(i,\tau)}\, d\tau + \delta_{(i,0)}, \quad \Delta\bar{\omega}_{(i,t)} = \frac{\omega_{(i,t)} - \omega_0}{\omega_0},\ \omega_0 = 2\pi f_0, \tag{2.11}$$

where $\omega_{(i,t)}$, $\delta_{(i,0)}$, f_0 and t are the angular frequency (in [rad/s]), the initial phase angle of the generator i-th (in [radians]), the nominal frequency of the grid in [Hz] and the time instant (in [seconds]), respectively. The process of modeling the electric network comprising its major elements such as loads and generators is now completed. However, synchronous generators are electromechanical devices and because of this, it is still required to define how they may exchange energy with the electric network. Thus, in the next section some popular dynamic models of generators is described in more detail.

2.3 Synchronous Generator Models

One of the key components of any power system is the energy resources that provide the required energy for the electrical network. Synchronous generators work by converting mechanical energy from different sources (such as fossil fuels, wind, etc.) into electrical energy and, as a result, their dynamics can have a significant impact on the reliability and stability of power systems. Therefore, in the following sections several models which are widely used for these key components will be reviewed in

more detail.

2.3.1 Second-Order Swing Model

In this Section a second-order model namely swing equations is utilized to describe the dynamics of each generator g_i in power system as (2.12) [Xu *et al.*, 2019; Wang, 2021]:

$$\begin{aligned} \frac{d\Delta\bar{\omega}_{(i,t)}}{dt} &= \frac{1}{M_i}\left(P^m_{(i,t)} - P^g_{(i,t)} - K^d_i\,\Delta\bar{\omega}_{(i,t)}\right), \quad M_i = 2H_i, \\ \frac{d\delta_{(i,t)}}{dt} &= \omega_0\,\Delta\bar{\omega}_{(i,t)}, \end{aligned} \tag{2.12}$$

where $\delta_{(i,t)}$ is the rotor angle in radians, $\omega_0 = 2\pi f_0$ is the nominal synchronous angular speed in [rad/s], $\Delta\bar{\omega}_{(i,t)}$ is the rotor speed deviation in per unit [p.u.]); $P^m_{(i,t)}$ is the mechanical power in p.u.; $P^g_{(i,t)}$ is the electric power in [p.u.]; H_i is the inertia constant in seconds, and K^d_i is the damping factor in [p.u.], respectively. This model will be used specifically in Chapter 6.

2.3.2 Fourth-Order Model

One of the models which is widely exploited for synchronous generator is the following fourth-order nonlinear state space model:

$$\begin{aligned} x &= [\delta\ \Delta\bar{\omega}\ e'_q\ e'_d]^T = [x_1\ x_2\ x_3\ x_4]^T, \\ \dot{x_1} &= \omega_0\,x_2, \\ \dot{x_2} &= \frac{1}{2H}(P^m - P^g - K^d\,x_2), \\ \dot{x_3} &= \frac{1}{T'_{do}}(E_{fd} - x_3 - (x_d - x'_d)\,i_d), \\ \dot{x_4} &= \frac{1}{T'_{qo}}(-x_4 - (x_q - x'_q)\,i_q), \end{aligned} \tag{2.13}$$

where, x_1 (i.e. δ) is the rotor angle in [rad], $\omega_0 = 2\pi f_0$ is the nominal synchronous angular speed in [rad/s], x_2 (i.e. $\Delta\bar{\omega}$) is the rotor speed deviation from the nominal speed in [p.u.], P^m is the mechanical input power in [p.u.], P^g is the approximate electrical output power in [p.u.], E_{fd} is the field voltage as seen from the armature

in [p.u.] and it is considered as the second input of the SG model, K^d is the damping factor in [p.u.], H is inertia constant in [s], x_d (resp. $x_d^{'}$) and x_q (resp. $x_q^{'}$) are the direct axis (resp. direct axis transient) and quadratic axis (resp. quadratic transient axis) reactances, $T^{'}_{do}$ (resp. $T^{'}_{qo}$) is the direct (resp. quadratic) transient open-circuit time constant (resp. d-axis transient open-circuit time constant), and x_3 (i.e. $e_q^{'}$) and x_4 (i.e. $e_d^{'}$) are the quadratic transient axis voltage and direct axis transient voltage behind the corresponding reactances, $x_q^{'}$ and $x_d^{'}$, respectively. Lastly, i_d and i_q are defined as (2.14) and (2.15) [Machowski *et al.*, 2020]:

$$i_d = \frac{e^{'}_q - V_B \cos(x_1)}{x_{td}}, \qquad x_{td} = x_d^{'} + x_e, \tag{2.14}$$

$$i_q = \frac{V_B \sin(x_1)}{x_{tq}}, \qquad x_{tq} = x_q + x_e, \tag{2.15}$$

where V_B is the bus voltage in [p.u.], and x_e is the line reactance in [p.u.]. The outputs of the generator are the active and reactive powers, defined respectively as:

$$P = \frac{V_B x_3 \sin(x_1)}{x_{td}} + \frac{V_B^2}{2}\left(\frac{1}{x_{tq}} - \frac{1}{x_{td}}\right)\sin(2x_1), \tag{2.16}$$

$$Q = -\frac{V_B^2}{x_{tq}}\sin^2(x_1) - \frac{V_B^2}{x_{td}}\cos^2(x_1) + \frac{V_B x_3}{x_{td}}\cos(x_1) + x_e\left(i_d^2 + i_q^2\right). \tag{2.17}$$

2.4 Conclusion

This Chapter reviewed a simple methodology for mathematically modeling a power system. The main components of the power system were described, and how to model each and combine them to obtain the whole model for the dynamic study was illustrated. In this direction, for synchronous generators, two popular models which are widely used in the scientific literature were explained. The information and concepts explained in this Chapter will be used principally later in Chapters 5 and 6.

Chapter 3

Overview of Dynamic State Estimation Methodologies Applied to the Power Systems

Contents

Controlling and monitoring are two crucial processes for maintaining the stability and reliability of power systems, but they cannot be achieved maturely without accurate and sufficient measurements, and effective state estimation approaches, and in this chapter it will be examined the current state of the art of DSE methods

in power systems, and then it will be examined three potent approaches, including EKF, UKF, and CKF, which have all been widely used.

This chapter is organized as follows. Section 3.1 discusses the existing works on realizing DSE in power systems. Section 3.2 describes the continuous state space model including the process model and measurement model for a nonlinear dynamic system. In Section 3.3, the steps through which a continuous model is converted into a discrete model are illustrated. Lastly, Section 3.4 describes the procedures associated with three well-known KF based filters, namely EKF, UKF, and CKF.

3.1 Introduction

Applying state estimation techniques to power systems dates back to [Schweppe and Wildes, 1970], which introduced the Weighted Least Square (WLS) to estimate power system static states (SEs). Any fluctuations in power generation and customers' loads in power systems with a high percentage of renewable energy sources and electric vehicles may seriously distort WLS estimation results [Valverde and Terzija, 2011]. For this reason, Kalman filtering techniques are proposed in order to address and estimate the dynamic states of power systems [Alhalali and El-Shatshat, 2019]. Estimation in power systems could be implemented in two major frameworks, static and dynamic estimation [Zhao *et al.*, 2019]. In static estimation quantities like voltage magnitudes and voltage phase angles are of interest, while in its dynamic counterparts states such as generator rotor angles and generator speeds are in the center of attention [Huang *et al.*, 2007].

A growing number of PMUs, which provide high sampling resolution synchronous measurements, makes DSE implementation more promising [Rostami and Lotfifard, 2018]. Considering what the researchers have accomplished until now in the context of DSE, it can be concluded that in the majority of the researches, Kalman filter methods have been playing the main role. EKF filter was used in [Huang *et al.*, 2007], along with PMU, to estimate the state of generators in a multi-machine electrical network. Although the estimation is accomplished under some noise assumptions, the dynamical model itself must be fully known. Ghahremani and Kamwa [2011] proposed extended Kalman filter with unknown input (EKF-UI) for dynamic state estimation of a synchronous generator connected to an infinite bus. Based on this approach, the authors managed to bypass measuring some necessary input sig-

nals, e.g. exciter output voltage, etc. Later on, in [Ghahremani and Kamwa, 2016], the authors extended the EKF-UI method of their previous work in [Ghahremani and Kamwa, 2011] to be functional in the case of multi-machines as well. It is observed that in both studies in [Ghahremani and Kamwa, 2011] and [Ghahremani and Kamwa, 2016], complete information about the dynamic model of each generator was required.

Huang *et al.* [2014] have exploited an EKF to implement a DSE for a multi-machine system. Some sensitivity analysis was also performed to examine the performance of this estimation method. Despite some errors in the parameters of the employed model, the EKF has demonstrated some good resilience to these errors. Aminifar *et al.* [2014] addressed DSE by using a mixed-integer programming approach to avoid predicted values whenever a drastic change comes up in the system state. In [Zhang *et al.*, 2014b], both static and dynamic state estimation were addressed, with an adaptive Kalman filter with inflatable noise variances proposed to overcome the impact of inaccurate system modeling and bad measurement data, thereby improving the robustness and reliability of the estimator. In [Tebianian and Jeyasurya, 2015], a fourth order model of the generator was considered, where EKF was used to estimate the dynamic state.

In [Zhou *et al.*, 2015], using Monte Carlo methods, four Bayesian-based filtering methodologies namely EKF, ensemble Kalman filter, UKF, and particle filter (PF) were reviewed, and their performances were examined on a two-area four-machine test system. The performance of these estimators was investigated in particular in relation to the PMU sampling rate, measurement interpolation methods, and outliers. Cui and Kavasseri [2015] implemented DSE using PF and compare its performance with UKF for a multi-machine power system, where the model of each generator is of 12-th order. However, as also stressed in this work, for PF two issues that must be carefully considered are the number of particles and measurement sampling. Increasing the number of particles will improve the accuracy of results at the expense of computation requirements. On the other hand, the probability of divergence in PF would increase when the sample time associated with measurement is lower than the filter's iteration computation time.

In Netto *et al.* [2016]'s work, a robust estimator based on EKF, which is called GM-EKF, was proposed that can function reasonably under gross errors in measurements if model's nonlinearity is not very severe and noise is Gaussian. Zhao *et al.*

[2017b] also proposed a robust filter based on EKF, named IEKF, which benefits from features such as fast computations and acceptable robustness to observation and innovation outliers, but it suffers from several weaknesses such as vulnerability to system parameter and topology errors, and unreliable state estimates under strong nonlinearities of the power system model. The work in [Zhao *et al.*, 2017b] was extended in Zhao *et al.* [2017a] to develop a robust estimator named GM-IEKF that was capable of tracking power system dynamic state variables under a few parameters with errors and/or a variety of cyber attacks, although it was vulnerable to a large number of inaccurate parameters in the model of the power system.

Additionally, Akhlaghi and Zhou [2017] demonstrated an adaptive EKF where the prediction step could be repeated several times in case of high nonlinearity to improve the estimation of dynamic states. Lavenius and Vanfretti [2018] proposed a new methodology, i.e., the nonlinear extended recursive three-step smoother (NERTSS), and a new alternative estimation model to tackle the problem of simultaneously estimating the states and unknown inputs of synchronous machines. In [Joseph *et al.*, 2018], based on the method in [Kitanidis, 1987], the authors attempted to solve the DSE problem in power systems. The authors claimed their methodology has better transient response comparing with the work in [Ghahremani and Kamwa, 2016]. Using S-estimator and EKF, Chakhchoukh *et al.* [2020] converted the EKF estimator to a robust one that can function effectively and precisely under phenomena like the presence of outliers, increased nonlinearities and measurement noise. Under bad data, PMU failures, external disturbances, extraneous noise, and bounded observer-gain perturbation conditions, Wang [2021] proposed a second-order fault-tolerant extended Kalman filter (SOFTEKF) framework for dynamic state estimation in power systems.

The UKF method, which has been utilized in estimators and filters for nonlinear systems, was proposed by [Julier *et al.*, 2000], and this method gained more attraction to be used in comparison with its EKF counterpart method owing to an easier implementation and more accuracy since no model linearization or Jacobian matrix computation is needed [Wang *et al.*, 2012; Valverde and Terzija, 2011]. A numerical stable UKF was proposed in [Qi *et al.*, 2018] to estimate the dynamic states of power systems. Zhao [2018] have proposed H_∞-EKF (HEKF) to overcome the problem of uncertainties in the system model but this method may suffer from some difficulties in terms of tuning its parameters as well as requiring a certain level of mathematics

to be understandable by users. Wang *et al.* [2012] solved the problem of DSE in multi-machine power systems by using UKF, but it required an exhaustive model of the system, and measurements are influenced by Gaussian noise. According to [Netto and Mili, 2018], a robust operator-based Kalman filter (KF) named the generalized maximum-likelihood Koopman operator-based Kalman filter (GM-KKF) has been proposed, which is a data-driven estimator, and was used to implement DSE in power systems. It appears that the results from this work are more accurate than the results from [Netto *et al.*, 2016]. A robust generalized maximum-likelihood-type unscented Kalman filter (GM-UKF) was developed by Zhao and Mili [2018b] for suppressing observation and innovation outliers and filtering non-Gaussian process and measurement noise. In [Zhao and Mili, 2018a], they report the development of a fast and robust unscented Kalman filter-based dynamic state estimator (DSE) capable of identifying and suppressing three types of outliers, including observation, innovation, and structural outliers. According to [Zhao and Mili, 2018a], observation outliers refer to the received PMU measurements providing unreliable metered values as a result of gross errors or cyber attacks; innovation outliers tend to be caused by impulsive system process noise, while structural outliers are caused by incorrect parameters of generators or the controllers that control them, such as exciters and speed governors.

Zhao and Mili [2019] have developed a methodology to estimate the dynamic state of power system by combining UKF and H_∞ namely HUKF to deal with the system nonlinearity as well as to suppress outliers which can not be done well with their earlier method in [Zhao, 2018]. Dang *et al.* [2022] introduced SRUKf-MM, a square root unscented Kalman filter with modified measurement, which is capable of directly adjusting measurement to weight error covariance and noise variance, which leads to more accurate estimation when the measurement noise is non-Gaussian or large. Yu *et al.* [2019] utilized the methods of the H_∞ filter and the extended particle filter (EPF), and by integrating static estimation into dynamic estimation, managed to improve overall dynamic state estimation (DSE). In [Wang *et al.*, 2020b], researchers proposed a robust mixed p-norm square root Kalman filter that functions properly in spite of non-Gaussian noise and outliers. In [Anagnostou and Pal, 2018], DSE of a power system performed in a decentralized derivative-free manner. The authors also consider an unknown input case for their proposed estimation methodology. Wang *et al.* [2020a] tested their novel method on the IEEE

68-bus system, and their results showed that their approach can effectively handle model errors of the power system caused by changing loads. In fact, the authors proposed a self-adaptive DSE method able to correct model errors and produce accurate estimates.

Based on the great work of Arasaratnam and Haykin [2009], Sharma *et al.* [2017] have developed a CKF filter to get through the problem of DSE in power system. However, their filter still required to have both an accurate model of the system and Gaussian noise. In contrast to such a conventional CKF estimator, in Li *et al.* [2019]'s work, a robust CKF filter has been presented that can work well even in the presence of noise with unknown statistics features like non-Gaussian measurement noise and/or outliers. For estimating the dynamic state of power systems against innovation outliers and observation outliers, Wang *et al.* [2019] proposed an adaptive robust cubature Kalman filter (RCKF), which included redundancy in observation data and an adaptive strategy for adjusting the state estimation error covariance matrix. In [Lee *et al.*, 2020], DSE with unknown inputs is implemented using both UKF and PF. It has been claimed that this method is appropriate to be deployed in estimating highly-nonlinear systems but since it is a three-stage algorithm with two different types of Kalman filters, its complexity and computational time might be problematic as the size of estimation problem is growing.

Despite the fact that UKFs and CKFs are generally known as sigma-point or derivative-free filters, and that they have been reported to have superior performance compared to EKFs, particularly when nonlinearities are severe, they still have some shortcomings that may affect their performance [Basetti *et al.*, 2022].

For instance, as stated in [Arasaratnam and Haykin, 2009; Sharma *et al.*, 2015], UKF performance is degraded due to growing the number of system states, which is likely to occur in systems like power systems. In contrast, CKF can offer some advantages over UKF in terms of accuracy, computational cost, and stability [Liu *et al.*, 2014] but because the CKF approach relies on square root and matrix inversion operations of the state covariance matrix, the positive definiteness of matrices could be disturbed during the operation of the CKF owing to some unpredictable variations in a system model or noise model, which would lead to instability and consequently inaccurate and erroneous results [Zhao *et al.*, 2015; Basetti *et al.*, 2022].

As a consequence, it cannot be recognized that one approach is better than another for one specific estimation problem, and because real-world systems are ex-

posed to a variety of changes, for example in their model or the model of noise, robust approaches may be more promising for use in real-world applications. Therefore, in Chapter 6, a robust solution will be provided to tackle the problem of system state estimation in the presence of some model mismatches.

3.2 Continuous Nonlinear System

In this section, the general state-space form including both the process and measurement equations for a continuous-time nonlinear system can be given as (3.1):

$$\begin{cases} \frac{d\mathbf{x}}{dt} = & \mathbf{f}(\mathbf{x}, \mathbf{u}, t) + \mathbf{w}_c, \\ \mathbf{z} = & \mathbf{h}(\mathbf{x}, t) + \mathbf{v}_c, \end{cases} \tag{3.1}$$

where, t indicates time, $\mathbf{z} = [z_{1,t}, \ldots, z_{q,t}]^T \in \mathbb{R}^q$ is the measurement vector and consists of the measured values of the available quantities. $\mathbf{w}_c \in \mathbb{R}^n$ and $\mathbf{v}_c \in \mathbb{R}^q$ are Gaussian white noises for the process and measurement equations respectively, and have properties like $\mathbb{E}\left[\mathbf{w}_c\mathbf{w}_c^T\right] = \mathbf{Q}$, $\mathbb{E}\left[\mathbf{v}_c\mathbf{v}_c^T\right] = \mathbf{R}$, and $\mathbb{E}\left[\mathbf{w}_c\mathbf{v}_c^T\right] = \mathbf{0}$; $\mathbf{x} = [x_{1,t}, \ldots, x_{n,t}]^T \in \mathbb{R}^n$ is the state vector, $\mathbf{u} = [u_{1,t}, \ldots, u_{m,t}]^T \in \mathbb{R}^m$ is the known input vector of the system. The scalars n, m and q are the number of states, the known inputs and the available quantities to be measured, respectively. $\mathbb{E}$ represents the expected value.

3.3 Discrete Form for Nonlinear System

A detailed explanation of two methods used to discretize the continuous model of a nonlinear system, namely Euler and Runge Kutta, is provided in this section.

3.3.1 Euler Method

Assuming a sample interval of Δt, using the Euler method, the discrete-time form of (3.1) is given by:

$$\frac{d\mathbf{x}}{dt} = \frac{\mathbf{x}_{k+1} - \mathbf{x}_k}{\Delta t} \qquad \Rightarrow \qquad \mathbf{x}_{k+1} = \mathbf{x}_k + \Delta t\, \mathbf{f}(\mathbf{x}_k, \mathbf{u}_k, k) + \mathbf{w}_k, \tag{3.2}$$

where, $k+1$ and k represent indeed $t = (k+1)\Delta t$ and $t = k\Delta t$, respectively. Assume that the value of Δt is small enough, and that, as explained in [Catlin, 1989], the discrete-time process noise $\mathbf{w}_{k-1}$ can be approximated by (3.3),

$$\mathbf{w}_{k-1} \approx \int_{(k-1)\Delta t}^{k\Delta t} \mathbf{w}_c(\tau) d\tau. \tag{3.3}$$

Considering (3.3) and the continuous covariance of the process noise, $\mathbf{Q}$, the discrete-time equivalent for this covariance can be given by:

$$\begin{aligned} \mathbf{Q}_{(k)}^d &\triangleq \mathbb{E}\left(\mathbf{w}_{k-1}\,\mathbf{w}_{k-1}^T\right) \\ &= \int_{(k-1)\Delta t}^{k\Delta t} \int_{(k-1)\Delta t}^{k\Delta t} \mathbb{E}\left[\mathbf{w}_c(\tau_1)\mathbf{w}_c^T(\tau_2)\right] d\tau_1 d\tau_2 \\ &= \int_{(k-1)\Delta t}^{k\Delta t} \int_{(k-1)\Delta t}^{k\Delta t} \mathbf{Q}\,\delta_\Delta(\tau_1 - \tau_2)\, d\tau_1 d\tau_2 = \mathbf{Q}\Delta t, \end{aligned} \tag{3.4}$$

where $\delta_\Delta()$ represents the Dirac delta function. Having obtained the state vector as its discrete form $\mathbf{x}_k$, the measurement equation can be simply written in a discretized form as follows:

$$\mathbf{z}_k = h(\mathbf{x}_k) + \mathbf{v}_k, \tag{3.5}$$

where $\mathbf{v}_k$ is the discrete-time output noise, and assuming its mean value is equal to zero, its covariance can be described by:

$$\mathbf{R}_{(k)}^d \triangleq \mathbb{E}\left(\mathbf{v}_k \mathbf{v}_k^T\right) = \mathbf{R}/\Delta t. \tag{3.6}$$

3.3.2 Fourth-Order Runge-Kutta Method

Assuming a sample interval of Δt is small enough, the discrete-time form of (3.1) is given by:

$$\begin{aligned} \int_{\mathbf{x}_{(k)}}^{\mathbf{x}_{(k+1)}} d\mathbf{x} &= \int_{k\Delta t}^{(k+1)\Delta t} \mathbf{f}(\mathbf{x}_{(\tau)}, \mathbf{u}_{(\tau)}, \tau)\, d\tau + \int_{k\Delta}^{(k+1)\Delta t} \mathbf{w}_c(\tau)\, d\tau, \\ \mathbf{x}_{(k+1)} &= \mathbf{x}_{(k)} + \int_{k\Delta t}^{(k+1)\Delta t} \mathbf{f}(\mathbf{x}_{(\tau)}, \mathbf{u}_{(\tau)}, \tau)\, d\tau + \int_{k\Delta t}^{(k+1)\Delta t} \mathbf{w}_c(\tau)\, d\tau, \end{aligned} \tag{3.7}$$

where k indicates the time at $k\Delta t$ and since $\mathbf{f}(\mathbf{x}_{(t)}, \mathbf{u}_{(t)}, t)$ is nonlinear and it is assumed that the inputs in this work do not change during sampling interval, the second term of (3.7) can be solved by numerical methods, e.g., 4th-order Runge-Kutta [Butcher, 2008] as (3.8):

$$\int_{k\Delta t}^{(k+1)\Delta t} \mathbf{f}(\mathbf{x}_{(\tau)}, \mathbf{u}_{(\tau)}, \tau)\, d\tau \approx \frac{\Delta t}{6}(\mathbf{k}_1 + 2\mathbf{k}_2 + 2\mathbf{k}_3 + \mathbf{k}_4), \tag{3.8}$$

where

$$\begin{aligned}
\mathbf{k}_1 &= \mathbf{f}(\mathbf{x}_{(k)}, \mathbf{u}_{(t)}, t = k\Delta t),\\
\mathbf{k}_2 &= \mathbf{f}(\mathbf{x}_{(k)} + 0.5\mathbf{k}_1, \mathbf{u}_{(t)}, t = (k+0.5), \Delta t)\\
\mathbf{k}_3 &= \mathbf{f}(\mathbf{x}_{(k)} + 0.5\mathbf{k}_2, \mathbf{u}_{(t)}, t = (k+0.5), \Delta t)\\
\mathbf{k}_4 &= \mathbf{f}(\mathbf{x}_{(k)} + \mathbf{k}_3, \mathbf{u}_{(t)}, t = (k+1)\Delta t).
\end{aligned}$$

Additionally, from (3.7) the discrete-time process noise $\mathbf{w}_{(k)}$ can be defined as follows:

$$\mathbf{w}_{(k)} = \int_{k\Delta t}^{(k+1)\Delta t} \mathbf{w}_c(\tau) d\tau. \tag{3.9}$$

Considering (3.9) and the continuous covariance of the process noise, $\mathbf{Q}$, the discrete-time equivalent for this covariance can be given by Simon [2006]:

$$\begin{aligned}
\mathbf{Q}^d &\triangleq \mathbb{E}\left(\mathbf{w}_{(k)}\, \mathbf{w}_{(k)}^T\right)\\
&= \int_{k\Delta t}^{(k+1)\Delta t} \int_{k\Delta t}^{(k+1)\Delta t} \mathbb{E}\left[\mathbf{w}_c(\tau_1)\mathbf{w}_c^T(\tau_2)\right] d\tau_1 d\tau_2\\
&= \int_{k\Delta t}^{(k+1)\Delta t} \int_{k\Delta t}^{(k+1)\Delta t} \mathbf{Q}\, \delta_\Delta(\tau_1 - \tau_2)\, d\tau_1 d\tau_2 = \mathbf{Q}\Delta t,
\end{aligned} \tag{3.10}$$

where $\delta_\Delta()$ represents the Dirac delta function. Using (3.8) and (3.9), equation (3.7) can be rewritten as:

$$\begin{aligned}
\mathbf{x}_{(k+1)} =& \mathbf{x}_{(k)} + \frac{\Delta t}{6}(\mathbf{k}_1 + 2\mathbf{k}_2 + 2\mathbf{k}_3 + \mathbf{k}_4) + \mathbf{w}_{(k)}\\
\equiv& \mathbf{g}(\mathbf{x}_{(k)}, \boldsymbol{\theta}_{(k)}) + \mathbf{w}_{(k)},
\end{aligned} \tag{3.11}$$

where

$$\begin{aligned}
\mathbf{g}(\mathbf{x}_{(k)}, \boldsymbol{\theta}_{(k)}) &= [g_1(\mathbf{x}_{(k)}, \boldsymbol{\theta}_{(k)}), \ldots, g_n(\mathbf{x}_{(k)}, \boldsymbol{\theta}_{(k)})]^T,\\
\boldsymbol{\theta}_{(k)} &= (\mathbf{u}_{(k)}, \mathbf{u}_{(k+0.5)}, \mathbf{u}_{(k+1)}).
\end{aligned} \tag{3.12}$$

In the current work, $\boldsymbol{\theta}_{(k)}$ is a tuple consisting of several parameters, but, as the inputs are assumed to be unchanged on each interval between the two consecutive samples k and $k+1$, $\boldsymbol{\theta}_{(k)}$ reduces to only one term, i.e., $\boldsymbol{\theta}_{(k)} = \mathbf{u}_{(k)}$. Therefore, for the sake of simplicity, since then, $\boldsymbol{\theta}_k$ will be replaced with $\mathbf{u}_{(k)}$. Having obtained the state vector as its discrete form $\mathbf{x}_{(k)}$, the measurement equation can be simply written in a discretized form as follows:

$$\mathbf{z}_{(k)} = \mathbf{h}(\mathbf{x}_{(k)}) + \mathbf{v}_{(k)}, \tag{3.13}$$

where $\mathbf{v}_{(k)}$ is the discrete-time output noise, and assuming its mean value is equal to zero, its covariance can be described by Simon [2006]:

$$\mathbf{R}^d_{(k)} \triangleq \mathbb{E}\left(\mathbf{v}_{(k)}\mathbf{v}^T_{(k)}\right) = \mathbf{R}/\Delta t. \tag{3.14}$$

3.4 Nonlinear Kalman Filter Based Approaches

In Section 3.1, it is stated that EKF, UKF and CKF are three well-known filters which have been widely utilized for implementing dynamic state estimation (DSE) in power systems, and for this reason, in this section the procedures that are taken for each of these three methods are given in more detail. In Chapter 6, these estimators are applied to an IEEE benchmark electrical network to analyze their performances with some model mismatches.

3.4.1 EKF

In Algorithm 3.1, the procedures for implementing the EKF approach are described.

3.4.2 UKF

In Algorithm 3.2, the procedures for implementing the UKF approach are described.

Algorithm 3.1 Implementation algorithm for EKF filter.

Input: an initial state vector $\mathbf{x}_0 \in \mathbb{R}^n$; a measurement series $\{\mathbf{z}_k\}_{k=1}^{T_{max}}$; and the maximum number of samples T_{max};

1. Initialize the filter at $k = 0$:

$$\hat{\mathbf{x}}_0 = \mathbb{E}\left[\mathbf{x}_0\right] \tag{3.15}$$

$$\hat{\mathbf{P}}_0 = \mathbb{E}\left[\left(\hat{\mathbf{x}}_0 - \mathbf{x}_0\right)\left(\hat{\mathbf{x}}_0 - \mathbf{x}_0\right)^T\right] \tag{3.16}$$

2. **for** $k = 0, \ldots, T_{max}$
   (a) Compute the Jacobian of $\mathbf{f}$:

$$\mathrm{A}_k \triangleq \left.\frac{\partial \mathbf{f}}{\partial \mathbf{x}}\right|_{\mathbf{x}=\hat{\mathbf{x}}_k} = \begin{bmatrix} \frac{\partial f_1(\hat{\mathbf{x}}_k,\, \mathbf{u}_k)}{\partial x_1} & \cdots & \frac{\partial f_1(\hat{\mathbf{x}}_k,\, \mathbf{u}_k)}{\partial x_n} \\ \vdots & \ddots & \vdots \\ \frac{\partial f_n(\hat{\mathbf{x}}_k,\, \mathbf{u}_k)}{\partial x_1} & \cdots & \frac{\partial f_n(\hat{\mathbf{x}}_k,\, \mathbf{u}_k)}{\partial x_n} \end{bmatrix}; \tag{3.17}$$

   (b) Prediction update step:

$$\hat{\mathbf{x}}_{k+1}^- = \mathbf{f}(\hat{\mathbf{x}}_k, \mathbf{u}_k), \tag{3.18}$$

$$\mathbf{P}_{k+1}^- = \mathbf{A}_k \mathbf{P}_k \mathbf{A}_k^\mathsf{T} + \mathbf{Q}^d; \tag{3.19}$$

   (c) Calculate the Jacobian of $\mathbf{h}$:

$$\mathbf{C}_k \triangleq \left.\frac{\partial \mathbf{h}}{\partial \mathbf{x}}\right|_{\mathbf{x}=\hat{\mathbf{x}}_{k+1}^-} = \begin{bmatrix} \frac{\partial h_1(\hat{\mathbf{x}}_{k+1}^-)}{\partial x_1} & \cdots & \frac{\partial h_1(\hat{\mathbf{x}}_{k+1}^-)}{\partial x_n} \\ \vdots & \ddots & \vdots \\ \frac{\partial h_n(\hat{\mathbf{x}}_{k+1}^-)}{\partial x_1} & \cdots & \frac{\partial h_n(\hat{\mathbf{x}}_{k+1}^-)}{\partial x_n} \end{bmatrix}; \tag{3.20}$$

   (d) Measurement update step:

$$\mathbf{K}_k = \mathbf{P}_{k+1}^- \mathbf{C}_k^\mathsf{T} (\mathbf{C}_k \mathbf{P}_{k+1}^- \mathbf{C}_k^\mathsf{T} + \mathbf{R}^d)^{-1} \tag{3.21}$$

$$\hat{\mathbf{x}}_{k+1} = \hat{\mathbf{x}}_{k+1}^- + \mathbf{K}_k \left(\mathbf{z}_k - \mathbf{h}(\hat{\mathbf{x}}_{k+1}^-)\right) \tag{3.22}$$

$$\mathbf{P}_{k+1} = (\mathbf{I} - \mathbf{K}_k\, \mathbf{C}_k)\mathbf{P}_{k+1}^- \tag{3.23}$$

   (e) Update $\hat{\mathbf{x}}_k$ and $\mathbf{P}_k$:

$$\hat{\mathbf{x}}_k \leftarrow \hat{\mathbf{x}}_{k+1};$$
$$\mathbf{P}_k \leftarrow \mathbf{P}_{k+1};$$

   (f) Store $\hat{\mathbf{x}}_k$, and $\mathbf{P}_k$.

3. **end for**

Output: State estimate series $\{\hat{\mathbf{x}}_k\}_{k=1}^{T_{max}}$;

3.4.3 CKF

In Algorithm 3.3, the procedures for implementing the CKF approach are described.

Algorithm 3.2 Implementation algorithm for UKF filter.

Input: An initial state vector $\mathbf{x}_0 \in \mathbb{R}^n$; a measurement series $\{\mathbf{z}_k\}_{k=1}^{T_{max}}$; and the maximum number of samples T_{max};

1: Initialize the filter at $k = 0$:

$$\hat{\mathbf{x}}_0 = \mathbb{E}\left[\mathbf{x}_0\right], \tag{3.24}$$

$$\hat{\mathbf{P}}_0 = \mathbb{E}\left[\left(\hat{\mathbf{x}}_0 - \mathbf{x}_0\right)\left(\hat{\mathbf{x}}_0 - \mathbf{x}_0\right)^T\right] \tag{3.25}$$

2: Calculate the scaling parameter λ:

$$\lambda = \alpha^2(n + \kappa) - n, \tag{3.26}$$

where n is the dimension of state vector $\mathbf{x}$, $0 \leq \alpha \leq 1$ is an appropriate choice for α, and a larger value for α will spread the sigma points farther away from the mean value. α is often set to a small positive real value (e.g., $1e^{-3}$). $\kappa = 3 - n$ is a good choice for κ and if n is greater than 3 then it is enough to set κ zero;

3: **for** $k = 0, \ldots, T_{max}$ **do**

4: Compute sigma points:

$$[\mathbf{X}]_1 = \hat{\mathbf{x}}_k, [\mathbf{X}]_{1+i} = \begin{cases} \hat{\mathbf{x}}_k + \left[\sqrt{(n+\lambda)\mathbf{P}_k}\right]_i, & \text{for } i = 1, \ldots, n, \\ \hat{\mathbf{x}}_k - \left[\sqrt{(n+\lambda)\mathbf{P}_k}\right]_{i-n}, & \text{for } i = (n+1), \ldots, 2n, \end{cases} \tag{3.27}$$

where the notation $[\mathbf{X}]_k$ denotes the k-th column of matrix $\mathbf{X}$;

5: Calculate weights corresponding to $[\mathbf{X}]_1$:

$$w_1^m = \frac{\lambda}{n + \lambda}, \tag{3.28}$$

$$w_1^c = \frac{\lambda}{n + \lambda} + 1 - \alpha^2 + \beta, \tag{3.29}$$

where $\beta = 2$ could be a good choice for Gaussian problems like the problem where it will be used in this thesis (Chapter 6);

6: Calculate weights corresponding to $[\mathbf{X}]_2$, ..., $[\mathbf{X}]_{2n+1}$:

$$w_i^m = w_i^c = \frac{1}{2n}, \quad \text{for } i = 2, \ldots, 2n + 1. \tag{3.30}$$

3.5 Conclusions

This chapter presented an overview of KF-based works corresponding to DSE in power systems. Also, the continuous and discrete form of a state space model for a nonlinear system was expressed. Three famous KF-based filters that have been widely used for nonlinear system state estimation were described explicitly, and their

7: Prediction update step:

1. Find the sigma points transformed by the nonlinear function $\mathbf{f}$:

$$\mathbf{Y} = \mathbf{f}(\mathbf{X}, \mathbf{u}_k); \tag{3.31}$$

2. Calculate $\hat{\mathbf{x}}_{k+1}^-$ and $\mathbf{P}_{k+1}^-$:

$$\hat{\mathbf{x}}_{k+1}^- = \sum_{i=1}^{2n+1} w_i^m \left[\mathbf{Y}\right]_i, \tag{3.32}$$

$$\mathbf{P}_{k+1}^- = \sum_{i=1}^{2n+1} w_i^c ([\mathbf{Y}]_i - \hat{\mathbf{x}}_{k+1}^-)([\mathbf{Y}]_i - \hat{\mathbf{x}}_{k+1}^-)^\mathsf{T} + \mathbf{Q}^d; \tag{3.33}$$

8: Measurement update step:

1. Find the projected sigma points through the nonlinear function $\mathbf{h}$ (measurement function):

$$\mathbf{Z} = \mathbf{h}(\mathbf{Y}); \tag{3.34}$$

2. Calculate $\boldsymbol{\mu}_z$ and $\mathbf{P}_z$:

$$\boldsymbol{\mu}_z = \sum_{i=1}^{2n+1} w_i^m \left[\mathbf{Z}\right]_i, \tag{3.35}$$

$$\mathbf{P}_z = \sum_{i=1}^{2n+1} w_i^c ([\mathbf{Z}]_i - \boldsymbol{\mu}_z)([\mathbf{Z}]_i - \boldsymbol{\mu}_z)^\mathsf{T} + \mathbf{R}^d; \tag{3.36}$$

3. Calculate $\mathbf{K}_k$, $\hat{\mathbf{x}}_{k+1}$, and $\mathbf{P}_{k+1}$:

$$\mathbf{K}_k = \left[\sum_{i=1}^{2n+1} w_i^c ([\mathbf{Y}]_i - \hat{\mathbf{x}}_{k+1}^-)([\mathbf{Z}]_i - \boldsymbol{\mu}_z)^\mathsf{T}\right] \mathbf{P}_z^{-1}, \tag{3.37}$$

$$\hat{\mathbf{x}}_{k+1} = \hat{\mathbf{x}}_{k+1}^- + \mathbf{K}_k \left(\mathbf{z}_k - \boldsymbol{\mu}_z\right), \tag{3.38}$$

$$\mathbf{P}_{k+1} = \mathbf{P}_{k+1}^- - \mathbf{K}_k \mathbf{P}_z \mathbf{K}_k^\mathsf{T}; \tag{3.39}$$

9: Update $\hat{\mathbf{x}}_k$ and $\mathbf{P}_k$:

$$\hat{\mathbf{x}}_k \leftarrow \hat{\mathbf{x}}_{k+1},$$
$$\mathbf{P}_k \leftarrow \mathbf{P}_{k+1};$$

10: Store $\hat{\mathbf{x}}_k$, and $\mathbf{P}_k$.

11: **end for**

Output: State estimate series $\{\hat{\mathbf{x}}_k\}_{k=1}^{T_{max}}$;

Algorithm 3.3 Implementation algorithm for CKF filter.

Input: An initial state vector $\mathbf{x}_0 \in \mathbb{R}^n$; a measurement series $\{\mathbf{z}_k\}_{k=1}^{T_{max}}$; and the maximum number of samples T_{max};

1: Initialize the filter at $k = 0$:

$$\hat{\mathbf{x}}_0 = \mathbb{E}\left[\mathbf{x}_0\right], \tag{3.40}$$

$$\hat{\mathbf{P}}_0 = \mathbb{E}\left[\left(\hat{\mathbf{x}}_0 - \mathbf{x}_0\right)\left(\hat{\mathbf{x}}_0 - \mathbf{x}_0\right)^T\right]; \tag{3.41}$$

2: **for** $k = 0, \ldots, T_{max}$ **do**

3: Compute sigma points:

$$[\mathbf{X}]_i = \begin{cases} \sqrt{(n)}\,[\mathbf{I}_n]_i\,, & \text{for } i = 1, \ldots, n, \\ -\sqrt{(n)}\,[\mathbf{I}_n]_{i-n}\,, & \text{for } i = (n+1), \ldots, 2n, \end{cases} \tag{3.42}$$

where n is the dimension of state vector $\mathbf{x}$, and the notation $[\mathbf{X}]_k$ denotes the k-th column of matrix $\mathbf{X}$;.

4: Calculate weights corresponding to $[\mathbf{X}]_1$, …, $[\mathbf{X}]_{2n}$:

$$w_i^m = w_i^c = \frac{1}{2n}, \quad \text{for } i = 1, \ldots, 2n; \tag{3.43}$$

5: Prediction update step:

1. Find the sigma points transformed by the nonlinear function $\mathbf{f}$ of the state transition equation:

$$\mathbf{Y} = \mathbf{f}(\mathbf{X}, \mathbf{u}_k); \tag{3.44}$$

2. Calculate $\hat{\mathbf{x}}_{k+1}^-$ and $\mathbf{P}_{k+1}^-$:

$$\hat{\mathbf{x}}_{k+1}^- = \sum_{i=1}^{2n+1} w_i^m\,[\mathbf{Y}]_i\,, \tag{3.45}$$

$$\mathbf{P}_{k+1}^- = \sum_{i=1}^{2n+1} w_i^c([\mathbf{Y}]_i - \hat{\mathbf{x}}_{k+1}^-)([\mathbf{Y}]_i - \hat{\mathbf{x}}_{k+1}^-)^{\mathsf{T}} + \mathbf{Q}^d; \tag{3.46}$$

benefits and shortcomings were briefly discussed. It is concluded that one promising trend for future research in the context of DSE is to develop robust methods that are resistant to more model mismatches. This will be discussed and addressed in Chapter 6.

6: Measurement update step:

1. Find the projected sigma points through the nonlinear measurement function $\mathbf{h}$:

$$\mathbf{Z} = \mathbf{h}(\mathbf{Y}); \tag{3.47}$$

2. Calculate $\boldsymbol{\mu}_z$ and $\mathbf{P}_z$:

$$\boldsymbol{\mu}_z = \sum_{i=1}^{2n+1} w_i^m \left[\mathbf{Z}\right]_i, \tag{3.48}$$

$$\mathbf{P}_z = \sum_{i=1}^{2n+1} w_i^c ([\mathbf{Z}]_i - \boldsymbol{\mu}_z)([\mathbf{Z}]_i - \boldsymbol{\mu}_z)^\mathsf{T} + \mathbf{R}^d; \tag{3.49}$$

3. Calculate $\mathbf{K}_k$, $\hat{\mathbf{x}}_{k+1}$ and $\mathbf{P}_{k+1}$:

$$\mathbf{K}_k = \left[\sum_{i=1}^{2n+1} w_i^c ([\mathbf{Y}]_i - \hat{\mathbf{x}}_{k+1}^-)([\mathbf{Z}]_i - \boldsymbol{\mu}_z)^\mathsf{T}\right] \mathbf{P}_z^{-1}, \tag{3.50}$$

$$\hat{\mathbf{x}}_{k+1} = \hat{\mathbf{x}}_{k+1}^- + \mathbf{K}_k \left(\mathbf{z}_k - \boldsymbol{\mu}_z\right), \tag{3.51}$$

$$\mathbf{P}_{k+1} = \mathbf{P}_{k+1}^- - \mathbf{K}_k \mathbf{P}_z \mathbf{K}_k^\mathsf{T}; \tag{3.52}$$

7: Update $\hat{\mathbf{x}}_k$ and $\mathbf{P}_k$:

$$\hat{\mathbf{x}}_k \leftarrow \hat{\mathbf{x}}_{k+1},$$
$$\mathbf{P}_k \leftarrow \mathbf{P}_{k+1};$$

8: Store $\hat{\mathbf{x}}_k$, and $\mathbf{P}_k$.

9: **end for**

Output: State estimate series $\{\hat{\mathbf{x}}_k\}_{k=1}^{T_{max}}$;

Chapter 4

Distributed Simultaneous Estimation of States and Unknown Inputs

Contents

4.1 Introduction

State estimation is a fundamental problem in industrial systems. Kalman filter (KF) is an effective method and has been widely used for the state estimation of linear systems since its introduction. In KF-based estimation usually it is assumed that the model of system and measurement are known, which is not always a valid assumption. In fact and in practice, uncertainties in the system model and systematic measurement errors are inevitable. In particular, it might be even necessary to estimate the states of a system using only a subset of states and/or unknown inputs in the system. Exemplar applications of such cases are: fault detection and diagnosis [Patton *et al.*, 1989], missile-target interception [Pan *et al.*, 2010], synchronous generator state estimation [Ghahremani and Kamwa, 2016], and autonomous vehicle navigation [Yong *et al.*, 2016]. Therefore, a question can be posed: how to optimally obtain an estimation of states and unknown inputs of a system? And with the increasingly application of large-scale and multi-agent systems, another question that may arise is how to configure such an estimation system to function more effectively. In this regard, this Chapter will address a simultaneous estimation of system's states and unknown inputs in a distributed manner.

Estimating systems can be categorized into central or distributed configurations. In the central configuration, it is assumed that measurements are made and transmitted to the processing center with no errors. Such assumptions are not likely to hold in practice. For example, if the normal functioning of central processing gets disrupted, the estimation system is not able to perform its function until the fault is cleared. On the other hand, distributed systems are more robust against accidental faults that enable them to perform reliably despite missing several measurements [Cattivelli and Sayed, 2011].

A summary of some of the most relevant distributed state estimation approaches is provided in Table 4.1. A key concept in distributed computations is the Consensus theory. The consensus rule makes the estimators reach to the same state estimation, although utilizing only the local measurements and information exchange with the neighborhood agents [Olfati-Saber, 2007b]. In [Olfati-Saber, 2005], an algorithm based on Kalman Filter was introduced for distributed consensus filter, called the Information Kalman Filter (IKF). It has the limitation that the process must be observable by the sensors and the observation matrices have to be identical. Then

Table 4.1: Some of the recent state estimation methods in the distributed configuration.

Reference	Estimated Variables	Approach/ Feature	Limitation
[Olfati-Saber, 2005]	NA	Information Kalman Filter (IKF)	The process must be observable by all sensors
[Riverso *et al.*, 2013]	States	Plug and Play (PnP)	Limited to distributed systems
[Lu, 2013]	States/unknown inputs	Consensus gains of local filters	No proof of the filter formula
[Millan *et al.*, 2017]	Obs./unobservable states	Local decomposition of states	Limited to state estimation
[Liu *et al.*, 2018]	States/unknown inputs	Cooperative distributed filters	NA

Olfati-Saber [2007a] further improved the algorithm for sensor networks application with different observation matrices. In [Riverso *et al.*, 2013] the Plug and Play (PnP) capability was introduced which makes the addition and removal of subsystems in a large-scale distributed system more efficient. In [Millan *et al.*, 2017] approach, a method to decompose the observable and unobservable states at every local estimation point was proposed which allows the designer to adjust independently the dynamics of the local observable states and unobservable states. In [Lu, 2013] an approach for consensus gain computation of local filters is proposed. However the paper did not discuss about the proof and features of the proposed filter (like unbiasedness or stability). Liu *et al.* [2018] utilized cooperative distributed filters to solve the simultaneous estimation of states and unknown inputs. In comparison with [Lu, 2013] which applied the estimation solution for a networked system, [Liu *et al.*, 2018], incorporating the results in [Gillijns and Moor, 2007a], adapted the estimation solution for a multi-agent system.

This chapter addresses the problem of simultaneous state estimation and unknown inputs estimation for linear systems with Gaussian noise. The special conditions under which some fundamental features of the proposed filter, such as unbiasedness, minimum variance, stability, and convergence, can be achieved will be discussed in more detail, and using a numerical example, the performance of the designed estimator will be assessed. This chapter indeed discusses the results of a study published in [Emami *et al.*, 2020]. This Chapter is organized as follows. Section 4.2 reviews some useful notations and definitions. Problem formulation is presented in Section 4.3. Sections 4.4, 4.5, and 4.6 describe the proposed methodology. The results from an illustrative example are detailed and analyzed in Section 4.7. Section 4.8 contains concluding remarks.

4.2 Preliminary Definitions

In this section some useful notations and definitions which are used throughout this section are reviewed. Considering a random vector, $\mathbf{v}$, $\mathbb{E}[\mathbf{v}]$ is the expectation value of $\mathbf{v}$. Also, assuming that $\mathbf{M} \in \mathbb{R}^{q\times q}$, its Moore-Penrose inverse is defined as follows:

$$\mathbf{M}^{\dagger} = \left(\mathbf{M}^{T}\,\mathbf{M}\right)^{-1}\,\mathbf{M}^{T}. \tag{4.1}$$

A. Estimation Theory: In estimation theory $\hat{\theta}$ is defined as an estimation of variable θ, and $\hat{\theta}$ is Minimum-variance unbiased (MVU), if $\mathbb{E}[\hat{\theta}] = \theta$ and the variance of $\hat{\theta}$ is not higher than any other unbiased estimates.

B. Graph Theory: In this chapter the main objective is to design a distributed estimator whose stability and convergence must be guaranteed. Imagine having a network of sensors or agents, where each sensor or agent only has access to local measurements of the system, but needs to estimate the overall state vector of the system. Under this condition, a distributed estimator is a computational algorithm that allows sensors or agents to exchange information with each other and perform calculations based on their local measurements, in order to collectively estimate the overall state vector of the system. The design of a distributed estimator involves enabling its agents to share information and collaborate effectively, while minimizing communication and computational overhead. A powerful tool for modeling the interactions between these agents is the Laplacian matrix in graph theory. In order to obtain the Laplacian matrix, it is needed to represent the network of agents in the form of a graph. The nodes of the graph represent agents, while the links of the graph indicate whether between any two nodes a communicational link exists or not. Taking into account these points, the communication graph among $N = |a|$ agents is defined by $W(a, E_w, \mathbf{B})$ where a represents the set of estimators, E_w comprises the set of links existing among the agents of the network, and $\mathbf{B}$ is the corresponding adjacency matrix of graph W. If $e_{ij} \in E_w$, then $e_{ji} \in E_w$, and the corresponding array of elements in the adjacent matrix $\mathbf{B}$ are equal to $b_{ij} = b_{ji} = 1$; Otherwise they are zero, meaning that there is no link between agents i and j. The data flow between two linked agents is assumed to be bi-directional, making $\mathbf{B}$ a symmetrical matrix with nonnegative-elements. If $b_{ij} = 1$ then agents i and j are neighbors, and N_i represents the set of agents which are the neighbors of agent i. The graph

W is connected if between any two distinct nodes (agents), there is at least one path. The degree matrix $\mathbf{D}$ is defined as a diagonal matrix showing the number of links connected to each node, and the Laplacian matrix is defined as $\mathbf{L} = \mathbf{D} - \mathbf{B}$ and $\mathbf{L} \in \mathbb{R}^{|a|\times|a|}$. If it is assumed that the graph of the communication network of agents is connected and undirected, which is always respected throughout this Chapter, the Laplacian matrix $\mathbf{L}$ for this graph would become positive semidefinite [Godsil and Royle, 2001]. Prior to expressing the corresponding equations when the system state is a vector, first, for the sake of understanding, it is assumed that each agent i ($i \in \{1, ..., |a|\}$) would estimate the system state, which is assumed to be a scalar. Thus, $\hat{x}^i \in \mathbb{R}$, which represents the state estimated by agent i ($i \in \{1, ..., |a|\}$), and by having a positive semidefinite Laplacian matrix $\mathbf{L}$ due to having a connected undirected graph, the following quadratic property holds for all the agents inside the network, and more specifically their corresponding estimated state values represented by $\hat{x}^i$ ($i \in \{1, ..., |a|\}$) [Sun, 2015; Olfati-Saber, 2007a; Godsil and Royle, 2001]

$$\begin{aligned}\sum_{i=1}^{|a|}\sum_{j\in N_i}\hat{x}^i(\hat{x}^j-\hat{x}^i) &= -\frac{1}{2}\sum_{(i,j)\in E_w}\|\hat{x}^j-\hat{x}^i\|^2 \\ &= -\hat{\mathbf{x}}^T\,\mathbf{L}\,\hat{\mathbf{x}},\end{aligned} \tag{4.2}$$

where $|a|$ is the cardinality of the set a and $\hat{\mathbf{x}} \in \mathbb{R}^{|a|}$ is defined as $\hat{\mathbf{x}} = \left[\hat{x}^1, ..., \hat{x}^{|a|}\right]^T$. Equation (4.2) is valid when the system state is scalar. However, in practice, the system state that is due to be estimated is a vector with more than one element (i.e. $\hat{\mathbf{x}}^i = [x_1^i, \ldots, x_n^i]^T \in \mathbb{R}^n$), where $n > 1$ is an integer number representing the total number of system states. Therefore, it is essential to extend (4.2) in order to include the more general form of vector state with $n \geq 2$. Thus, the matrix $\hat{\mathbf{X}}$ is defined to aggregate the state vector of the existing estimators as (4.3):

$$\hat{\mathbf{X}} = [\hat{\mathbf{x}}^1, \ldots, \hat{\mathbf{x}}^i, \ldots, \hat{\mathbf{x}}^{|a|}]. \tag{4.3}$$

If the state to be estimated is a vector rather than a scalar, then a more general

form of (4.2) can be defined as (4.4):

$$\begin{aligned}\sum_{l=1}^{n}\sum_{i=1}^{|a|}\sum_{j\in N_i}\hat{x}_l^i(\hat{x}_l^j-\hat{x}_l^i) &= -\frac{1}{2}\sum_{l=1}^{n}\sum_{i=1}^{|a|}\sum_{j\in N_i}\|\hat{x}_l^j-\hat{x}_l^i\|^2\\ &= -\frac{1}{2}\sum_{i=1}^{|a|}\sum_{j\in N_i}(\hat{\mathbf{x}}^j-\hat{\mathbf{x}}^i)^T(\hat{\mathbf{x}}^j-\hat{\mathbf{x}}^i)\\ &= \sum_{i=1}^{|a|}\sum_{j\in N_i}(\hat{\mathbf{x}}^i)^T(\hat{\mathbf{x}}^j-\hat{\mathbf{x}}^i)\\ &= -\sum_{l=1}^{n}\boldsymbol{\delta}^l\,\hat{\mathbf{X}}\,\mathbf{L}\,\left(\boldsymbol{\delta}^l\,\hat{\mathbf{X}}\right)^T,\end{aligned} \tag{4.4}$$

where $\boldsymbol{\delta}^l \in \mathbb{R}^{1\times n}$, and its entries are defined as (4.5):

$$\begin{aligned}\boldsymbol{\delta}^l &= [\delta_1^l \cdots \delta_n^l],\\ \delta_j^l &= \begin{cases}1 & \text{if } j = l,\\ 0 & \text{if } j \neq l.\end{cases}\end{aligned} \tag{4.5}$$

Equation (4.4) is used in Section 4.6.4 to verify the stability proof of the proposed estimator. During this Chapter, since the function of each agent is to estimate the vector state of the system, instead of using the word "agent", the word "estimator" is sometimes used, and both terms are equivalent and can therefore be used interchangeably.

4.3 Problem Description

The studied system is defined by the linear discrete-time state equation (4.6), and the available output measurement at estimator $i \in a$ is given by (4.7)

$$\mathbf{x}_{(k+1)} = \mathbf{A}_{(k)}\,\mathbf{x}_{(k)} + \mathbf{G}_{(k)}\,\mathbf{d}_{(k)} + \boldsymbol{\omega}_{(k)}, \tag{4.6}$$

$$\mathbf{y}_{(k)}^i = \mathbf{C}_{(k)}^i\,\mathbf{x}_{(k)} + \mathbf{v}_{(k)}^i, \tag{4.7}$$

where $\mathbf{x}_{(k)} \in \mathbb{R}^n$ is the state vector, $\mathbf{d}_{(k)} \in \mathbb{R}^m$ is an unknown input vector, $\mathbf{y}_{(k)}^i \in \mathbb{R}^q$ is the measurement vector at the i-th estimator. $\mathbf{A}_{(k)}$, $\mathbf{G}_{(k)}$, and $\mathbf{C}_{(k)}^i$ are deterministic known matrices with appropriate dimensions. The process noise $\boldsymbol{\omega}_{(k)} \in \mathbb{R}^n$,

and the measurement noise $\mathbf{v}^i_{(k)} \in \mathbb{R}^q$ are considered mutually uncorrelated, zero-mean, white noises with known covariance matrices, $\mathbf{Q}_{(k)} = \mathbb{E}[\boldsymbol{\omega}_{(k)}\, \boldsymbol{\omega}^T_{(k)}] \geq 0$, and $\mathbf{R}^i_{(k)} = \mathbb{E}[\mathbf{v}^i_{(k)}\, (\mathbf{v}^i_{(k)})^T] > 0$, respectively. Throughout this Chapter the notation of time 'k' may be dropped for the sake of simplicity.

The aim is to estimate the states and unknown inputs of the system from the available series of outputs up to time K, $\{\mathbf{y}^i_{(k)}\}^K_{k=1}, \forall i \in a$ in a distributed manner. No specific conditions were considered for the unknown input $\mathbf{d}_{(k)}$.

4.4 Estimation Development

In this section the recursive filter equations are defined for the distributed estimation of a system's states and unknown inputs as follows:

$$\hat{\mathbf{x}}^{i-}_{(k)} = \mathbf{A}_{(k-1)}\, \hat{\mathbf{x}}^i_{(k-1)}, \tag{4.8}$$

$$\hat{\mathbf{d}}^i_{(k-1)} = -\mathbf{M}^i_{d(k)} \left(\mathbf{C}^i_{(k)} \hat{\mathbf{x}}^{i-}_{(k)} - \mathbf{y}^i_{(k)}\right), \tag{4.9}$$

$$\hat{\mathbf{x}}^{i*}_{(k)} = \hat{\mathbf{x}}^{i-}_{(k)} + \mathbf{G}_{(k-1)}\, \hat{\mathbf{d}}^i_{(k-1)}, \tag{4.10}$$

$$\begin{aligned} \hat{\mathbf{x}}^i_{(k)} = {} & \hat{\mathbf{x}}^{i*}_{(k)} - \mathbf{M}^i_{x(k)} \left(\mathbf{C}^i_{(k)} \hat{\mathbf{x}}^{i*}_{(k)} - \mathbf{y}^i_{(k)}\right) \\ & + \mathbf{N}^i_{x(k)} \sum_{j \in N_i} \left(\hat{\mathbf{x}}^{j-}_{(k)} - \hat{\mathbf{x}}^{i-}_{(k)}\right), \end{aligned} \tag{4.11}$$

where gain matrices $\mathbf{M}^i_{d(k)} \in \mathbb{R}^{m \times q}$, $\mathbf{M}^i_{x(k)} \in \mathbb{R}^{n \times q}$, and $\mathbf{N}^i_{x(k)} \in \mathbb{R}^{n \times n}$ are still to be determined. The required conditions for calculating $\mathbf{M}^i_{d(k)}$ are given in Section 4.5. $\mathbf{N}^i_{x(k)}$ is a consensus gain and a poor choice of it may lead to either the lack of stability of error dynamics in the distributed estimator (4.11) or absence of consensus among the local estimators. Therefore, it should be carefully considered in the design of the estimator. The calculation of gains $\mathbf{M}^i_{x(k)}$ and $\mathbf{N}^i_{x(k)}$ are given in Section 4.6. The variables $\hat{\mathbf{x}}^i_{(k)}$ and $\hat{\mathbf{d}}^i_{(k)}$ are the estimations of $\mathbf{x}_{(k)}$ and $\hat{\mathbf{d}}^i_{(k)}$ obtained by the i-th estimator, respectively.

4.5 Unknown Input Estimation

In this section the calculation of $\hat{\mathbf{d}}^i_{(k)}$ are investigated in more detail. It is inspired by the method discussed in [Gillijns and Moor, 2007a]. First, in Section 4.5.1 the

condition which is required for the gain matrix $\mathbf{M}^i_{d(k)}$ to make $\hat{\mathbf{d}}^{\,i}_{(k)}$ unbiased, i.e. $\mathbb{E}\left[\hat{\mathbf{d}}^{\,i}_{(k)}\right] = \mathbf{d}_{(k)}$, is demonstrated.

Assumption 1. $\text{rank}\left(\mathbf{C}^i_{(k)}\mathbf{G}_{(k-1)}\right) = \text{rank}\left(\mathbf{G}_{(k-1)}\right) = m$, for all k [Gillijns and Moor, 2007a; Ding and Fang, 2017].

From Assumption 1, it can be deduced that $n \geq m$ and $q \geq m$.

4.5.1 Unbiased Unknown Input Estimation

First, the innovation $\tilde{\mathbf{y}}^i(k)$ is defined as [Gillijns and Moor, 2007a]:

$$\tilde{\mathbf{y}}^i_{(k)} \triangleq \mathbf{C}^i_{(k)}\hat{\mathbf{x}}^{i-}_{(k)} - \mathbf{y}^i_{(k)}. \tag{4.12}$$

From (4.6), (4.7), and (4.8),

$$\begin{aligned}
\tilde{\mathbf{y}}^i_{(k)} &= \mathbf{C}^i_{(k)}\mathbf{A}_{(k-1)}\,\hat{\mathbf{x}}^i_{(k-1|k-1)} - \mathbf{C}^i_{(k)}\,\left(\mathbf{A}_{(k-1)}\,\mathbf{x}_{(k-1)} + \mathbf{G}_{(k-1)}\,\mathbf{d}_{(k-1)} + \boldsymbol{\omega}_{(k-1)}\right) - \mathbf{v}^i_{(k)} \\
&= \mathbf{C}^i_{(k)}\mathbf{A}_{(k-1)}\,\tilde{\mathbf{x}}^i_{(k-1)} - \mathbf{C}^i_{(k)}\,\mathbf{G}_{(k-1)}\,\mathbf{d}_{(k-1)} - \mathbf{C}^i_{(k)}\,\boldsymbol{\omega}_{(k-1)} - \mathbf{v}^i_{(k)} \\
&= -\mathbf{C}^i_{(k)}\mathbf{G}_{(k-1)}\mathbf{d}_{(k-1)} + \mathbf{e}^i_{(k)},
\end{aligned} \tag{4.13}$$

where

$$\mathbf{e}^i_{(k)} = \mathbf{C}^i_{(k)}\left(\mathbf{A}_{(k-1)}\tilde{\mathbf{x}}^i_{(k-1)} - \boldsymbol{\omega}_{(k-1)}\right) - \mathbf{v}^i_{(k)}, \tag{4.14}$$

and $\tilde{\mathbf{x}}^i_{(k)} \triangleq \hat{\mathbf{x}}^i_{(k)} - \mathbf{x}_{(k)}$. Assuming that $\hat{\mathbf{x}}^i_{(k-1)}$ is unbiased, then it follows from (4.14) that $\mathbb{E}\left[\mathbf{e}^i_{(k)}\right] = \mathbf{0}$. Therefore, from (4.13)

$$\mathbb{E}\left[\tilde{\mathbf{y}}^i_{(k)}\right] = -\mathbf{C}^i_{(k)}\mathbf{G}_{(k-1)}\mathbf{d}_{(k-1)}. \tag{4.15}$$

Substituting (4.13) into (4.9), $\hat{\mathbf{d}}^{\,i}_{(k-1)}$ is written as

$$\hat{\mathbf{d}}^{\,i}_{(k-1)} = \mathbf{M}^i_{d(k)}\mathbf{C}^i_{(k)}\mathbf{G}_{(k-1)}\mathbf{d}_{(k-1)} - \mathbf{M}^i_{d(k)}\mathbf{e}^i_{(k)}. \tag{4.16}$$

Now assume that

$$\mathbf{M}^i_{d(k)}\mathbf{C}^i_{(k)}\mathbf{G}_{(k-1)} = \mathbf{I}_m. \tag{4.17}$$

From (4.17) and (4.16) it is seen that $\hat{\mathbf{d}}^{\,i}_{(k-1)}$ is unbiased.

Estimators of $\mathbf{d}_{(k)}$ can be implemented using Least-squares (LS) solutions of equation (4.13) for every agent (estimator). However, because $\mathbf{e}^i_{(k)}$ does not have unit variance, and thus (4.13) does not meet the assumptions of the Guass-Markov theorem [Kailath *et al.*, 2000], then such estimators of $\mathbf{d}_{(k)}$ are still not MVU. To achieve MVU estimators of $\mathbf{d}_{(k)}$, a weighted LS (WLS) estimation method with weighting matrix $\left(\mathbb{E}[\mathbf{e}^i_{(k)}\,\mathbf{e}^i_{(k)}{}^T]\right)^{-1}$ is utilized in Section 4.5.2.

4.5.2 Minimum-Variance Unbiased Input Estimation

As mentioned in Section 4.5.1, if $\mathbf{M}^i_{d(k)}$ satisfies condition (4.17), then the estimators of $\mathbf{d}_{(k)}$ obtained by LS solutions of (4.13) for every agent are unbiased. The variance of $\mathbf{e}^i_{(k)}$ defined as

$$\tilde{\mathbf{R}}^{\,i}_{(k)} = \mathbb{E}\left[\mathbf{e}^i_{(k)}(\mathbf{e}^i_{(k)})^T\right] = \mathbf{C}^i_{(k)}\left[\mathbf{A}_{(k)}\mathbf{P}^i_{(k-1)}\mathbf{A}^T_{(k)} + \mathbf{Q}_{(k-1)}\right]\left(\mathbf{C}^i_{(k)}\right)^T + \mathbf{R}^i_{(k)}, \tag{4.18}$$

where $\mathbf{P}^i_{(k)} \triangleq \mathbb{E}\left[\tilde{\mathbf{x}}^i_{(k)}\,\left(\tilde{\mathbf{x}}^i_{(k)}\right)^T\right]$.

Defining $\mathbf{P}^{i-}_{(k)} \triangleq \mathbb{E}[\tilde{\mathbf{x}}^{i-}_{(k)}(\tilde{\mathbf{x}}^{i-}_{(k)})^T]$, then

$$\mathbf{P}^{i-}_{(k)} = \mathbf{A}_{(k-1)}\mathbf{P}^i_{(k-1)}\mathbf{A}^T_{(k-1)} + \mathbf{Q}_{(k-1)}, \tag{4.19}$$

$$\tilde{\mathbf{R}}^{\,i}_{(k)} = \mathbf{C}^i_{(k)}\mathbf{P}^{i-}_{(k)}\left(\mathbf{C}^i_{(k)}\right)^T + \mathbf{R}^i_{(k)}. \tag{4.20}$$

An MVU unknown input estimate is then attained as described in Theorem 4.5.1.

Theorem 4.5.1. *Consider that Assumption 1, the unbiasedness of $\hat{\mathbf{x}}_{(k-1)}$, and the positive definiteness of $\tilde{\mathbf{R}}^{\,i}_{(k)}$ are satisfied, then $\mathbf{M}^i_{d(k)}$ is as*

$$\mathbf{M}^i_{d(k)} = -((\mathbf{F}^i_{(k)})^T(\tilde{\mathbf{R}}^{\,i}_{(k)})^{-1}\mathbf{F}^i_{(k)})^{-1}(\mathbf{F}^i_{(k)})^T(\tilde{\mathbf{R}}^{\,i}_{(k)})^{-1}, \tag{4.21}$$

where $\mathbf{F}^i_{(k)} = \mathbf{C}^i_{(k)}\mathbf{G}_{(k-1)}$. Then, (4.9) gives the MVU estimates of $\mathbf{d}_{(k-1)}$, and the variance of the corresponding unknown input estimate $\hat{\mathbf{d}}^{\,i}_{(k-1)}$ is obtained by $((\mathbf{F}^i_{(k)})^T(\tilde{\mathbf{R}}^{\,i}_{(k)})^{-1}\mathbf{F}^i_{(k)})^{-1}$.

Proof. If the positive definiteness of $\tilde{\mathbf{R}}^{\,i}_{(k)}$ is satisfied, then an invertible matrix

$\tilde{\mathbf{Z}}^i_{(k)} \in \mathbb{R}^{q\times q}$ exists satisfying $\tilde{\mathbf{Z}}^i_{(k)}(\tilde{\mathbf{Z}}^i_{(k)})^T = \tilde{\mathbf{R}}^i_{(k)}$. As one solution this matrix can be the Cholesky factorization of $\tilde{\mathbf{R}}^i_{(k)}$. Therefore, from (4.13)

$$(\tilde{\mathbf{Z}}^i_{(k)})^{-1}\tilde{\mathbf{y}}^i_{(k)} = -(\tilde{\mathbf{Z}}^i_{(k)})^{-1}\mathbf{C}^i_{(k)}\mathbf{G}_{(k-1)}\mathbf{d}_{(k-1)} + (\tilde{\mathbf{Z}}^i_{(k)})^{-1}\mathbf{e}^i_{(k)}. \tag{4.22}$$

Since $\tilde{\mathbf{Z}}^i_{(k)}$ is invertible, then from Assumption 1, $(\tilde{\mathbf{Z}}^i_{(k)})^{-1}\mathbf{C}^i_{(k)}\mathbf{G}_{(k-1)}$ has full column rank, and therefore the LS solution of (4.22) is obtained by

$$\hat{\mathbf{d}}^i_{(k-1)} = ((\mathbf{F}^i_{(k)})^T(\tilde{\mathbf{R}}^i_{(k)})^{-1}\mathbf{F}^i_{(k)})^{-1}(\mathbf{F}^i_{(k)})^T(\tilde{\mathbf{R}}^i_{(k)})^{-1}\tilde{\mathbf{y}}^i_{(k)}, \tag{4.23}$$

where $\mathbf{F}^i_{(k)} = \mathbf{C}^i_{(k)}\mathbf{G}_{(k-1)}$, and $(\tilde{\mathbf{Z}}^i_{(k)})^{-1}\mathbf{e}^i_{(k)}$ has unit variance. Therefore, equation (4.22) meets the assumption of the Gauss-Markov theorem and thus, it is concluded that the estimate of $\mathbf{d}_{(k-1)}$ is MVU [Kailath *et al.*, 2000]. The proof is complete. □

4.6 State Estimation

Taking into consideration the models of the system and the corresponding measurements (4.6) and (4.7), and the recursive distributed filter defined by equations (4.8)-(4.11); Then the goal is to obtain the conditions on the gains $\mathbf{M}^i_{x(k)}$ and $\mathbf{N}^i_{x(k)}$ required for the estimator $\hat{\mathbf{x}}^i_{(k)}$ (4.8)-(4.11) of $\mathbf{x}_{(k)}$ to be unbiased and with minimum variance.

4.6.1 Unbiased State Estimation

The conditions for unbiasedness of the state estimator introduced by (4.8)-(4.11) is investigated in Theorem 4.6.1.

Theorem 4.6.1. *Assuming that* $\hat{\mathbf{x}}^i_{(k-1)}$ *and* $\hat{\mathbf{d}}^i_{(k-1)}$ *are unbiased estimators of* $\mathbf{x}_{(k-1)}$ *and* $\mathbf{d}_{(k-1)}$*, respectively, i.e.* $\mathbb{E}[\tilde{\mathbf{x}}^i_{(k-1)}] \triangleq \mathbb{E}[\hat{\mathbf{x}}^i_{(k-1)} - \mathbf{x}_{(k-1)}] = \mathbf{0}$ *and* $\mathbb{E}[\tilde{\mathbf{d}}^i_{(k-1)}] \triangleq \mathbb{E}[\hat{\mathbf{d}}^i_{(k-1)} - \mathbf{d}_{(k-1)}] = \mathbf{0}$*, then (4.10) and (4.11) are unbiased estimators of* $\mathbf{x}_{(k)}$ *for any* $\mathbf{M}^i_{x(k)}$ *and* $\mathbf{N}^i_{x(k)}$.

Proof. By substituting (4.8), and (4.10) into (4.11) it can be obtained:

$$\mathbb{E}[\tilde{\mathbf{x}}^i] = \mathbb{E}\Big[\mathbf{A}_{(k-1)}\tilde{\mathbf{x}}^i_{(k-1)} + \mathbf{G}_{(k-1)}\tilde{\mathbf{d}}^i_{(k-1)} - \boldsymbol{\omega}_{(k-1)} - \mathbf{M}^i_{x(k)}\mathbf{C}^i_{(k)}\mathbf{A}_{(k-1)}\tilde{\mathbf{x}}^i_{(k-1)}$$

$$
\begin{aligned}
&- \mathbf{M}^i_{x(k)}\mathbf{C}^i_{(k)}\mathbf{G}_{(k-1)}\tilde{\mathbf{d}}^i_{(k-1)} + \mathbf{M}^i_{x(k)}\mathbf{C}^i_{(k)}\boldsymbol{\omega}_{(k-1)} + \mathbf{M}^i_{x(k)} \\
&+\mathbf{N}^i_{x(k)}\mathbf{A}_{(k-1)} \sum_{j\in N_i}\left(\tilde{\mathbf{x}}^j_{(k-1)} - \tilde{\mathbf{x}}^i_{(k-1)}\right)\Bigg] \\
&= \quad \left(\mathbf{I}_n - \mathbf{M}^i_{x(k)}\mathbf{C}^i_{(k)}\right)\left(\mathbf{A}_{(k-1)}\,\mathbb{E}[\tilde{\mathbf{x}}^i_{(k-1)}] - \mathbb{E}[\boldsymbol{\omega}_{(k-1)}] + \mathbf{G}_{(k-1)}\,\mathbb{E}[\tilde{\mathbf{d}}^i_{(k-1)}]\right) \\
&+ \mathbf{M}^i_{x(k)}\,\mathbb{E}[\mathbf{v}^i_{(k)}] + \mathbf{N}^i_{x(k)}\mathbf{A}_{(k-1)}\left(\sum_{j\in N_i}\mathbb{E}[\tilde{\mathbf{x}}^j_{(k-1)}] - \sum_{j\in N_i}\mathbb{E}[\tilde{\mathbf{x}}^i_{(k-1)}]\right) = \mathbf{0}
\end{aligned}
\tag{4.24}
$$

Since $\mathbb{E}\left[\boldsymbol{\omega}_{(k-1)}\right] = \mathbb{E}\left[\mathbf{v}^i_{(k)}\right] = \mathbf{0}$, then the value of (4.24) for any value of $\mathbf{M}^i_x$ and $\mathbf{N}^i_x$ equals to zero and the proof is complete. □

4.6.2 Minimum Variance Unbiased State Estimation

By defining $\tilde{\mathbf{x}}^i_{(k)} \triangleq \hat{\mathbf{x}}^i_{(k)} - \mathbf{x}_{(k)}$ and substitution of (4.11) and (4.6) for $\hat{\mathbf{x}}^i_{(k)}$ and $\mathbf{x}_{(k)}$ respectively, the covariance matrix $\mathbf{P}^{ij}_{(k)}$ can be obtained as (4.25):

$$
\begin{aligned}
\mathbf{P}^{ij}_{(k)} &\triangleq \mathbb{E}\left[\tilde{\mathbf{x}}^i_{(k)}(\tilde{\mathbf{x}}^j_{(k)})^T\right] \\
&= \{\mathbf{I}_n - \mathbf{M}^i_{x(k)}\mathbf{C}^i_k\}\,\mathbf{A}_{(k-1)}\,\mathbb{E}\left[\tilde{\mathbf{x}}^i_{(k-1)}(\tilde{\mathbf{x}}^j_{(k-1)})^T\right]\,\mathbf{A}^T_{(k-1)}\,\{\mathbf{I}_n - \mathbf{M}^j_{x(k)}\mathbf{C}^j_k\}^T \\
&- \{\mathbf{I}_n - \mathbf{M}^i_{x(k)}\mathbf{C}^i_k\}\,\mathbf{A}_{(k-1)}\,\mathbb{E}\left[\tilde{\mathbf{x}}^i_{(k-1)}(\tilde{\mathbf{x}}^j_{(k-1)})^T\right]\,\mathbf{A}^T_{(k-1)}(\mathbf{C}^j_{(k-1)})^T(\mathbf{M}^j_{d(k)})^T\,\mathbf{G}^T_{(k-1)}\,\{\mathbf{I}_n - \mathbf{M}^j_{x(k)}\mathbf{C}^j_k\}^T \\
&+ \{\mathbf{I}_n - \mathbf{M}^i_{x(k)}\mathbf{C}^i_k\}\,\mathbf{A}_{(k-1)}\sum_{s\in N_j}\left(\mathbb{E}\left[\tilde{\mathbf{x}}^i_{(k-1)}(\tilde{\mathbf{x}}^s_{(k-1)})^T\right] - \mathbb{E}\left[\tilde{\mathbf{x}}^i_{(k-1)}(\tilde{\mathbf{x}}^j_{(k-1)})^T\right]\right)\,\mathbf{A}^T_{(k-1)}(\mathbf{N}^j_{x(k)})^T \\
&- \{\mathbf{I}_n - \mathbf{M}^i_{x(k)}\mathbf{C}^i_k\}\,\mathbf{G}_{(k-1)}\,\mathbf{M}^i_{d(k)}\mathbf{C}^i_{(k-1)}\mathbf{A}_{(k-1)}\mathbb{E}\left[\tilde{\mathbf{x}}^i_{(k-1)}(\tilde{\mathbf{x}}^j_{(k-1)})^T\right]\,\mathbf{A}^T_{(k-1)}\,\{\mathbf{I}_n - \mathbf{M}^j_{x(k)}\mathbf{C}^j_k\}^T \\
&+ \{\mathbf{I}_n - \mathbf{M}^i_{x(k)}\mathbf{C}^i_k\}\,\mathbf{G}_{(k-1)}\,\mathbf{M}^i_{d(k)}\mathbf{C}^i_{(k-1)}\mathbf{A}_{(k-1)}\mathbb{E}\left[\tilde{\mathbf{x}}^i_{(k-1)}\tilde{\mathbf{x}}^j_{(k-1)})^T\right]\mathbf{A}^T_{(k-1)}(\mathbf{C}^j_{(k-1)})^T(\mathbf{M}^j_{d(k)})^T\,\mathbf{G}^T_{(k-1)} \\
&\times \{\mathbf{I}_n - \mathbf{M}^j_{x(k)}\mathbf{C}^j_k\}^T + \{\mathbf{I}_n - \mathbf{M}^i_{x(k)}\mathbf{C}^i_k\}\,\mathbf{G}_{(k-1)}\,\mathbf{M}^i_{d(k)}\mathbf{C}^i_k Q(\mathbf{C}^j_k)^T(\mathbf{M}^j_{d(k)})^T\,\mathbf{G}^T_{(k-1)}\,\{\mathbf{I}_n - \mathbf{M}^j_{x(k)}\mathbf{C}^j_k\}^T \\
&+ \{\mathbf{I}_n - \mathbf{M}^i_{x(k)}\mathbf{C}^i_k\}\,\mathbf{G}_{(k-1)}\,\mathbf{M}^i_{d(k)}\mathbb{E}\left[\mathbf{v}^i_{(k)}(\mathbf{v}^j_{(k)})^T\right](\mathbf{M}^j_{d(k)})^T\,\mathbf{G}^T_{(k-1)}\,\{\mathbf{I}_n - \mathbf{M}^j_{x(k)}\mathbf{C}^j_k\}^T \\
&- \{\mathbf{I}_n - \mathbf{M}^i_{x(k)}\mathbf{C}^i_k\}\,\mathbf{G}_{(k-1)}\,\mathbf{M}^i_{d(k)}\mathbf{C}^i_k\,\mathbf{Q}\,\{\mathbf{I}_n - \mathbf{M}^j_{x(k)}\mathbf{C}^j_k\}^T \\
&+ \{\mathbf{I}_n - \mathbf{M}^i_{x(k)}\mathbf{C}^i_k\}\,\mathbf{G}_{(k-1)}\,\mathbf{M}^i_{d(k)}\mathbb{E}\left[\mathbf{v}^i_{(k)}(\mathbf{v}^j_{(k)})^T\right](M^j_{x\,(k)})^T \\
&- \{\mathbf{I}_n - \mathbf{M}^i_{x(k)}\mathbf{C}^i_k\}\,\mathbf{G}_{(k-1)}\,\mathbf{M}^i_{d(k)}\mathbf{C}^i_k\mathbf{A}_{(k-1)}\sum_{s\in N_j}\left(\mathbb{E}\left[\tilde{\mathbf{x}}^i_{(k-1)}(\tilde{\mathbf{x}}^s_{(k-1)})^T\right] - \mathbb{E}\left[\tilde{\mathbf{x}}^i_{(k-1)}(\tilde{\mathbf{x}}^j_{(k-1)})^T\right]\right) \\
&\times \mathbf{A}^T_{(k-1)}(\mathbf{N}^j_{x(k)})^T - \{\mathbf{I}_n - \mathbf{M}^i_{x(k)}\mathbf{C}^i_k\}\,\mathbf{Q}\,(\mathbf{C}^j_k)^T(\mathbf{M}^j_{d(k)})^T\,\mathbf{G}^T_{(k-1)}\,\{\mathbf{I}_n - \mathbf{M}^j_{x(k)}\mathbf{C}^j_k\}^T \\
&+ \{\mathbf{I}_n - \mathbf{M}^i_{x(k)}\mathbf{C}^i_k\}\,\mathbf{Q}\,\{\mathbf{I}_n - \mathbf{M}^j_{x(k)}\mathbf{C}^j_k\}^T \\
&+ \mathbf{M}^i_{x(k)}\,\mathbb{E}\left[\mathbf{v}^i_{(k)}(\mathbf{v}^j_{(k)})^T\right](\mathbf{M}^j_{d(k)})^T\,\mathbf{G}^T_{(k-1)}\,\{\mathbf{I}_n - \mathbf{M}^j_{x(k)}\mathbf{C}^j_k\}^T + \mathbf{M}^i_{x(k)}\,\mathbb{E}\left[\mathbf{v}^i_{(k)}(\mathbf{v}^j_{(k)})^T\right](M^j_{x\,(k)})^T \\
&+ \mathbf{N}^i_{x(k)}\,\mathbf{A}_{(k-1)}\sum_{r\in N_i}\left(\mathbb{E}\left[\tilde{\mathbf{x}}^r_{(k-1)}(\tilde{\mathbf{x}}^j_{(k-1)})^T\right] - \mathbb{E}\left[\tilde{\mathbf{x}}^i_{(k-1)}(\tilde{\mathbf{x}}^j_{(k-1)})^T\right]\right)\,\mathbf{A}^T_{(k-1)}\,\{\mathbf{I}_n - \mathbf{M}^j_{x(k)}\mathbf{C}^j_k\}^T
\end{aligned}
$$

$$
\begin{aligned}
&- \mathbf{N}^i_{x(k)}\,\mathbf{A}_{(k-1)} \sum_{r\in N_i} \left(\mathbb{E}\left[\tilde{\mathbf{x}}^r_{(k-1)}(\tilde{\mathbf{x}}^j_{(k-1)})^T\right] - \mathbb{E}\left[\tilde{\mathbf{x}}^i_{(k-1)}(\tilde{\mathbf{x}}^j_{(k-1)})^T\right]\right) \mathbf{A}^T_{(k-1)}(\mathbf{C}^j_{(k-1)})^T \\
&\times (\mathbf{M}^j_{d(k)})^T\,\mathbf{G}^T_{(k-1)}\,\{\mathbf{I}_n - \mathbf{M}^j_{x(k)}\mathbf{C}^j_k\}^T + \mathbf{N}^i_{x(k)}\,\mathbf{A}_{(k-1)} \sum_{r\in N_i}\sum_{s\in N_j} \left(\mathbb{E}\left[\tilde{\mathbf{x}}^r_{(k-1)}(\tilde{\mathbf{x}}^s_{(k-1)})^T\right]\right. \\
&\left. - \mathbb{E}\left[\tilde{\mathbf{x}}^r_{(k-1)}(\tilde{\mathbf{x}}^j_{(k-1)})^T\right] - \mathbb{E}\left[\tilde{\mathbf{x}}^i_{(k-1)}(\tilde{\mathbf{x}}^s_{(k-1)})^T\right] + \mathbb{E}\left[\tilde{\mathbf{x}}^i_{(k-1)}(\tilde{\mathbf{x}}^j_{(k-1)})^T\right]\right)\, \mathbf{A}^T_{(k-1)}(\mathbf{N}^j_{x(k)})^T. \qquad (4.25)
\end{aligned}
$$

By setting $i = j$ in (4.25) the error covariance matrix $\mathbf{P}^i_{(k)} \triangleq \mathbf{P}^{ii}_{(k)}$ at estimator i can be calculated by (4.26) as follows:

$$
\begin{aligned}
\mathbf{P}^i_{(k)} &\triangleq \mathbb{E}\left[\tilde{\mathbf{x}}^i_{(k)}(\tilde{\mathbf{x}}^i_{(k)})^T\right] \\
&= \mathbf{P}^{i-}_{(k)} - \mathbf{P}^{i-}_{(k)}(\mathbf{C}^i_{(k)})^T(\mathbf{M}^i_{x(k)})^T \\
&- (\mathbf{M}^i_{x(k)}\mathbf{C}^i_{(k)})\,\mathbf{P}^{i-}_{(k)} + \mathbf{M}^i_{x(k)}\tilde{\mathbf{R}}^i_{(k)}(\mathbf{M}^i_{x(k)})^T \\
&- \mathbf{P}^{i-}_{(k)}(\mathbf{C}^i_{(k)})^T(\mathbf{M}^i_{d(k)})^T\,\mathbf{G}^T_{(k-1)} \\
&+ \mathbf{P}^{i-}_{(k)}(\mathbf{C}^i_{(k)})^T(\mathbf{M}^i_{d(k)})^T\,\mathbf{G}^T_{(k-1)}\,(\mathbf{C}^i_{(k)})^T(\mathbf{M}^i_{x(k)})^T \\
&+ \mathbf{M}^i_{x(k)}\,\tilde{\mathbf{R}}^i_{(k)}\,(\mathbf{M}^i_{d(k)})^T\,\mathbf{G}^T_{(k-1)} \\
&- \mathbf{M}^i_{x(k)}\,\tilde{\mathbf{R}}^i_{(k)}\,(\mathbf{M}^i_{d(k)})^T\,\mathbf{G}^T_{(k-1)}\,(\mathbf{C}^i_{(k)})^T(\mathbf{M}^i_{x(k)})^T \\
&+ \mathbf{A}_{(k-1)} \sum_{s\in N_i} \left(\mathbf{P}^{is}_{(k-1)} - \mathbf{P}^i_{(k-1)}\right)\,\mathbf{A}^T_{(k-1)}(\mathbf{N}^i_{x(k)})^T \\
&+ \mathbf{N}^i_{x(k)}\,\mathbf{A}_{(k-1)} \sum_{r\in N_i} \left(\mathbf{P}^{ri}_{(k-1)} - \mathbf{P}^i_{(k-1)}\right)\,\mathbf{A}^T_{(k-1)} \\
&- (\mathbf{M}^i_{x(k)}\mathbf{C}^i_{(k)})\,\mathbf{A}_{(k-1)} \sum_{s\in N_i} \left(\mathbf{P}^{is}_{(k-1)} - \mathbf{P}^i_{(k-1)}\right)\,\mathbf{A}^T_{(k-1)}(\mathbf{N}^i_{x(k)})^T \\
&- \mathbf{N}^i_{x(k)}\,\mathbf{A}_{(k-1)} \sum_{r\in N_i} \left(\mathbf{P}^{ri}_{(k-1)} - \mathbf{P}^i_{(k-1)}\right)\,\mathbf{A}^T_{(k-1)}\,(\mathbf{C}^i_{(k)})^T(\mathbf{M}^i_{x(k)})^T \\
&- \mathbf{G}_{(k-1)}\mathbf{M}^i_{d(k)}\mathbf{C}^i_{(k)}\,\mathbf{P}^{i-}_{(k)} \\
&+ \mathbf{G}_{(k-1)}\mathbf{M}^i_{d(k)}\,\tilde{\mathbf{R}}^i_{(k)}\,(\mathbf{M}^i_{x(k)})^T \\
&+ (\mathbf{M}^i_{x(k)}\mathbf{C}^i_{(k)})\mathbf{G}_{(k-1)}\mathbf{M}^i_{d(k)}\,\mathbf{C}^i_{(k)}\mathbf{P}^{i-}_{(k)} \\
&- (\mathbf{M}^i_{x(k)}\mathbf{C}^i_{(k)})\mathbf{G}_{(k-1)}\mathbf{M}^i_{d(k)}\,\tilde{\mathbf{R}}^i_{(k)}\,(\mathbf{M}^i_{x(k)})^T \\
&+ \mathbf{G}_{(k-1)}\mathbf{M}^i_{d(k)}\,\tilde{\mathbf{R}}^i_{(k)}\,(\mathbf{M}^i_{d(k)})^T\,\mathbf{G}^T_{(k-1)} \\
&- \mathbf{G}_{(k-1)}\mathbf{M}^i_{d(k)}\,\tilde{\mathbf{R}}^i_{(k)}\,(\mathbf{M}^i_{d(k)})^T\,\mathbf{G}^T_{(k-1)}\,(\mathbf{C}^i_{(k)})^T(\mathbf{M}^i_{x(k)})^T \\
&- (\mathbf{M}^i_{x(k)}\mathbf{C}^i_{(k)})\mathbf{G}_{(k-1)}\mathbf{M}^i_{d(k)}\,\tilde{\mathbf{R}}^i_{(k)}\,(\mathbf{M}^i_{d(k)})^T\,\mathbf{G}^T_{(k-1)} \\
&+ (\mathbf{M}^i_{x(k)}\mathbf{C}^i_{(k)})\mathbf{G}_{(k-1)}\mathbf{M}^i_{d(k)}\,\tilde{\mathbf{R}}^i_{(k)}\,(\mathbf{M}^i_{d(k)})^T\,\mathbf{G}^T_{(k-1)}\,(\mathbf{C}^i_{(k)})^T(\mathbf{M}^i_{x(k)})^T \\
&- G_{(k-1)}\,\mathbf{M}^i_{d(k)}\mathbf{C}^i_{(k)}\mathbf{A}_{(k-1)} \sum_{s\in N_i} \left(\mathbf{P}^{is}_{(k-1)} - \mathbf{P}^i_{(k-1)}\right)\,\mathbf{A}^T_{(k-1)}(\mathbf{N}^i_{x(k)})^T
\end{aligned}
$$

$$
\begin{aligned}
&- \mathbf{N}^i_{x(k)}\, \mathbf{A}_{(k-1)} \sum_{r\in N_i} \left(\mathbf{P}^{ri}_{(k-1)} \; - \mathbf{P}^i_{(k-1)}\right) \mathbf{A}^T_{(k-1)} (\mathbf{C}^i_{(k)})^T (\mathbf{M}^i_{d(k)})^T\, \mathbf{G}^T_{(k-1)} \\
&+ (\mathbf{M}^i_{x(k)} \mathbf{C}^i_{(k)}) G_{(k-1)}\, \mathbf{M}^i_{d(k)} \mathbf{C}^i_{(k)} \mathbf{A}_{(k-1)} \sum_{s\in N_i} \left(\mathbf{P}^{is}_{(k-1)} - \mathbf{P}^i_{(k-1)}\right)\, \mathbf{A}^T_{(k-1)} (\mathbf{N}^i_{x(k)})^T \\
&+ \mathbf{N}^i_{x(k)}\, \mathbf{A}_{(k-1)} \sum_{r\in N_i} \left(\mathbf{P}^{ri}_{(k-1)} \; - \mathbf{P}^i_{(k-1)}\right) \mathbf{A}^T_{(k-1)} (\mathbf{C}^i_{(k)})^T (\mathbf{M}^i_{d(k)})^T\, \mathbf{G}^T_{(k-1)}\, (\mathbf{C}^i_{(k)})^T (\mathbf{M}^i_{x(k)})^T \\
&+ \mathbf{N}^i_{x(k)}\, \mathbf{A}_{(k-1)} \sum_{r\in N_i} \sum_{s\in N_i} \left(P^{rs}_{(k-1|k-1)} - \mathbf{P}^{ri}_{(k-1)} - \mathbf{P}^{is}_{(k-1)} + \mathbf{P}^i_{(k-1)}\right)\, \mathbf{A}^T_{(k-1)} (\mathbf{N}^i_{x(k)})^T. \quad (4.26)
\end{aligned}
$$

where $\mathbf{P}^{is} = (\mathbf{P}^{si})^T = \mathbb{E}[\tilde{\mathbf{x}}^i(\tilde{\mathbf{x}}^s)^T]$, $\mathbf{P}^{rs} = \mathbb{E}[\tilde{\mathbf{x}}^r(\tilde{\mathbf{x}}^s)^T]$, $\mathbf{P}^{ri} = \mathbb{E}[\tilde{\mathbf{x}}^r(\tilde{\mathbf{x}}^i)^T]$ and $\mathbf{P}^{ii} = \mathbf{P}^i = \mathbb{E}[\tilde{\mathbf{x}}^i(\tilde{\mathbf{x}}^i)^T]$. To find the optimal gain for $\mathbf{M}^i_x$ to minimize the variance of the error states, the partial derivative of $tr[\mathbf{P}^i_{(k)}]$ to $\mathbf{M}^i_x$ is computed:

$$
\begin{aligned}
&\frac{\partial\{tr[\mathbf{P}^i_{(k)}]\}}{\partial \mathbf{M}^i_{x(k)}} = \mathbf{M}^i_{x(k)}\, \tilde{\mathbf{R}}^i_{(k)} \\
&- \mathbf{M}^i_{x(k)}\, \tilde{\mathbf{R}}^i_{(k)}\, (\mathbf{M}^i_{d(k)})^T\, \mathbf{G}^T_{(k-1)}\, (\mathbf{C}^i_{(k)})^T \\
&- \mathbf{M}^i_{x(k)}\, \mathbf{C}^i_{(k)}\, \mathbf{G}_{(k-1)}\, \mathbf{M}^i_{d(k)}\, \tilde{\mathbf{R}}^i_{(k)} \\
&+ \mathbf{M}^i_{x(k)} \mathbf{C}^i_{(k)} \mathbf{G}_{(k-1)} \mathbf{M}^i_{d(k)}\, \tilde{\mathbf{R}}^i_{(k)}\, (\mathbf{M}^i_{d(k)})^T\, \mathbf{G}^T_{(k-1)}\, (\mathbf{C}^i_{(k)})^T \\
&+ \mathbf{P}^{i-}_{(k)}\, (\mathbf{C}^i_{(k)})^T\, (\mathbf{M}^i_{d(k)})^T\, \mathbf{G}^T_{(k-1)}\, (\mathbf{C}^i_{(k)})^T \\
&- \mathbf{P}^{i-}_{(k)} (\mathbf{C}^i_{(k)})^T + \mathbf{G}_{(k-1)} \mathbf{M}^i_{d(k)}\, \tilde{\mathbf{R}}^i_{(k)} \\
&- \mathbf{N}^i_{x(k)}\, \mathbf{A}_{(k-1)} \sum_{r\in N_i} \left(\mathbf{P}^{ri}_{(k-1)} \; - \mathbf{P}^i_{(k-1)}\right)\, \mathbf{A}^T_{(k-1)}\, (\mathbf{C}^i_{(k)})^T \\
&- G_{(k-1)} (\mathbf{M}^i_{d(k)})\, \tilde{\mathbf{R}}^i_{(k)}\, (\mathbf{M}^i_{d(k)})^T\, \mathbf{G}^T_{(k-1)} (\mathbf{C}^i_{(k)})^T \\
&+ \mathbf{N}^i_{x(k)}\, \mathbf{A}_{(k-1)} \sum_{r\in N_i} \left(\mathbf{P}^{ri}_{(k-1)} \; - \mathbf{P}^i_{(k-1)}\right) \mathbf{A}^T_{(k-1)} (\mathbf{C}^i_{(k)})^T (\mathbf{M}^i_{d(k)})^T\, \mathbf{G}^T_{(k-1)}\, (\mathbf{C}^i_{(k)})^T.
\end{aligned} \quad (4.27)
$$

By setting $\frac{\partial\{tr[\mathbf{P}^i(k)]\}}{\partial \mathbf{M}^i_{x(k)}} = 0$, the optimal $\mathbf{M}^i_x$ is:

$$
\begin{aligned}
\mathbf{M}^i_{x(k)} \tilde{\mathbf{R}}^{i\,*}_{(k)} = &\left[\mathbf{P}^{i-}_{(k)} (\mathbf{C}^i_{(k)})^T - \mathbf{G}_{(k-1)} \mathbf{M}^i_{d(k)}\, \tilde{\mathbf{R}}^i_{(k)} \; - \mathbf{N}^i_{x(k)}\, \mathbf{A}_{(k-1)} \sum_{r\in N_i} \left(\mathbf{P}^{ri}_{(k-1)} \; - \mathbf{P}^i_{(k-1)}\right)\right. \\
&\left. \times \mathbf{A}^T_{(k-1)} (\mathbf{C}^i_{(k)})^T\right] \left(\mathbf{I} - (\mathbf{M}^i_{d(k)})^T\, \mathbf{G}^T_{(k-1)}\, (\mathbf{C}^i_{(k)})^T\right), \quad (4.28)
\end{aligned}
$$

where

$$\tilde{\mathbf{R}}^{i*} = [\mathbf{I}_q - \mathbf{C}^i_{(k)}\mathbf{G}_{(k-1)}\mathbf{M}^i_{d(k)}]\,\tilde{\mathbf{R}}^{i}\,[\mathbf{I}_q - \mathbf{C}^i_{(k)}\mathbf{G}_{(k-1)}\mathbf{M}^i_{d(k)}]^T, \tag{4.29}$$

and $\mathbf{I}_q$ is the identity matrix of dimension q. From (4.28) it can be inferred that there is a unique solution for $\mathbf{M}^i_x$ if $\tilde{\mathbf{R}}^{i*}$ is invertible (full rank or non singular). Furthermore, from (4.28) it can be seen that the value of $\mathbf{M}^i_x$ depends on the consensus gain $\mathbf{N}^i_x$ and on the aggregated difference of error covariance of node i with its neighbor nodes ($\sum_{r\in N_i}\{\mathbf{P}^{ri}_{(k)} - \mathbf{P}^i_{(k)}\}$).

Now $\tilde{\mathbf{R}}^{i*}$ will be examined because its rank can affect the uniqueness of the solution for $\mathbf{M}^i_x$ (4.28).

Lemma 1. *Assuming condition (4.17) is satisfied then the term* $[\mathbf{I}_q - \mathbf{C}^i_{(k)}\mathbf{G}_{(k-1)}\mathbf{M}^i_{d(k)}]$ *has rank* $q - m$*, where* $\mathbf{I}_q$ *is the identity matrix of dimension* q*.*

Proof. From (4.17) $\mathbf{M}^i_{d(k)}\mathbf{C}^i_{(k)}\mathbf{G}_{(k-1)} = \mathbf{I}_m$, it can be deduced that $\mathbf{M}^i_{d(k)}$ is a left inverse of $\mathbf{C}^i_{(k)}\mathbf{G}_{(k-1)}$. Therefore, both $[\mathbf{C}^i_{(k)}\mathbf{G}_{(k-1)}\mathbf{M}^i_{d(k)}]$ and $[\mathbf{I}_q - \mathbf{C}^i_{(k)}\mathbf{G}_{(k-1)}\mathbf{M}^i_{d(k)}]$ are idempotent. Thus, the rank of $[\mathbf{I}_q - \mathbf{C}^i_{(k)}\mathbf{G}_{(k-1)}\mathbf{M}^i_{d(k)}]$ is equal to $\text{rank}(\mathbf{I}_q) - \text{rank}(\mathbf{C}^i_{(k)}\mathbf{G}_{(k-1)}\mathbf{M}^i_{d(k)}) = q - m = r$. □

It is inferred from Lemma 1 that $\mathbf{M}^i_{x(k)}$ is not unique since $\tilde{\mathbf{R}}^{i*}$ is not full rank (it is singular). In Section 4.6.3, the generalized inverse of $\tilde{\mathbf{R}}^{i*}$ is explored.

4.6.3 Generalized Inverse Calculation

Using singular value decomposition (SVD) [Klema and Laub, 1980], $\tilde{\mathbf{R}}^{i*} \in \mathbb{R}^{q\times q}$ is

$$\tilde{\mathbf{R}}^{i*} = \mathbf{U}^{i*}\begin{bmatrix} \mathbf{D}^{i*}_{r\times r} & \mathbf{0}_{r\times(q-r)} \\ \mathbf{0}_{(q-r)\times r} & \mathbf{0}_{(q-r)\times(q-r)} \end{bmatrix}(\mathbf{V}^{i*})^T, \tag{4.30}$$

where matrices $\mathbf{U}^{i*} \in \mathbb{R}^{q\times q}$ and $\mathbf{V}^{i*} \in \mathbb{R}^{q\times q}$ are orthogonal, $\mathbf{D}^{i*} \triangleq diag[\sigma^{i*}_1, \ldots, \sigma^{i*}_r]$ and $\sigma^{i*}_1 \geqslant \sigma^{i*}_2 \geqslant \ldots \geqslant \sigma^{i*}_r > 0$ are the positive singular values of $\tilde{\mathbf{R}}^{i*}$. Thus, the generalized inverse of $\tilde{\mathbf{R}}^{i*}$ is

$$(\tilde{\mathbf{R}}^{i*})^{\dagger} = (\mathbf{V}^{i*})\begin{bmatrix} (\mathbf{D}^{i*})^{-1}_{r\times r} & \mathbf{0}_{r\times(q-r)} \\ \mathbf{0}_{(q-r)\times r} & \mathbf{0}_{(q-r)\times(q-r)} \end{bmatrix}(\mathbf{U}^{i*})^T. \tag{4.31}$$

Having obtained $(\tilde{\mathbf{R}}^{i*})^{\dagger}$ in (4.31), then similar to (4.28), $\mathbf{M}^i_{x(k)}$ can be written as:

$$\mathbf{M}^i_{x(k)} = \Bigg[\mathbf{P}^{i-}_{(k)}(\mathbf{C}^i_{(k)})^T - \mathbf{G}_{(k-1)}\mathbf{M}^i_{d(k)}\tilde{\mathbf{R}}^i_{(k)} - \mathbf{N}^i_{x(k)}\, A_{(k-1)} \sum_{r\in N_i}\left(\mathbf{P}^{ri}_{(k-1)} - \mathbf{P}^i_{(k-1)}\right) \times \mathbf{A}^T_{(k-1)}(\mathbf{C}^i_{(k)})^T\Bigg]\left(\mathbf{I} - (\mathbf{M}^i_{d(k)})^T\,\mathbf{G}^T_{(k-1)}\,(\mathbf{C}^i_{(k)})^T\right)(\tilde{\mathbf{R}}^{i*})^{\dagger} \tag{4.32}$$

From (4.32) it has been seen that $\mathbf{M}^i_x$ depends on the consensus gain $\mathbf{N}^i_x$. Later in Section 4.6.4, it will be discussed that the proposed distributed estimator can be stable and will converge under certain conditions. As a result, assuming the convergence of the filter, the term $\sum_{r\in N_i}\left(\mathbf{P}^{ri}_{(k-1)} - \mathbf{P}^i_{(k-1)}\right)$ in (4.32) can be considered approximately zero. Therefore, this approximation leads to have a suboptimal but still good approximate solution for $\mathbf{M}^i_{x(k)}$ as (4.33):

$$\mathbf{M}^i_{x(k)} = \left[\mathbf{P}^{i-}_{(k)}(\mathbf{C}^i_{(k)})^T - \mathbf{G}_{(k-1)}\mathbf{M}^i_{d(k)}\tilde{\mathbf{R}}^i_{(k)}\right] \times \left(\mathbf{I} - (\mathbf{M}^i_{d(k)})^T\,\mathbf{G}^T_{(k-1)}\,(\mathbf{C}^i_{(k)})^T\right)(\tilde{\mathbf{R}}^{i*})^{\dagger}. \tag{4.33}$$

This assumption and consequently, the suboptimal solution for $\mathbf{M}^i_{x(k)}$ clearly have two advantages. First, it makes the performance of estimator more robust and reliable since the calculation of local gain $\mathbf{M}^i_{x(k)}$ is only dependent on the available data of local estimator and not its neighbor's data. Second, it contributes to be able to consider this proposed estimator as a distributed method based on what is defined in [Liu *et al.*, 2018]. Yet, $\mathbf{N}^i_{x(k)}$ is unknown, and is required to be determined. This will be addressed in Section 4.6.4 where the stability of the studied distributed estimator is assessed.

4.6.4 Stability and Convergence of Estimator

The equation for the error dynamics of the distributed filter is written as (4.34). To obtain (4.34) the noises are assumed to be zero, and condition (4.17) is assumed to be met, implying that the unknown input does not have any effect on the error dynamics of the estimator.

$$\begin{aligned}\tilde{\mathbf{x}}^i_{(k)} &= \hat{\mathbf{x}}^i_{(k)} - \mathbf{x}_{(k)} \\ &= \mathbf{H}^i_{(k)}\mathbf{A}_{(k-1)}\tilde{\mathbf{x}}^i_{(k-1)} + \mathbf{N}^i_{x(k)}\mathbf{u}^i_{(k-1)}.\end{aligned} \tag{4.34}$$

$\mathbf{H}^i_{(k)}$ and $\mathbf{u}^i_{(k)}$ are defined in (4.35) and (4.36) respectively.

$$\mathbf{H}^i_{(k)} = \mathbf{I}_n - \mathbf{M}^i_{x(k)}\mathbf{C}^i_{(k)} - \mathbf{G}_{(k-1)}\,\mathbf{M}^i_{d(k)}\mathbf{C}^i_{(k)} + \mathbf{M}^i_{x(k)}\mathbf{C}^i_{(k)}\mathbf{G}_{(k-1)}\,\mathbf{M}^i_{d(k)}\mathbf{C}^i_{(k)}, \quad (4.35)$$

$$\mathbf{u}^i_{(k)} = \mathbf{A}_{(k)} \sum_{r\in N_i} \left(\tilde{\mathbf{x}}^r_{(k)} - \tilde{\mathbf{x}}^i_{(k)}\right). \quad (4.36)$$

Before investigating the stability of the distributed estimator (4.8)-(4.11) in Theorem 4.6.2 below, Lemma 2 is given:

Lemma 2. *Assuming that* $\mathbf{A}^{-1}_{(k)}\mathbf{G}_{(k)} \neq \mathbf{0}$*, and that condition (4.17) is met and* $\mathbf{N}^i_{x(k)} = \mathbf{0}$*, then the error dynamics (4.34) of each estimator, i, will be globally asymptotically stable.*

Proof. The proof is made as follows: the discrete-time Lyapunov function [Haddad and Chellaboina, 2008] $V^i = (\tilde{\mathbf{x}}^i_{(k)})^T\tilde{\mathbf{x}}^i_{(k)}$ is defined. Then, it is shown that $\Delta V^i = V^i_{(k+1)} - V^i_{(k)} < 0$. From (4.34), since it is assumed that $\mathbf{N}^i_{x(k)} = \mathbf{0}$, then ΔV^i is written as:

$$\begin{aligned}
\Delta V^i &= V^i_{(k+1)} - V^i_{(k)} \\
&= (\tilde{\mathbf{x}}^i_{(k+1)})^T\,\tilde{\mathbf{x}}^i_{(k+1)} - (\tilde{\mathbf{x}}^i_{(k)})^T\tilde{\mathbf{x}}^i_{(k)} \\
&= (\tilde{\mathbf{x}}^i_{(k)})^T\left(\mathbf{A}^T_{(k)}(\mathbf{H}^i_{(k+1)})^T\,\mathbf{H}^i_{(k+1)}\mathbf{A}_{(k)} - \mathbf{I}_n\right)\tilde{\mathbf{x}}^i_{(k)} \\
&= (\tilde{\mathbf{x}}^i_{(k)})^T\boldsymbol{\Omega}^i\,(\tilde{\mathbf{x}}^i_{(k)}),
\end{aligned} \quad (4.37)$$

where

$$\boldsymbol{\Omega}^i = \mathbf{A}^T_{(k)}(\mathbf{H}^i_{(k+1)})^T\,\mathbf{H}^i_{(k+1)}\mathbf{A}_{(k)} - \mathbf{I}_n. \quad (4.38)$$

In order to show that (4.37) is negative, it is sufficient to show that $\boldsymbol{\Omega}^i$ is negative definite for all $k \geq 0$. From (4.38), since it is assumed that $\mathbf{A}^{-1}_{(k)}\mathbf{G}_{(k)} \neq \mathbf{0}$ it can be written that

$$\begin{aligned}
\boldsymbol{\Omega}^i\,\mathbf{A}^{-1}_{(k)}\,\mathbf{G}_{(k)} &= \left(\mathbf{A}^T_{(k)}(\mathbf{H}^i_{(k+1)})^T\,\mathbf{H}^i_{(k+1)}\mathbf{A}_{(k)} - \mathbf{I}_n\right)\mathbf{A}^{-1}_{(k)}\mathbf{G}_{(k)}, \\
(\boldsymbol{\Omega}^i + \mathbf{I}_n)\mathbf{A}^{-1}_{(k)}\mathbf{G}_{(k)} = \mathbf{0} &\Rightarrow \boldsymbol{\Omega}^i = -\mathbf{I}_n.
\end{aligned} \quad (4.39)$$

The result in (4.39) is obtained because $\mathbf{H}^i_{(k)}\mathbf{G}_{(k-1)} = \mathbf{0}$. Using (4.17), namely $\mathbf{M}^i_{d(k)}\mathbf{C}^i_{(k)}\mathbf{G}_{(k-1)} = \mathbf{I}_m$, then from (4.35) the term $\mathbf{H}^i_{(k)}\mathbf{G}_{(k-1)} = \mathbf{0}$. Since $\boldsymbol{\Omega}^i_{(k)}$ for all

i is constant and equal to $-\mathbf{I}_n$, $\mathbf{\Omega}^i_{(k)}$ can be denoted by $\mathbf{\Omega}$.

$$\Delta V^i = V^i_{(k+1)} - V^i_{(k)} = -(\tilde{\mathbf{x}}^i_{(k)})^T (\tilde{\mathbf{x}}^i_{(k)}) < 0, \forall \tilde{\mathbf{x}}^i \neq \mathbf{0}.$$

Therefore, the proof is complete. □

Theorem 4.6.2. *Suppose that the error dynamics of estimator i is defined as (4.34), and let*

$$\mathbf{N}^i_{x(k)} = \beta \, \mathbf{H}^i_{(k)} \tag{4.40}$$

Then, the error dynamics of the distributed estimator (4.11) is globally asymptotically stable for $0 \leq \beta \leq 1/2$.

Proof. The proof is made as follows: the discrete-time Lyapunov function [Haddad and Chellaboina, 2008] is defined

$$V_{(k)} = \sum_{i=1}^{|a|} \left((\tilde{\mathbf{x}}^i_{(k)})^T \tilde{\mathbf{x}}^i_{(k)} \right). \tag{4.41}$$

Then, it is shown that $\Delta V \triangleq V_{(k+1)} - V_{(k)} < 0$.

From the error dynamics of the filter (4.34), (4.35), (4.36), Lemma 2 and Lyapunov function (4.41):

$$\begin{aligned}
\Delta V &\triangleq V_{(k+1)} - V_{(k)} \\
&= \sum_{i=1}^{|a|} \left[(\tilde{\mathbf{x}}^i_{(k+1)})^T \tilde{\mathbf{x}}^i_{(k+1)} - (\tilde{\mathbf{x}}^i_{(k)})^T \tilde{\mathbf{x}}^i_{(k)} \right] \\
&= \sum_{i=1}^{|a|} (\tilde{\mathbf{x}}^i_{(k)})^T \left[\mathbf{A}^T_{(k)} \, (\mathbf{H}^i_{(k+1)})^T \, \mathbf{H}^i_{(k+1)} \mathbf{A}_{(k)} - \mathbf{I}_n \right] \tilde{\mathbf{x}}^i_{(k)} \\
&+ \sum_{i=1}^{|a|} (\tilde{\mathbf{x}}^i_{(k)})^T \mathbf{A}^T_{(k)} (\mathbf{H}^i_{(k+1)})^T \, \mathbf{N}^i_{x(k+1)} \mathbf{u}^i_{(k)} \\
&+ \sum_{i=1}^{|a|} (\mathbf{u}^i_{(k)})^T (\mathbf{N}^i_{x(k+1)})^T \, \mathbf{N}^i_{x(k+1)} \mathbf{u}^i_{(k)} \\
&= \sum_{i=1}^{|a|} (\tilde{\mathbf{x}}^i_{(k)})^T \mathbf{\Omega}^i \tilde{\mathbf{x}}^i_{(k)} + \sum_{i=1}^{|a|} (\tilde{\mathbf{x}}^i_{(k)})^T \mathbf{A}^T_{(k)} (\mathbf{H}^i_{(k+1)})^T \, \mathbf{N}^i_{x(k+1)} \mathbf{u}^i_{(k)}
\end{aligned}$$

$$+ \sum_{i=1}^{|a|} (\mathbf{u}^i_{(k)})^T (\mathbf{N}^i_{x(k+1)})^T \mathbf{N}^i_{x(k+1)} \mathbf{u}^i_{(k)}. \tag{4.42}$$

Equation in (4.42) comprises the sum of three terms. The first term in (4.42) is negative definite according to Lemma 2, and if $\mathbf{N}^i_{x(k)}$ is chosen as (4.40), with the aid of property (4.4) of undirected graphs, the second and third terms can be converted into forms by which verifying the stability proof become much more straightforward. Before continuing the above hypothesis, it is required to define matrix $\tilde{\mathbf{X}}_{(k)}$, similar to (4.3), as:

$$\tilde{\mathbf{X}}_{(k)} = [\tilde{\mathbf{x}}^1_{(k)}, \ldots, \tilde{\mathbf{x}}^i_{(k)}, \ldots, \tilde{\mathbf{x}}^{|a|}_{(k)}] \tag{4.43}$$

where $\tilde{\mathbf{x}}^i_{(k)} \in \mathbb{R}^n$ represents the error of state vector corresponding to the ith estimator. For the second term of (4.42), by replacing $\mathbf{N}^i_{x(k)}$ with (4.40) and $\mathbf{u}^i_{(k)}$ with (4.36) as:

$$\sum_{i=1}^{|a|} (\tilde{\mathbf{x}}^i_{(k)})^T \mathbf{A}^T_{(k)} (\mathbf{H}^i_{(k+1)})^T \ \mathbf{N}^i_{x(k+1)} \mathbf{u}^i_{(k)} =$$
$$\beta \sum_{i=1}^{|a|} \sum_{r \in N_i} (\mathbf{H}^i_{(k+1)} \mathbf{A}_{(k)} \tilde{\mathbf{x}}^i_{(k)})^T \left(\mathbf{H}^i_{(k+1)} \mathbf{A}_{(k)} \tilde{\mathbf{x}}^r_{(k)} - \mathbf{H}^i_{(k+1)} \mathbf{A}_{(k)} \tilde{\mathbf{x}}^i_{(k)} \right). \tag{4.44}$$

Comparing the result obtained in (4.44) with (4.4), and by replacing in (4.4) $\hat{\mathbf{x}}$ with $\mathbf{H}^i_{(k+1)} \mathbf{A}_{(k)} \tilde{\mathbf{x}}^i$, it is possible to rewrite (4.44) as (4.46):

$$\sum_{i=1}^{|a|} (\tilde{\mathbf{x}}^i_{(k)})^T \mathbf{A}^T_{(k)} (\mathbf{H}^i_{(k+1)})^T \ \mathbf{N}^i_{x(k+1)} \mathbf{u}^i_{(k)} = \tag{4.45}$$
$$- \beta \sum_{l=1}^{n} \left(\boldsymbol{\delta}^l \right)^T \left(\mathbf{H}^i_{(k+1)} \mathbf{A}_{(k)} \right)^T \ \mathbf{H}^i_{(k+1)} \mathbf{A}_{(k)} \ \tilde{\mathbf{X}}_{(k)} \, \mathbf{L} \, \tilde{\mathbf{X}}^T_{(k)} \boldsymbol{\delta}^l \tag{4.46}$$

so the second term of (4.42) is obtained in the form of a quadratic form. Considering (4.36) and (4.40), the third term in (4.42) can be rewritten in a compact form as (4.47):

$$\sum_{i=1}^{|a|} \left(\mathbf{u}^i_{(k)} \right)^T \left(\mathbf{N}^i_{x(k+1)} \right)^T \mathbf{N}^i_{x(k+1)} \mathbf{u}^i_{(k)} =$$

$$
\begin{aligned}
=&\beta^2 \sum_{i=1}^{|a|} \sum_{r\in N_i} \left(\tilde{\mathbf{x}}^r_{(k)} - \tilde{\mathbf{x}}^i_{(k)}\right)^T \mathbf{A}^T_{(k)} \left(\mathbf{H}^i_{(k+1)}\right)^T \mathbf{H}^i_{(k+1)} \mathbf{A}_{(k)} \left(\tilde{\mathbf{x}}^r_{(k)} - \tilde{\mathbf{x}}^i_{(k)}\right) \\
=&-2\beta^2 \sum_{i=1}^{|a|} \sum_{r\in N_i} \left(\mathbf{H}^i_{(k+1)} \mathbf{A}_{(k)} \tilde{\mathbf{x}}^i_{(k)}\right)^T \left(\mathbf{H}^i_{(k+1)} \mathbf{A}_{(k)} \tilde{\mathbf{x}}^r_{(k)} - \mathbf{H}^i_{(k+1)} \mathbf{A}_{(k)} \tilde{\mathbf{x}}^i_{(k)}\right) \\
=&\, 2\beta^2 \sum_{l=1}^{n} \left(\boldsymbol{\delta}^l\right)^T \left(\mathbf{H}^i_{(k+1)} \mathbf{A}_{(k)}\right)^T \mathbf{H}^i_{(k+1)} \mathbf{A}_{(k)} \tilde{\mathbf{X}}_{(k)} \mathbf{L} \tilde{\mathbf{X}}^T_{(k)} \boldsymbol{\delta}^l. \qquad (4.47)
\end{aligned}
$$

The final result in (4.47) has been got from the state of the art of graph theory in (4.4) with similar operation that has been done for the second term in (4.46). Considering (4.46) and (4.47), ΔV in (4.42) can be rewritten as:

$$
\begin{aligned}
\Delta V =& \sum_{l=1}^{n} \left(\boldsymbol{\delta}^l\right)^T \tilde{\mathbf{X}}_{(k)} \boldsymbol{\Omega} \tilde{\mathbf{X}}^T_{(k)} \boldsymbol{\delta}^l \\
&+ (2\beta^2 - \beta) \sum_{l=1}^{n} \left(\boldsymbol{\delta}^l\right)^T \left(\mathbf{H}^i_{(k+1)} \mathbf{A}_{(k)}\right)^T \mathbf{H}^i_{(k+1)} \mathbf{A}_{(k)} \tilde{\mathbf{X}}_{(k)} \mathbf{L} \tilde{\mathbf{X}}^T_{(k)} \boldsymbol{\delta}^l. \qquad (4.48)
\end{aligned}
$$

In order to have $\tilde{\mathbf{X}}_{(k)} = \mathbf{0}$, as time is passing and, as a result distributed estimator is asymptotically stable, the second term in (4.48) (i.e. $+ (2\beta^2 - \beta) \sum_{l=1}^{n} \left(\boldsymbol{\delta}^l\right)^T \left(\mathbf{H}^i_{(k+1)} \mathbf{A}_{(k)}\right)^T \mathbf{H}^i_{(k+1)} \mathbf{A}_{(k)} \tilde{\mathbf{X}}_{(k)} L \tilde{\mathbf{X}}^T_{(k)} \boldsymbol{\delta}^l$) is enough to be negative or zero. $(2\beta^2 - \beta)$ has two root (0 and $\frac{1}{2}$) and it is negative for $(0 \leq \beta \leq \frac{1}{2})$ and for other values outside the aforementioned range is positive, so by tuning β, the stability of the proposed distributed estimator can be guaranteed. Definitely one assured answer for β can be $\beta = 0.5$. However, depending on the value of $(\sum_{l=1}^{n} \left(\boldsymbol{\delta}^l\right)^T \left(\mathbf{H}^i_{(k+1)} \mathbf{A}_{(k)}\right)^T \mathbf{H}^i_{(k+1)} \mathbf{A}_{(k)} \tilde{\mathbf{X}}_{(k)} \mathbf{L} \tilde{\mathbf{X}}^T_{(k)} \boldsymbol{\delta}^l)$, surely, there are other values for β (with possibly $(2\beta^2 - \beta)$ of time-varying signal) which would guarantee the stability, too. Therefore, with having $\Delta V < 0$ for any $\tilde{\mathbf{X}}_{(k)} \neq \mathbf{0}$, it can be stated that $\tilde{\mathbf{X}}_{(k)}$ will converge to $\mathbf{0}$ and the studied distributed estimator is globally asymptomatically stable. Therefore, the stability proof is complete. □

4.7 Illustrative example

In this section, the method for distributed estimation (described previously) will be applied to a sample system which is very similar to the system expressed in [Cheng *et al.*, 2009] with the known parameters $n = 5$ state variables, $q = 3$ measurement variables, and $m = 2$ unknown inputs. The number of estimators is 4 and the

Figure 4.1: Connection diagram of four-estimator distributed system.

diagram of their communicational connections is illustrated in Figure 4.1. As can be seen from the connection diagram in Figure 4.1 for instance "Estimator 1" is connected to "Estimator 2" and "Estimator 4" but it is not neighbor of "Estimator 3" since there is no direct connection link between them. Similarly, one can interpret this diagram for any other estimators as well. The process and measurements noise covariances are diagonal and their values are defined as $\mathbf{Q} = 10^{-4} \times \mathbf{I}_5$ and $\mathbf{R}^i = 0.01 \times \mathbf{I}_3$ for $i = 1, \ldots, 4$. The matrices of system (4.6) and measurement (4.7) are given as follows:

$$\mathbf{A} = \begin{bmatrix} 0.5 & 2 & 0 & 0 & 0 \\ 0 & 0.2 & 1 & 0 & 1 \\ 0 & 0 & 0.3 & 0 & 1 \\ 0 & 0 & 0 & 0.7 & 1 \\ 0 & 0 & 0 & 0 & 0.1 \end{bmatrix}, \tag{4.49}$$

$$\mathbf{G} = \begin{bmatrix} 1 & 1 & 0 & 0 & 0 \\ -0.3 & 0 & 0 & 0 & 0 \end{bmatrix}^T, \tag{4.50}$$

$$\mathbf{C}^1 = \begin{bmatrix} 1 & 0 & 0 & 0 & 0 \\ 0 & 1 & 0 & 0 & 0 \\ 0 & 0 & 1 & 0 & 0 \end{bmatrix}, \mathbf{C}^2 = \begin{bmatrix} 1 & 1 & 0 & 0 & 0 \\ 0 & 1 & 1 & 0 & 0 \\ 0 & 0 & 0 & 1 & 1 \end{bmatrix}, \tag{4.51}$$

$$\mathbf{C}^3 = \begin{bmatrix} 0 & 0 & 1 & 0 & 0 \\ 1 & 1 & 0 & 1 & 0 \\ 0 & 1 & 0 & 0 & 1 \end{bmatrix}, \mathbf{C}^4 = \begin{bmatrix} 0 & 1 & 0 & 0 & 0 \\ 0 & 0 & 1 & 0 & 0 \\ 1 & 0 & 0 & 0 & 1 \end{bmatrix}. \tag{4.52}$$

Furthermore, $\beta = 0.5$ is considered equally for the four estimators. The unknown inputs of the system are depicted in Figure 4.2. The initial values of the estimators

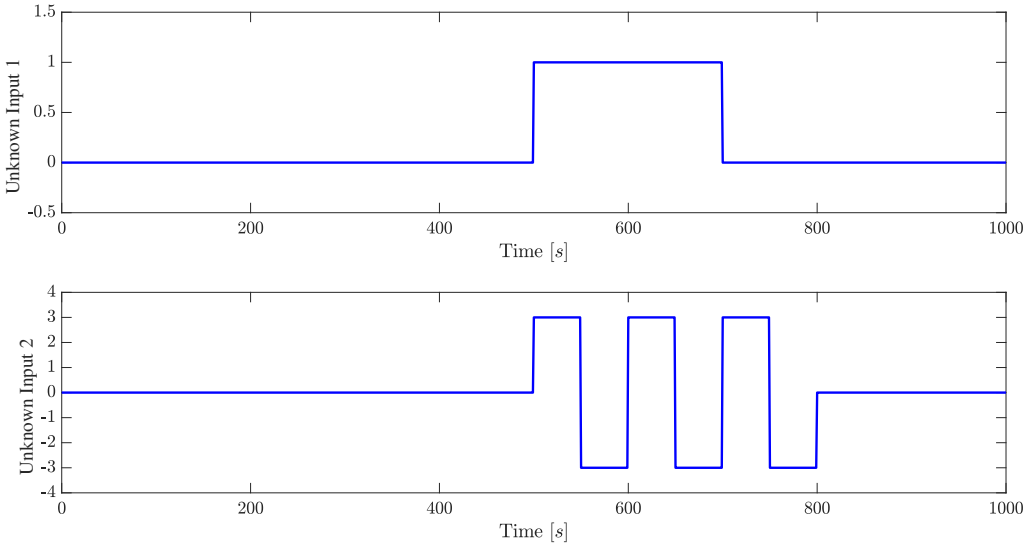

Figure 4.2: Unknown inputs of the given system.

are defined as follows:

$$\begin{aligned} \mathbf{P}^{i}_{(0)} &= 10^{3}, \\ \hat{\mathbf{x}}^{i}_{(0)} &= \begin{bmatrix} 1 & 1 & 1 & 1 & 1 \end{bmatrix}^{T}, \ i = 1, \ldots, 4. \end{aligned} \tag{4.53}$$

In order to analyze the performance of the mentioned distributed estimator (DE) method, its root-mean-square error (RMSE) of unknown and states estimations are compared with the corresponding results in its counterpart centralized estimator (CE) presented in [Gillijns and Moor, 2007a]. For the CE, the centralized measurement matrix is defined as $\mathbf{C} = [(\mathbf{C}^1)^T, (\mathbf{C}^2)^T, (\mathbf{C}^3)^T, (\mathbf{C}^4)^T]^T$. The RMSE for the states and unknown inputs of the DE and CE are specified and compared in Table 4.2. According to the results, the RMSE of the inputs in the DE is considerably higher than the one in the CE. As a result, these higher errors in estimation of input could degrade the estimation of the first two states, which are directly affected by the unknown inputs, in comparison with the results of its counterpart CE. However, the state errors of the DE are not very different from the CE's error which shows the effectiveness of presented distributed estimator.

In Figures 4.3 and 4.4 the actual first and second elements of the state vector together with their corresponding estimates are demonstrated, respectively.

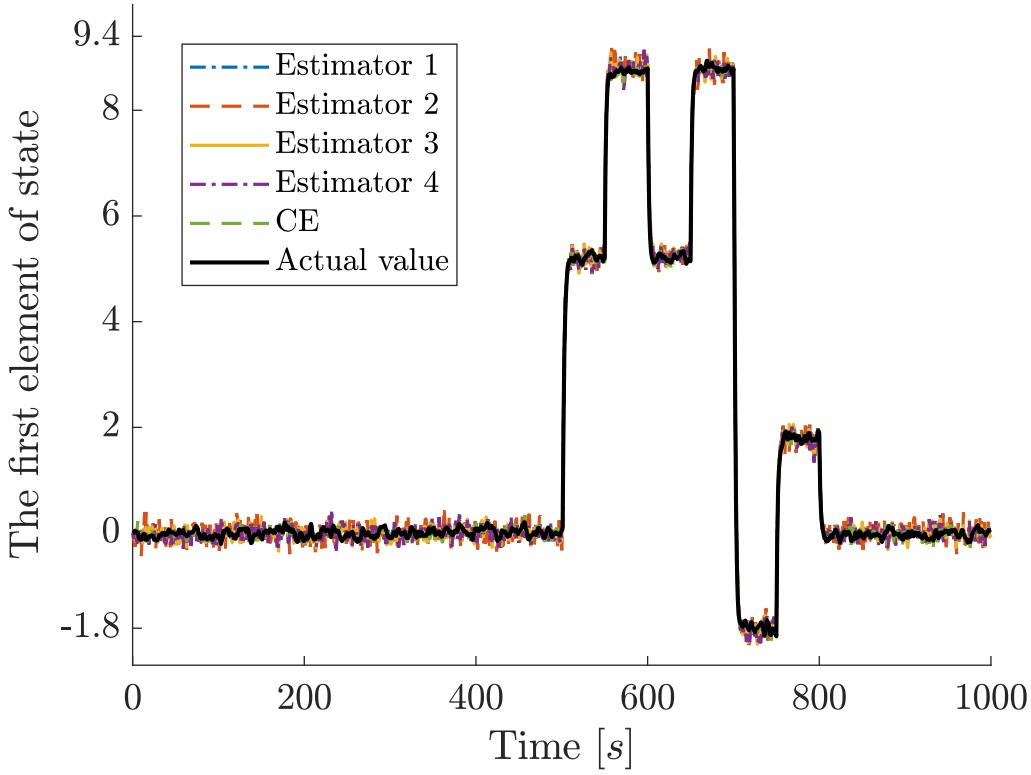

Figure 4.3: The actual and corresponding state estimation of the first component of state vector.

Table 4.2: Comparison of distributed estimation and centralized estimation in term of RMSE.

	Est. 1	**Est. 2**	**Est. 3**	**Est. 4**	**Est. CE**
States					
x_1	0.0712	0.1348	0.0846	0.1004	0.0530
x_2	0.0718	0.0970	0.0703	0.0999	0.0442
x_3	0.0151	0.0151	0.0153	0.0155	0.0148
x_4	0.0213	0.0199	0.0215	0.0213	0.0186
x_5	0.0101	0.0100	0.0101	0.0101	0.0099
Inputs					
d_1	0.1017	0.1014	0.1005	0.1055	0.0517
d_2	0.6449	0.8625	0.8332	0.7908	0.3676

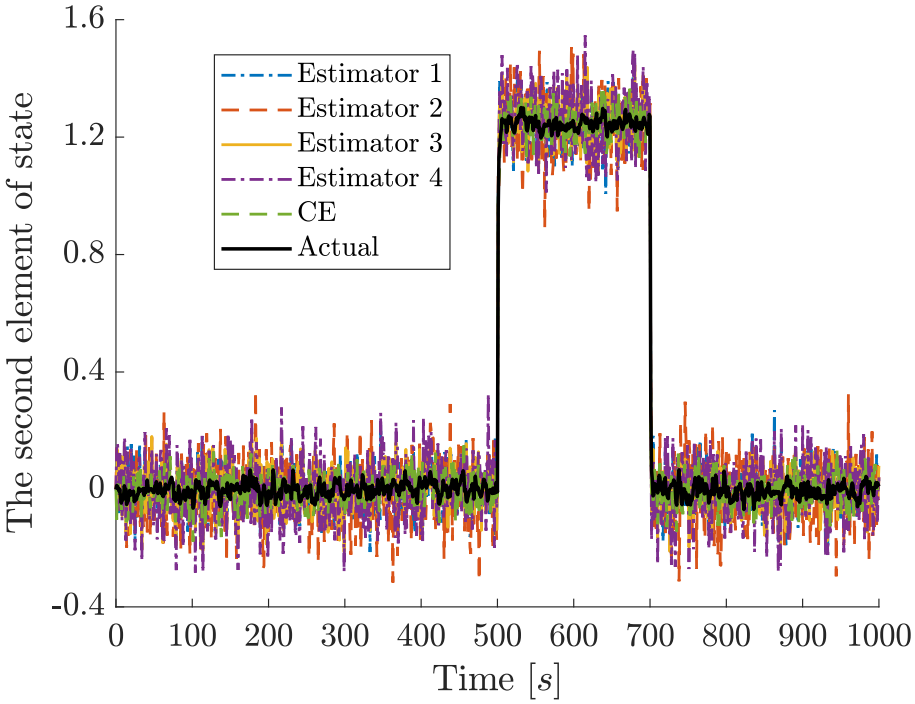

Figure 4.4: The actual and corresponding state estimation of the second component of state vector.

4.8 Conclusion

In this Chapter we developed a distributed method for the simultaneous estimation of states and unknown inputs for linear discrete-time systems. The unbiasedness and minimum variance of the state and unknown input estimation were investigated and verified. The condition making the estimator stable was stated, from which the sufficient distributed gain was extracted. Finally, the proposed method was applied to a system and its results were compared to the results of the centralized estimator. Due to the proposed distributed approach, all individual estimators can estimate state variables and unknown input variables precisely, as evidenced by the example results.

Chapter 5

A Systematic Approach to Modeling Synchronous Generator Using Markov Parameters and T-S Fuzzy Systems

Contents

5.1 Introduction

Synchronous generators (SGs) are key components in power system stability, energy delivery, and energy efficiency. SGs have been the object of research in a variety of applications and problems involving control, monitoring, and estimation. To address these problems, the SG model is a fundamental issue. A SG is a highly nonlinear and long-term time-varying device, and phenomena such as load and temperature variations, aging, or even a critical event like a three-phase short-circuit at the SG's terminals can lead to noticeable changes in its model [Zaker *et al.*, 2016; Micev *et al.*, 2021; Mitra *et al.*, 2021].

In order to obtain synchronous generator models, a variety of identification methods have been proposed, and these methods can be divided into two main categories [Micev *et al.*, 2022]. In the first category [Hasni *et al.*, 2021; Mouni *et al.*, 2008; Hasni *et al.*, 2010; Lidenholm and Lundin, 2010; Vandoorn *et al.*, 2010; IEEE, 2010; Wamkeue *et al.*, 2011; Arjona *et al.*, 2011; Belqorchi *et al.*, 2019; Faria *et al.*, 2020; Ma *et al.*, 2020; Micev *et al.*, 2021; Arastou *et al.*, 2021a; Micev *et al.*, 2022], the generator must be disconnected from the grid before the identification process can be performed (off-grid mode), whereas in the second category [Shamsollahi and Malik, 1996; Fard *et al.*, 2005; Ganjefar and Alizadeh, 2011; Karrari and Malik, 2004; Karrari *et al.*, 2006; Dehghani and Nikravesh, 2008; Ghahremani *et al.*, 2008; Dehghani *et al.*, 2010; Khodadadi *et al.*, 2018; Huang *et al.*, 2020; Mitra *et al.*, 2021; Grillo *et al.*, 2021; Bendaoud *et al.*, 2021; Arastou *et al.*, 2021b; Shariati *et al.*, 2021], the generator can remain in service without having to be disconnected from the grid (on-grid mode).

IEEE standards cover some off-grid methods, known as traditional methods [IEEE, 2010]. However, there are some others, such as open-circuit frequency response (OCFR) [Mouni *et al.*, 2008], stand-still frequency response (SSFR) [Belqorchi *et al.*, 2019], and DC excitation-based [Hasni *et al.*, 2010], that can also be considered as off-grid methods. The downsides of these methods include, but are not limited to, being time-consuming, costly, and difficult to implement, and above all unable to maintain accuracy as the SG status changes due to, for instance, aging or

saturation effects [Mitra *et al.*, 2021].

In order to overcome these drawbacks, on-grid methods have been proposed. These methods can be categorized into two groups, gray-box and black-box [Zaker *et al.*, 2016]. For the former, a model structure derived from physical-mathematical principles is assumed, and its parameters are determined from the defined input and output (I/O) data measured from the system (i.e. SG) [Brus *et al.*, 2008]. There are two aspects to be determined for all these methods, namely their model structure and order (3rd-, 4th-, 5th-, or 7th-order, etc) and the quantities to be measured as inputs and outputs.

While gray-box methods are widely used, as can be seen in many works that have incorporated these approaches [Shamsollahi and Malik, 1996; Fard *et al.*, 2005; Ganjefar and Alizadeh, 2011; Karrari and Malik, 2004; Karrari *et al.*, 2006; Dehghani and Nikravesh, 2008; Ghahremani *et al.*, 2008; Dehghani *et al.*, 2010; Khodadadi *et al.*, 2018; Huang *et al.*, 2020; Mitra *et al.*, 2021; Grillo *et al.*, 2021; Bendaoud *et al.*, 2021; Arastou *et al.*, 2021b; Shariati *et al.*, 2021], assuming a model that is required for these methods can limit the identification process in two ways. First, they may not utilize all the capacity provided by the measured data to calculate a model of higher rank and, consequently, higher accuracy. Secondly, to use these methods, one must have some basic knowledge of the generator model.

Also, these methods may have some other limitations. For example, in [Shariati *et al.*, 2021] the authors proposed a method based on Artificial Neural Network (ANN) to determine the dynamic parameters of salient-pole generators, but this method requires the application of disturbances to the generator under test, and the obtained parameters may suffer from some inaccuracies depending on the disturbance and/or the machine operating point. In a recent work [Grillo *et al.*, 2021], an online method was proposed to determine a subset of the synchronous generator parameters from online measurements while the generator is in normal operation and experiencing small disturbances. However, the successful application of this method depends on the estimation of load angle.

On the other hand, with black-box methods there is no need to assume any special physical-mathematical-based model structure since these methods simply use the measured I/O data obtained from the system (i.e. SG) [Liu *et al.*, 2020] under study, and then attempt to attain a model with the ability to precisely map a set of inputs to a set of outputs. Forward Neural Network (FNN) [Shamsollahi and

Malik, 1996], Volterra series [Fard *et al.*, 2005], and Self-Recurrent Wavelet Neural Networks (SRWNNs) [Ganjefar and Alizadeh, 2011] are some techniques that have been employed to implement a black-box method. However, these studies were all conducted under the infinite-bus condition.

Besides the discussed limitations associated with existing off-grid and on-grid methods, it is inspiring that fuzzy logic has shown big successes in a variety of applications, including control systems engineering [Mendes *et al.*, 2020], electric machines [Chang *et al.*, 2016], clustering [Pehlivan and Turksen, 2021], inventory planning models [Ketsarapong *et al.*, 2012], identification and modeling [Rastegar *et al.*, 2017; Precup *et al.*, 2021] as well as fuzzy inference system modeling [Pozna *et al.*, 2012]. Furthermore, the Takagi Sugeno (T-S) fuzzy system, which is a type of fuzzy inference system, has shown a noticeable ability to model nonlinear systems using linear sub-models [Mani *et al.*, 2021], and its successful application in areas such as electric machines [Kuppusamy and Joo, 2021], and identification and modeling [Rastegar *et al.*, 2017; Precup *et al.*, 2021] also confirms its capabilities. Motivated by these facts, in this chapter, a Takagi-Sugeno (T-S) fuzzy system has been chosen for achieving an accurate global model for a real synchronous generator, where the obtained model is expected to be suitable for deploying into controllers such as model predictive controllers (MPCs) [Hadla and Cruz, 2017; Gonçalves *et al.*, 2019; Mendes *et al.*, 2013].

The process of fuzzy modeling consists of two main tasks, namely structure and parameter determination are needed to be planned and accomplished [Wiktorowicz and Krzeszowski, 2019]. Structure determination is concerned with determining the number of rules and the linear state space models, which involves computing the parameters of the state space models, in the consequent part of the T-S fuzzy model, whereas parameter determination is concerned with finding fuzzy set parameters in the antecedent part of T-S fuzzy model. The initial number of rules can be determined arbitrarily based mainly on the available number of datasets and their corresponding sizes (refer to Section 5.5), and as the number of rules increases, the accuracy of the overall model could improve, but at the cost of more required computational resources.

To calculate the parameters of the state space model, for each existing T-S fuzzy rule, a subspace identification method (SIM) has been applied that involves a combination of observer/Kalman filter identification (ORKID) [Aitken and Clarke,

2012] and eigensystem realization algorithm (ERA) [Aitken and Clarke, 2012; Tsai *et al.*, 2007] called ORKID/ERA [Aitken and Clarke, 2012; Tsai *et al.*, 2007]. The choice has been made because, on the one hand, the identification method has been validated in a variety of applications, as reported for example in [Aitken and Clarke, 2012; Kim and Lynch, 2012; Zhang *et al.*, 2014a; Everett and Dubay, 2017; Fan and Miao, 2021; Mejia-Ruiz *et al.*, 2021], and on the other hand, owing to its simplicity, stability [Zhou *et al.*, 2017], and ability to handle bias issues [Qin, 2006]. Since the successful implementation of SIM is crucial to the success of the final model, two important steps in this method, namely calculating Markov parameters (MPs) and implementing ERA, are discussed in more detail in Section 5.4.

As a main contribution, this work contributes to the methods for developing more accurate models for highly nonlinear systems like SG, which are essential, e.g. to techniques such as model predictive controllers (MPCs). This chapter presents a new data-driven approach based on T-S fuzzy and SIM for finding a global model for a synchronous generator. Unlike the methods in [Karrari and Malik, 2004; Ghahremani *et al.*, 2008; Dehghani and Nikravesh, 2008; Dehghani *et al.*, 2010; Grillo *et al.*, 2021], where connection to an infinite bus is necessary, such a condition is not required for the proposed approach, due to taking generator terminal voltage into account as an input. Micev *et al.* [2022] highlighted that most existing on-grid identification methods like [Dehghani *et al.*, 2010; Khodadadi *et al.*, 2018; Huang *et al.*, 2020; Mitra *et al.*, 2021; Grillo *et al.*, 2021; Bendaoud *et al.*, 2021] require additional equipment to inject extra signals for identification purposes, increasing the setup costs, while in this work, there is no need to inject extra signals. The proposed method leads to a hybrid model (a model possessing the main features of models obtained from either gray-box or black-box methods) that can be utilized by any user, regardless of their knowledge of the system (here SGs). However, a professional user can even gain more insight into the generator structure and condition since the sub-models computed from I/O data are in the form of state space equations, as discussed in Section 5.4.2. Indeed, the state space representations allow the determination of, for example, the order of sub-models or even comparisons between corresponding current and earlier sub-models, which can be used to detect faults and/or monitor the condition of the synchronous generator, as in [Gopinath *et al.*, 2016]. Furthermore, the presence of noise in some works, such as [Dehghani and Nikravesh, 2008], and saturation effects in some other works, such as [Kar-

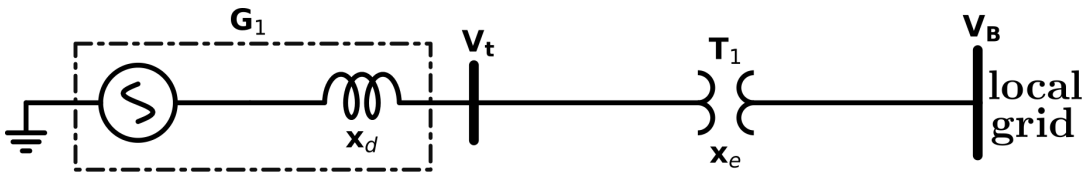

Figure 5.1: The studied system diagram.

rari and Malik, 2004; Dehghani and Nikravesh, 2008; Ghahremani *et al.*, 2008], can negatively affect the performance of the models proposed therein, but the model obtained from the method proposed in this chapter does not have such problems and can accurately approximate the active and reactive powers of the generator for a wide range of operating inputs.

The results of the simulation and experimental case studies, which serve as validations of the proposed methodology, confirm its effectiveness.

This Chapter is organized as follows. In Section 5.2 the main problem is explained. In Section 5.3 the Fuzzy model strategies are given in more detail. Subspace state-space identification is discussed in more detail in Section 5.4. In Section 5.5, both a simulation and a experimental case studies are employed to validate the proposed approach. Finally, concluding remarks are presented in Section 5.6.

5.2 Problem Description

The main objective of this Chapter is to propose a method to identify and model a real synchronous generator in a more systematic and flexible way. For this purpose, the generator is arranged in a circuit, as illustrated in Figure 5.1, where it is connected to a local bus via the transmission line x_e. The new methodology is not only applied to a real-world generator, but also to a nonlinear fourth-order model, which is widely used in simulation frameworks to represent synchronous generators due to the following reasons. First, most researchers are familiar with this model, and they can access it easily if they want to replicate the results, or it could serve as a benchmark for any future similar research. Secondly, since a linearized approximation model of this nonlinear model can be obtained analytically with some computational efforts, the local sub-models' results of the proposed method can also be compared with those of the linear model. Thirdly, in some situations, simulation can be more useful than an experimental test to demonstrate the capability of a pro-

posed methodology. This is especially true when the devices used in the real testing setup may have some technical limitations, like ranges or input rates. In Section 5.5.1, two examples of such situations will be presented. The nonlinear fourth-order model of the generator and its linearized model will be described next.

5.2.1 Synchronous Generator Model

In order to generate the needed data samples for testing the proposed approach in simulation studies, a synchronous generator model, which is based on the model described in Section 2.3.2 is utilized. The linearized equations corresponding to the nonlinear model of a synchronous generator, which is defined in (2.13), will be computed in Section 5.2.2.

5.2.2 Linearized Synchronous Generator Model

A linearized model of (2.13) can be computed and is given by:

$$
\begin{aligned}
\Delta\dot{x_1} &= \omega_0 \Delta x_2, \qquad (5.1)\\
\Delta\dot{x_2} &= -\frac{1}{2H}\left[\frac{V_B}{x_{td}} x_3^0 \cos(x_1^0)\right.\\
&\quad \left. + (V_B)^2 \left(\frac{1}{x_{tq}} - \frac{1}{x_{td}}\right)\cos(2x_1^0)\right]\Delta x_1\\
&\quad - \frac{K^d}{2H}\Delta x_2 - \frac{V_B}{2H\, x_{td}}\sin(x_1^0)\,\Delta x_3 + \frac{1}{2H}\,\Delta P^m,\\
\Delta\dot{x_3} &= \frac{-V_B}{T'_{do}\, x_{td}}\,(x_d - x'_d)\,\sin(x_1^0)\,\Delta x_1\\
&\quad - \frac{1}{T'_{do}}\left(1 + \frac{x_d - x'_d}{x_{td}}\right)\Delta x_3 + \frac{1}{T'_{do}}\Delta E_{fd},\\
\Delta\dot{x_4} &= \frac{-1}{T'_{qo}\, x_{tq}}\,(x_q - x'_q) V_B \cos(x_1^0)\,\Delta x_1 - \frac{1}{T'_{qo}}\,\Delta x_4.
\end{aligned}
$$

The linearized model of active and reactive powers can be found as (5.2) and

(5.3):

$$\begin{aligned}\Delta P = &\left[\frac{V_B}{x_{td}} x_3^0 \cos(x_1^0) + V_B^2 \left(\frac{1}{x_{tq}} - \frac{1}{x_{td}}\right) \cos(2x_1^0)\right] \Delta x_1 \\ &+ \frac{V_B \sin(x_1^0)}{x_{td}} \Delta x_3, \qquad (5.2)\\ \Delta Q = &\left[\left(\frac{-1}{x_{tq}} + \frac{1}{x_{td}}\right) V_B^2 \sin(2x_1^0) + \left(\frac{-x_e}{x_{td}^2} + \frac{x_e}{x_{tq}^2}\right) V_B^2 \sin(2x_1^0)\right. \\ &\left. + \left(\frac{2x_e}{x_{td}^2} - \frac{1}{x_{td}}\right) V_B x_3^0 \sin(x_1^0)\right] \Delta x_1 \\ &+ \left[\left(\frac{-2x_e}{x_{td}^2} + \frac{1}{x_{td}}\right) V_B \cos(x_1^0) + 2\frac{x_e\, x_3^0}{x_{td}^2}\right] \Delta x_3, \qquad (5.3)\end{aligned}$$

where $x_i^0, i = 1, \ldots, 4$ define the operating point of the nonlinear system. From (5.1), (5.2), and (5.3), it is possible to write the linearized equations in a compact state-space form as follows:

$$\begin{aligned}\Delta \dot{\mathbf{x}} &= \mathbf{A}\, \Delta \mathbf{x} + \mathbf{B}\, \Delta \mathbf{u},\\ \Delta \mathbf{y} &= \mathbf{C} \Delta \mathbf{x}, \qquad (5.4)\end{aligned}$$

where $\Delta \mathbf{u} = [\Delta P_m \ \Delta E_{fd}]^T$, $\Delta \mathbf{x} = [\Delta x_1 \ \Delta x_2 \ \Delta x_3 \ \Delta x_4]^T$, $\Delta \mathbf{y} = [\Delta P \ \Delta Q]^T$, and the entries of matrices $\mathbf{A}$, $\mathbf{B}$ and $\mathbf{C}$, which are indeed the coefficients corresponding to $\Delta \mathbf{x}$, $\Delta \mathbf{u}$, and $\Delta \mathbf{y}$, respectively, can be obtained easily from (5.1), (5.2), and (5.3).

5.3 Fuzzy Modeling

In this chapter, a synchronous generator is represented by the following fuzzy structure:

$$\begin{aligned}R^i : &\textbf{IF } z_{(1,k)} \text{ is } F_1^i \text{ and } \ldots \text{ and } z_{(p,k)} \text{ is } F_p^i\\ &\textbf{THEN} \begin{cases} \mathbf{x}_{(k+1)}^i &= \mathbf{A}^i \mathbf{x}_{(k)}^i + \mathbf{B}^i \mathbf{u}_{(k)},\\ \mathbf{y}_{(k)}^i &= \mathbf{C}^i \mathbf{x}_{(k)}^i + \mathbf{D}^i \mathbf{u}_{(k)}, \end{cases} \qquad (5.5)\end{aligned}$$

where R^i represents the i-th fuzzy inference rule ($i = 1, 2, \ldots, R$), $\mathbf{z}_{(k)} = [z_{(1,k)}, z_{(2,k)}, \ldots, z_{(p,k)}]^T$ is the vector of antecedent variables on the k-th instant of time, F_j^i is the i-th fuzzy set of the j-th antecedent variable ($j = 1, 2, \ldots, p$). In

the consequent part, $\mathbf{A}^i \in \mathbb{R}^{n\times n}$, $\mathbf{B}^i \in \mathbb{R}^{n\times m}$, $\mathbf{C}^i \in \mathbb{R}^{q\times n}$ and $\mathbf{D}^i \in \mathbb{R}^{q\times m}$, are the parameters of the i-th submodel of the n-th order system with m inputs, and q outputs. $\mathbf{x}^i_{(k)} = [x^i_{(1,k)}, x^i_{(2,k)}, \ldots, x^i_{(n,k)}]^T \in \mathbb{R}^n$ is the state vector of the i-th submodel, $\mathbf{y}^i_{(k)} = [y^i_{(1,k)}, y^i_{(2,k)}, \ldots, y^i_{(q,k)}]^T \in \mathbb{R}^q$ is the output vector of the i-th submodel and $\mathbf{u}_{(k)} = [u_{(1,k)}, u_{(2,k)}, \ldots, u_{(m,k)}]^T \in \mathbb{R}^m$ is the input vector of the system. In order to identify the model of the system defined by (2.13), the measured quantities which are available as inputs are P^m (mechanical power), E_{fd} (field voltage), and V_t (terminal voltage), while as outputs, P (electrical active power) and Q (electrical reactive power) are measured (thus, $m = 3$ and $q = 2$).

Let $\mu^i_{F^i_j}(z_{(j,k)}) : R \to [0,1]$ $(j = 1, \ldots, p)$ be the membership function of the antecedent fuzzy set F^i_j at the k-th sample of the linguistic variable, $z_{(j,k)}$, in a universe of discourse U_{z_j} partitioned by fuzzy sets, or linguistic terms, F^i_j, then the activation degree of the i-th fuzzy rule is given by:

$$h^i_{(k)} = \mu^i_{F^i_1}(z_{(1,k)}) \circ \mu^i_{F^i_2}(z_{(2,k)}) \circ \cdots \circ \mu^i_{F^i_p}(z_{(p,k)}), \tag{5.6}$$

where the symbol $\circ$ represents a t-norm operator [Jin, 2017].

The normalized activation degree of the i-th rule is given by [Szedlak-Stinean *et al.*, 2022]:

$$\gamma^i(\mathbf{z}_{(k)}) = \frac{h^i_{(k)}}{\sum_{i=1}^R h^i_{(k)}}. \tag{5.7}$$

The output of the fuzzy TS model is given by:

$$\begin{cases} \tilde{\mathbf{x}}_{(k+1)} = \sum_{i=1}^R \gamma^i(\mathbf{z}_{(k)})\mathbf{x}^i_{(k+1)}, \\ \tilde{\mathbf{y}}_{(k)} = \sum_{i=1}^R \gamma^i(\mathbf{z}_{(k)})\mathbf{y}^i_{(k)}. \end{cases} \tag{5.8}$$

Substituting (5.5) into (5.8) results in:

$$\begin{cases} \tilde{\mathbf{x}}_{(k+1)} = \sum_{i=1}^R \mathbf{A}^i\gamma^i(\mathbf{z}_{(k)})\mathbf{x}^i_{(k)} + \sum_{i=1}^R \mathbf{B}^i\gamma^i(\mathbf{z}_{(k)})\mathbf{u}_{(k)}, \\ \tilde{\mathbf{y}}^i_{(k)} = \sum_{i=1}^R \mathbf{C}^i\gamma^i(\mathbf{z}_{(k)})\mathbf{x}^i_{(k)} + \sum_{i=1}^R \mathbf{D}^i\gamma^i(\mathbf{z}_{(k)})\mathbf{u}_{(k)}. \end{cases} \tag{5.9}$$

5.3.1 Batch Fuzzy Clustering Algorithm

Fuzzy clustering algorithms can be used to determine the antecedent fuzzy sets F_j^i in (5.5) by using experimental datasets of the system. Among the most well known algorithms are the Fuzzy C-Means (FCM); and the Fuzzy Maximum Likelihood Estimates (FMLE). In this work, the FCM algorithm is selected for clustering. The objective of the FCM is to find a membership matrix $\mathbf{U} = [\mu^1; \mu^2; \cdots; \mu^c] \in \mathbb{R}^{N\times c}$, and a centers matrix $\mathbf{V} = [\mathbf{v}_1; \mathbf{v}_2; \cdots; \mathbf{v}_c]$ with $\mathbf{v}_i \in \mathbb{R}^p$, where c is the number of clusters, N is the number of data points, and p is the dimensionality of a dataset $\mathbf{z}_{(k)}$ such that the following objective function J_m is minimized [Mendes *et al.*, 2013]:

$$J_m = \sum_{k=1}^{N}\sum_{i=1}^{c}(\mu^i(\mathbf{z}_{(k)}))^\eta (d^i_{(k)})^2, \tag{5.10}$$

where $\mu^i(\mathbf{z}_{(k)})$ is the membership function of the k-th data point in the i-th cluster, $\eta \in (1, \infty)$ is a weighting constant that controls the degree of fuzzy overlap, and $d^i_{(k)} = ||\mathbf{z}_{(k)} - \mathbf{v}_i||$ is the Euclidean distance between $\mathbf{z}_{(k)}$ and cluster center $\mathbf{v}_i$. Assuming that $||\mathbf{z}_{(k)} - \mathbf{v}_i|| \neq 0$, $\forall\, k = 1, \ldots, N$, $\forall\, i = 1, \ldots, c$, then $\mathbf{U}$ and $\mathbf{V}$ is a local minimum for J_m if:

$$\mu^i(\mathbf{z}_{(k)}) = \left(\frac{\sum_{i=1}^{c}||\mathbf{z}_{(k)} - \mathbf{v}_i||}{||\mathbf{z}_{(k)} - \mathbf{v}_i||}\right)^{\frac{2}{\eta-1}}, \tag{5.11}$$

where

$$\mathbf{v}_i = \frac{\sum_{k=1}^{N}\left(\mu^i(\mathbf{z}_{(k)})\right)^\eta \mathbf{z}_{(k)}}{\sum_{k=1}^{N}\left(\mu^i(\mathbf{z}_{(k)})\right)}. \tag{5.12}$$

The FCM algorithm performs several iterations in order to reduce as much as possible the objective function defined in (5.10) until either (5.13) or (5.14) are met:

$$||\mathbf{U}^{(l+1)} - \mathbf{U}^l|| < \epsilon, \tag{5.13}$$

$$||J_m^{(l+1)} - J_m^l|| < \epsilon, \tag{5.14}$$

where l is the current iteration number and ϵ is a specified minimum threshold or tolerance. The fuzzy C-Means algorithm is implemented as specified in Algorithm

Algorithm 5.1 Fuzzy C-Means Clustering Algorithm

Receives a dataset $\{\mathbf{z}_{(k)}\}$ with $k = 1, 2, \ldots, N$ data points;
Fixes $c \in \{2, 3, \ldots, N-1\}$ and $\eta \in (1, \infty)$;
Initialize $\mathbf{U}^{(0)}$, i.e. randomly initialize the cluster membership values, μ^i;
repeat
  Compute the c mean vectors or centers using (5.12);
  Update $\mathbf{U}^{(l)}$ to $\mathbf{U}^{(l+1)}$ according to (5.11);
  Calculate the objective function J_m with (5.10);
until $||\mathbf{U}^{(l+1)} - \mathbf{U}^{(l)}|| < \epsilon$ **or** $||J_m^{(l+1)} - J_m^{(l)}|| < \epsilon$.

5.1. In the current work, despite the fact that each dataset sample can be assigned to more than one cluster at the same time using FCM, for simplicity each sample will be assigned to only one cluster in which it has the highest degree of membership. The FCM method identifies the number of fuzzy rules (clusters) as well as the centers v_i of the Gaussian membership functions [Boulkaibet *et al.*, 2017]

$$\mu_{F_j^i}(z_{(j,k)}) = \exp\left[-\frac{1}{2}\left(\frac{z_{(j,k)} - v_i}{\sigma_j^i}\right)^2\right], \tag{5.15}$$

associated to each fuzzy set F_j^i. To determine the optimal width (σ_j^i) of each membership function, one can use Particle Swarm Optimization (PSO), as shown, for example, in [Shihabudheen *et al.*, 2018]. A function that is to be minimized can for example be the mean square error (MSE) defined as follows:

$$\begin{aligned} &\min_{\sigma_j^i} \quad \text{MSE}(\hat{y}_k)\,, && \text{MSE}\,(\hat{y}_k) \triangleq \frac{1}{L}\sum_{k=1}^{L} ||\hat{y}_k - y_k||^2, \\ &\text{s.t.} \quad \sigma_j^i > 0 \end{aligned} \tag{5.16}$$

where, $y_k \in \mathbb{R}$ is the true value of each available output getting from the real (nonlinear) system at the sample time k, $\hat{y}_k$ is the value of the corresponding output obtained from the identified model at the sample time k, and L is the total number of data samples. Indeed, the PSO stage is the final stage of training. To realize this step, a different dataset from the one which has been utilized for sub-models identification (refer to Section 5.4), will be used. This will be illustrated more explicitly in Section 5.5, where proposed approach is validated by using simulation and experimental case studies. Another issue that is important to be taken into

consideration, is the number of rules. The number of clusters is determined by the user, which would depend on the size of dataset (the number of available sampled inputs and outputs). Using the FCM method, the dataset is partitioned into clusters. Using each cluster, the parameters of the state-space sub-model, corresponding to the cluster, can be calculated. Therefore, the number of clusters at the beginning represents the number of rules as well. Nevertheless, in practice, only a subset of the initial rules are maintained, and other rules are eliminated during the process of testing sub-models (comparing the outputs of computed state space models with true values). Keeping or removing such rules can be based on a variety of general objectives. For instance, in this work, one can keep rules whose state space sub-models result in more precise active power, reactive power or both. It is obvious that by taking such an action, the effective number of rules is reduced. As a result, PSO has less computational operations, due to decreasing the number of parameters that need to be optimized. Moreover, the problem of overfitting in data-driven modeling is always of concern, this issue will be discussed in Section 5.5, where it is explained with examples how stages like training and testing are conducted. Section 5.4 outlines the steps to calculate the parameters of each sub-model (state space model parameters) corresponding to the consequent part of each existing T-S fuzzy rule.

5.4 Subspace State-Space Identification Method

In this section, the identification of each sub-model from the clustered (I/O) data, and more specifically, computing the state-space parameters of each submodel in (5.5) (i.e. $\mathbf{A}^i, \mathbf{B}^i, \mathbf{C}^i$, and $\mathbf{D}^i$) is presented in more detail. Thus, for the sake of convenience, the i-th local model of the system defined in the consequent part of equation (5.5), with a slight change in its input term $\mathbf{u}_{(k)}$, is represented by (5.17)-(5.18), where the input is given by $\mathbf{u}^i_{(k)}$:

$$\mathbf{x}^i_{(k+1)} = \mathbf{A}^i\,\mathbf{x}^i_{(k)} + \mathbf{B}^i\,\mathbf{u}^i_{(k)}, \tag{5.17}$$

$$\mathbf{y}^i_{(k)} = \mathbf{C}^i\,\mathbf{x}^i_{(k)} + \mathbf{D}^i\,\mathbf{u}^i_{(k)}. \tag{5.18}$$

This change in the input term is due to the fact that, for the purpose of identification, only the values of the inputs corresponding to the cluster i are utilized,

and not all values for the inputs corresponding the dataset. To identify each model i, first the system Markov parameters are obtained by using the observer/Kalman filter identification (OKID) approach [Aitken and Clarke, 2012]. Then, using the ERA algorithm [Aitken and Clarke, 2012] the order of each submodel i and the corresponding state space matrices (i.e. $\mathbf{A}^i, \mathbf{B}^i, \mathbf{C}^i, \mathbf{D}^i$), will be calculated.

5.4.1 Markov Parameters Calculation

In this section, the concept of the system Markov parameters is explained and then it is presented how these parameters for each local submodel i are extracted from the clustered data. Before continuing with the definition and calculation of the Markov parameters, some preliminary notations will be defined. The dataset $S := \{(\mathbf{u}_{(k)}^T, \mathbf{y}_{(k)}^T) | \, k = 0, 1, 2, \ldots, l-1\}$ consists of all the manipulated inputs $\mathbf{u}_{(k)} \in \mathbb{R}^m$ and the corresponding measured outputs $\mathbf{y}_{(k)} \in \mathbb{R}^q$ at the time steps $k = 0, \ldots, l-1$, where $l := |S|$ indicates the whole number of available data samples. Additionally, for the purpose of identification, using the clustering method given in Section 5.3.1, the dataset S is partitioned into c smaller datasets S^i, $i \in \{1, 2, \ldots, c\}$, and similarly for each dataset S^i, the total number of samples is represented by $l^i := |S^i|$.

The clustered samples S^i are used to determine the Markov parameters of the local subsystem, i, for $i = 1, \ldots, c$. In this way, assuming $\mathbf{x}_{(0)}^i = \mathbf{0}$, then from (5.18) for the l^i samples:

$$\mathbf{y}^i = \mathbf{Y}^i \, \mathbf{U}^i, \tag{5.19}$$

where

$$\mathbf{y}^i = \left[\mathbf{y}^i_{(0)}, \mathbf{y}^i_{(1)}, \ldots, \mathbf{y}^i_{(l^i-1)}\right] \in \mathbb{R}^{q\times l^i},$$
$$\mathbf{Y}^i = \left[\mathbf{D}^i \quad \mathbf{C}^i\,\mathbf{B}^i \quad \mathbf{C}^i\,\mathbf{A}^i\,\mathbf{B}^i \quad \cdots \quad \mathbf{C}^i\left(\mathbf{A}^i\right)^{l^i-2}\mathbf{B}^i\right] \in \mathbb{R}^{q\times(m\,l^i)},$$
$$\mathbf{U}^i = \begin{bmatrix} \mathbf{u}^i_{(0)} & \mathbf{u}^i_{(1)} & \mathbf{u}^i_{(2)} & \cdots & \mathbf{u}^i_{(l^i-1)} \\ \mathbf{0} & \mathbf{u}^i_{(0)} & \mathbf{u}^i_{(1)} & \cdots & \mathbf{u}^i_{(l^i-2)} \\ \mathbf{0} & \mathbf{0} & \mathbf{u}^i_{(0)} & \cdots & \mathbf{u}^i_{(l^i-3)} \\ \mathbf{0} & \mathbf{0} & \mathbf{0} & \ddots & \vdots \\ \mathbf{0} & \mathbf{0} & \mathbf{0} & \mathbf{0} & \mathbf{u}^i_{(0)} \end{bmatrix} \in \mathbb{R}^{(m\,l^i)\times l^i}. \tag{5.20}$$

Matrix $\mathbf{Y}^i$ consists of all the Markov parameters $\mathbf{D}^i, \mathbf{C}^i\,\mathbf{B}^i, \mathbf{C}^i\,\mathbf{A}^i\,\mathbf{B}^i, \cdots, \mathbf{C}^i\left(\mathbf{A}^i\right)^{l^i-2}\mathbf{B}^i$, which need to be computed. q and m are the numbers of outputs and inputs, respectively and taking into account equations (5.19) and (5.20), it is deduced that if $m > 1$, which is also the case of the current work, then the number of unknown parameters in the matrix $\mathbf{Y}^i$ exceeds the number of known equations which is determined by the dimension of $\mathbf{y}^i$ in (5.20), since obviously $(q \times l^i) < (q \times m\,l^i)$. This implies that matrix $\mathbf{Y}^i$ cannot be determined uniquely, and it is necessary to take this issue into consideration. For example, if each submodel i defined by (5.17)-(5.18) is asymptotically stable, then the eigenvalues of matrix $\mathbf{A}^i$ are inside the unit circle centered at the origin, and as a result, $\left(\mathbf{A}^i\right)^k$, and eventually the corresponding parameters inside matrix $\mathbf{Y}^i$ that have the term $\left(\mathbf{A}^i\right)^k$ will decay to zero for $k \geqslant p$, for some sufficiently large integer p. Therefore, it is sufficient to calculate only the Markov parameters such as $\mathbf{D}^i, \mathbf{C}^i\,\mathbf{B}^i, \mathbf{C}^i\,\mathbf{A}^i\,\mathbf{B}^i, \cdots, \mathbf{C}^i\left(\mathbf{A}^i\right)^{p-1}\mathbf{B}^i$ as the other parameters inside $\mathbf{Y}^i$ can be assumed to be approximately zero. Thus, the truncated form of (5.19) can be given by

$$\mathbf{y}^i = \tilde{\mathbf{Y}}^i\,\tilde{\mathbf{U}}^i, \tag{5.21}$$

where

$$
\begin{aligned}
\mathbf{y}^i &= \left[\mathbf{y}^i_{(0)}, \mathbf{y}^i_{(1)}, \mathbf{y}^i_{(2)}, \ldots, \mathbf{y}^i_{(p)}, \ldots, \mathbf{y}^i_{(l^i-1)}\right] \in \mathbb{R}^{q\times l^i},\\
\tilde{\mathbf{Y}}^i &= \begin{bmatrix} \mathbf{D}^i & \mathbf{C}^i\,\mathbf{B}^i & \cdots & \mathbf{C}^i\left(\mathbf{A}^i\right)^{p-1}\mathbf{B}^i \end{bmatrix} \in \mathbb{R}^{q\times m\,(p+1)},\\
\tilde{\mathbf{U}}^i &= \begin{bmatrix}
\mathbf{u}^i_{(0)} & \mathbf{u}^i_{(1)} & \mathbf{u}^i_{(2)} & \cdots & \mathbf{u}^i_{(p)} & \cdots & \mathbf{u}^i_{(l^i-1)}\\
\mathbf{0} & \mathbf{u}^i_{(0)} & \mathbf{u}^i_{(1)} & \cdots & \mathbf{u}^i_{(p-1)} & \cdots & \mathbf{u}^i_{(l^i-2)}\\
\mathbf{0} & \mathbf{0} & \mathbf{u}^i_{(0)} & \cdots & \mathbf{u}^i_{(p-2)} & \cdots & \mathbf{u}^i_{(l^i-3)}\\
\mathbf{0} & \mathbf{0} & \cdots & \ddots & & \cdots & \vdots\\
\mathbf{0} & \mathbf{0} & \cdots & & \mathbf{u}^i_{(0)} & \cdots & \mathbf{u}^i_{(l^i-p-1)}
\end{bmatrix}.
\end{aligned}
\tag{5.22}
$$

As can be seen, (5.22) can be addressed as a least-squares problem, and consequently can be solved using a variety of approaches, e.g. singular-value decomposition [Emami *et al.*, 2020], [Govindarajan *et al.*, 2020]. Considering the fact that both $\mathbf{y}^i$ and $\tilde{\mathbf{U}}^i \in \mathbb{R}^{m\,(p+1)\times l^i}$ are known and available from the dataset, if $m(p+1) \leq l^i$, then the number of equations will be equal to, or greater than, the number of unknown parameters, and if the rows of $\tilde{\mathbf{U}}^i$ are linearly independent, then by calculating $(\tilde{\mathbf{U}}^i)^\dagger$, which is the pseudo-inverse of $\tilde{\mathbf{U}}^i$, $\tilde{\mathbf{Y}}^i$ can be computed as $\tilde{\mathbf{Y}}^i = \mathbf{y}^i(\tilde{\mathbf{U}}^i)^\dagger$. Clearly, the more independent the rows are, the more accuracy would be achieved in this computation.

If the system is lightly damped, then for the state matrix $\mathbf{A}^i$, $\left(\mathbf{A}^i\right)^k$ could be considered approximately zero, only for $k \geq p$ and for a very large value of p. In this condition, it is still possible to decrease the value of p and consequently, the computational operation needed for obtaining the Markov parameters by means of approach here called observer approach, where using the feedback concepts, e.g. by adding and subtracting the term $\mathbf{M}^i\mathbf{y}^i_{(k)}$ to the right-hand side of the state equation (5.17) of the i-th local model of the system defined in (5.17)-(5.18), and getting the observer system model for submodel i as follows:

$$
\begin{aligned}
\mathbf{x}^i_{(k+1)} &= \mathbf{A}^i\,\mathbf{x}^i_{(k)} + \mathbf{B}^i\,\mathbf{u}^i_{(k)} + \mathbf{M}^i\mathbf{y}^i_{(k)} - \mathbf{M}^i\mathbf{y}^i_{(k)}\\
&= \left(\mathbf{A}^i + \mathbf{M}^i\mathbf{C}^i\right)\mathbf{x}^i_{(k)} + \left(\mathbf{B}^i + \mathbf{M}^i\mathbf{D}^i\right)\mathbf{u}^i_{(k)} - \mathbf{M}^i\mathbf{y}^i_{(k)}\\
&= \bar{\mathbf{A}}^i\mathbf{x}^i_{(k)} + \bar{\mathbf{B}}^i\,\mathbf{v}^i_{(k)}, \qquad (5.23)\\
\mathbf{y}^i_{(k)} &= \mathbf{C}^i\,\mathbf{x}^i_{(k)} + \mathbf{D}^i\,\mathbf{u}^i_{(k)}, \qquad (5.24)
\end{aligned}
$$

where

$$\begin{aligned}\bar{\mathbf{A}}^{i} &= \mathbf{A}^{i} + \mathbf{M}^{i}\mathbf{C}^{i},\\ \bar{\mathbf{B}}^{i} &= \left[\mathbf{B}^{i} + \mathbf{M}^{i}\mathbf{D}^{i}, \quad -\mathbf{M}^{i}\right],\\ \mathbf{v}^{i}_{(k)} &= \left[\left(\mathbf{u}^{i}_{(k)}\right)^{T} \quad \left(\mathbf{y}^{i}_{(k)}\right)^{T}\right]^{T},\end{aligned} \tag{5.25}$$

and $\mathbf{M}^{i}$ is an $n \times q$ arbitrary gain matrix to adjust the eigenvalues of matrix $\bar{\mathbf{A}}^{i}$ in order to make it as stable as desired, and/or to make the system response characteristics as wished, e.g. by attempting to place the eigenvalues of $\bar{\mathbf{A}}^{i}$ as close as possible to the origin to increase the damping of the observer system. Using observer techniques can decrease the computational effort by reducing the number of dataset samples required for calculating the aforementioned Markov parameters. Therefore, instead of calculating the Markov parameters of the main local system i defined by (5.17)-(5.18), it is more convenient and faster to find those of the observer local system i defined by (5.23)-(5.24). In the end, having the Markov parameters of the observer local system i defined by (5.23)-(5.24), the Markov parameters of (5.17)-(5.18) and $\mathbf{M}^{i}$ can be obtained by performing some mathematical manipulations as will be described in the following paragraphs.

Likewise the procedures given to calculate the Markov parameters of the main submodel i, it is possible to obtain the Markov parameters of the observer submodel i. Assuming that $\mathbf{x}^{i}_{(0)} = \mathbf{0}$, and replacing (5.23) into (5.24), then the output $\mathbf{y}^{i}_{(k)}$ can be rewritten into its batch matrix form as follows:

$$\mathbf{y}^{i} = \bar{\mathbf{Y}}^{i}\,\bar{\mathbf{V}}^{i}, \tag{5.26}$$

where

$$\begin{aligned}
\mathbf{y}^i &= \left[\mathbf{y}^i_{(0)}, \mathbf{y}^i_{(1)}, \ldots, \mathbf{y}^i_{(p)}, \ldots, \mathbf{y}^i_{(l^i-1)}\right] \in \mathbb{R}^{q\times l^i},\\
\bar{\mathbf{Y}}^i &= \Big[\mathbf{D}^i, \mathbf{C}^i\,\bar{\mathbf{B}}^i, \mathbf{C}^i\,\bar{\mathbf{A}}^i\,\bar{\mathbf{B}}^i, \cdots,\\
&\quad \mathbf{C}^i\left(\bar{\mathbf{A}}^i\right)^{p-1}\bar{\mathbf{B}}^i, \cdots, \mathbf{C}^i\left(\bar{\mathbf{A}}^i\right)^{l^i-2}\bar{\mathbf{B}}^i\Big] \in \mathbb{R}^{q\times[m+(q+m)(l^i-1)]},\\
\bar{\mathbf{V}}^i &= \begin{bmatrix}
\mathbf{u}^i_{(0)} & \mathbf{u}^i_{(1)} & \mathbf{u}^i_{(2)} & \cdots & \mathbf{u}^i_{(p)} & \cdots & \mathbf{u}^i_{(l^i-1)}\\
\mathbf{0} & \mathbf{v}^i_{(0)} & \mathbf{v}^i_{(1)} & \cdots & \mathbf{v}^i_{(p-1)} & \cdots & \mathbf{v}^i_{(l^i-2)}\\
\mathbf{0} & \mathbf{0} & \mathbf{v}^i_{(0)} & \cdots & \mathbf{v}^i_{(p-2)} & \cdots & \mathbf{v}^i_{(l^i-3)}\\
\mathbf{0} & \mathbf{0} & \ldots & \ddots & \vdots & \cdots & \vdots\\
\mathbf{0} & \mathbf{0} & \ldots & \mathbf{0} & \mathbf{v}^i_{(0)} & \cdots & \mathbf{v}^i_{(l^i-p-1)}\\
\mathbf{0} & \mathbf{0} & \ldots & \ldots & \mathbf{0} & \ddots & \vdots\\
\mathbf{0} & \mathbf{0} & \ldots & \ldots & \ldots & \mathbf{0} & \mathbf{v}^i_{(0)}
\end{bmatrix},
\end{aligned} \tag{5.27}$$

where $\bar{\mathbf{V}}^i \in \mathbb{R}^{[m+(q+m)(l^i-1)]\times l^i}$ and matrix $\bar{\mathbf{Y}}^i$ contains all the Markov parameters $\mathbf{D}^i, \mathbf{C}^i\,\bar{\mathbf{B}}^i, \mathbf{C}^i\,\bar{\mathbf{A}}^i\,\bar{\mathbf{B}}^i, \cdots, \mathbf{C}^i\left(\bar{\mathbf{A}}^i\right)^{l^i-2}\bar{\mathbf{B}}^i$ of the invented observer submodel i (5.23)-(5.24). Thanks to utilizing the observer gain $\mathbf{M}^i$, the observer submodel i defined by (5.23)-(5.24) can be asymptotically stable and damped enough, so that $(\bar{\mathbf{A}}^i)^k$, and eventually, the corresponding parameters within the matrix $\tilde{\mathbf{Y}}^i$ that have the term $\left(\bar{\mathbf{A}}^i\right)^k\bar{\mathbf{B}}^i$ will decay to nearly zero, for all $k \geqslant p$, where p is a sufficiently large integer. Therefore, again, it is sufficient to calculate only the Markov parameters of the observer submodel i, $\mathbf{D}^i, \mathbf{C}^i\,\bar{\mathbf{B}}^i, \mathbf{C}^i\,\bar{\mathbf{A}}^i\,\bar{\mathbf{B}}^i, \cdots, \mathbf{C}^i\left(\bar{\mathbf{A}}^i\right)^{p-1}\bar{\mathbf{B}}^i$, as the other parameters inside $\bar{\mathbf{Y}}^i$ can be assumed to be approximately zero. Thus, to achieve this goal, the truncated form of (5.26) and (5.27) can be given as follows:

$$\mathbf{y}^i = \tilde{\bar{\mathbf{Y}}}^i\,\tilde{\bar{\mathbf{V}}}^i,\ \left(\tilde{\bar{\mathbf{Y}}}^i \in \mathbb{R}^{q\times[m+(m+q)p]}, \tilde{\bar{\mathbf{V}}} \in \mathbb{R}^{[m+(m+q)p]\times l^i}\right), \tag{5.28}$$

where

$$\mathbf{y}^i = \left[\mathbf{y}^i_{(0)}, \mathbf{y}^i_{(1)}, \ldots, \mathbf{y}^i_{(p)}, \ldots, \mathbf{y}^i_{(l^i-1)}\right] \in \mathbb{R}^{q\times l^i},$$
$$\tilde{\bar{\mathbf{Y}}} = \begin{bmatrix}\mathbf{D}^i & \mathbf{C}^i\,\bar{\mathbf{B}}^i & \mathbf{C}^i\,\bar{\mathbf{A}}^i\,\bar{\mathbf{B}}^i & \cdots & \mathbf{C}^i\left(\bar{\mathbf{A}}^i\right)^{p-1}\,\bar{\mathbf{B}}^i\end{bmatrix},$$
$$\tilde{\bar{\mathbf{V}}}^i = \begin{bmatrix}\mathbf{u}^i_{(0)} & \mathbf{u}^i_{(1)} & \mathbf{u}^i_{(2)} & \cdots & \mathbf{u}^i_{(p)} & \cdots & \mathbf{u}^i_{(l^i-1)}\\ \mathbf{0} & \mathbf{v}^i_{(0)} & \mathbf{v}^i_{(1)} & \cdots & \mathbf{v}^i_{(p-1)} & \cdots & \mathbf{v}^i_{(l^i-2)}\\ \mathbf{0} & \mathbf{0} & \mathbf{v}^i_{(0)} & \cdots & \mathbf{v}^i_{(p-2)} & \cdots & \mathbf{v}^i_{(l^i-3)}\\ \mathbf{0} & \mathbf{0} & \mathbf{0} & \ddots & \vdots & \cdots & \vdots\\ \mathbf{0} & \mathbf{0} & \mathbf{0} & \mathbf{0} & \mathbf{v}^i_{(0)} & \cdots & \mathbf{v}^i_{(l^i-p-1)}\end{bmatrix}. \tag{5.29}$$

Considering the fact that both $\mathbf{y}^i$ and $\tilde{\bar{\mathbf{V}}}^i$ are known and available from the dataset, if $l^i \geq m(p+1)+qp$, then the number of equations will be equal or greater than the number of unknown parameters and if also the rows of $\tilde{\bar{\mathbf{V}}}^i$ are linearly independent, then by calculating $(\tilde{\bar{\mathbf{V}}}^i)^\dagger$, which is the pseudo-inverse of $\tilde{\bar{\mathbf{V}}}^i$, $\tilde{\bar{\mathbf{Y}}}^i$ can be computed as $\tilde{\bar{\mathbf{Y}}}^i = \mathbf{y}^i(\tilde{\bar{\mathbf{V}}}^i)^\dagger$. In fact, again the more independent the rows are, the more accuracy would be achieved in this computation. Furthermore, it is important to notice that the value of p can increase to the extent which the independence of the rows in $\tilde{\bar{\mathbf{V}}}^i$ would not be disturbed and this fact can determine the maximum of the parameter p for the observer representation. Furthermore, the solution matrix $\tilde{\bar{\mathbf{Y}}}^i$ gives the Markov parameters of the observer submodel i defined by (5.23)-(5.24), while the objective is to achieve the Markov parameters of the main submodel i defined by (5.17)-(5.18). In this regard, matrix $\tilde{\bar{\mathbf{Y}}}^i$ defined in (5.29) can be written as

$$\tilde{\bar{\mathbf{Y}}}^i = \begin{bmatrix}\bar{\mathbf{Y}}^i_{-1} & \bar{\mathbf{Y}}^i_0 & \bar{\mathbf{Y}}^i_1 & \ldots & \bar{\mathbf{Y}}^i_{p-1}\end{bmatrix}, \tag{5.30}$$

where

$$\begin{aligned}
\tilde{\bar{\mathbf{Y}}}^i_{-1} &= \mathbf{D}^i, \\
\tilde{\bar{\mathbf{Y}}}^i_{k} &= \mathbf{C}^i \left(\bar{\mathbf{A}}^{\,i}\right)^k \bar{\mathbf{B}}^i \\
&= \begin{bmatrix} \left(\mathbf{C}^i \left(\mathbf{A}^i + \mathbf{M}^i\mathbf{C}^i\right)^k \left(\mathbf{B}^i + \mathbf{M}^i\mathbf{D}^i\right)\right)^T \\ \left(-\mathbf{C}^i \left(\mathbf{A}^i + \mathbf{M}^i\mathbf{C}^i\right)^k \mathbf{M}^i\right)^T \end{bmatrix}^T \\
&\equiv \left[\tilde{\bar{\mathbf{Y}}}^{i\,(1)}_k \quad \tilde{\bar{\mathbf{Y}}}^{i\,(2)}_k\right], \;\; k = 0, 1, 2, \ldots, p-1.
\end{aligned} \tag{5.31}$$

Using (5.31) and (5.28), the general relationship between the observer Markov parameters and the i-th submodel's system Markov parameters can be written as [Aitken and Clarke, 2012]:

$$\mathbf{Y}^i_k = \tilde{\bar{\mathbf{Y}}}^{i\,(1)}_k + \sum_{s=0}^{k-1} \tilde{\bar{\mathbf{Y}}}^{i\,(2)}_s \tilde{\bar{\mathbf{Y}}}^{i}_{k-s-1} + \tilde{\bar{\mathbf{Y}}}^{i\,(2)}_k \mathbf{D}^i, \qquad k = 0, 1, \ldots, p-1, \tag{5.32}$$

and clearly $\mathbf{Y}^i_{-1} = \tilde{\bar{\mathbf{Y}}}^i_{-1} = \mathbf{D}^i$ based on the restructured form of $\mathbf{Y}^i$ in (5.20) which is defined as

$$\mathbf{Y}^i = \left[\mathbf{Y}^i_{-1} \quad \mathbf{Y}^i_0 \quad \mathbf{Y}^i_1 \quad \ldots \quad \mathbf{Y}^i_{l^i-2}\right]. \tag{5.33}$$

For example, considering (5.20) and (5.32), then $\mathbf{Y}^i_0 = \mathbf{C}^i\,\mathbf{B}^i$ can be easily written in accordance with (5.32) as (5.34):

$$\begin{aligned}
\mathbf{Y}^i_0 =& \mathbf{C}^i\,\mathbf{B}^i = \mathbf{C}^i \left(\mathbf{B}^i + \mathbf{M}^i\,\mathbf{D}^i\right) - \left(\mathbf{C}^i\,\mathbf{M}^i\right)\,\mathbf{D}^i \\
=& \tilde{\bar{\mathbf{Y}}}^{i\,(1)}_0 + \tilde{\bar{\mathbf{Y}}}^{i\,(2)}_0\,\mathbf{D}^i.
\end{aligned} \tag{5.34}$$

Here, it seems that (5.32) can only give a portion of the Markov parameters of the main submodel system i such as $\mathbf{Y}^i_0, \mathbf{Y}^i_1, \ldots, \mathbf{Y}^i_p$, while it is due to be calculated all the Markov parameters of the main submodel system i i.e. $\mathbf{Y}^i_0, \mathbf{Y}^i_1, \ldots, \mathbf{Y}^i_{l^i-1}$. To address this issue, considering the definitions of $\tilde{\bar{\mathbf{Y}}}^{i\,(1)}_k$ and $\tilde{\bar{\mathbf{Y}}}^{i\,(2)}_k$ in (5.31), the assumption that $\left(\bar{\mathbf{A}}^{\,i}\right)^k \approx 0$ for all time steps k if $k \geqslant p$ as well as assuming that $p \ll l^i$ remains valid, both $\tilde{\bar{\mathbf{Y}}}^{i\,(1)}_k$ and $\tilde{\bar{\mathbf{Y}}}^{i\,(2)}_k$ can be assumed to be zero for all k,

$k \geqslant p$ and it is possible to have approximated values for the Markov parameters $\mathbf{Y}^i_{p+1}, \mathbf{Y}^i_{p+2}, \ldots, \mathbf{Y}^i_{l^i-1}$ using (5.32). Having the Markov parameters of each main submodel i ready, then in Section 5.4.2, the procedures to calculate the state-space matrices of the submodel i, as well as the observer gain $\mathbf{M}^i$ are defined.

Before finishing this section, it is worth mentioning two more points. First, in general, using the observer approach could decrease the value of p. Hence, this could reduce the computational operation due to the reduction in the size of the matrices. Secondly, in case that the observer approach is not necessary to be used (e.g. when the system is damped and enough samples exist), the problem can be solved by using (5.21) and (5.22), where it is still possible to calculate more than p parameters by just replacing p with $p + I$, where I is an arbitrary integer number and $p + I < l^i$. However, it is highly recommended to use the observer approach, as it can reduce the computational operation, irrespective of the given system being damped enough or weakly-damped. For the current work also the Markov parameters are calculated based on the observer approach.

5.4.2 Eigensystem Realization Algorithm

In Section 5.4.1, the Markov parameters of each submodel i for each fuzzy rule i defined in Section 5.3, have been computed. Having these parameters from (5.33), the following generalized Hankel matrix can be defined [Aitken and Clarke, 2012]:

$$\mathbf{H}^i_\gamma \triangleq \begin{bmatrix} \mathbf{Y}^i_\gamma & \mathbf{Y}^i_{\gamma+1} & \cdots & \mathbf{Y}^i_{\gamma+N-1} \\ \mathbf{Y}^i_{\gamma+1} & \mathbf{Y}^i_{\gamma+2} & \cdots & \mathbf{Y}^i_{\gamma+N} \\ \vdots & \vdots & \ddots & \vdots \\ \mathbf{Y}^i_{\gamma+p-1} & \mathbf{Y}^i_{\gamma+p} & \cdots & \mathbf{Y}^i_{\gamma+p+N-2} \end{bmatrix} \in \mathbb{R}^{qp \times Nm}, \tag{5.35}$$

or its decomposed form:

$$\begin{aligned}
\mathbf{H}_{\gamma}^{i} &= \begin{bmatrix} \mathbf{C}^{i}\left(\mathbf{A}^{i}\right)^{\gamma}\mathbf{B}^{i} & \cdots & \mathbf{C}^{i}\left(\mathbf{A}^{i}\right)^{N+\gamma-1}\mathbf{B}^{i} \\ \mathbf{C}^{i}\left(\mathbf{A}^{i}\right)^{1+\gamma}\mathbf{B}^{i} & \cdots & \mathbf{C}^{i}\left(\mathbf{A}^{i}\right)^{N+\gamma}\mathbf{B}^{i} \\ \vdots & \ddots & \vdots \\ \mathbf{C}^{i}\left(\mathbf{A}^{i}\right)^{p+\gamma-1}\mathbf{B}^{i} & \cdots & \mathbf{C}^{i}\left(\mathbf{A}^{i}\right)^{p+N+\gamma-2}\mathbf{B}^{i} \end{bmatrix} \\
&= \begin{bmatrix} \mathbf{C}^{i} \\ \mathbf{C}^{i}\mathbf{A}^{i} \\ \vdots \\ \mathbf{C}^{i}\left(\mathbf{A}^{i}\right)^{p-1} \end{bmatrix} \left(\mathbf{A}^{i}\right)^{\gamma} \begin{bmatrix} \mathbf{B}^{i} & \mathbf{A}^{i}\mathbf{B}^{i} & \cdots & \left(\mathbf{A}^{i}\right)^{N-1}\mathbf{B}^{i} \end{bmatrix} \\
&= \mathbf{P}^{i}\left(\mathbf{A}^{i}\right)^{\gamma}\mathbf{Q}^{i}, \qquad (5.36)
\end{aligned}$$

where $\gamma = 0, 1$; N should be a sufficiently large integer; $\mathbf{P}^{i}$ and $\mathbf{Q}^{i}$ are defined as the observability and controllability matrices of the identified local linear system i, respectively [Aitken and Clarke, 2012], and each entry of $\mathbf{H}_{\gamma}^{i}$ is determined based on the analysis given in Section 5.4.1, and more specifically, the result in (5.33). For example, by replacing $\gamma = 0$, then the first entry of $\mathbf{H}_{\gamma}^{i}\big|_{\gamma=0} \equiv \mathbf{H}_{0}^{i}$ is $\mathbf{Y}_{0}^{i} = \mathbf{C}^{i}\mathbf{B}^{i}$, based on the definition of $\mathbf{Y}^{i}$ in (5.33), and considering (5.35) as well as (5.36), H_{0}^{i} can be written as

$$\begin{aligned}
\mathbf{H}_{0}^{i} &= \begin{bmatrix} \mathbf{Y}_{0}^{i} & \mathbf{Y}_{1}^{i} & \cdots & \mathbf{Y}_{N-1}^{i} \\ \mathbf{Y}_{1}^{i} & \mathbf{Y}_{2}^{i} & \cdots & \mathbf{Y}_{N}^{i} \\ \vdots & \vdots & \ddots & \vdots \\ \mathbf{Y}_{p-1}^{i} & \mathbf{Y}_{p}^{i} & \cdots & \mathbf{Y}_{p+N-2}^{i} \end{bmatrix} \\
&= \begin{bmatrix} \mathbf{C}^{i}\mathbf{B}^{i} & \mathbf{C}^{i}\mathbf{A}^{i}\mathbf{B}^{i} & \cdots & \mathbf{C}^{i}\left(\mathbf{A}^{i}\right)^{N-1}\mathbf{B}^{i} \\ \mathbf{C}^{i}\mathbf{A}^{i}\mathbf{B}^{i} & \mathbf{C}^{i}\left(\mathbf{A}^{i}\right)^{2}\mathbf{B}^{i} & \cdots & \mathbf{C}^{i}\left(\mathbf{A}^{i}\right)^{N}\mathbf{B}^{i} \\ \vdots & \vdots & \ddots & \vdots \\ \mathbf{C}^{i}\left(\mathbf{A}^{i}\right)^{p-1}\mathbf{B}^{i} & \mathbf{C}^{i}\left(\mathbf{A}^{i}\right)^{p}\mathbf{B}^{i} & \cdots & \mathbf{C}^{i}\left(\mathbf{A}^{i}\right)^{p+N-2}\mathbf{B}^{i} \end{bmatrix} \\
&= \mathbf{P}^{i}\mathbf{Q}^{i}. \qquad (5.37)
\end{aligned}$$

It is assumed that each subsystem i is observable and controllable, and has order n. This means that the minimum dimension of the state matrix $\mathbf{A}^{i}$ would be $n \times n$

(i.e. $\mathbf{A}^i \in \mathbb{R}^{n\times n}$), and the observability matrix ($\mathbf{P}^i$) and controllability matrix ($\mathbf{Q}^i$) are of rank n, too. Therefore, assuming $qp < mN$, then if $\mathbf{H}_0^i$ defined by (5.37) is sufficiently large, i.e. $qp \geq n$, then its rank is also n, since it is the product of two matrices of rank n [Aitken and Clarke, 2012]. In fact, the condition $qp \geq n$ defines the lower bound for the value of the parameter p that must be considered throughout the design process. The matrix $\mathbf{H}_0^i$ defined in (5.37), can be decomposed by Singular Value Decomposition (SVD) [Govindarajan *et al.*, 2020] as follows:

$$\begin{aligned}\mathbf{H}_0^i &= \mathbf{R}^i\mathbf{\Sigma}^i(\mathbf{S}^i)^T = \begin{bmatrix}\mathbf{R}_n^i & \bar{\mathbf{R}}_n^i\end{bmatrix}\mathbf{\Sigma}^i\begin{bmatrix}\mathbf{S}_n^i & \bar{\mathbf{S}}_n^i\end{bmatrix}^T,\\ \mathbf{\Sigma}^i &= \begin{bmatrix}\mathbf{\Sigma}_n^i & \mathbf{0}\\ \mathbf{0} & \mathbf{0}\end{bmatrix},\end{aligned} \tag{5.38}$$

where $\mathbf{\Sigma}^i$ is a rectangular matrix whose zero-value entries represent zero matrices with appropriate dimensions. $\mathbf{R}^i$, $\mathbf{R}_n^i$, $\mathbf{S}^i$, and $\mathbf{S}_n^i$, are all orthogonal matrices with appropriate dimensions. $\bar{\mathbf{R}}_n^i$ and $\bar{\mathbf{S}}_n^i$ are zero matrices with proper dimensions. $\mathbf{\Sigma}_n^i$ is defined as

$$\mathbf{\Sigma}_n^i = \text{diag}\left[\sigma_1^i, \sigma_2^i, \ldots, \sigma_n^i\right], \tag{5.39}$$

where $\sigma_j^i, j = 1, 2, \ldots, n$ are n nonzero singular values of the matrix $\mathbf{H}_0^i$, i.e., $\sigma_1^i > \sigma_2^i > \ldots > \sigma_n^i > 0$. The reduced matrix $\mathbf{H}_{0r}^i$ can be written as

$$\mathbf{H}_{0r}^i = \mathbf{R}_n^i\mathbf{\Sigma}_n^i(\mathbf{S}_n^i)^T, \text{ where } \mathbf{R}_n^i(\mathbf{R}_n^i)^T = \mathbf{S}_n^i(\mathbf{S}_n^i)^T = \mathbf{I}_n. \tag{5.40}$$

By comparing and examining (5.36) (replacing $\gamma = 0$) and (5.40), the following outcome can be inferred:

$$\mathbf{H}_{0r}^i = \mathbf{R}_n^i(\mathbf{\Sigma}_n^i)^{\frac{1}{2}}(\mathbf{\Sigma}_n^i)^{\frac{1}{2}}(\mathbf{S}_n^i)^T \approx \mathbf{P}^i\mathbf{Q}^i. \tag{5.41}$$

The reason for this approximation is that the reduced form of the Hankel matrix (i.e., $\mathbf{H}_{0r}^i$) only contains information about the dominant modes of the system, while the controllability and observability matrices contain information about all modes of the system. Therefore, the reduced form of the Hankel matrix may not accurately capture the behavior of the system for all frequencies or time scales. However, in practice, the reduced form of the Hankel matrix obtained using SVD is often

a good approximation of the controllability and observability matrices, especially for systems with dominant modes that decay quickly. This approximation can be improved by increasing the number of singular values included in the reduced form of the Hankel matrix. Considering (5.41), one possible choice can be $\mathbf{P}^i = \mathbf{R}_n^i \sqrt{\mathbf{\Sigma}_n^i}$ and $\mathbf{Q}^i = \sqrt{\mathbf{\Sigma}_n^i}(\mathbf{S}_n^i)^T$. Thus, if $\gamma = 0$, then based on (5.36) and knowing m and q, which are the numbers of inputs and outputs, respectively, the matrices $\mathbf{B}^i$, and $\mathbf{C}^i$ of the i-th local model can be determined as follows:

$$\begin{aligned} \mathbf{B}^i &= \text{the first } m \text{ columns of } (\mathbf{\Sigma}_n^i)^{\frac{1}{2}}(\mathbf{S}_n^i)^T, \\ \mathbf{C}^i &= \text{the first } q \text{ rows of } \mathbf{R}_n^i\,(\mathbf{\Sigma}_n^i)^{\frac{1}{2}}. \end{aligned} \tag{5.42}$$

Next, to calculate $\mathbf{A}^i$, by replacing $\gamma = 1$ in (5.35), the Hankel matrix $\mathbf{H}_1^i$ can be written as

$$\mathbf{H}_1^i = \begin{bmatrix} \mathbf{Y}_1^i & \mathbf{Y}_2^i & \cdots & \mathbf{Y}_N^i \\ \mathbf{Y}_2^i & \mathbf{Y}_3^i & \cdots & \mathbf{Y}_{N+1}^i \\ \vdots & \vdots & \ddots & \vdots \\ \mathbf{Y}_p^i & \mathbf{Y}_{p+1}^i & \cdots & \mathbf{Y}_{p+N-1}^i \end{bmatrix}. \tag{5.43}$$

By replacing $\gamma = 1$ in (5.36) and having $\mathbf{P}^i = \mathbf{R}_n^i \sqrt{\mathbf{\Sigma}_n^i}$, $\mathbf{Q}^i = \sqrt{\mathbf{\Sigma}_n^i}(\mathbf{S}_n^i)^T$, and $\mathbf{H}_1^i$ in (5.43), the state matrix $\mathbf{A}^i$ can be calculated as:

$$\mathbf{A}^i = (\mathbf{\Sigma}_n^i)^{-\frac{1}{2}}\,(\mathbf{R}_n^i)^T\,\mathbf{H}_1^i\,\mathbf{S}_n^i\,(\mathbf{\Sigma}_n^i)^{-\frac{1}{2}}. \tag{5.44}$$

Matrix $\mathbf{D}^i$ can be directly extracted from the obtained matrix $\mathbf{Y}^i$ in (5.33) as follows:

$$\mathbf{D}^i = \mathbf{Y}_{-1}^i \text{ (the first element of } \mathbf{Y}^i). \tag{5.45}$$

The last remaining parameter required to be calculated is the observer gain $\mathbf{M}^i$. In this regard, the sequence of parameters $\mathbf{Z}_k^i$ is defined as (5.46),

$$\mathbf{Z}_k^i = \mathbf{C}^i \left(\bar{\mathbf{A}}^i\right)^k \mathbf{M}^i, \quad k = 0, 1, 2, \ldots, \tag{5.46}$$

and based on [Juang *et al.*, 1993] each parameter $\mathbf{Z}_k^i$ can be obtained from the

observer Markov parameters of the submodel i, using the general formula as (5.47):

$$\mathbf{Z}_k^i = -\tilde{\tilde{\mathbf{Y}}}_k^{i\,(2)} + \sum_{s=0}^{k-1} \tilde{\tilde{\mathbf{Y}}}_s^{i\,(2)}\, \mathbf{Z}_{k-s-1}^i, \tag{5.47}$$

where $\tilde{\tilde{\mathbf{Y}}}_k^{i\,(2)}$ can be calculated, using (5.31). For example, by replacing $k = 0$ in (5.31) and considering (5.46), then $\mathbf{Z}_0^i = \mathbf{C}^i\,\mathbf{M}^i = -\tilde{\tilde{\mathbf{Y}}}_0^{i\,(2)}$. Having calculated the values of sequence $\mathbf{Z}_k^i$ using (5.47), and based on the definition in (5.46), $\mathbf{Z}^i$ can be represented as

$$\mathbf{Z}^i = \begin{bmatrix} \mathbf{Z}_0^i \\ \vdots \\ \mathbf{Z}_k^i \end{bmatrix} = \begin{bmatrix} \mathbf{C}^i\,\mathbf{M}^i \\ \vdots \\ \mathbf{C}^i \left(\mathbf{A}^i\right)^k \mathbf{M}^i \end{bmatrix}, \tag{5.48}$$

and, $\mathbf{F}^i$ can be defined as

$$\mathbf{F}^i = \begin{bmatrix} \mathbf{C}^i \\ \vdots \\ \mathbf{C}^i \left(\mathbf{A}^i\right)^k \end{bmatrix}. \tag{5.49}$$

Thus, from (5.48) and (5.49), the observer gain $\mathbf{M}^i$ can be computed using the pseudo-inverse of $\mathbf{F}^i$ as

$$\mathbf{M}^i = \left(\left(\mathbf{F}^i\right)^T \mathbf{F}^i\right)^{-1} \left(\mathbf{F}^i\right)^T \mathbf{Z}^i. \tag{5.50}$$

Having computed all the state-space parameters associated with sub-models, it is time to summarize the main steps defined in this work for the proposed approach, as illustrated in Section 5.4.3.

5.4.3 Approach Summary

This subsection summarizes the main steps of the proposed new approach, which are also illustrated in Figure 5.2, as follows: **1)** Assign the input and output signals which are to be used to construct the dataset; **2)** Construct the required datasets from the measured input and output data; **3)** Partition the dataset into a defined

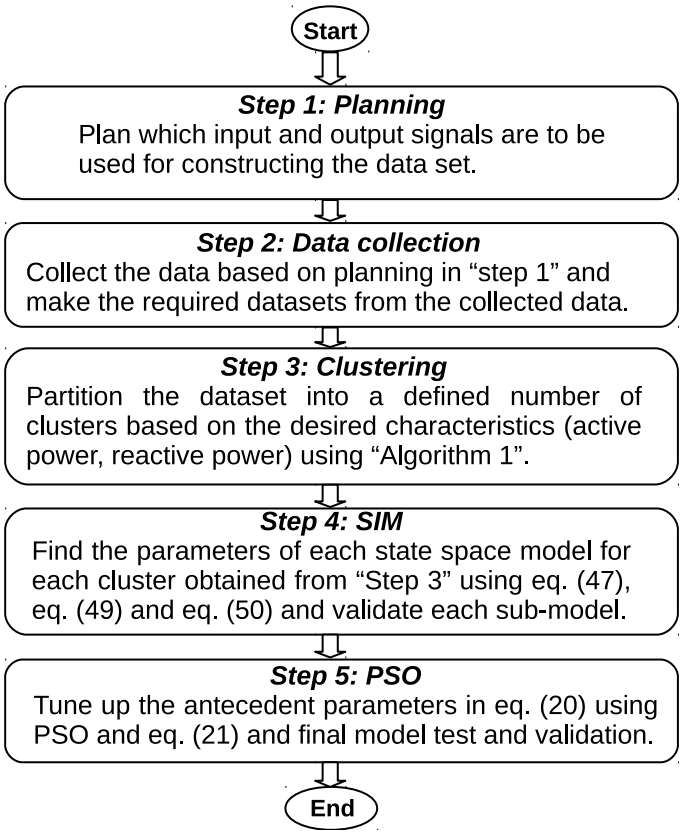

Figure 5.2: Flowchart for the proposed modeling approach.

number of clusters based on the desired characteristics (e.g. active power, reactive power, etc) using the approach described in Section 5.3.1; **4)** Find the parameters of the state space models for the clusters obtained from Step 3, using the approach described in Section 5.4; **5)** Utilize T-S fuzzy modeling, as explained in Section 5.3, to form a global model for the given synchronous generator, which includes determining the degree of activation of each rule defined by (5.6). To this end, it suffices to use PSO to determine the width (σ_j^i) of each Gaussian membership function defined by (5.15) using a dataset different from the one already used for calculating the parameters of each state-space sub-model that is inside the consequent part of each fuzzy rule. Once the PSO task is complete, for testing and validating the final T-S fuzzy model another dataset different from the first two ones is deployed. These steps alongside the required datasets will be explained more explicitly in Section 5.5.

5.5 Approach Evaluation

In this section, the proposed approach will be validated both in a simulation case study and in an experimental case study. Three types of datasets are planned and constructed for the new proposed method, in order to avoid over-fitting issues and guarantee the accuracy of the final model. The first dataset, termed state-space dataset, is partitioned into several clusters (rules) by the FCM method given in Algorithm 5.1, and each cluster is used to extract state-space model parameters of the consequent part of the corresponding rule.

It is important to note that the initial number of rules is calculated by multiplying the number of outputs by the number of clusters. The values of the computed sub-model are compared with the true values of the system under study for each output, and if these values are approximately close, the rule including the computed sub-model is retained, otherwise it would be removed. Therefore, it is very likely that the final number of rules will be less than the initial number. The metric that can be used for this purpose is the MSE defined as:

$$\text{MSE}\left(\hat{y}_k\right) \triangleq \frac{1}{L}\sum_{k=1}^{L}||\hat{y}_k - y_k||^2, \tag{5.51}$$

where, $y_k \in \mathbb{R}$ is the true (measured) value of each available output getting from the nonlinear system simulations, or the real-world system at the sample time k, $\hat{y}_k$ is the value of the corresponding output obtained from the computed sub-model at the sample time k, and L is the total number of data samples corresponding to the utilized cluster.

Once the rules and the parameters of the state-space sub-models corresponding to the rules' consequent parts are determined, PSO can be used to optimize (minimize) the objective function defined by (5.16) using a dataset known as the PSO dataset, which is entirely different from the state-space dataset. During the optimization process, the parameters for each antecedent part of a rule (more precisely the width (σ_j^i) of each membership function) are determined, followed by the activation degree of each sub-model in the consequent part of the corresponding rule. Indeed, by finishing the PSO operation, the model's training phase is completed.

Regarding making the datasets, the first dataset, namely the state-space dataset, is constructed by applying a wide range of values to the generator voltage field input,

while the generator mechanical power input is kept relatively constant. To construct the second dataset, namely, the PSO dataset, the generator mechanical power input is fed with a wide range of power values, whereas the generator voltage field input is maintained at a constant nominal value. Thus, by using these two datasets in which either a wide range of mechanical power values or a wide range of field voltage values is utilized, the training phase can be accomplished more effectively due to sweeping a wide area of generator dynamics by applying a wide range of values to the generator inputs.

Similar to the second dataset, the third dataset is constructed by varying the generator mechanical power input while maintaining the generator voltage field input at a constant nominal value. The main function of synchronous generators in power systems is to convert mechanical power into electrical power, supplying power to electrical networks. Therefore, this choice of test dataset makes sense. The third dataset is used to validate and test the final tuned T-S model. The MSE defined in (5.51) is the metric used to assess the accuracy of the final T-S fuzzy model.

Simulation and experimental case studies are presented in Sections 5.5.1 and 5.5.2 to describe how the proposed modeling approach, which includes the construction of the three aforementioned datasets, can be implemented in practice.

5.5.1 Simulation Case Study

In this section, the nonlinear synchronous generator model mentioned in Section 5.2.1 and defined by (2.13) is simulated under a variety of rated values of its inputs, and the corresponding output signal waveforms of this nonlinear model alongside the input signal waveforms are collected and stored, as can be seen in Figure 5.3. These waveforms form the data of the first dataset, i.e., the state space dataset. As can be seen in Figure 5.3 three different cases are simulated, where in each case, the mechanical power can possess one specific value (Figure 5.3a), while terminal voltages (Figure 5.3a) and particularly, field voltage input (Figure 5.3b) can take on various values. Therefore, it can be stated that the state space dataset consists of three smaller datasets corresponding to each case. Using FCM, each dataset is partitioned into several clusters (here the number of clusters for each case is set to 2), and subsequently using the approach given in Section 5.4, the sub-models in the form of state space models are obtained. Assuming to have two clusters for each case and

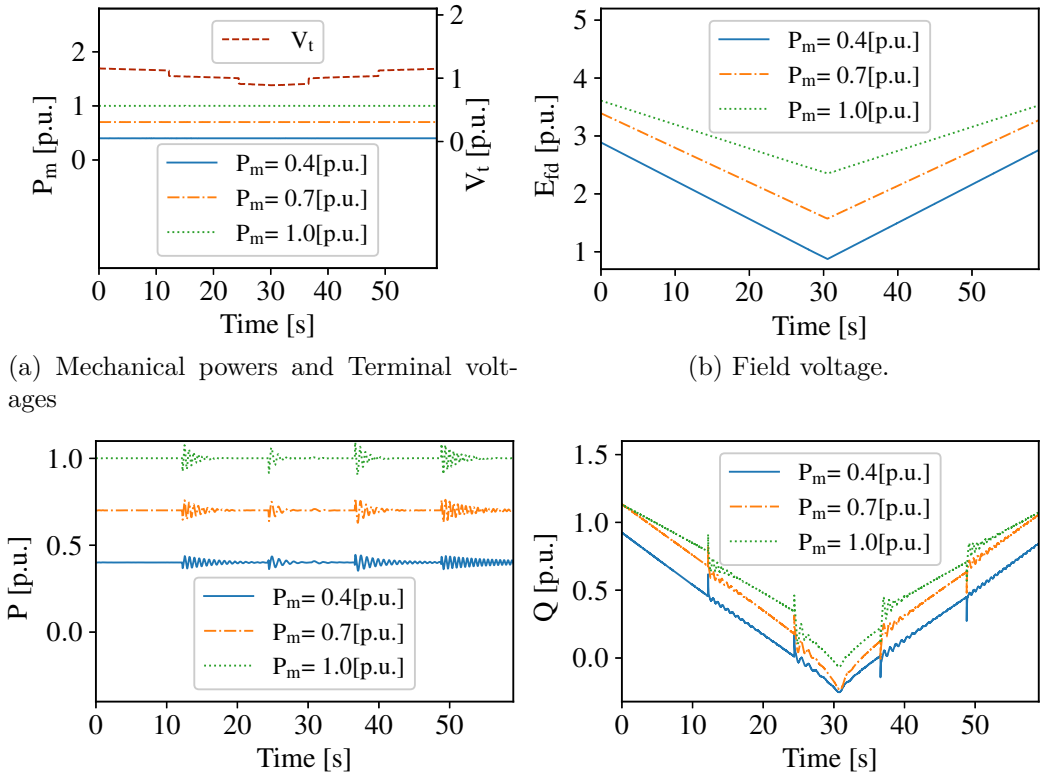

(a) Mechanical powers and Terminal voltages

(b) Field voltage.

(c) Active electrical power.

(d) Reactive electrical power.

Figure 5.3: Three inputs (a)-(b) and two corresponding outputs (c)-(d) which are used to form the state-space dataset (simulation case).

two outputs, namely active and reactive powers, the initial number of rules becomes 12, as explained in Section 5.5. However, upon comparison of the output values of the computed sub-models with the output values of the model under several simulations, only the case with the lowest mechanical power is represented by 4 rules, while each of the two other cases are represent by only 2 rules. Thus, the total number of rules is reduced to 8. In Figure 5.4, the active and reactive power outputs obtained from the dataset as well as those obtained from a sub-model calculated from a chosen cluster of the dataset, are illustrated. Approximately 7500 samples are used to compute the sub-model, while the utilized dataset contains around 17000 samples, and the sub-model is tested on all the 17000 samples. Having all the sub-models associated with the consequent parts of the T-S fuzzy rules ready, the next step is to apply PSO for optimizing the rule antecedent parammeters. The waveforms associated with the applied inputs and the corresponding waveforms of the outputs obtained

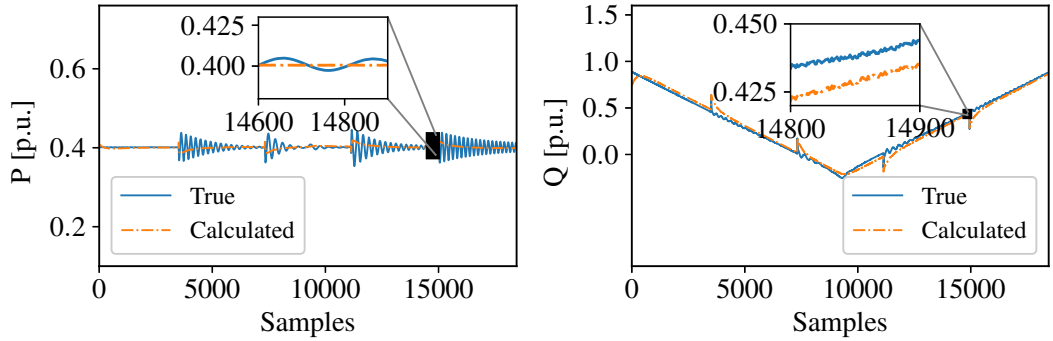

(a) Active power. (b) Reactive power.

Figure 5.4: Comparison of active and reactive power outputs: true vs. computed state space model values for an arbitrary cluster of dataset. (simulation case study).

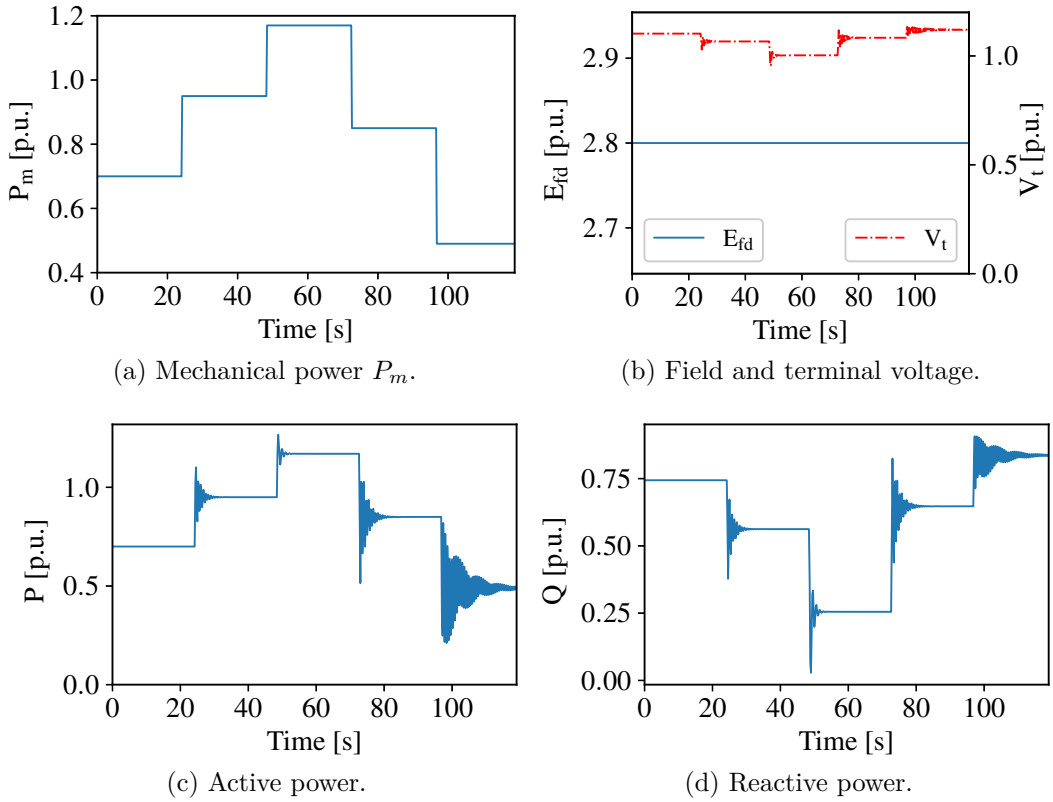

(a) Mechanical power P_m. (b) Field and terminal voltage.

(c) Active power. (d) Reactive power.

Figure 5.5: Three inputs (a)-(b) and two corresponding outputs (c)-(d) used to form the PSO dataset (simulation case).

from simulation, are illustrated in Figure 5.5. Moreover, the maximum number of iterations given to PSO for attaining a reasonable result (MSE $<$ 0.0005) for each

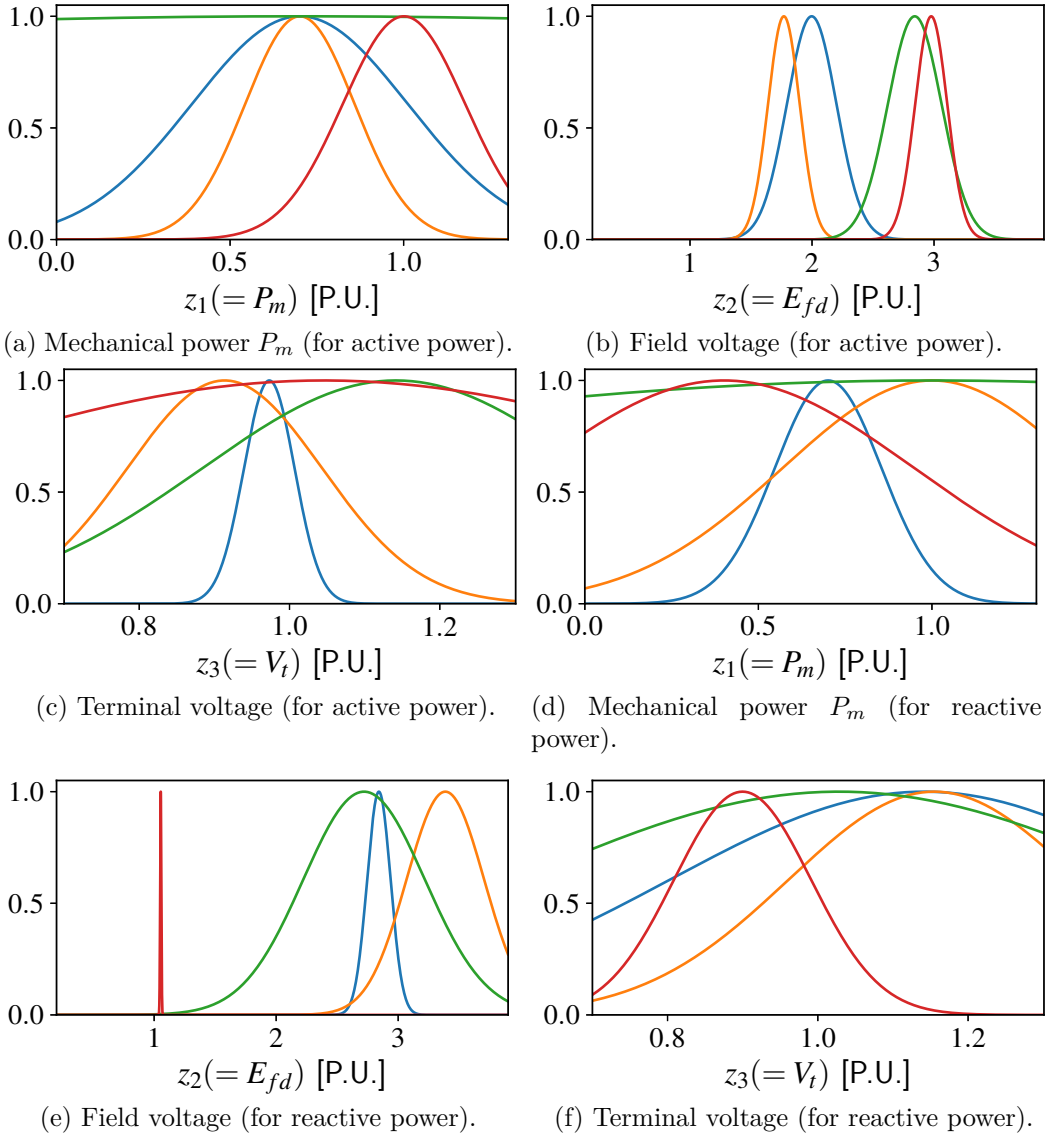

(a) Mechanical power P_m (for active power).

(b) Field voltage (for active power).

(c) Terminal voltage (for active power).

(d) Mechanical power P_m (for reactive power).

(e) Field voltage (for reactive power).

(f) Terminal voltage (for reactive power).

Figure 5.6: Input membership functions corresponding to the active power output (a)-(c), and reactive power output (a)-(c) obtained from training the T-S fuzzy model (simulation case).

output is set to 150. Figure 5.6 shows the optimized membership functions as a result of PSO for the three inputs of the T-S fuzzy model, namely P_m (mechanical power), E_{fd} (field voltage), and V_t (terminal voltage) in this case study. Finally, for testing and evaluating the optimized T-S fuzzy model, the waveforms shown in Figure 5.7 are applied to the inputs of the T-S fuzzy model and linear model, and

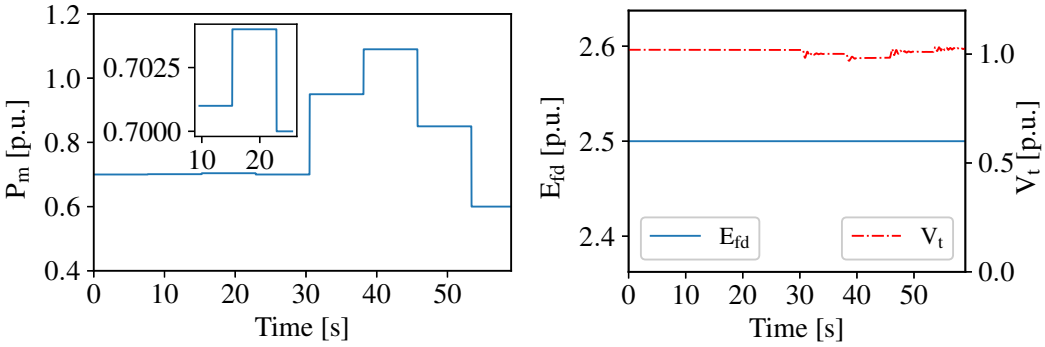

(a) Mechanical power P_m. (b) Field and terminal voltages.

Figure 5.7: Signals applied to the inputs of the trained T-S fuzzy model to evaluate the model performance (simulation case).

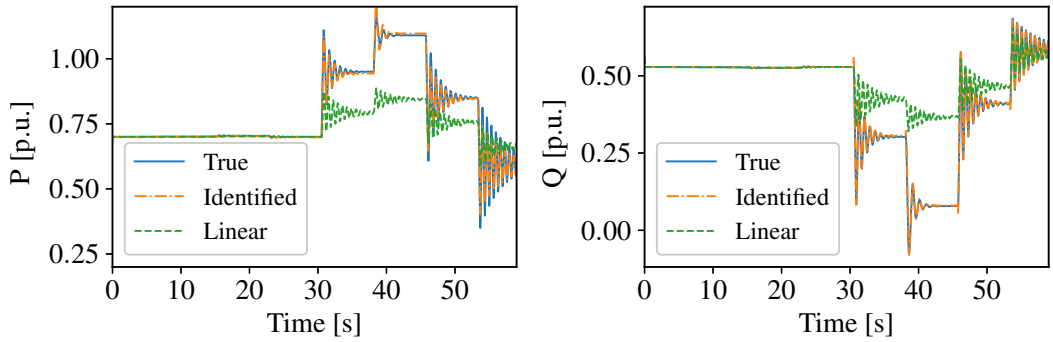

(a) Active power. (b) Reactive power.

Figure 5.8: Comparison of the response of the true, the identified, and the linearized models to the large-signal mechanical input (simulation case).

their outputs, namely the active power and the reactive power, are compared with those of the simulated nonlinear model, which is indeed considered as true model, as illustrated in Figure 5.8. By observing the linear model outputs in Figure 5.8, it can be concluded that a linear model with specific parameters is only valid for a very narrow band of the synchronous generator's operating points around that specific operating-point, and it is always required to update the parameters of the model as the synchronous generator's operating points diverge from that particular point. Therefore, for nonlinear systems such as the one studied here, methods leading to models with a wider valid operational range are necessary, especially in power system applications where such operating point variations may occur more frequently.

In addition to pictorial comparison, it is useful to express the accuracy of the T-S

Table 5.1: The MSE metric for the identified.

	Active power (P)	Reactive power (Q)
Obtained model	0.000185	0.000070
Linearized model	0.026244	0.023409

Table 5.2: Parameters of the synchronous generator.

Parameter	Value	Parameter	Value
S_b^{sg}	6.5 [kVA]	K^d	0.05 [p.u.]
V_B	1.02 [p.u.]	ω_0	314.16 [rad/s]
T'_{do}	0.13 [s]	T'_{qo}	0.013 [s]
x_d	2.06 [p.u.]	x_q	1.21 [p.u.]
$x_d^{'}$	0.37 [p.u.]	$x_q^{'}$	0.37 [p.u.]
H	5 [s]	x_e	0.193 [p.u.]

Table 5.3: Operating data for synchronous generator.

Parameters	O.p.1
δ^0 [rad]	0.72
V_B [p.u.]	1.02
E_{fd} [p.u.]	2.29
P^m [p.u.]	0.75

fuzzy model and the linearized model results using MSE defined in (5.51). Table 5.1 shows the MSE metric associated with the outputs of the T-S fuzzy model obtained using the proposed approach for the simulation case study, as well as the MSE results obtained for the linearized model. According to the results in Table 5.1, for the T-S fuzzy model, the MSE remains low for both active power (P) and reactive power (Q), even though the mechanical power input is changing widely.

The parameters characterizing the given synchronous generator are presented in Table 5.2. Additionally, the data necessary for the linear model defined in (5.1) can be found in Table 5.3, where the parameters and their corresponding values are given at one specific operating point, namely O.p.1.

This research work is primarily concerned with developing methods to apply to real-world synchronous generators, as will be verified in Section 5.5.2, however, the simulation case study is also included for two main reasons. Firstly, to demonstrate how the new obtained model behaves when the mechanical power experiences drastic changes. In practice, such a drastic change in a short period would be unusual and

Table 5.4: Parameters used for the simulation case study.

Parameter	Value
Number of MPs	1000
Sampling rate [Samples/s]	1000
Number of Fuzzy rules (per output)	4
Obtained order for the state space model	4

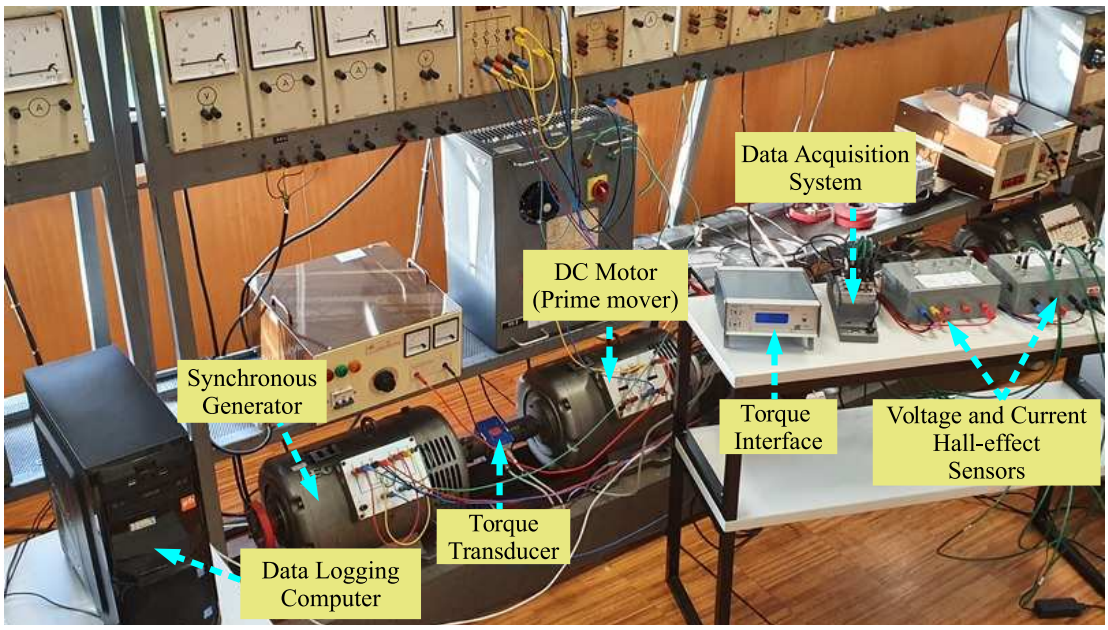

Figure 5.9: Experimental setup for testing at the laboratory.

abnormal because it might cause extraordinary and abnormal tensions and damages to the generator. The second reason is to illustrate the high performance of this approach even when the voltage bus at which the generator is connected is not very stable and may experience some fluctuations.

The important parameters which are used for this case study are summarized in Table 5.4.

5.5.2 Experimental Case Study

The physical testing setup and its corresponding diagram are illustrated in Figure 5.9 and Figure 5.10, respectively. As can be seen from the diagram, the prime mover for rotating the synchronous generator is a DC motor, of 3 [kW]. The mechanical

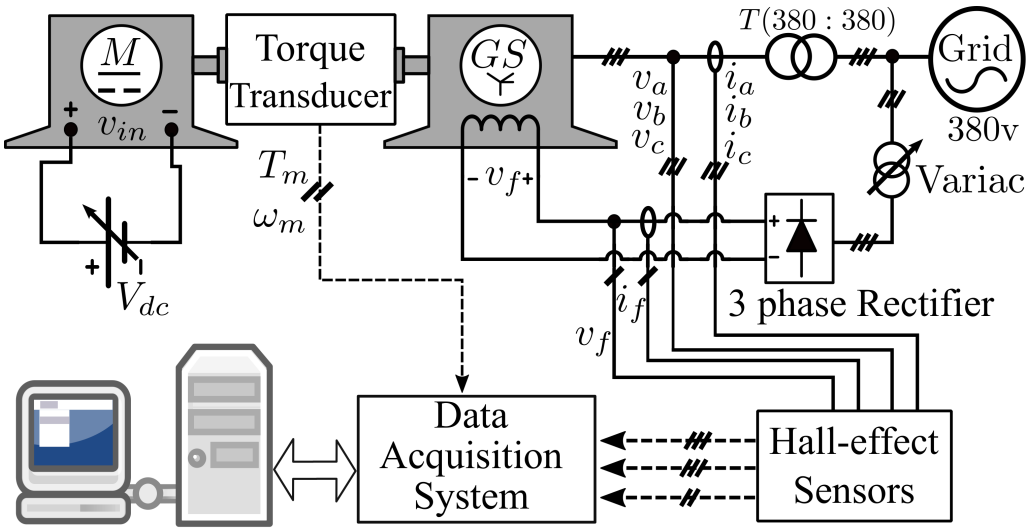

Figure 5.10: Schematic overview of the laboratory setup.

Table 5.5: Synchronous generator parameters.

Parameter	Value	Parameter	Value
Rated power	3.8 [kVA]	Rated voltage	380 [v]
Rated current	5.8 [A]	Pole number	4
Rated speed	1500 [rpm]	Active power	3 [kW]

torque in [Nm] and mechanical speed in [rad/s] are measured by the torque transducer RWT310 [Test and Measurement, 2021]. The nameplate rating data of the synchronous generator is given in Table 5.5. The field winding of the generator rotor is excited by a variable three-phase full-wave diode rectifier. The measured voltages and currents are from the phases or from the exciting system, and are measured by precise hall-effect sensors. All the measured data are sampled and acquired by the data acquisition system (DAQ) including analogue input module NI 9215 [Instruments, 2021b] and Embedded controller cRIO-9066 [Instruments, 2021a]. The rate for the data sampling is fixed to 1 [kHz] for each channel of the DAQ. The generator is connected to the local grid through a proper transformer. Figure 5.11 shows the wave shapes applied to the generator inputs and the resulting output wave shapes that are used to construct the dataset, i.e., state space dataset. As can be seen, three different cases are considered, where in each case, the mechanical power can possess one specific value (Figure 5.11a), terminal voltages (Figure 5.11a) are almost constant since the electrical network voltage is stable and constant, and only field

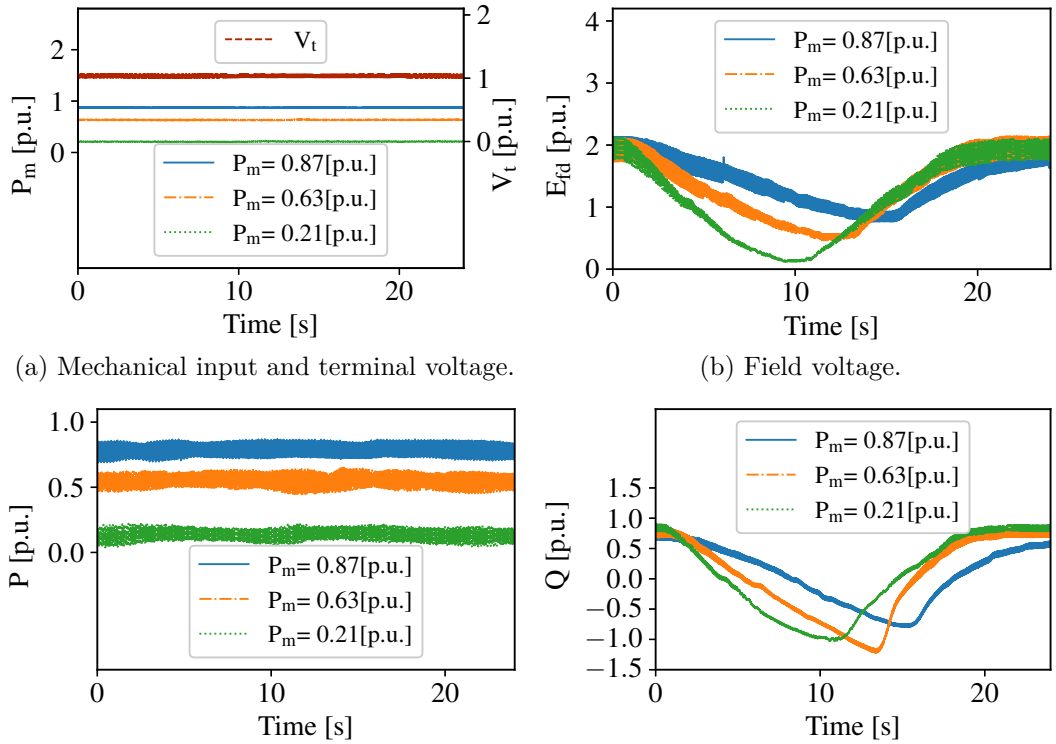

(a) Mechanical input and terminal voltage.

(b) Field voltage.

(c) Active electrical power.

(d) Reactive electrical power.

Figure 5.11: Three inputs (a)-(b) and two corresponding outputs (c)-(d) which are used for the identification process (experimental case).

voltage input (Figure 5.11b) can take on a variety of values. Therefore, it can be stated that the state space dataset consists of three smaller datasets corresponding to each case.

Using FCM, each dataset is partitioned into several clusters (here the number of clusters for each case is set to 2), and subsequently using the approach given in Section 5.4, the sub-models in the form of state space models are obtained. Assuming to have two clusters for each case and two outputs, namely active and reactive powers, the initial number of rules becomes 12, as explained in Section 5.5. Since all the computed sub-models generate fairly accurate outputs, none of them will be removed, and as a result the final number of rules is kept at 12.

In Figure 5.12, the active and reactive power outputs obtained from the dataset as well as those obtained from a sub-model calculated from a chosen cluster of the dataset, are illustrated. Approximately 3000 samples are used to compute the sub-model, while the utilized dataset contains 6000 samples, and the sub-model is tested

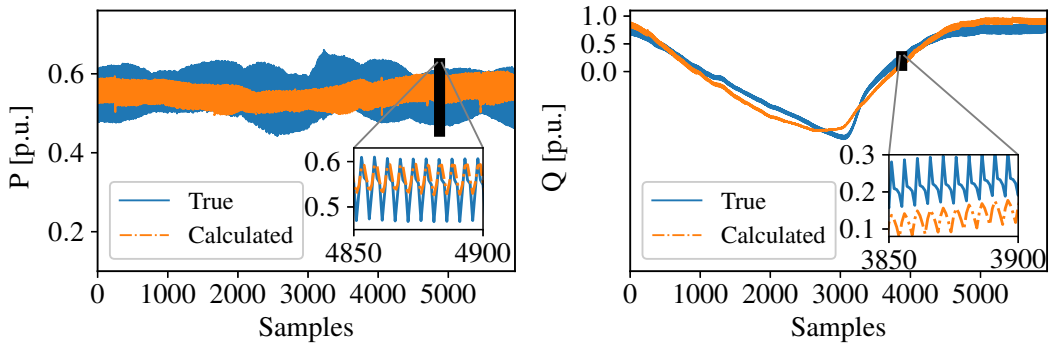

(a) Active power.

(b) Reactive power.

Figure 5.12: Comparison of active and reactive power outputs: true vs. computed state space model values for an arbitrary cluster of dataset. (experimental case study).

Table 5.6: The MSE metric for the identified model (experimental case study).

	Active power (P)	Reactive power (Q)
Obtained model	0.00127	0.00138

on all the 6000 samples.

Having all the sub-models associated with the consequent parts of the T-S fuzzy rules ready, the next step is to apply PSO for optimizing purpose. The waveforms associated with the applied inputs and the corresponding waveforms of the outputs obtained from the experimental setup, are illustrated in Figure 5.13. Moreover, the maximum number of iterations given to PSO for attaining a reasonable result (MSE $<$ 0.0005) for each output is set to 150. Figure 5.14 shows the optimized membership functions as a result of PSO for the three inputs of the T-S fuzzy model, namely P_m (mechanical power), E_{fd} (field voltage), and V_t (terminal voltage) in this case study.

Finally, for testing and evaluating the optimized T-S fuzzy model, the waveforms shown in Figure 5.15 are applied to the inputs of the T-S fuzzy model, and its outputs, namely active power and reactive power, are compared with those of the real-system setup, as illustrated in Figure 5.16. Additionally, to better evaluate the accuracy of the T-S fuzzy model, the MSE metric is calculated and presented in Table 5.6 for both the active power and the reactive power.

The important parameters which are used to configure the proposed identification algorithms are given in Table 5.7.

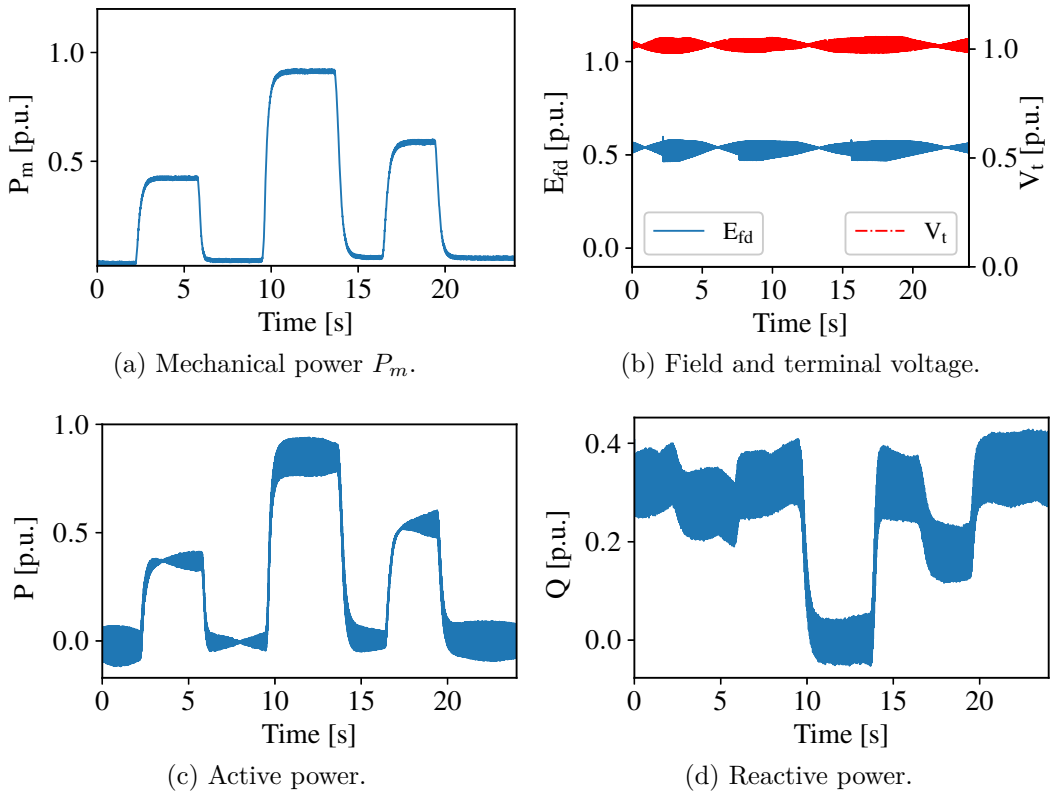

(a) Mechanical power P_m.

(b) Field and terminal voltage.

(c) Active power.

(d) Reactive power.

Figure 5.13: Three inputs (a)-(b) and two corresponding outputs (c)-(d) used to form the PSO dataset (experimental case study).

Table 5.7: Values of the parameters used for identification purposes (experimental setup).

Parameter	Value
Number of MPs	1000
sampling rate [Samples/s]	1000
Number of Fuzzy rules (per output)	6
Obtained order for the state space model	4

5.6 Conclusion

A novel approach for developing a global model for a real synchronous generator is presented in this Chapter. The approach combines the subspace identification method with T-S fuzzy modeling. In particular, all the developed procedures like dataset construction, clustering, local model identification, and T-S fuzzy modeling are thoroughly illustrated with simulation and experiential case studies. The results

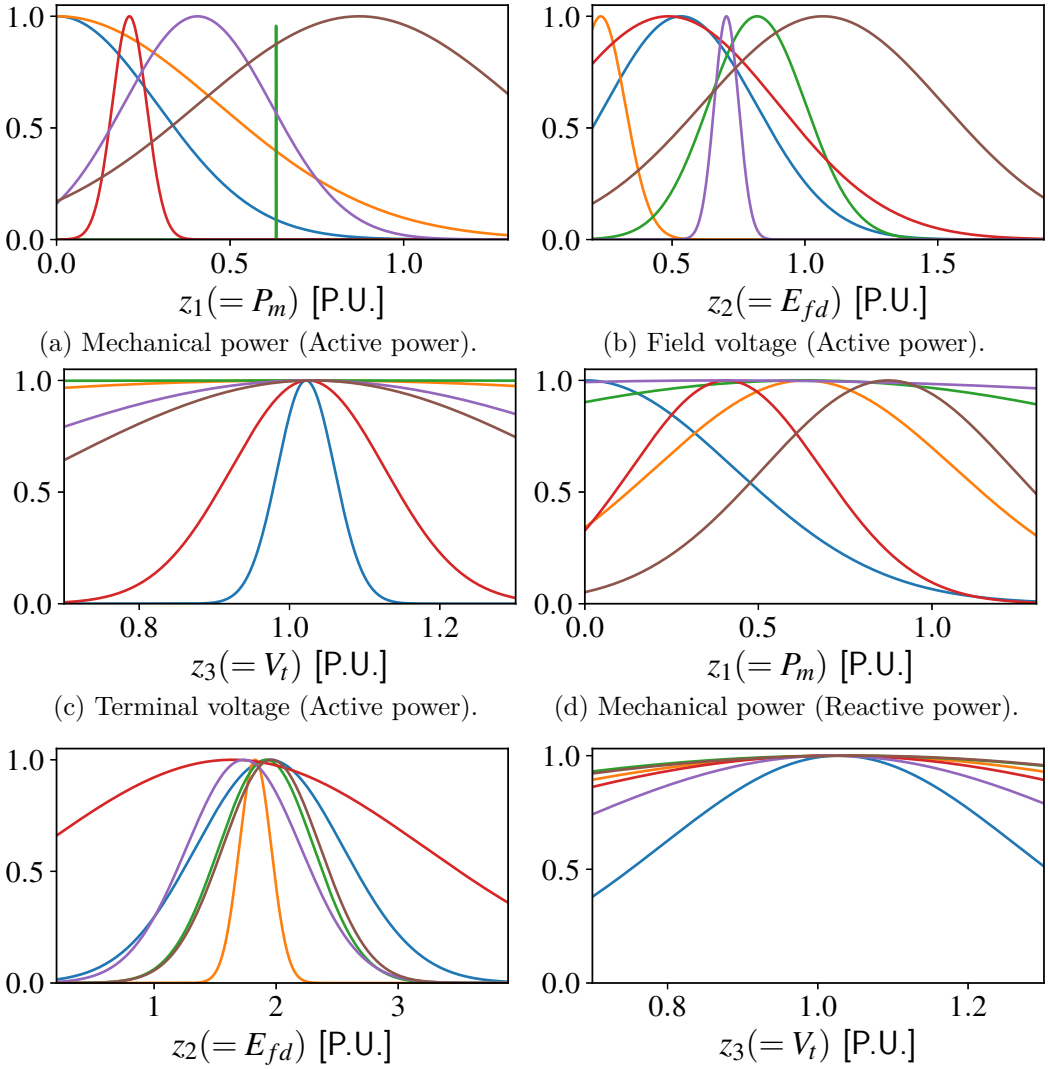

(a) Mechanical power (Active power).
(b) Field voltage (Active power).
(c) Terminal voltage (Active power).
(d) Mechanical power (Reactive power).
(e) Field voltage (Reactive power).
(f) Terminal voltage (Reactive power).

Figure 5.14: Input membership functions corresponding to the active power output (a)-(c), and to the reactive power output (a)-(c) obtained from training the T-S fuzzy model (experimental case).

from these case studies demonstrate that even under some unfavorable conditions such as noise, saturation issues, or variable terminal voltages, etc, which may occur during SG operations, the proposed novel approach can still lead to a precise global model. Therefore, the new approach is efficient, flexible, and robust enough to be used in a variety of scenarios and/or environments. Also, the model is composed of several linear sub-models in the form of state space representation, so it can be

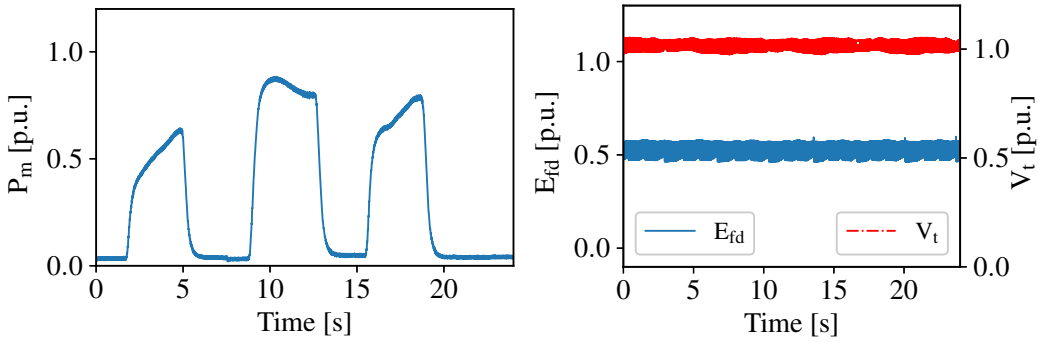

(a) Mechanical power P_m. (b) Field and terminal voltages.

Figure 5.15: Signals applied to inputs of the trained T-S fuzzy model to evaluate the model performance (experimental case).

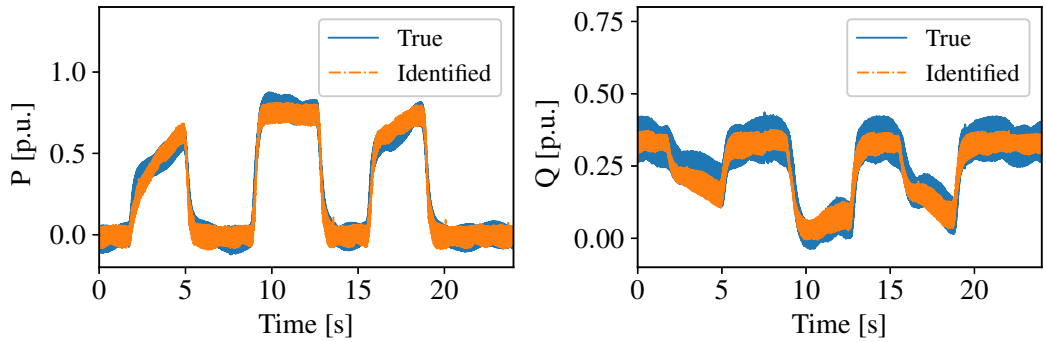

(a) Active power. (b) Reactive power.

Figure 5.16: Comparison of the real outputs with the identified model outputs as the mechanical input varies as shown in Figure 5.15a (experimental case).

easily applied in control and estimation applications as well. As a future work, it would be interesting to examine the performance of the identified model in control and estimation methodologies like model predictive control (MPC) and Kalman-based filters, where an accurate model is usually required. As another future work, establishing an adaptive mechanism for the obtained model would improve its accuracy and reduce the necessity to repeat the whole proposed modeling procedure over time.

Chapter 6

Engineering Approach to Construct Robust Filter for Mismatched Nonlinear Dynamic Systems

Contents

6.1 Introduction

Modeling a real-world system can often be a big challenge for scientists and researchers owing to various issues such as nonlinearities, unknown parameters, temperature and environmental variations and so on. Therefore, although estimators might use models somehow different from the real models, they still must be able to estimate states precisely.

Due to their ability to work in real-time and with Gaussian noises, Kalman filter (KF)-based methods such as the extended Kalman filter (EKF) [Simon, 2006], the unscented Kalman filter (UKF) [Julier and Uhlmann, 2004], and the cubature Kalman filter (CKF) [Arasaratnam and Haykin, 2009] have been widely used to estimate states of nonlinear systems in applications such as power systems [Ghahremani and Kamwa, 2011; Zhou *et al.*, 2015; Anagnostou and Pal, 2018], robotics [Chang *et al.*, 2011; Li and Yang, 2021], navigation [Eckenhoff *et al.*, 2021], etc. Nevertheless, these methods can be less effective when the system model is not accurate and/or the noise is not Gaussian. Thus, a considerable number of robust approaches have been proposed in an attempt to mitigate issues caused by noises [Li *et al.*, 2019] or outliers [Li *et al.*, 2019; Zhao and Mili, 2019; Gandhi and Mili, 2010]. Yet, the number of works addressing the model mismatch for nonlinear system is still limited [Abdallah *et al.*, 2022].

Hrustic *et al.* [2021] combined EKF and the linear constraints (LC) method of [Vilà-Valls *et al.*, 2020] to solve the problem of mismatch modeling for a nonlinear system, but a lack of precision in linearization might disrupt the consistency of the method, as discussed in [Chauchat *et al.*, 2022]. Accordingly, Abdallah *et al.* [2022] attempted to replace the EKF of [Hrustic *et al.*, 2021] with a type of sigma-point Gaussian filter which is a square-root CKF (SCKF) previously proposed in ZEMAMI, but since, as shown, e.g., in [Dang *et al.*, 2020], the computational time of SCKF may exceed the EKF computational time, especially as the state dimensionality of a system grows, then the use of this method might be problematic.

Considering the limited number of works as well as the aforementioned issues that may arise when using estimators such as those in [Hrustic *et al.*, 2021] or [Abdallah *et al.*, 2022], this study proposes a new methodology to guarantee the continuation of the estimation process even if there is a mismatch in the process model for a class of nonlinear system exposed to Gaussian noises. Specifically, the main contributions of the present work are fourfold: *(i)* A new adaptive methodology based on EKF is proposed to tackle the model mismatch problem for nonlinear dynamic systems without imposing any linear constraints (refer to Section 6.3). *(ii)* Providing a practical mechanism to incorporate and utilize the designer's knowledge and experience from the system's behavior in designing its corresponding filter. In other words, it will be shown that by choosing a proper estimation strategy along with having a true comprehension of the system behaviours, it is still possible to

develop an estimator that can operate precisely under model errors and inaccuracies (refer to Section 6.3). *(iii)* Considering power systems to be some of the most important nonlinear and dynamic systems in human life, this work will explicate the proposed method by applying it to an IEEE power system benchmark (IEEE 14-bus 5-generator). Since one of the features of this approach is to incorporate the designer's knowledge into the design of the estimator, some concepts about power system modeling are also described in a very basic manner to help readers who are not familiar with power systems (refer to Chapter 2). *(iv)* Results of the resultant estimator are compared to those of EKF, UKF, and CKF.

It is worth noting that even though the proposed approach is explained and validated for a dynamical power system, it can be applied to any real-system once the designer knowledge would provide the necessary information to construct the corresponding unknown input matrix as it will be discussed in Section 6.3. Moreover, in order to enhance the characterization of the results, Monte Carlo (MC) methods are applied to the results obtained by comparing the statistical performance of each estimation method.

In Chapter 2, it is illustrated how to model a power system, while in Chapter 3 several well-known Kalman Filter-based filters are given. Based on the information in these Chapters, this Chapter proposes an engineering approach to develop a state estimator for the purpose of implementing Dynamic State Estimation (DSE) to be applied in nonlinear systems. In this chapter the application case-study is in power systems. In fact, many researches have been accomplished concerning the DSE in electric grids and the majority of them have attempted to implement/improve estimators based on having thorough knowledge of the system model. However, in this work, it will show that it is still possible to achieve quite precise and reasonable results by designing a systematic approach, despite of not having thorough knowledge about the electric network. Indeed, here, it is tried to follow some general intuitive rules, concepts, and forehand knowledge and design an estimator which although its model is not so accurate, it still manages to fulfill the objective of dynamic state estimation efficiently. All the design procedures are explained step by step and to show the effectiveness of this proposed approach, its performance results are compared with those of three well-known estimators i.e. unscented kalman filter (UKF), cubature kalman filter (CKF), EKF, on the IEEE 5-generator 14-bus benchmark.

This Chapter is organized as follows. In Section 6.2 the problem is formulated

and described. Section 6.3 deals with the proposed estimator model.Next, the results obtained from examining the proposed estimator on the IEEE 14-bus power system are illustrated in Section 6.4. Finally, the conclusion and future work are provided in Section 6.5.

6.2 System Modeling and Description

As mentioned in Section 6.1, one feature of the proposed approach is that it incorporates the designer's knowledge of system behavior into the problem of robust filter design. In this context, in order to evaluate and implement the proposed estimation methodology, a power system is chosen. Climate change and air pollution have pushed power operating companies (POCs) to use more renewable energy sources (RES), electric vehicle charging stations, distributed energy resources (DERs), and power electronic devices (PEDs), which makes power system dynamics and models more complex, stochastic, and sporadic. As a result, power system state estimation may become more difficult and challenging, and consequently, power system monitoring, control, and protection might be at risk, since monitoring, control, and protection systems in electric grids are dependent upon accurate state information. Taking into account the above issues, for power systems of today, developing estimation methodologies that work accurately under model inaccuracies is crucial and essential. This section discusses a power system whose model is obtained as explained in Chapter 2. This modeling exercise will produce a power system model that mimics a real-world system. While a real power system can be much more complex than what is described in this Chapter, since the purpose of this work is to explain the robust approach tackle model mismatch in a more general sense, so a more complex model is not useful and beneficial.

Considering Figure 2.1 and equation (2.12), if there are N generators in the power

system, it is worth rewriting (2.12) into the form (6.1) to include all N generators:

$$\frac{d}{dt}\begin{bmatrix} \Delta\bar{\omega}_{(1,t)} \\ \vdots \\ \Delta\bar{\omega}_{(N,t)} \\ \delta_{(1,t)} \\ \vdots \\ \delta_{(N,t)} \end{bmatrix} = \begin{bmatrix} \frac{1}{M_1}\left(P^m_{(1,t)} - P^g_{(1,t)} - K^d_1\,\Delta\bar{\omega}_{(1,t)}\right) \\ \vdots \\ \frac{1}{M_N}\left(P^m_{(N,t)} - P^g_{(N,t)} - K^d_N\,\Delta\bar{\omega}_{(N,t)}\right) \\ \omega_0\Delta\bar{\omega}_{(1,t)} \\ \vdots \\ \omega_0\Delta\bar{\omega}_{(N,t)} \end{bmatrix}. \tag{6.1}$$

To compact and generalize model (6.1), the notations are generalized to a general state-space model form as follows:

$$\begin{cases} \frac{d\mathbf{x}}{dt} = & \mathbf{f}\left(\mathbf{x}_{(t)}, \mathbf{u}_{(t)}, t\right) + \mathbf{w}_c, \\ \mathbf{z}_{(t)} = & \mathbf{h}\left(\mathbf{x}_{(t)}, t\right) + \mathbf{v}_c, \end{cases} \tag{6.2}$$

where, the first and second equations are the state and measurement equations, respectively. $\mathbf{z} \in \mathbb{R}^q$ is the measurement vector and consists of the measured values of the available quantities. $\mathbf{w}_c \in \mathbb{R}^n$ and $\mathbf{v}_c \in \mathbb{R}^q$ are Gaussian white noises with known covariance matrices $\mathbb{E}\left[\mathbf{w}_c\mathbf{w}_c^T\right] = \mathbf{Q}$ and $\mathbb{E}\left[\mathbf{v}_c\mathbf{v}_c^T\right] = \mathbf{R}$. Considering the physics of the problem, $\mathbf{w}_c$ can be interpreted as white acceleration and velocity signals, while $\mathbf{v}_c$ represents the noise signals on the measurements. $\mathbf{x}_{(t)} = [x_{(1,t)}, \ldots, x_{(n,t)}]^T \in \mathbb{R}^n$ is the state vector, $\mathbf{u}_{(t)} = [u_{(1,t)}, \ldots, u_{(m,t)}]^T \in \mathbb{R}^m$ is the known input vector of the system. The scalars n, m and q are the number of states, the number of known inputs, and the number of variables available to be measured, respectively.

In case the system is given by (6.1) then $\mathbf{x}_{(t)} = \left[\Delta\bar{\omega}_{(1,t)}, \ldots, \Delta\bar{\omega}_{(N,t)}, \delta_{(1,t)} \ldots, \delta_{(N,t)}\right]^T$; $\mathbf{u}_{(t)} = [P^m_{(1,t)}, \ldots, P^m_{(N,t)}]^T$ is the known input vector including the mechanical powers, and depending on the available measurements, one possible measurement vector, e.g., can be $\mathbf{z}_{(t)} = \left[P^g_{(1,t)}, \ldots, P^g_{(N,t)}, Q^g_{(1,t)}, \ldots, Q^g_{(N,t)}, V_{(1,t)}, \ldots, V_{(S,t)}, \theta_{(1,t)}, \ldots, \theta_{(S,t)}\right]^T$, where, $P^g_{(i,t)}$, $Q^g_{(i,t)}$, which are given by (2.7) and (2.8), are the active and reactive powers of the generator $i \in \{1, \ldots N\}$, and V_j and θ_j are the voltage amplitude and phase angle of bus $j \in \{1, \ldots, S\}$. It is worth mentioning that the estimation method presented here is in fact a centralized method, so for the estimation to be successful, all measurements must be sampled and transmitted to the center at a reasonable

rate (for example 50 samples per second).

6.3 Proposed Estimator

As mentioned in Section 3.3.2, the model of the system can be considered as (3.11), but the main goal of this work is to design an estimator to ensure that the estimation of the state vector is as precise as possible even when there may be unknown incidents in the electric network, such as switching off/on loads or switching out a line, which might cause model mismatches. Thus, to achieve this goal, it is suggested to use a slightly different model for the process model of the system, as illustrated in the discrete-time model (6.3):

$$\begin{aligned} \mathbf{x}_{(k+1)} &= \mathbf{g}(\mathbf{x}_{(k)}, \mathbf{u}_{(k)}) + \mathbf{G}\,\mathbf{d}_{(k)} + \mathbf{w}_{(k)}, \\ \mathbf{z}_{(k)} &= \mathbf{h}(x_{(k)}) + \mathbf{v}_{(k)}, \end{aligned} \tag{6.3}$$

where term $\mathbf{G}\,\mathbf{d}_{(k)}$ is added to compensate for the model mismatch, and due to its role in compensating, $\mathbf{G} \in \mathbb{R}^{n\times m}$ and $\mathbf{d} \in \mathbb{R}^m$ are named compensation matrix and compensation input vector, respectively. Matrix $\mathbf{G}$ here is not known, unlike its counterpart in, for example, [Liu *et al.*, 2022], and must be designed based on the designer's understanding of the system's behavior. Prior to determining matrix $\mathbf{G}$, it would be useful to examine the input vector $\mathbf{d}$ more closely. If it is considered a power system such as the one described in Section 6.2, intuitively, it is hypothesized that any changes in the network may lead to some power changes in this power system. As a result, vector $\mathbf{d}$ is unknown, but each element of vector $\mathbf{d}$ can be viewed as a power change variable associated with each generator in the electric grid. Due to this assumption for $\mathbf{d}$, finding a reasonable value for matrix $\mathbf{G}$ can be more straightforward and will be explained in the following paragraphs.

In the first step, it is required to obtain the discrete form of (6.1) with the aid

of the Runge-Kutta method explained in Section 3.3.2, yielding:

$$\begin{bmatrix} \Delta\bar{\omega}_{(1,k+1)} \\ \vdots \\ \Delta\bar{\omega}_{(N,k+1)} \\ \delta_{(1,k+1)} \\ \vdots \\ \delta_{(N,k+1)} \end{bmatrix} = \begin{bmatrix} \Delta\bar{\omega}_{(1,k)} \\ \vdots \\ \Delta\bar{\omega}_{(N,k)} \\ \delta_{(1,k)} \\ \vdots \\ \delta_{(N,k)} \end{bmatrix} + \begin{bmatrix} \frac{\Delta t}{M_1} P^m_{(1,k)} - \int_{k\Delta t}^{(k+1)\Delta t} \left(P^g_{(1,\tau)} + K^d_1 \, \Delta\bar{\omega}_{(1,\tau)} \right) d\tau \\ \vdots \\ \frac{\Delta t}{M_N} P^m_{(N,k)} - \int_{k\Delta t}^{(k+1)\Delta t} \left(P^g_{(N,\tau)} + K^d_N \, \Delta\bar{\omega}_{(N,\tau)} \right) d\tau \\ \omega_0 \int_{k\Delta t}^{(k+1)\Delta t} \Delta\bar{\omega}_{(1,\tau)} d\tau = c \, \Delta t \, \Delta\bar{\omega}_{(1,k)} \\ \vdots \\ \omega_0 \int_{k\Delta t}^{(k+1)\Delta t} \Delta\bar{\omega}_{(N,\tau)} d\tau = c \, \Delta t \, \Delta\bar{\omega}_{(N,k)} \end{bmatrix}, \tag{6.4}$$

where c is a constant brought into existence due to applying the operation given in (3.7), and inputs ($P^m_{(1,k)}$ to $P^m_{(N,k)}$), which are in fact mechanical power values associating with the each generator, are known and are assumed to be unchanged in the interval between the two consecutive samples. Taking into account (6.4), it can be observed that the values of these mechanical inputs, which are represented by $P^m_{(i,k)}$, where $i \in \{1, 2, \ldots, N\}$, can affect the frequency of the network by a coefficient equal to the inverse of parameter M_i (i.e. the inertia constant) multiplied by the sample time $\Delta\, t$, i.e. $\Delta\, t/M_i$ for each generator. Moreover, considering the second equation in (2.12), since the derivative of angle δ_i is proportional to the generator frequency deviation ($\Delta\bar{\omega}_{(i,k)}$), it is inferred that each given mechanical power value can also affect the corresponding term associating with rotor angle (δ_i) of the corresponding generator in (6.4) by a coefficient equal to the inverse of the parameter M_i multiplied by the square of sample time $\Delta\, t$, i.e. $\Delta\, t^2/M_i$. Eventually, these coefficients are proposed to be used for making the compensation matrix $\mathbf{G}$. Also, it is assumed that the size of the compensation vector $\mathbf{d}$ is identical to the number of known inputs in (6.4), which is equal to N, and it is assumed that each element of $\mathbf{d}$ can impact only one generator and hence they are independent. Thus,

the proposed $\mathbf{G}$ is written as (6.5):

$$\mathbf{G} = \begin{bmatrix} \frac{1}{M_1} & 0 & \dots & 0 \\ \vdots & \vdots & \ddots & \vdots \\ 0 & 0 & \dots & \frac{1}{M_n} \\ \frac{\omega_0 \Delta t}{M_1} & 0 & \dots & 0 \\ \vdots & \vdots & \ddots & \vdots \\ 0 & 0 & \dots & \frac{\omega_0 \Delta t}{M_N} \end{bmatrix}. \tag{6.5}$$

As can be seen in (6.5), Δt is factored out and it is assumed to be inside the unknown input vector $\mathbf{d}$ instead. This mathematical operation will make matrix $\mathbf{G}$ less sensitive, more constant and robust to the sample time, Δt. Having matrix $\mathbf{G}$ ready and in order to apply the centralized estimation approach, which is described in [Gillijns and Moor, 2007b] or [Emami *et al.*, 2020], to the system defined by (6.3), it is necessary to provide some extra calculations such as linearized models for the process and measurement models in (6.3) using the procedures provided in [Lavenius and Vanfretti, 2018]. In this direction, recursive filter equations are defined for the estimation of the system states as follows [Lavenius and Vanfretti, 2018]:

$$\hat{\mathbf{x}}^{-}_{(k)} = \mathbf{g}(\hat{\mathbf{x}}_{(k-1)}, \mathbf{u}_{(k-1)}), \tag{6.6}$$

$$\mathbf{d}_{(k-1)} = -\mathbf{M}^{d}_{(k)} \left(\mathbf{h}(\hat{\mathbf{x}}^{-}_{(k)}) - \mathbf{z}_{(k)} \right), \tag{6.7}$$

$$\hat{\mathbf{x}}^{\star}_{(k)} = \hat{\mathbf{x}}^{-}_{(k)} + \mathbf{G}\,\mathbf{d}_{(k-1)}, \tag{6.8}$$

$$\hat{\mathbf{x}}_{(k)} = \hat{\mathbf{x}}^{\star}_{(k)} - \mathbf{M}^{x}_{(k)} \left(\mathbf{h}(\hat{\mathbf{x}}^{\star}_{(k)}) - \mathbf{z}_{(k)} \right), \tag{6.9}$$

where $\hat{\mathbf{x}}^{-}_{(k)}$ and $\hat{\mathbf{x}}_{(k)}$ are a prior and a posterior estimates, respectively. The variable $\hat{\mathbf{x}}_{(k)}$ represents the estimator's estimation of $\mathbf{x}_{(k)}$, and $\mathbf{d}_{(k)}$ represents the compensation vector that is multiplied by matrix $\mathbf{G}$ to mitigate the impacts of model mismatch and consequently improve the estimated states. Also, the gain matrices $\mathbf{M}^{d}_{(k)} \in \mathbb{R}^{m \times q}$, and $\mathbf{M}^{x}_{(k)} \in \mathbb{R}^{n \times q}$ are still to be determined. The formula for calculating $\mathbf{M}^{d}_{(k)}$ is given by (6.10) as [Emami *et al.*, 2020] (refer to Chapter 4)

$$\mathbf{M}^{d}_{(k)} = -\left(\mathbf{F}^{T}_{(k)} (\tilde{\mathbf{R}}_{(k)})^{-1} \mathbf{F}_{(k)} \right)^{-1} \mathbf{F}^{T}_{(k)} \tilde{\mathbf{R}}^{-1}_{(k)}, \tag{6.10}$$

where $\mathbf{F}_{(k)} = \mathbf{C}_{(k)}\,\mathbf{G}$, and for $\mathbf{M}^{d}_{(k)}$ in (6.10) to be computable, it is enough to

have the condition that rank($\mathbf{F}_{(k)}$)=rank($\mathbf{G}$) for all k [Emami *et al.*, 2020] (refer to Chapter 4). Let $\mathbf{C}_{(k)}$ be defined as follows [Lavenius and Vanfretti, 2018]:

$$\mathbf{C}_{(k)} = \begin{bmatrix} \dfrac{\partial h_1(\hat{\mathbf{x}}_{(k)})}{\partial x_{(1,k)}} & \cdots & \dfrac{\partial h_1(\hat{\mathbf{x}}_{(k)})}{\partial x_{(n,k)}} \\ \vdots & \ddots & \vdots \\ \dfrac{\partial h_q(\hat{\mathbf{x}}_{(k)})}{\partial x_{(1,k)}} & \cdots & \dfrac{\partial h_q(\hat{\mathbf{x}}_{(k)})}{\partial x_{(n,k)}} \end{bmatrix}. \tag{6.11}$$

Similarly to (4.20), $\tilde{\mathbf{R}}_{(k)}$ is given by

$$\tilde{\mathbf{R}}_{(k)} = \mathbf{C}_{(k)}\mathbf{P}^{-}_{(k)}\left(\mathbf{C}_{(k)}\right)^T + \mathbf{R}^d_{(k)}. \tag{6.12}$$

Also, considering $\tilde{\mathbf{x}}^{-}_{(k)} \triangleq \hat{\mathbf{x}}^{-}_{(k)} - \mathbf{x}_{(k)}$, then $\mathbf{P}^{-}_{(k)} \triangleq \mathbb{E}[\tilde{\mathbf{x}}^{-}_{(k)}(\tilde{\mathbf{x}}^{-}_{(k)})^T]$ is defined as

$$\mathbf{P}^{-}_{(k)} = \mathbf{A}_{(k-1)}\mathbf{P}_{(k-1)}\mathbf{A}^T_{(k-1)} + \mathbf{Q}^d_{(k-1)}, \tag{6.13}$$

where $\mathbf{A}_k$ is given by [Lavenius and Vanfretti, 2018]:

$$\mathbf{A}_{(k)} = \begin{bmatrix} \dfrac{\partial g_1(\hat{\mathbf{x}}_{(k)},\, \mathbf{u}_{(k)})}{\partial x_{(1,k)}} & \cdots & \dfrac{\partial g_1(\hat{\mathbf{x}}_{(k)},\, \mathbf{u}_{(k)})}{\partial x_{(n,k)}} \\ \vdots & \ddots & \vdots \\ \dfrac{\partial g_n(\hat{\mathbf{x}}_{(k)},\, \mathbf{u}_{(k)})}{\partial x_{(1,k)}} & \cdots & \dfrac{\partial g_n(\hat{\mathbf{x}}_{(k)},\, \mathbf{u}_{(k)})}{\partial x_{(n,k)}} \end{bmatrix}. \tag{6.14}$$

$\mathbf{R}^d_{(k)}$ and $\mathbf{Q}^d_{(k-1)}$ are given in (3.14), and (3.10), respectively. Since in this case there is a single centralized estimator, then by setting the consensus coefficient $\mathbf{N}^i_{x(k)} = \mathbf{0}$ in (4.28), matrix $\mathbf{M}^x_{(k)}$ can be calculated from

$$\mathbf{M}^x_{(k)}\,\tilde{\mathbf{R}}^{\star}_{(k)} = \left[\mathbf{P}^{-}_{(k)}(\mathbf{C}_{(k)})^T - \mathbf{G}\,\mathbf{M}^d_{(k)}\,\tilde{\mathbf{R}}_{(k)}\right]\left(\mathbf{I} - (\mathbf{M}^d_{(k)})^T\,\mathbf{G}^T\,(\mathbf{C}_{(k)})^T\right), \tag{6.15}$$

where $\tilde{\mathbf{R}}^{\star}_{(k)}$

$$\tilde{\mathbf{R}}^{\star}_{(k)} = [\mathbf{I}_q - \mathbf{C}_{(k)}\mathbf{G}\,\mathbf{M}^d_{(k)}]\,\tilde{\mathbf{R}}_{(k)}\,[\mathbf{I}_q - \mathbf{C}_{(k)}\mathbf{G}\,\mathbf{M}^d_{(k)}]^T, \tag{6.16}$$

and considering $\tilde{\mathbf{x}}_{(k)} \triangleq \hat{\mathbf{x}}_{(k)} - \mathbf{x}_{(k)}$, $\mathbf{P}_{(k)}$ can be defined and obtained as [Gillijns and

Moor, 2007b]

$$\begin{aligned}\mathbf{P}_{(k)} &\triangleq \mathbb{E}\left[\tilde{\mathbf{x}}_{(k)}\,\tilde{\mathbf{x}}_{(k)}^{T}\right] \\ &= \mathbf{M}_{(k)}^{x}\,\tilde{\mathbf{R}}_{(k)}^{\star}\,(\mathbf{M}_{(k)}^{x})^{T} - \mathbf{V}_{(k)}^{\star}(\mathbf{M}_{(k)}^{x})^{T} - \mathbf{M}_{(k)}^{x}\,(\mathbf{V}_{(k)}^{\star})^{T} + \mathbf{P}_{(k)}^{\star},\end{aligned} \tag{6.17}$$

where $\mathbf{P}_{(k)}^{\star}$ and $\mathbf{V}_{(k)}^{\star}$ are denoted by (6.18) and (6.19), respectively:

$$\mathbf{P}_{(k)}^{*} = \left(\mathbf{I}_n - \mathbf{G}\,\mathbf{M}_{(k)}^{d}\,\mathbf{C}_{(k)}\right)\,\mathbf{P}_{(k)}^{-}\left(\mathbf{I}_n - \mathbf{G}\,\mathbf{M}_{(k)}^{d}\,\mathbf{C}_{(k)}\right)^{T}, \tag{6.18}$$

$$\mathbf{V}_{(k)}^{\star} = \mathbf{P}_{(k)}^{\star}\,\mathbf{C}_{(k)}^{T} - \mathbf{G}\,\mathbf{M}_{k}^{d}\,\mathbf{R}^{d}. \tag{6.19}$$

Now it seems that the main goal to design an estimator which is able to perform well and efficiently even when the available model is not complete and precise is realized. However, the compensation matrix $\mathbf{G}$ in (6.5) is not so precise since it was not analytically calculated from a known model. Indeed, $\mathbf{G}$ is designed based on some basic and limited knowledge of the studied system and its corresponding states. As a result, it is essential in an engineering approach to find a safe and secure solution to release some conditions at the price of achieving more accurate results. The fact behind this statement is that generally the available model of any system is not the exact model existing in the real world. Later, in Section 6.4, it can be observed that the conventional EKF filter with unknown input (EKF-UI), which is defined by equations (6.6)-(6.9) suffers noticeably from more fluctuations in its outputs which can degrade its effective performance. Thus, as another contribution, in this work, to mitigate this problem a new version for the computation of $\mathbf{d}$ is proposed in (6.20) which is an attenuated adaptive version of the $\mathbf{d}$ defined in (6.7):

$$\mathbf{d}_{(k)} = -\,\boldsymbol{\alpha}_{(k)}^{T}\mathbf{M}_{(k)}^{d}\left(\mathbf{h}(\hat{\mathbf{x}}_{(k)}^{-}) - \mathbf{z}_{(k)}\right) \tag{6.20}$$

$$\boldsymbol{\alpha}_{(k)} = 0.15\,\tanh\left(\sigma\frac{||\mathbf{h}(\hat{\mathbf{x}}_{(k)}^{-}) - \mathbf{z}_{(k)}||_2}{\mathbf{d}_{(k-1)}}\right), \tag{6.21}$$

where $\boldsymbol{\alpha}_{(k)} \in \mathbb{R}^m$ is the attenuated adaptive coefficient, σ is the standard deviation of the measurement white noise, and $||\cdot||_2$ denotes the Euclidean norm. In Section

6.4, using the attenuated $\mathbf{d}$ as a result of the proposed adaptive coefficient vector ($\boldsymbol{\alpha}_{(k)}$) defined in (6.21), it will be shown that the fluctuation problem existing in the outputs of the EKF-UI will be noticeably mitigated. In the following sections, the proposed estimator is termed as the Attenuated EKF-UI, or more briefly AEKF-UI.

This completes the definition of the proposed AEKF-UI estimator. In Section 3.4, the estimators whose performances are to be compared with this estimator, were briefly reviewed.

To sum up, the procedures which are accomplished here to realize the engineering approach for the proposed estimator, are summarized as follows:

1. Using the available information about the model of the system, a simple EKF estimator is designed based on (3.11), (3.13), (6.14), and (6.11).

2. Inspecting the known input matrix in (6.22),

$$\mathbf{B}_{(k)} = \begin{bmatrix} \dfrac{\partial g_1(\hat{\mathbf{x}}_{(k)},\, \mathbf{u}_{(k)})}{\partial u_{(1,k)}} & \cdots & \dfrac{\partial g_1(\hat{\mathbf{x}}_{(k)},\, \mathbf{u}_{(k)})}{\partial u_{(m,k)}} \\ \vdots & \ddots & \vdots \\ \dfrac{\partial g_n(\hat{\mathbf{x}}_{(k)},\, \mathbf{u}_{(k)})}{\partial u_{(1,k)}} & \cdots & \dfrac{\partial g_n(\hat{\mathbf{x}}_{(k)},\, \mathbf{u}_{(k)})}{\partial u_{(m,k)}} \end{bmatrix}, \tag{6.22}$$

   the objective is to identify how these inputs can affect the different states of the system and more specifically to determine all the coefficients of these inputs.

3. Considering the results obtained in Step 2, as an intuitive assumption, the number of the compensation inputs (the dimensionality of $\mathbf{d}$) is considered to be equal to that of the known inputs (the dimensionality of $\mathbf{u}$), and subsequently the initial value of matrix $\mathbf{G}$ will be equal to the known input matrix in (6.22).

4. Before the last step, a kind of clean-up can be done, where the goal is to make $\mathbf{G}$ more constant, robust, and less sensitive to parameters. This step can be tricky, and the designer's knowledge of the system can be fundamental and determining.

5. Finally, the estimation of the states can be obtained using equations (6.6), (6.8), (6.9), and (6.20).

Table 6.1: Generators data.[Pai and Chatterjee, 2014]

Parameter / Generator No.	x_d	H	K^d
$\mathbf{g_1}$	0.2995 [p.u.]	5.148 [s]	2.0 [p.u.]
$\mathbf{g_2}$	0.1850 [p.u.]	6.540 [s]	2.0 [p.u.]
$\mathbf{g_3}$	0.1850 [p.u.]	6.540 [s]	2.0 [p.u.]
$\mathbf{g_4}$	0.2320 [p.u.]	5.060 [s]	2.0 [p.u.]
$\mathbf{g_5}$	0.2320 [p.u.]	5.060 [s]	2.0 [p.u.]

6.4 Numerical Experiments

In this section, an IEEE 14-bus benchmark is selected as the test system for estimation studies. The generators' data is given in Table 6.1. The other required data relating to this IEEE electric network such as transmission lines data and the result of the load flow analysis can be found, e.g. in either [Pai and Chatterjee, 2014], [Milano, 2002], or [Milano, 2005].

In order to evaluate the performance of the understudied estimators (refer to Section 6.3 for more information) under different model mismatch conditions, three main test cases are planned, wherein four different scenarios are taken into account for each test case. In this work, the defined scenarios are based on two very probable incidents that may take place very often during any power system operation. These two types of incidents, which lead to sudden changes in any electrical grid, include switching out a line, in which the line between two buses in a grid may be switched off as a result of a fault or maintenance objectives, and a noticeable sudden load change, an incident which is very common and usual in power systems. Furthermore, the Monte Carlo (MC) method is used to repeat the simulations using various random noise instances to mitigate the drawbacks of analytical solutions and get more reliable and deterministic estimations of the states. Therefore, by averaging these results samples, the approximation of the probabilistic distribution of estimated states under different circumstances could be significantly more reliable.

To evaluate and compare the performance of all the considered Kalman filter

based estimators, the root mean squared error (RMSE) is quantified as:

$$\text{RMSE}\left(\hat{\mathbf{x}}_{(k)}\right) \triangleq \sqrt{\frac{1}{KM}\sum_{k=1}^{K}\sum_{m=1}^{M}||\hat{\mathbf{x}}_{(k)}^{m} - \mathbf{x}_{(k)}||_2^2}, \tag{6.23}$$

where $\mathbf{x}_{(k)} \in \mathbb{R}^n$ is the true state vector, $\hat{\mathbf{x}}_k^m$ is the estimated state vector at the m-th Monte Carlo (MC) iteration, $||\cdot||_2$ denotes the Euclidean norm, K is the total number of samples considered for $\mathbf{x}_{(k)}$ and M is the total number of MC simulations. The value of M depends on the problem that is to be solved and should be large enough to guarantee the convergence of the estimated RMSE. On the other hand, it is always reasonable to define a maximum value for M to avoid unnecessary computational burden. For example, in the current work, it is found that the RMSE of the estimated state vector does not change significantly for the values larger than $M = 35$, hence the maximum value of M is determined to be $M = 60$ to have a good margin of safety.

IEEE 14-bus power system. Figure 6.1 illustrates the network topology, the bus locations where the phasor measurement units (PMUs) are installed similar to the results presented in [Müller and Castro, 2016] or [Roy *et al.*, 2012], and the quantities being measured, such as voltage (V), active power (P), and reactive power (Q). This study assumes that the PMUs are accurate and without noticeable transmission delays, and their time-resolution is around 50 samples per second. Moreover, as it was stated in Section 6.3 , the response of EKF-UI is very fluctuating and noisy as can be observed, for example in Figure 6.2. Thus, thereafter, in order to keep the following figures clearer and more understandable, it will be avoided to display the responses of the conventional EKF-UI. As the first test case, it is assumed that the dynamical model of the generators within the understudied case study is entirely known by all the estimators' model and that the buses within the electrical network that are connected to the generator are monitored by a PMU through measuring quantities such as voltage (V), active power (P), and reactive power (Q), as shown in Figure 6.1. Under such a situation, four scenarios are planned to be carried out, and the obtained results are given in Figures 6.3–6.6. Figure 6.3 illustrates the results of the estimators for the first scenario, where the correct electrical network model (calculation procedure is available in Section 6.2) is available both pre- and post-

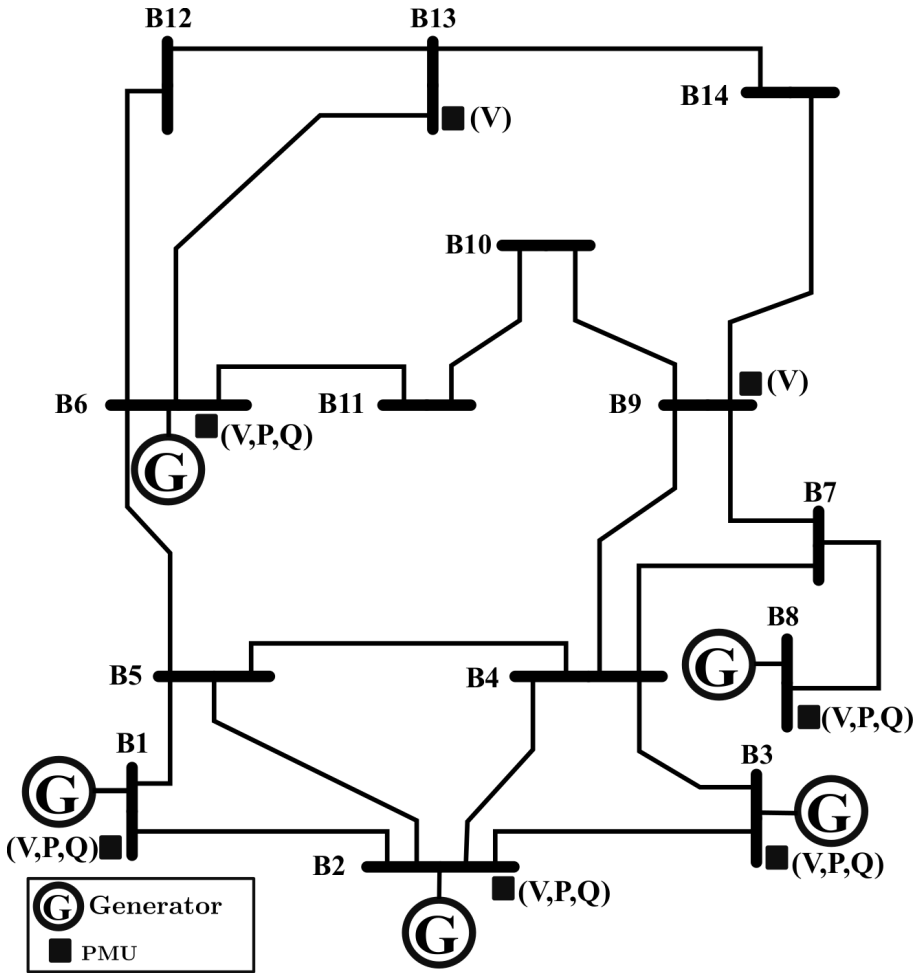

Figure 6.1: The single-line diagram of the IEEE 5-generator 14-bus electric network.

incident of line outage. Figure 6.4 demonstrates the estimation results in the second scenario, in which, unlike in the first scenario, the network model for the under examined estimators is not updated after a line outage occurs. Figure 6.5 illustrates the results of the third scenario, where a considerable load increase at bus B5 occurs while the correct electrical network model is available for both the pre- and post-incident of the load increase. Figure 6.6 shows the fourth scenario in which the electrical network model is fixed and not updated after a load increase occurs on bus B5. The assessment of these figures for the described four scenarios suggests that the estimator derived from the proposed approach is able to follow closely and accurately the dynamic states, namely speed deviation and angular position, while

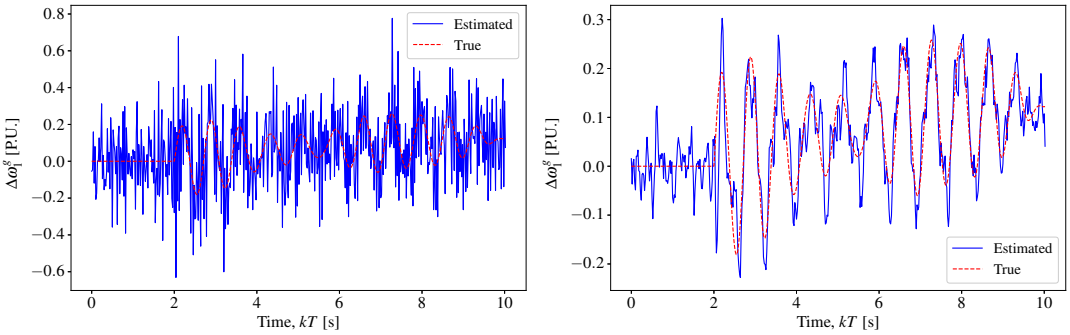

(a) EKF-UI output. (b) AEKF-UI output.

Figure 6.2: Comparing one of the estimated state of EKF-UI ($\Delta\omega_1^g$ of the generator g_1) with that of AEKF-UI.

other estimators, such as EKF, UKF, and CKF, especially when considerable model mismatch exists, are unable to track the speed deviation accurately.

For the second test case, the inertia parameters of existing generators in the considered case study system are assumed with 50 percent error, i.e., the inertia parameters in the model utilized for the estimators are about 50 percent less than their true values in the studied system model. Having such errors in the inertia parameters (M_i) of generators (refer to equation (2.12)), four scenarios are considered and the results for these four scenarios are shown in Figures 6.7–6.10. Figure 6.7 illustrates the results of the estimators for the first scenario, where the correct electrical network model (calculation procedure is available in Section 6.2) is available both pre- and post-incident of line outage. Figure 6.8 demonstrates the estimation results in the second scenario, in which, unlike in the first scenario, the network model for the under examined estimators is not updated after a line outage occurs. Figure 6.9 illustrates the results of the third scenario, where a considerable load increase at bus B5 occurs while the correct electrical network model is available for both the pre- and post- incident of the load increase. Figure 6.10 shows the fourth scenario in which the electrical network model is fixed and not updated after a load increase occurs on bus B5. The assessment of these figures for the described four scenarios suggests that the estimator derived from the proposed approach is able to follow closely and accurately the dynamic states, namely speed deviation and angular position, while other estimators, such as EKF, UKF, and CKF, especially when considerable model mismatch exists, are unable to track the speed deviation

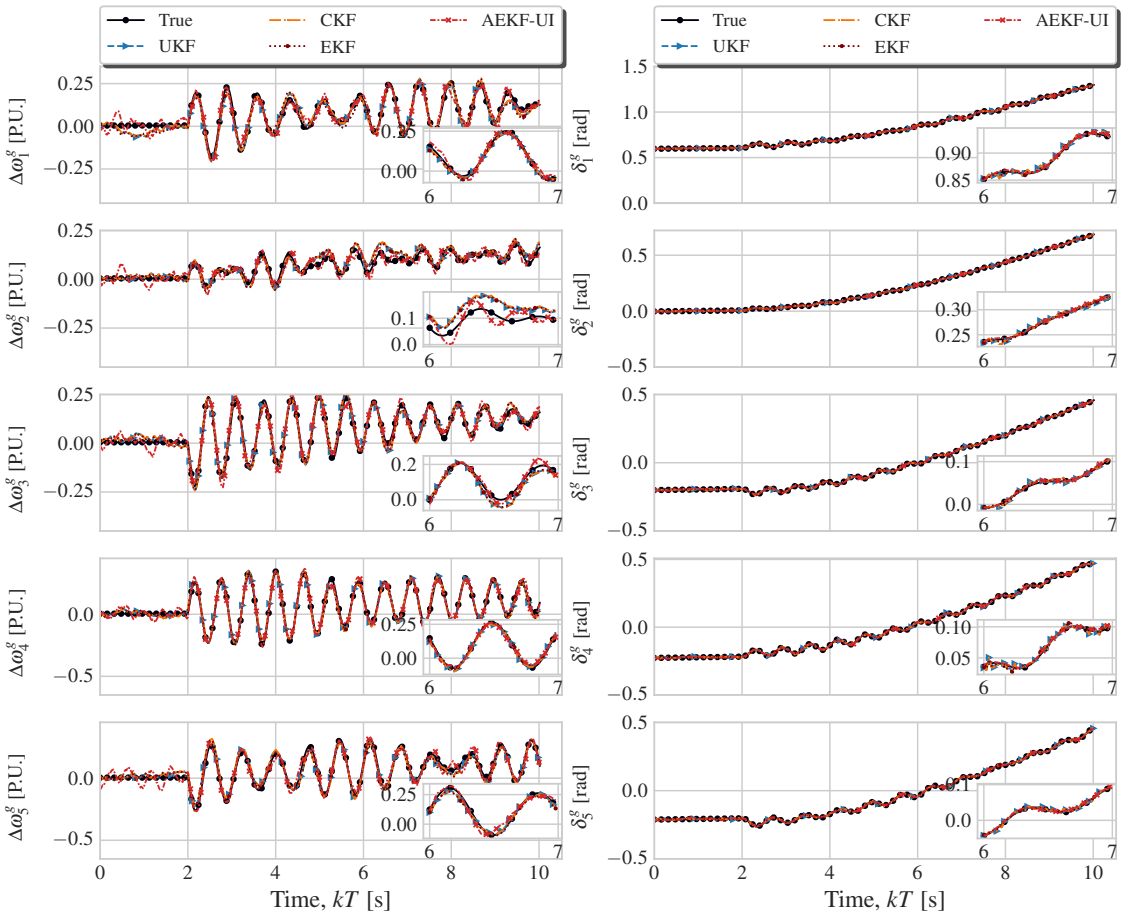

Figure 6.3: The estimated $\Delta\omega$ and δ of all generators in case of switching off line between buses 4 and 5, under the condition that the correct model of the electric network is always available.

accurately.

Finally, for the third designated test case, it is assumed that the measurements taken by the PMU installed at bus B1 would not be available to the estimators. In such a situation, four different scenarios are carried out. The results for these four scenarios are shown in Figures 6.11–6.14. Figure 6.11 illustrates the results of the estimators for the first scenario, where the correct electrical network model is available both pre- and post-incident of line outage. Figure 6.12 demonstrates the estimation results in the second scenario, in which, unlike in the first scenario, the network model for the under examined estimators is not updated after a line outage

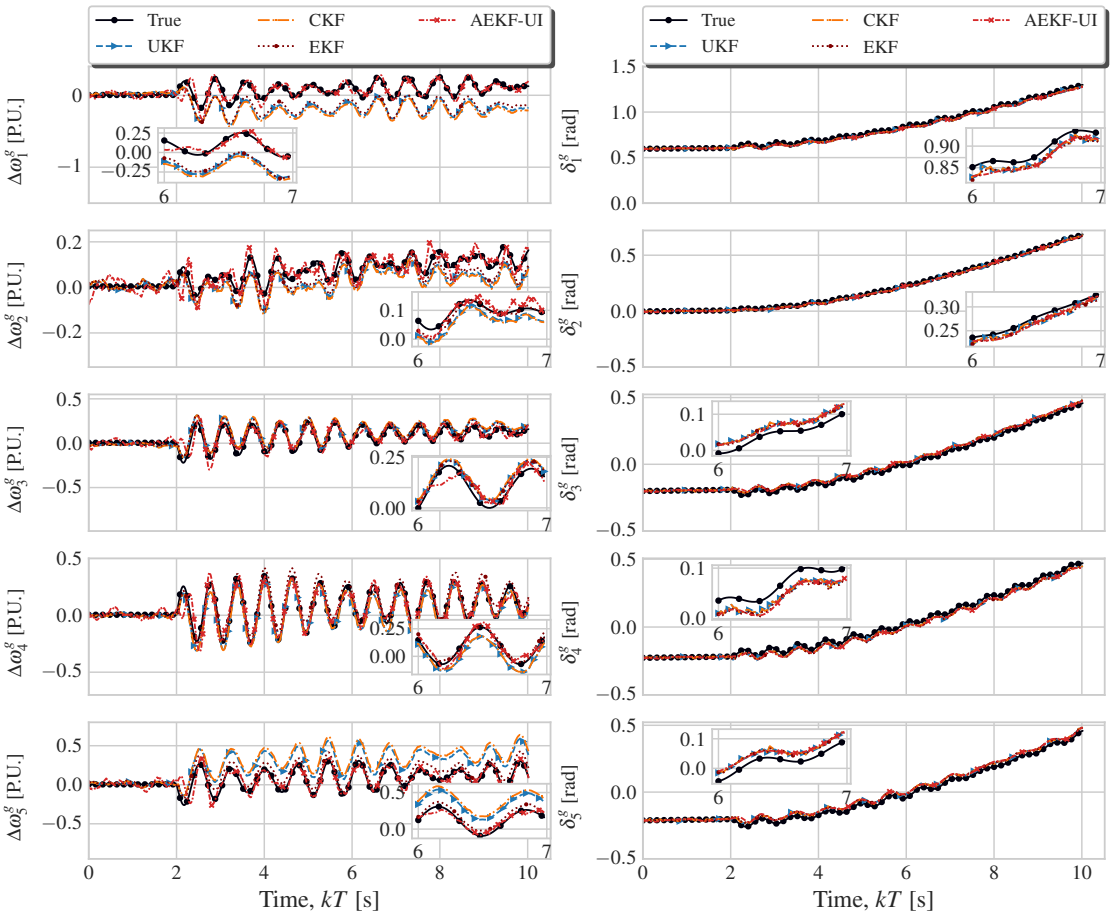

Figure 6.4: The estimated $\Delta\omega$ and δ of all generators in case of switching off the line between buses 4 and 5, under the condition that the correct model of the electric network is not available after the incident.

occurs. Figure 6.13 illustrates the results of the third scenario, where a considerable load increase at bus B5 occurs while the correct electrical network model is available for both the pre- and post- incident of the load increase. Figure 6.14 shows the fourth scenario in which the electrical network model is fixed and not updated after a load increase occurs on bus B5. The assessment of these figures for the described four scenarios suggests that the estimator derived from the proposed approach is able to follow closely and accurately the dynamic states, namely speed deviation and angular position, while other estimators, such as EKF, UKF, and CKF, especially when considerable model mismatches exists, are unable to track the speed deviation

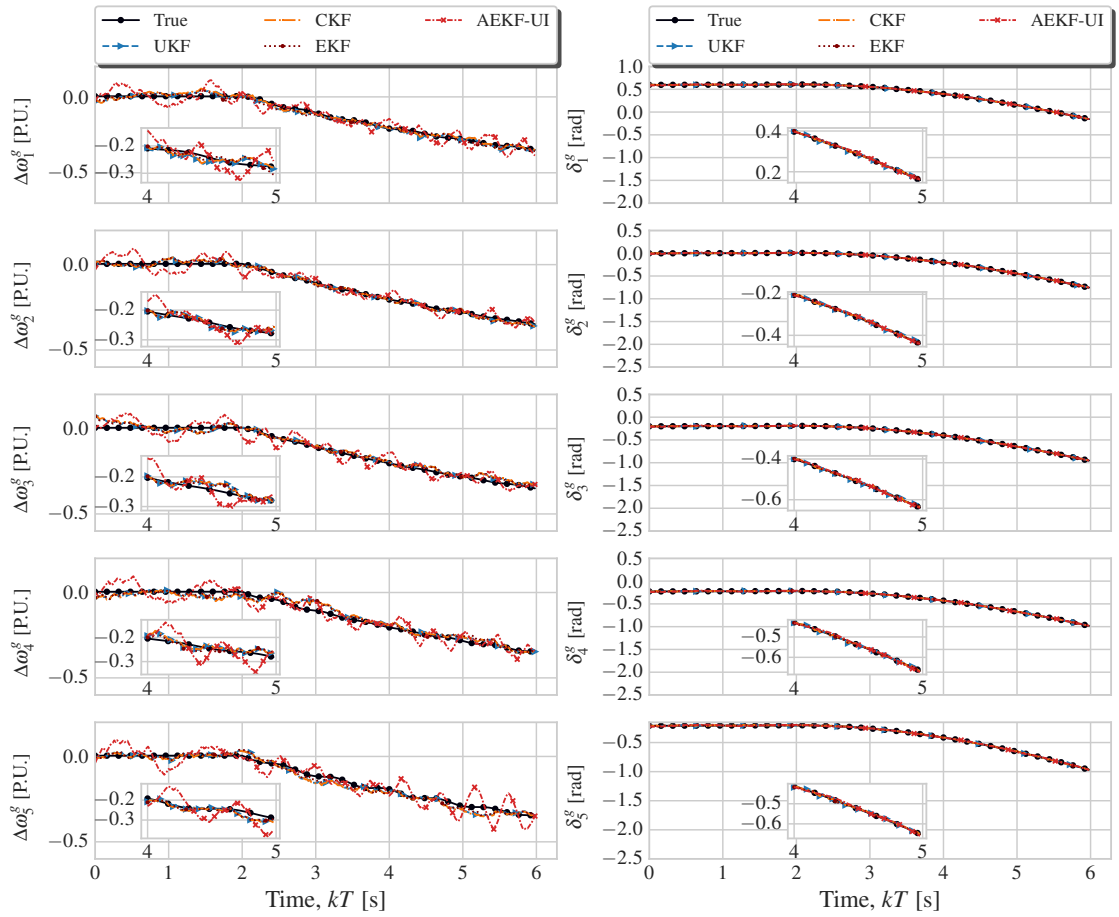

Figure 6.5: The estimated $\Delta\omega$ and δ of all generators in case of switching on the load at the bus 9 under the condition that the correct model of the electric network is always available.

accurately. Particularly, comparing that part of the results from the third test case that can be seen in Figure 6.12 and Figure 6.14, with their counterpart results in the first test case, i.e., Figure 6.4 and Figure 6.6, or their counterpart results in the second test case, i.e., Figure 6.8 and Figure 6.10, shows that missing measurements may adversely affect the accuracy of results in conventional estimators like EKF, UKF and CKF, but the estimator resulting from the proposed approach, AEKF, can track the states of the generators especially the generators' speed deviation.

Although the illustrated figures have shown the performance of each estimator under the different circumstances quite well, the RMSE index that was defined in

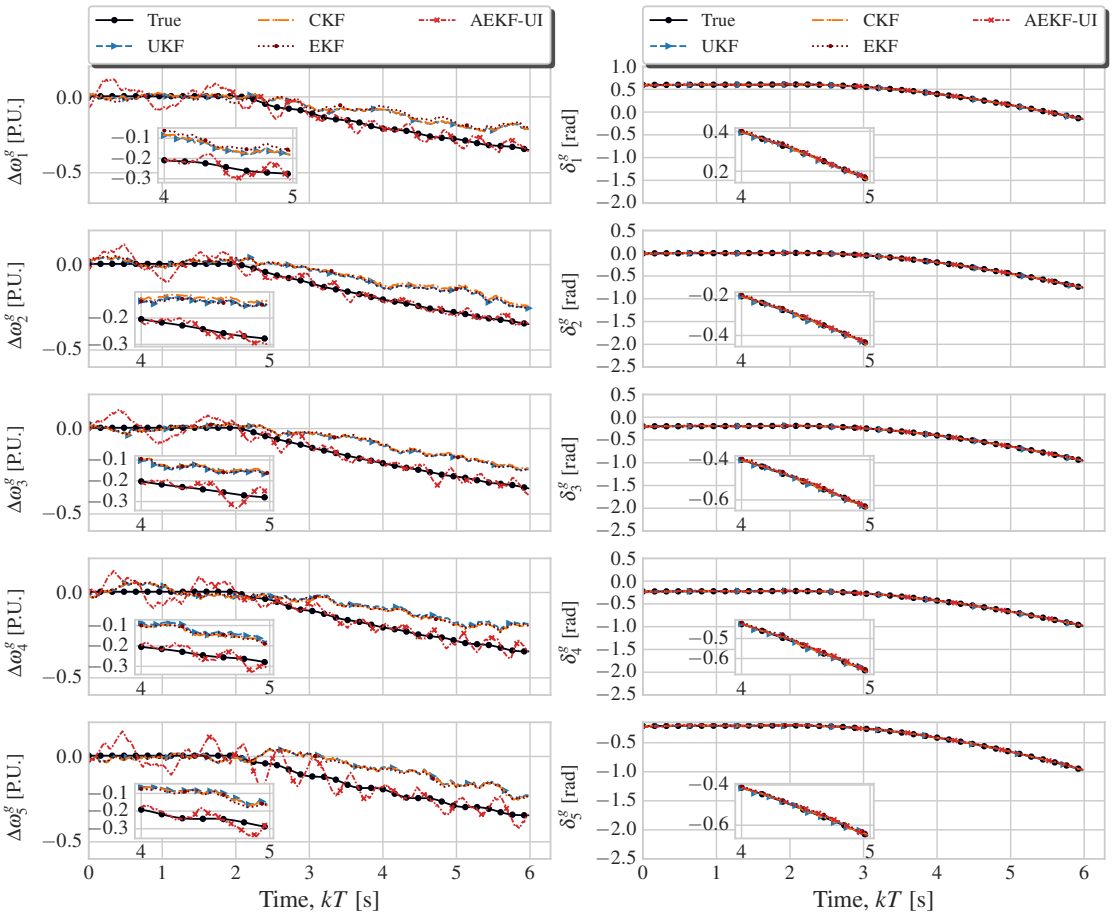

Figure 6.6: The estimated $\Delta\omega$ and δ of all generators in case of switching on the load at the bus 9 under the condition that the correct model of the electric network is not available after the incident.

(6.23) can also be a useful metric in evaluating how much successful an estimator is in performing its estimation task. RMSE values for all estimators under the aforementioned three test cases are presented in Table 6.2 , Table 6.3 and Table 6.4 , and as can be observed, the proposed estimator, AEKF-UI, results in smaller RMSE values than its rivals in cases where noticeable model mismatches have occurred.

To realize the simulations, it is assumed that measurement white noise has $\sigma = 0.01$, i.e., $\mathbf{R}^d = (0.01)^2\mathbf{I}$. Moreover, the process noise is also set to 0.01 p.u, i.e., $\mathbf{Q}^d = (0.01)^2\mathbf{I}$. In addition, the sampling rate used for generating the measurement data is assumed to be 50 samples per second, and such a sample time is utilized

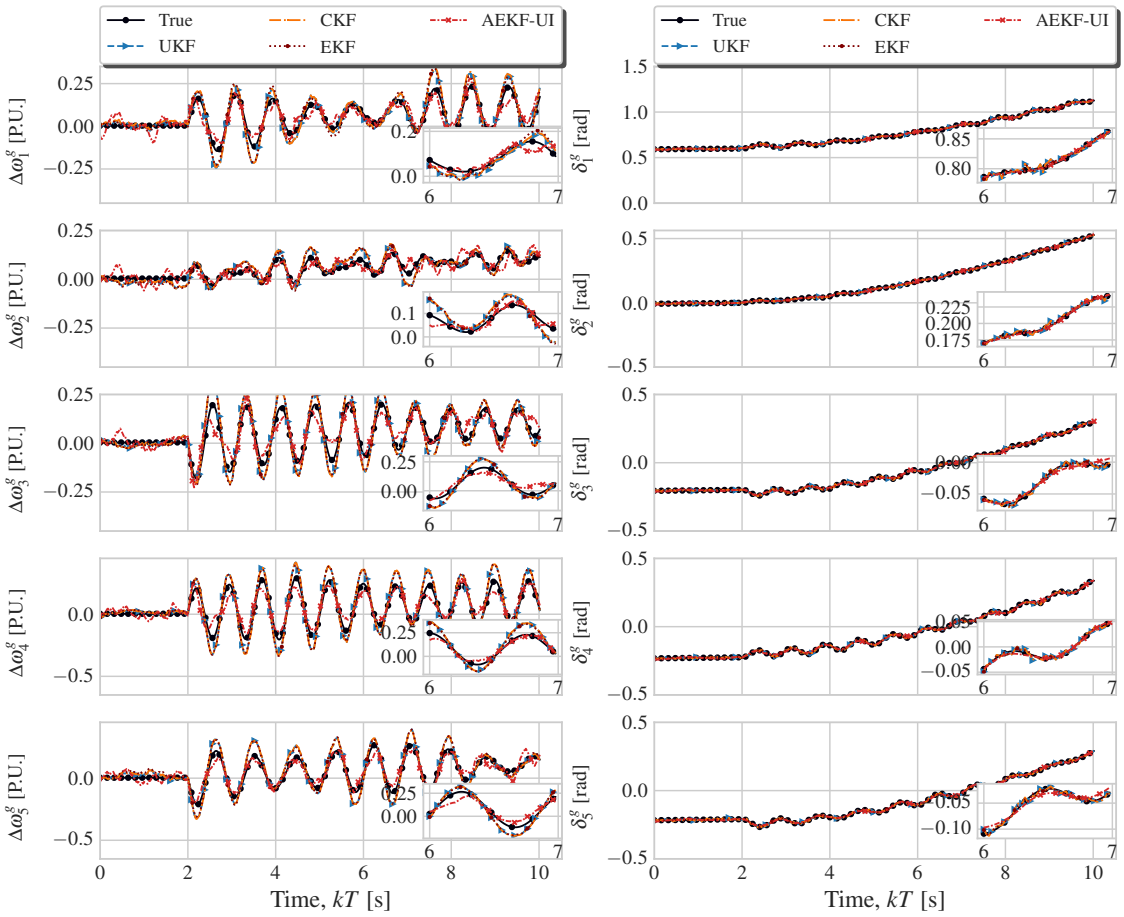

Figure 6.7: The estimated $\Delta\omega$ and δ of all generators in case of switching off line between buses 4 and 5, under the condition that the correct model of the electric network is always available (with inertia error).

for the estimation processes, as well. All the programming codes and simulations have been implemented in Python programming language and performed on an Intel Core i5 CPU with 8-GB RAM.

6.5 Conclusion

Due to the numerous and often unexpected factors such as aging, temperature, nonlinearity, faults, etc. that can affect a real-world system's model, this work addresses the issue of model mismatching for KF-based estimators. To achieve the goal

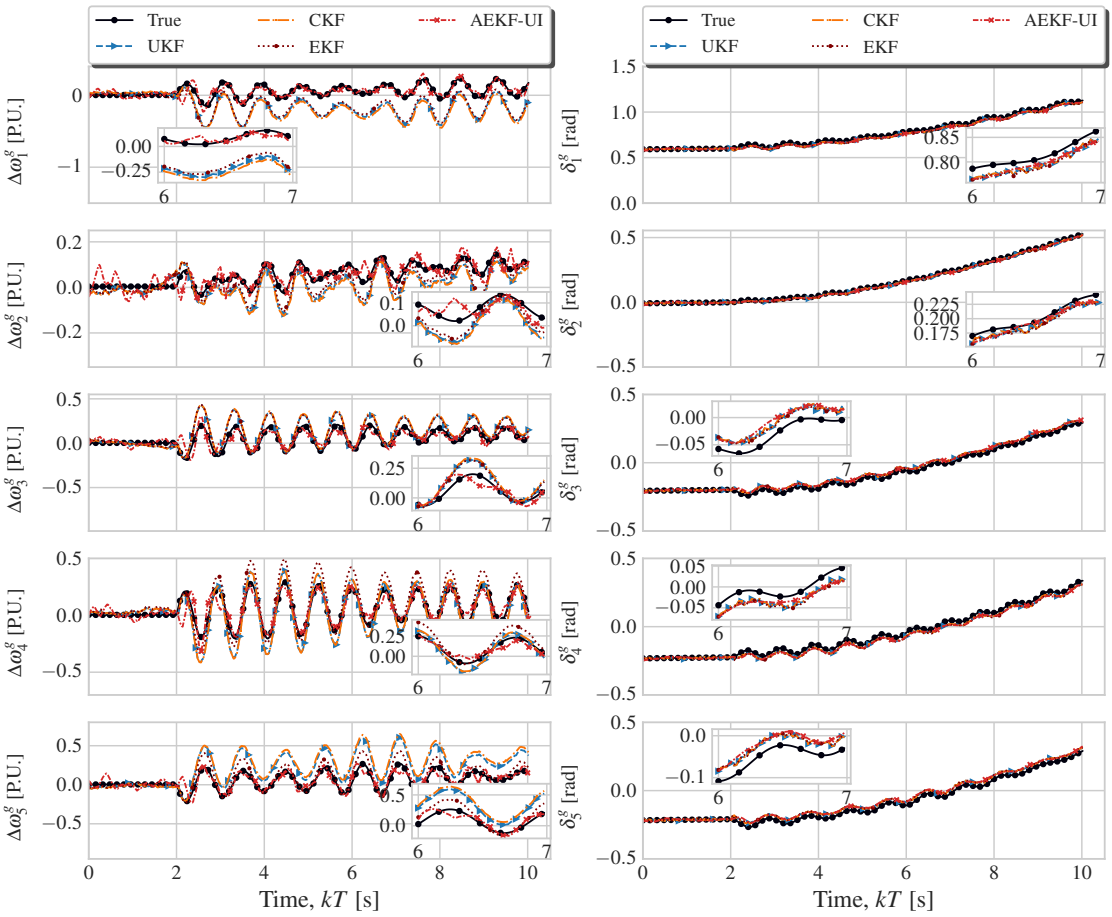

Figure 6.8: The estimated $\Delta\omega$ and δ of all generators in case of switching off the line between buses 4 and 5, under the condition that the correct model of the electric network is not available after the incident (with inertia error).

of developing a robust estimator working under model inaccuracies, an engineering approach was presented, wherein not only the concept of the estimation strategy but also the designer's understanding of the behavior of the system is considered and utilized. An implementation of the proposed approach resulting in a robust estimator is explained explicitly using the IEEE 14-bus 5-generator benchmark. The resulting estimator is observed to be robust to the noticeable model mismatches occurring during the system operation. Also, during this implementation, it was found that even if the Jacobian matrix of the resulting estimator is not updated and is kept its initial value, the estimator functions properly. This results in a significant reduc-

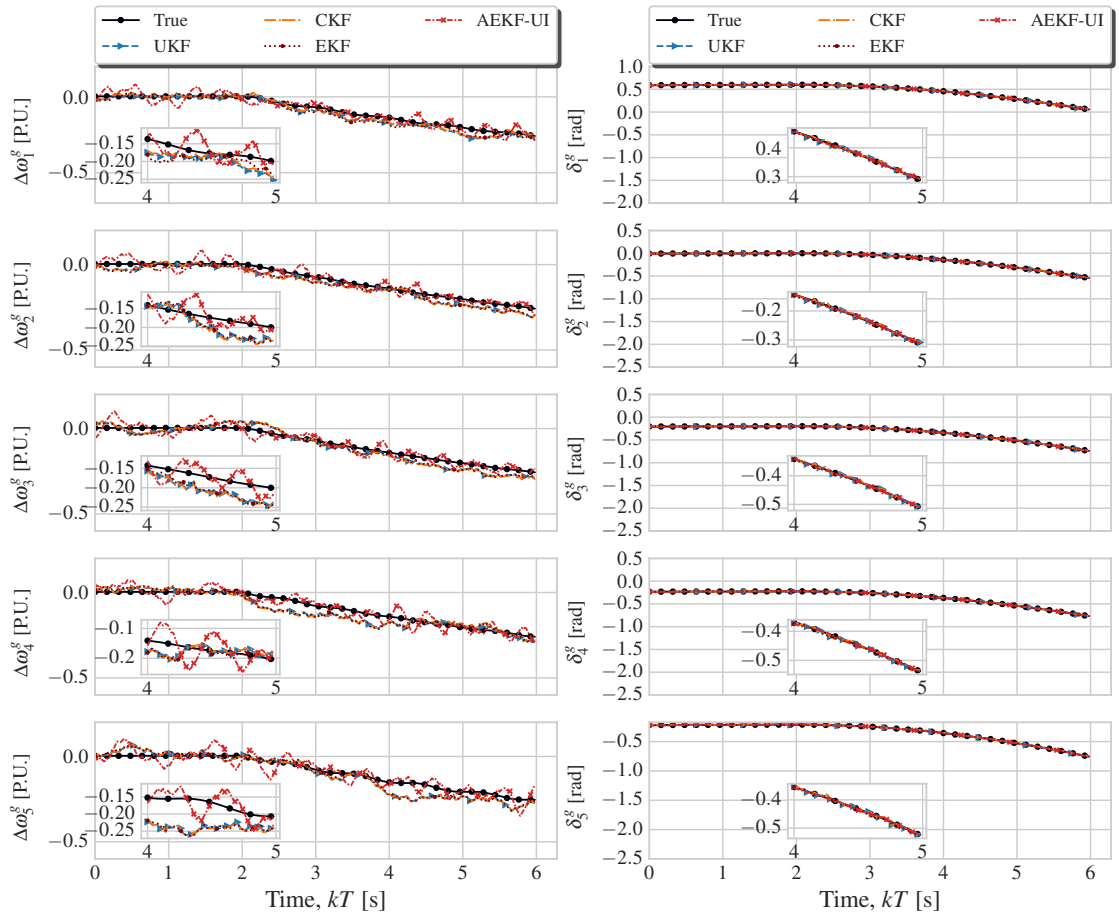

Figure 6.9: The estimated $\Delta\omega$ and δ of all generators in case of switching on the load at the bus 9 under the condition that the correct model of the electric network is always available (with inertia error).

tion in computational time. Comparing the performance of the estimator resulting from the proposed methodology with that of standard estimators like EKF, UKF, and CKF, demonstrates that the suggested approach yields a robust estimator for a nonlinear system even when model errors are present and Gaussian noise exists. As a future work, this methodology will be adapted to be implemented in a distributed framework rather than a centralized one, which could be beneficial for huge systems such as a power system with many components and sensors.

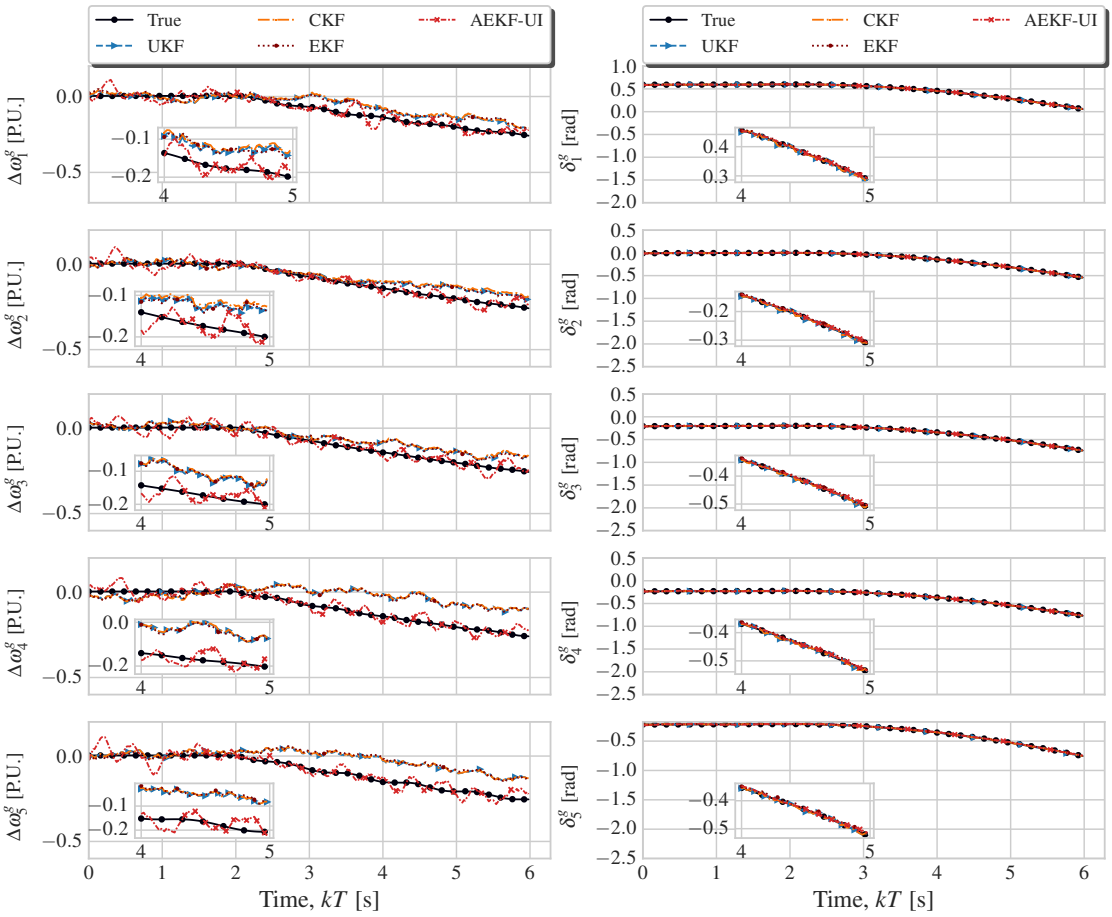

Figure 6.10: The estimated $\Delta\omega$ and δ of all generators in case of switching on the load at the bus 9 under the condition that the correct model of the electric network is not available after the incident (with inertia error).

Table 6.2: The comparison of the RMSE for UKF, CKF, EKF, EKF-UI, and AEKF-UI.

Estimator	Line Switching		Load Increasing	
	Accurate grid Mdl	Inaccurate grid Mdl	Accurate grid Mdl	Inaccurate grid Mdl
UKF	0.01625	0.10905	0.014119	0.07262
CKF	0.01765	0.12307	0.015413	0.07354
EKF	0.01697	0.09205	0.015093	0.07228
EKF-UI	0.15362	0.15802	0.165746	0.15213
AEKF-UI	0.02674	0.04240	0.021258	0.02210

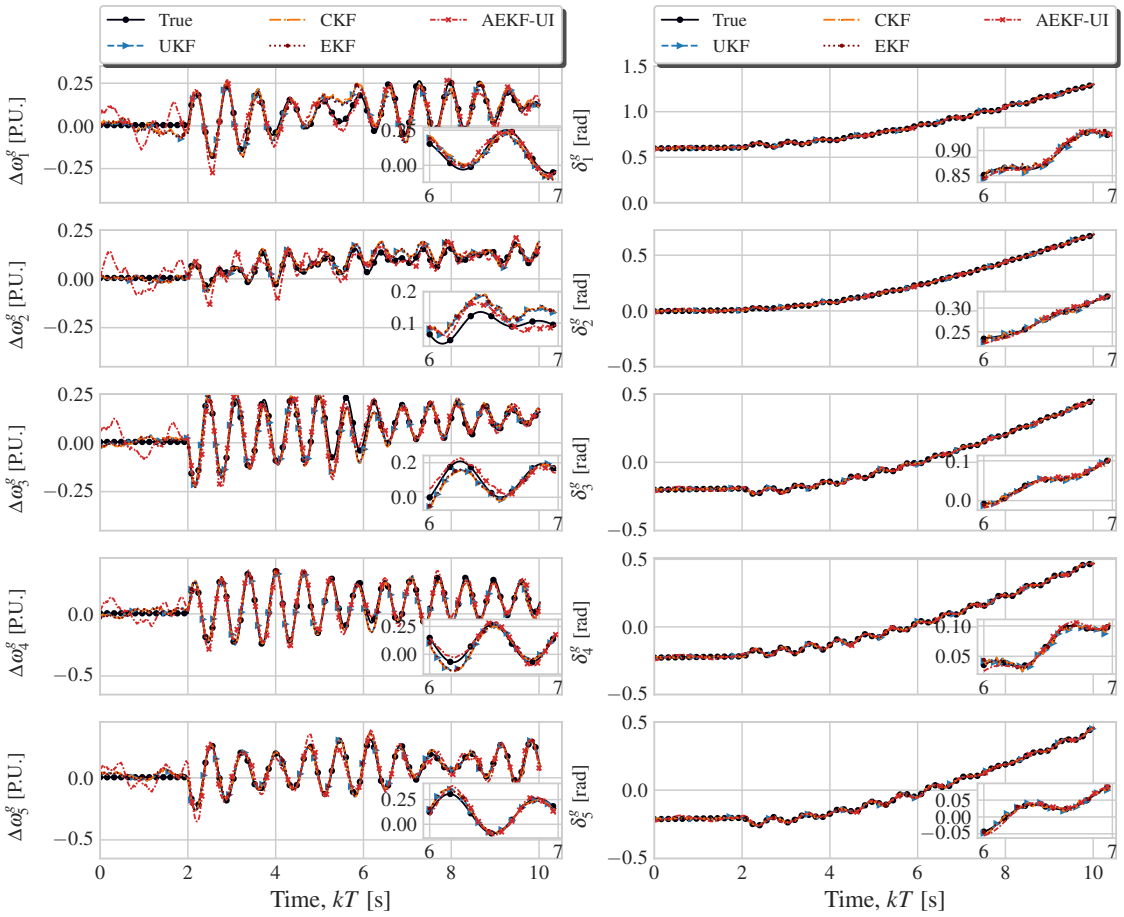

Figure 6.11: The estimated $\Delta\omega$ and δ of all generators in case of switching off the line between buses 4 and 5, under the conditions that the correct model of the electric network is always available and no measurements available from PMU at B1.

Table 6.3: The comparison of the RMSE for UKF, CKF, EKF, EKF-UI, and AEKF-UI (inertia errors).

Estimator	Line Switching		Load Increasing	
	Accurate grid Mdl	Inaccurate grid Mdl	Accurate grid Mdl	Inaccurate grid Mdl
UKF	0.03477	0.11223	0.022773	0.05809
CKF	0.03567	0.12582	0.023305	0.05906
EKF	0.03455	0.08606	0.023158	0.05756
EKF-UI	0.16981	0.16610	0.159836	0.16077
AEKF-UI	0.03783	0.03893	0.024418	0.02732

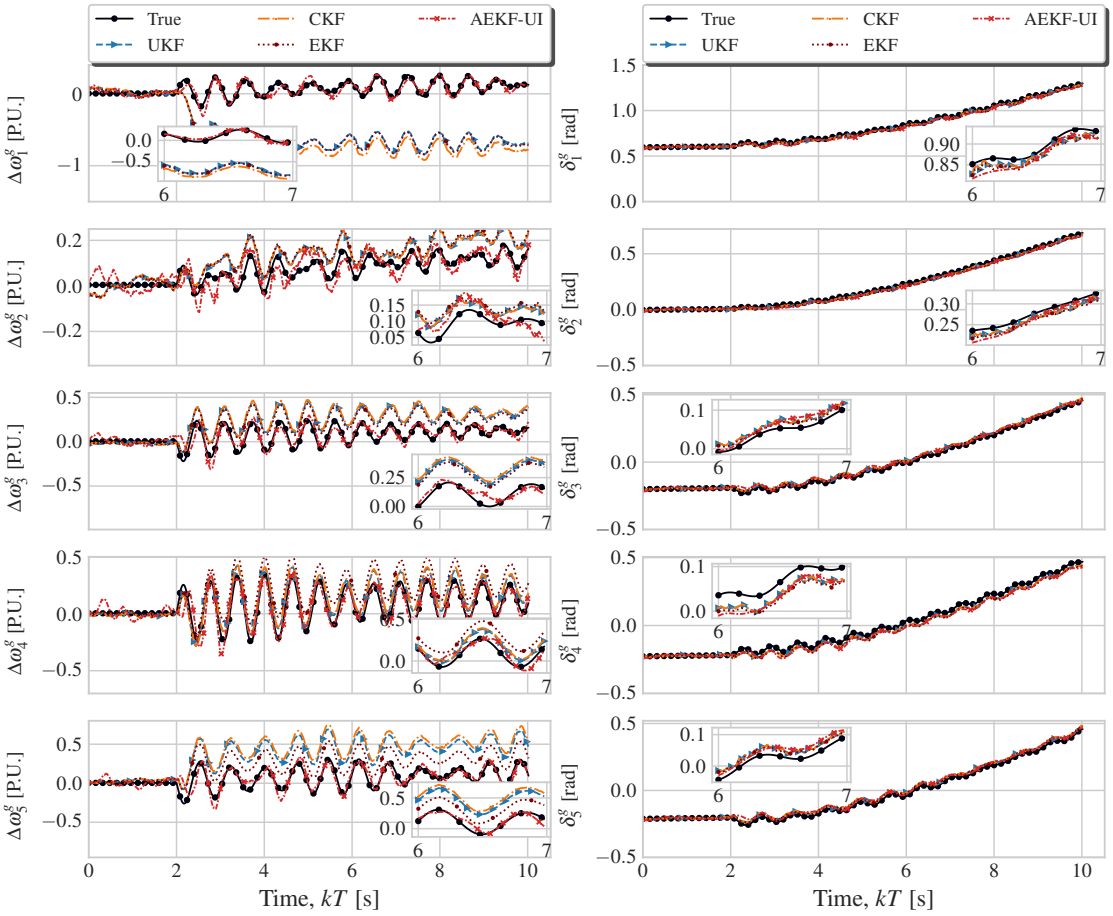

Figure 6.12: The estimated $\Delta\omega$ and δ of all generators in case of switching off the line between buses 4 and 5, under the conditions that the correct model of the electric network is not available after the incident and no measurements available from PMU at B1.

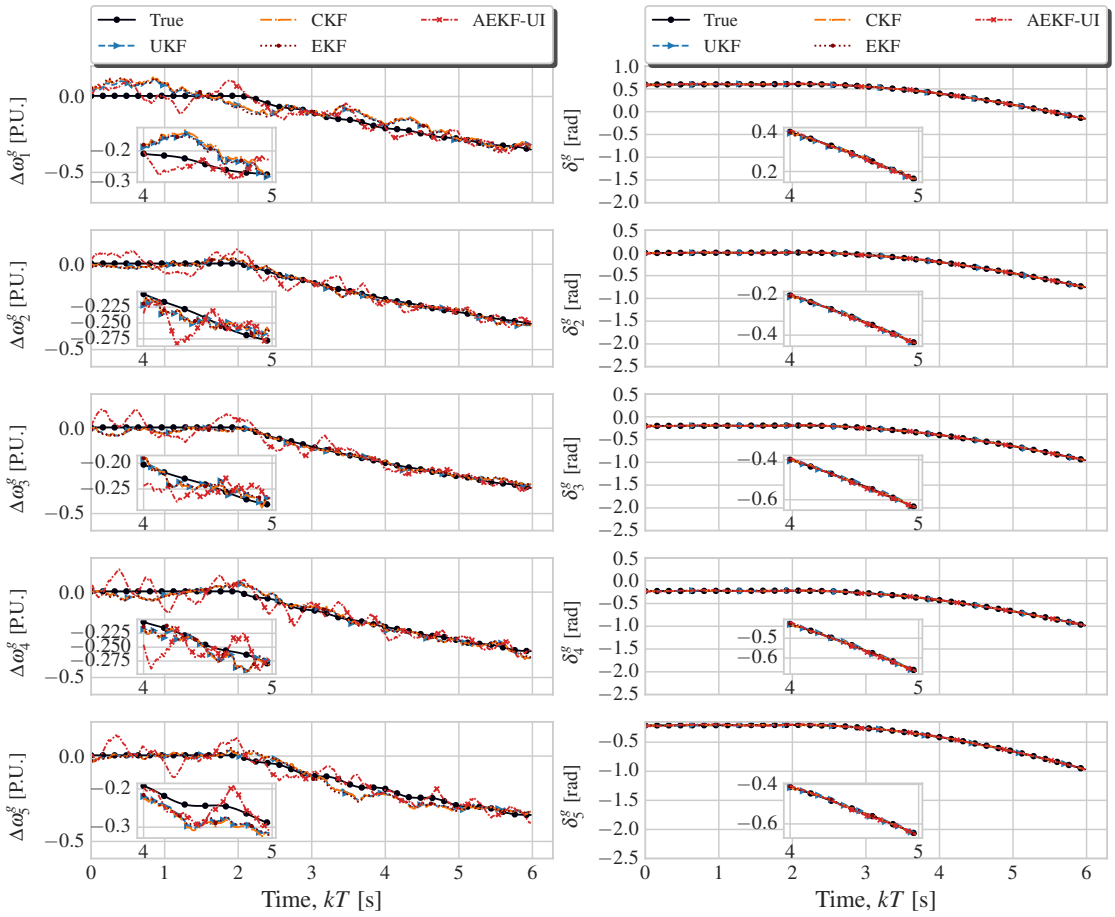

Figure 6.13: The estimated $\Delta\omega$ and δ of all generators in case of switching on the load at the bus 9 under the conditions that the correct model of the electric network is always available and no measurements available from PMU at B1.

Table 6.4: The comparison of the RMSE for UKF, CKF, EKF, EKF-UI, and AEKF-UI (missing measurements from PMU at B1).

Estimator	Line Switching		Load Increasing	
	Accurate grid Mdl	Inaccurate grid Mdl	Accurate grid Mdl	Inaccurate grid Mdl
UKF	0.02088	0.24686	0.01860	0.07456
CKF	0.02257	0.27386	0.01980	0.07929
EKF	0.02090	0.24090	0.01856	0.08221
EKF-UI	0.20288	0.20372	0.20694	0.20777
AEKF-UI	0.02625	0.04693	0.02365	0.03220

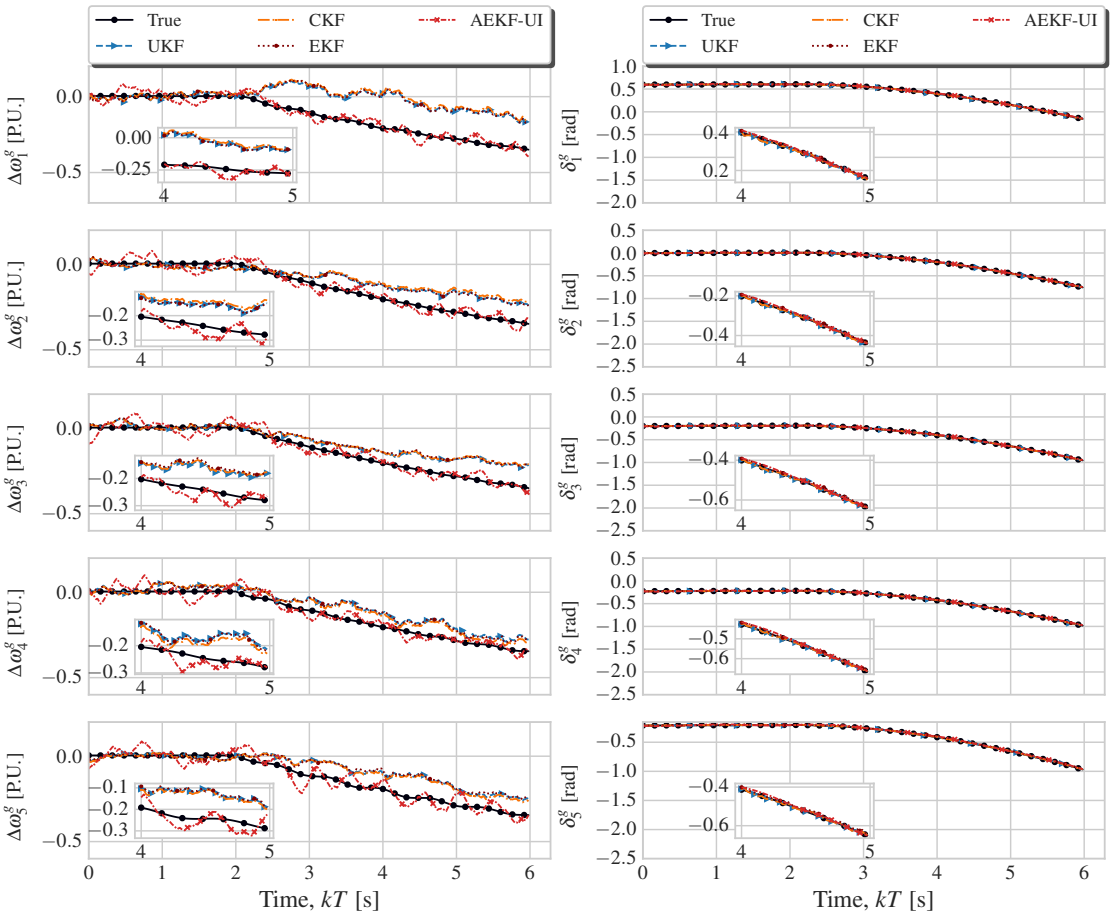

Figure 6.14: The estimated $\Delta\omega$ and δ of all generators in case of switching on the load at the bus 9 under the conditions that the correct model of the electric network is not available after the incident and no measurements available from PMU at B1.

Chapter 7

Conclusion

Nowadays power systems including electrical grids and/or microgrids play a fundamental and crucial role in providing electric energy to consumers across the globe. Since humans are highly dependent on electricity, their lives can be seriously jeopardized without electrical grids. Therefore, the more precise the estimates of the state variables are, the better the chance of controlling and monitoring systems regardless of the methodologies that are considered and planned for these systems. Undoubtedly, two areas that can definitely contribute to having more accurate state variables of a system are state estimation and system modeling and identification. Chapter 2 of the thesis explained a set of procedures to mathematically model a power system. The main benefit of such a mathematical modeling approach is that it allows researchers to discover more deeply the concepts and events hidden beneath technical software. Therefore, all research works in this PhD thesis are based on the concepts and the models described in this chapter. Furthermore, Chapter 3, reviewed most recent works as well as the state of the art in dynamic state estimation and in this direction, several well-known KF-based filters like EKF, UKF, and CKF, which are generally suitable for nonlinear system applications, are explored in more detail.

Motivated by the current problems and challenges exist in electrical grids from the perspective of modeling and estimation, this thesis explores and develops several approaches that can be used for estimating and model identification in power systems. The main contributions of the thesis is the proposal of several methodologies for improving state estimation as well as modeling in power system applications. The simulations results obtained using several benchmark models as well as experimental

results obtained using real-world systems verify the effectiveness and reliability of the new proposed methods. Specially, the proposed data-driven approach for modeling a real synchronous generator can be considered as a great and promising work in the direction of using AI methods and measured I/O data to find an accurate model of real-world systems like a synchronous generator.

In Chapter 4, a novel method was developed for the distributed simultaneous estimation of states and unknown inputs for linear discrete-time systems. The main contribution of this work was the Lyapunov stability proof provided for guaranteeing the stability and convergence of the proposed distributed filter. Additionally, the unbiasedness and minimum variance of state and unknown input estimation were investigated and verified. The condition making the estimator stable was stated, from which a sufficient distributed gain was extracted. Finally, the proposed method was applied to a system and its results were compared to the results of the centralized estimator. Based on the test results, the distributed estimators performed as well as the centralized estimator in terms of estimating states and unknown inputs, which is a great accomplishment, since besides keeping the estimation of states and unknown inputs accurate, the decentralization process of estimation brings more reliability and robustness to estimation results because central processing failures are no longer a problem.

Chapter 5 presents a novel approach for creating a global model for a real synchronous generator by combining subspace identification method with T-S fuzzy modeling. The main contribution of this work is the proposal a data-driven based approach for finding a global model for a real synchronous generator. All the developed procedures, such as dataset construction, clustering, local model identification, and T-S fuzzy modeling, are thoroughly illustrated with simulations and experiential case studies. The results from these case studies demonstrate that even under some unfavorable conditions such as noise, saturation issues, or variable terminal voltages, etc, which may occur during SG operations, the proposed novel approach can still lead to a precise global model. Therefore, the newly developed approach is efficient, flexible, and robust enough to be used in a variety of scenarios and/or environments. Also, the model is composed of several linear submodels in the form of state space representation, so it can be easily applied in control and estimation applications as well.

In Chapter 6, an engineering approach to develop a robust estimator in the

presence of some model mismatches is presented. In the proposed approach, not only the concept of estimation strategy but also the designer's understanding of the behavior of the system is considered and utilized. An implementation of the proposed approach which leads to a robust estimator is explained explicitly using the IEEE 14-bus 5-generator benchmark and it is observed that the resultant estimator is resistant to the noticeable model mismatches occurring during the operation of the power system. Comparing the performance of the resultant estimator with that of standard estimators like EKF, UKF, and CKF, demonstrates that the suggested approach yields a robust estimator for a nonlinear system even when model errors are present and Gaussian noise exists.

In this thesis, state estimation and modeling problems related to electrical grids were addressed; and several methodologies were proposed and developed to overcome such issues. The suggested approaches were compared with state-of-the-art approaches: a distributed estimator for linear systems to simultaneously estimate system state variables and its unknown inputs, was developed and necessary conditions for its stability and convergence were investigated (Chapter 4); T-S fuzzy modeling and SIM were utilized to create a data-driven approach to find a global model for a real synchronous generator (Chapter 5); A new adaptive approach based on EKF was proposed to tackle the model mismatch problem for nonlinear systems estimation, where the designer's knowledge and experience from the system's behavior were considered and utilized as well (Chapter 6). As a result, all the proposed approaches can be applied to problems relating to state estimation and modeling of nonlinear systems in power systems. However, there are still some issues that need future work, which could improve the performance of the proposed methodologies, such as:

- The distributed approach to simultaneously estimating state variables of the system as well as unknown inputs has shown to be stable and convergent under special conditions. However, if some conditions like unbiasedness or Gaussian noise can be relaxed, the proposed approach can be applied to a wider class of linear systems (Chapter 4).

- A data-driven approach was proposed for modeling a real synchronous generator but it would be interesting to examine the performance of the identified model in control and estimation methodologies like model predictive control

(MPC) and Kalman-based filters, where an accurate model is usually required. As another future work, establishing an adaptive mechanism for the obtained model would improve its accuracy and reduce the necessity to repeat the whole explained modeling procedure over time. (Chapter 5).

- The adaptive engineering approach for nonlinear systems estimation was an implemented framework. However, converting this work in a decentralized and distributed manner would be promising for huge systems like power systems, where it is possible to partition the power system into several regions and treat each region as an independent agent (Chapter 6).

Bibliography

[Abdallah *et al.*, 2022] Rayen Ben Abdallah, Gaël Pagès, Damien Vivet, Jordi Vilà-Valls, and Eric Chaumette. Robust Linearly Constrained Square-Root Cubature Kalman Filter for Mismatched Nonlinear Dynamic Systems. *IEEE Control Systems Letters*, vol. 6, pp. 2335–2340, February 2022. (Cited in page 98).

[Aitken and Clarke, 2012] Jonathan M. Aitken and Tim Clarke. Observer/Kalman Filter Identification With Wavelets. *IEEE Transactions on Signal Processing*, vol. 60, no. 7, pp. 3476–3485, July 2012. (Cited in pages 60, 61, 69, 75, 76, 77, and 78).

[Akhlaghi and Zhou, 2017] S. Akhlaghi and N. Zhou. Adaptive multi-step prediction based EKF to power system dynamic state estimation. In: *2017 IEEE Power and Energy Conference at Illinois (PECI)*, IEEE Power and Energy Conference, pp. 1–8. Feb. 23-24 2017. (Cited in page 18).

[Alhalali and El-Shatshat, 2019] Safoan Alhalali and Ramadan El-Shatshat. Cubature Particle Filtering Approach for State Estimation in Electrical Distribution Systems. In: *2019 IEEE Power & Energy Society General Meeting (PESGM)*, 2019 IEEE Power & Energy Society General Meeting (PESGM), pp. 1–5. August 4-8 2019. (Cited in page 16).

[Aminifar *et al.*, 2014] F. Aminifar, M. Shahidehpour, M. Fotuhi-Firuzabad, and S. Kamalinia. Power System Dynamic State Estimation With Synchronized Phasor Measurements. *IEEE Transactions on Instrumentation and Measurement*, vol. 63, no. 2, pp. 352–363, Feb. 2014. (Cited in page 17).

[Anagnostou and Pal, 2018] G. Anagnostou and B. C. Pal. Derivative-Free Kalman Filtering Based Approaches to Dynamic State Estimation for Power Systems With

Unknown Inputs. *IEEE Transactions on Power Systems*, vol. 33, no. 1, pp. 116–130, Jan. 2018. (Cited in pages 19, and 98).

[Arasaratnam and Haykin, 2009] Ienkaran Arasaratnam and Simon Haykin. Cubature Kalman Filters. *IEEE Transactions on Automatic Control*, vol. 54, no. 6, pp. 1254–1269, June 2009. (Cited in pages 20, and 98).

[Arastou *et al.*, 2021a] A. Arastou, M. Karrari, and B. Zaker. New Method for Synchronous Generator Parameters Estimation Using Load Rejection Tests Data Considering Operational Limitations. *Electric Power Systems Research*, vol. 192, p. 106999, March 2021. (Cited in page 58).

[Arastou *et al.*, 2021b] Alireza Arastou, Hadi Rabieyan, and Mehdi Karrari. A Novel PSS-based Online Test Procedure for Parameter Estimation of Synchronous Generator Using the Governor System. *IEEE Transactions on Energy Conversion*, vol. 36, no. 4, pp. 3178–3187, Dec. 2021. (Cited in pages 58, and 59).

[Arjona *et al.*, 2011] M. A. Arjona, M. Cisneros-González, and C. Hernández. Parameter Estimation of a Synchronous Generator Using a Sine Cardinal Perturbation and Mixed Stochastic–Deterministic Algorithms. *IEEE Transactions on Industrial Electronics*, vol. 58, no. 2, pp. 486–493, Feb. 2011. (Cited in page 58).

[Basetti *et al.*, 2022] Vedik Basetti, Ashwani Kumar Chandel, and Chandan Kumar Shiva. Square-root cubature Kalman filter based power system dynamic state estimation. *Sustainable Energy, Grids and Networks*, vol. 31, p. 100712, September 2022. (Cited in page 20).

[Belqorchi *et al.*, 2019] Abdelghafour Belqorchi, Ulas Karaagac, Jean Mahseredjian, and Innocent Kamwa. Standstill Frequency Response Test and Validation of a Large Hydrogenerator. *IEEE Transactions on Power Systems*, vol. 34, no. 3, pp. 2261–2269, May 2019. (Cited in page 58).

[Bendaoud *et al.*, 2021] Elrachid Bendaoud, Hammoud Radjeai, and Oussama Boutalbi. Identification of Nonlinear Synchronous Generator Parameters Using Stochastic Fractal Search Algorithm. *Journal of Control, Automation and Electrical Systems*, vol. 32, no. 6, pp. 1639–1651, Dec. 2021. (Cited in pages 58, 59, and 61).

[Boulkaibet *et al.*, 2017] Ilyes Boulkaibet, Khaled Belarbi, Sofiane Bououden, Tshilidzi Marwala, and Mohammed Chadli. A new T-S fuzzy model predictive control for nonlinear processes. *Expert Systems with Applications*, vol. 88, pp. 132–151, Dec. 2017. (Cited in page 67).

[Brus *et al.*, 2008] Linda Brus, Torbjörn Wigren, and Bengt Carlsson. Initialization of a Nonlinear Identification Algorithm Applied to Laboratory Plant Data. *IEEE Transactions on Control Systems Technology*, vol. 16, no. 4, pp. 708–716, July 2008. (Cited in page 59).

[Butcher, 2008] J. C. Butcher. *Numerical Methods for Ordinary Differential Equations*. John Wiley & Sons, Ltd, 2nd ed., 2008. (Cited in page 23).

[Catlin, 1989] Donald E. Catlin. *Estimation, Control, and the Discrete Kalman Filter*. Applied Mathematical Sciences. Springer, 1989. (Cited in page 22).

[Cattivelli and Sayed, 2011] F. S. Cattivelli and A. H. Sayed. Analysis of Spatial and Incremental LMS Processing for Distributed Estimation. *IEEE Transactions on Signal Processing*, vol. 59, no. 4, pp. 1465–1480, April 2011. (Cited in pages 3, and 32).

[Chakhchoukh *et al.*, 2020] Yacine Chakhchoukh, Hangtian Lei, and Brian K. Johnson. Diagnosis of Outliers and Cyber Attacks in Dynamic PMU-Based Power State Estimation. *IEEE Transactions on Power Systems*, vol. 35, no. 2, pp. 1188–1197, March 2020. (Cited in page 18).

[Chang *et al.*, 2011] Chun-Hua Chang, Shao-Chen Wang, and Chieh-Chih Wang. Vision-based cooperative simultaneous localization and tracking. In: *2011 IEEE International Conference on Robotics and Automation*, 2011 IEEE International Conference on Robotics and Automation, pp. 5191–5197. May 9-13 2011. (Cited in page 98).

[Chang *et al.*, 2016] Yuan-Chih Chang, Chien-Hua Chen, Zhong-Chuan Zhu, and Yi-Wen Huang. Speed Control of the Surface-Mounted Permanent-Magnet Synchronous Motor Based on Takagi–Sugeno Fuzzy Models. *IEEE Transactions on Power Electronics*, vol. 31, no. 9, pp. 6504–6510, September 2016. (Cited in page 60).

[Chauchat *et al.*, 2022] Paul Chauchat, Jordi Vilà-Valls, and Eric Chaumette. On the asymptotic behavior of linearly constrained filters for robust multi-channel signal processing. *Signal Processing*, vol. 196, p. 108500, July 2022. (Cited in page 98).

[Cheng *et al.*, 2009] Yue Cheng, Hao Ye, Yongqiang Wang, and Donghua Zhou. Unbiased minimum-variance state estimation for linear systems with unknown input. *Automatica*, vol. 45, no. 2, pp. 485–491, Feb 2009. (Cited in page 49).

[Cui and Kavasseri, 2015] Yinan Cui and Rajesh Kavasseri. A Particle Filter for Dynamic State Estimation in Multi-Machine Systems With Detailed Models. *IEEE Transactions on Power Systems*, vol. 30, no. 6, pp. 3377–3385, November 2015. (Cited in page 17).

[Dang *et al.*, 2020] Lujuan Dang, Badong Chen, Shiyuan Wang, Wentao Ma, and Pengju Ren. Robust Power System State Estimation With Minimum Error Entropy Unscented Kalman Filter. *IEEE Transactions on Instrumentation and Measurement*, vol. 69, no. 11, pp. 8797–8808, Nov. 2020. (Cited in page 98).

[Dang *et al.*, 2022] Lujuan Dang, Wanli Wang, and Badong Chen. Square Root Unscented Kalman Filter With Modified Measurement for Dynamic State Estimation of Power Systems. *IEEE Transactions on Instrumentation and Measurement*, vol. 71, pp. 1–13, March 2022. (Cited in page 19).

[Dehghani *et al.*, 2010] M. Dehghani, M. Karrari, W. Rosehart, and O.P. Malik. Synchronous machine model parameters estimation by a time-domain identification method. *International Journal of Electrical Power & Energy Systems*, vol. 32, no. 5, pp. 524–529, June 2010. (Cited in pages 4, 58, 59, and 61).

[Dehghani and Nikravesh, 2008] Maryam Dehghani and Seyyed Kamaleddin Yadavar Nikravesh. State-Space Model Parameter Identification in Large-Scale Power Systems. *IEEE Transactions on Power Systems*, vol. 23, no. 3, pp. 1449–1457, Aug. 2008. (Cited in pages 4, 58, 59, 61, and 62).

[Ding and Fang, 2017] Bo Ding and Huajing Fang. Adaptive Modified Input and State Estimation for Linear Discrete-Time System with Unknown Inputs. *Circuits, Systems, and Signal Processing*, vol. 36, no. 9, pp. 3630–3649, Sep 2017. (Cited in page 38).

[Eckenhoff *et al.*, 2021] Kevin Eckenhoff, Patrick Geneva, and Guoquan Huang. MIMC-VINS: A Versatile and Resilient Multi-IMU Multi-Camera Visual-Inertial Navigation System. *IEEE Transactions on Robotics*, vol. 37, no. 5, pp. 1360–1380, Oct. 2021. (Cited in page 98).

[Emami *et al.*, -] Alireza Emami, Rui Araújo, Sérgio Cruz, and A. Pedro Aguiar. Engineering Approach to Construct Robust Filter for Mismatched Nonlinear Dynamic Systems. *International Journal of Robust and Nonlinear Control*, Under-reviewing -. (Cited in page 4).

[Emami *et al.*, 2020] Alireza Emami, Rui Araújo, and Alireza Asvadi. Distributed Simultaneous Sstimation of States and Unknown Inputs. *Systems & Control Letters*, vol. 138, p. 104660, April 2020. (Cited in pages 4, 33, 71, 104, and 105).

[Emami *et al.*, 2024] Alireza Emami, Rui Araújo, Sérgio Cruz, Hazem Hadla, and A. Pedro Aguiar. A Systematic Approach to Modeling Synchronous Generator Using Markov Parameters and T-S Fuzzy Systems. *Expert Systems with Applications*, vol. 235, p. 121122, January 2024. (Cited in page 4).

[Everett and Dubay, 2017] Scott E. Everett and Rickey Dubay. A sub-space artificial neural network for mold cooling in injection molding. *Expert Systems with Applications*, vol. 79, pp. 358–371, Feb. 2017. (Cited in page 61).

[Fan and Miao, 2021] Lingling Fan and Zhixin Miao. Time-Domain Measurement-Based *DQ*-Frame Admittance Model Identification for Inverter-Based Resources. *IEEE Transactions on Power Systems*, vol. 36, no. 3, pp. 2211–2221, May 2021. (Cited in page 61).

[Fard *et al.*, 2005] R. D. Fard, M. Karrari, and O. P. Malik. Synchronous generator model identification for control application using volterra series. *IEEE Transactions on Energy Conversion*, vol. 20, no. 4, pp. 852–858, Dec. 2005. (Cited in pages 58, 59, and 60).

[Faria *et al.*, 2020] Victor A.D. Faria, J.V. Bernardes, and Edson C. Bortoni. Parameter estimation of synchronous machines considering field voltage variation during the sudden short-circuit test. *International Journal of Electrical Power & Energy Systems*, vol. 114, p. 105421, Jan. 2020. (Cited in page 58).

[Gandhi and Mili, 2010] Mital A. Gandhi and Lamine Mili. Robust Kalman Filter Based on a Generalized Maximum-Likelihood-Type Estimator. *IEEE Transactions on Signal Processing*, vol. 58, no. 5, pp. 2509–2520, May 2010. (Cited in page 98).

[Ganjefar and Alizadeh, 2011] Soheil Ganjefar and Mojtaba Alizadeh. On-line Identification of Synchronous Generator Using Self Recurrent Wavelet Neural Networks via Adaptive Learning Rates. In: *2011 5th International Power Engineering and Optimization Conference*, 2011 5th International Power Engineering and Optimization Conference, pp. 243–248. June 6-7 2011. (Cited in pages 58, 59, and 60).

[Ghahremani and Kamwa, 2011] E. Ghahremani and I. Kamwa. Dynamic State Estimation in Power System by Applying the Extended Kalman Filter With Unknown Inputs to Phasor Measurements. *IEEE Transactions on Power Systems*, vol. 26, no. 4, pp. 2556–2566, November 2011. (Cited in pages 16, 17, and 98).

[Ghahremani and Kamwa, 2016] E. Ghahremani and I. Kamwa. Local and Wide-Area PMU-Based Decentralized Dynamic State Estimation in Multi-Machine Power Systems. *IEEE Transactions on Power Systems*, vol. 31, no. 1, pp. 547–562, Jan. 2016. (Cited in pages 17, 18, and 32).

[Ghahremani *et al.*, 2008] E. Ghahremani, M. Karrari, and O.P. Malik. Synchronous generator third-order model parameter estimation using online experimental data. *IET Generation, Transmission & Distribution*, vol. 2, no. 5, pp. 708–719, September 2008. (Cited in pages 4, 58, 59, 61, and 62).

[Gillijns and Moor, 2007a] Steven Gillijns and Bart De Moor. Unbiased Minimum-Variance Input and State Estimation for Linear Discrete-Time Systems. *Automatica*, vol. 43, no. 1, pp. 111–116, 2007. (Cited in pages 33, 37, 38, and 51).

[Gillijns and Moor, 2007b] Steven Gillijns and Bart De Moor. Unbiased minimum-variance input and state estimation for linear discrete-time systems. *Automatica*, vol. 43, no. 1, pp. 111–116, January 2007. (Cited in pages 104, and 105).

[Godsil and Royle, 2001] Chris Godsil and Gordon F. Royle. *Algebraic Graph Theory*. Springer-Verlag, 2001. (Cited in page 35).

[Gonçalves *et al.*, 2019] P. F. C. Gonçalves, S. M. A. Cruz, and A. M. S. Mendes. Finite Control Set Model Predictive Control of Six-Phase Asymmetrical Machines–An Overview. *Energies*, vol. 12, no. 24, pp. 1–42, December 2019. (Cited in page 60).

[Gopinath *et al.*, 2016] R. Gopinath, C. Santhosh Kumar, K.I. Ramachandran, V. Upendranath, and P.V.R. Sai Kiran. Intelligent fault diagnosis of synchronous generators. *Expert Systems with Applications*, vol. 45, pp. 142–149, March 2016. (Cited in page 61).

[Govindarajan *et al.*, 2020] Suganya Govindarajan, Jayalalitha Subbaiah, Andrea Cavallini, Kannan Krithivasan, and Jaikanth Jayakumar. Partial Discharge Random Noise Removal Using Hankel Matrix-Based Fast Singular Value Decomposition. *IEEE Transactions on Instrumentation and Measurement*, vol. 69, no. 7, pp. 4093–4102, July 2020. (Cited in pages 71, and 78).

[Grigsby, 2012] Leonard L. Grigsby. *The Electric Power Engineering Handbook: Power Systems*. CRC Press, 2012. doi:10.1201/b12111-5. (Cited in page 9).

[Grillo *et al.*, 2021] Luis Otavio S. Grillo, Aguinaldo S. E. Silva, and Fabrizio L. Freitas. A Method for Online Identification of a Subset of Synchronous Generator Fundamental Parameters from Monitoring Systems Data. *Journal of Control, Automation and Electrical Systems*, vol. 32, no. 3, pp. 672–681, February 2021. (Cited in pages 4, 58, 59, and 61).

[Haddad and Chellaboina, 2008] Wassim M. Haddad and VijaySekhar Chellaboina. *Nonlinear Dynamical Systems and Control: A Lyapunov-Based Approach*. Princeton University Press, Princeton, NJ, USA, 2008. (Cited in pages 46, and 47).

[Hadla and Cruz, 2017] H. Hadla and S. M. A. Cruz. Predictive Stator Flux and Load Angle Control of Synchronous Reluctance Motor Drives Operating in a Wide Speed Range. *IEEE Transactions on Industrial Electronics*, vol. 64, no. 9, pp. 6950–6959, September 2017. (Cited in page 60).

[Hasni *et al.*, 2010] M. Hasni, O. Touhami, R. Ibtiouen, M. Fadel, and S. Caux. Estimation of synchronous machine parameters by standstill tests. *Mathematics and Computers in Simulation*, vol. 81, no. 2, pp. 277–289, Jan. 2010. (Cited in page 58).

[Hasni *et al.*, 2021] M. Hasni, O. Touhami, R. Ibtiouen, M. Fadel, and S. Caux. Estimation of synchronous machine parameter by standstill frequency response tests. *Journal of Control, Automation and Electrical Systems*, vol. 32, no. 6, pp. 1639–1651, Dec. 2021. (Cited in page 58).

[Hrustic *et al.*, 2021] Emir Hrustic, Rayen Ben Abdallah, Jordi Vilà-Valls, Damien Vivet, Gaël Pagès, and Eric Chaumette. Robust linearly constrained extended Kalman filter for mismatched nonlinear systems. *International Journal of Robust and Nonlinear Control*, vol. 31, no. 3, pp. 787–805, November 2021. (Cited in page 98).

[Huang *et al.*, 2020] Chao-Ming Huang, Yann-Chang Huang, Shin-Ju Chen, and Sung-Pei Yang. A Hierarchical Optimization Method for Parameter Estimation of Diesel Generators. *IEEE Access*, vol. 8, pp. 176467–176479, Sept. 2020. (Cited in pages 58, 59, and 61).

[Huang *et al.*, 2014] Z. Huang, K. Schneider, J. Nieplocha, and N. Zhou. Estimating power system dynamic states using extended Kalman Filter. In: *2014 IEEE PES General Meeting | Conference & Exposition*, IEEE PES General Meeting, pp. 1–5. July 27-31 2014. (Cited in page 17).

[Huang *et al.*, 2007] Zhenyu Huang, K. Schneider, and J. Nieplocha. Feasibility studies of applying Kalman Filter techniques to power system dynamic state estimation. In: *International Power Engineering Conference (IPEC 2007)*, IPEC 2007, pp. 376–382. 3-6 Dec. 2007. (Cited in page 16).

[IEEE, 2010] IEEE. IEEE Guide for Test Procedures for Synchronous Machines Part I–Acceptance and Performance Testing Part II–Test Procedures and Parameter Determination for Dynamic Analysis. *IEEE Std 115-2009 (Revision of IEEE Std 115-1995)*, pp. 1–219, May 2010. (Cited in page 58).

[Instruments, 2021a] National Instruments. CompactRIO cRIO-9066 Embedded Controller. https://www.ni.com/en-us/support/model.crio-9066.html, 2021. URL `https://www.ni.com/en-us/support/model.crio-9066.html`. (Cited in page 90).

[Instruments, 2021b] National Instruments. NI 9215 Analog Input Module. https://www.ni.com/en-us/support/model.ni9215.html, 2021. URL `https://www.ni.com/en-us/support/model.ni9215.html`. (Cited in page 90).

[Jin, 2017] LeSheng Jin. Vector t-Norms With Applications. *IEEE Transactions on Fuzzy Systems*, vol. 25, no. 6, pp. 1644–1654, Dec. 2017. (Cited in page 65).

[Joseph *et al.*, 2018] Thomas Joseph, Barjeev Tyagi, and Vishal Kumar. Dynamic Generator State Estimation using PMU Measurements for Unknown Generator Input. In: *2018 IEEE Power & Energy Society General Meeting (PESGM)*, 2018 IEEE Power & Energy Society, pp. 1–5. Aug. 5-10 2018. (Cited in page 18).

[Juang *et al.*, 1993] Jer-Nan Juang, Minh Phan, Lucas G. Horta, and Richard W. Longman. Identification of Observer/Kalman Filter Markov Parameters - Theory and Experiments. *Journal of Guidance, Control, and Dynamics*, vol. 16, no. 2, pp. 320–329, March 1993. (Cited in page 79).

[Julier *et al.*, 2000] S. Julier, J. Uhlmann, and H. F. Durrant-Whyte. A new method for the nonlinear transformation of means and covariances in filters and estimators. *IEEE Transactions on Automatic Control*, vol. 45, no. 3, pp. 477–482, March 2000. (Cited in page 18).

[Julier and Uhlmann, 2004] S.J. Julier and J.K. Uhlmann. Unscented filtering and nonlinear estimation. *Proceedings of the IEEE*, vol. 92, no. 3, pp. 401–422, March 2004. (Cited in page 98).

[Kailath *et al.*, 2000] Thomas Kailath, Ali H. Sayed, and Babak Hassibi. *Linear Estimation*. Prentice Hall, New Jersey, 2000. (Cited in pages 39, and 40).

[Karrari and Malik, 2004] M. Karrari and O.P. Malik. Identification of Physical Parameters of a Synchronous Generator from On-line Measurements. *IEEE Transactions on Energy Conversion*, vol. 19, no. 2, pp. 407–415, June 2004. (Cited in pages 4, 58, 59, and 61).

[Karrari *et al.*, 2006] M. Karrari, W. Rosehart, O.P. Malik, and A.H. Givehchi. Identification of Synchronous Generators Using "4SID" Identfication Method and Neural Networks. *IFAC Proceedings Volumes*, vol. 39, no. 7, pp. 71–76, April 2006. (Cited in pages 58, and 59).

[Ketsarapong *et al.*, 2012] Suphattra Ketsarapong, Varathorn Punyangarm, Kongkiti Phusavat, and Binshan Lin. An experience-based system supporting inventory planning: A fuzzy approach. *Expert Systems with Applications*, vol. 39, no. 8, pp. 6994–7003, June 2012. (Cited in page 60).

[Khodadadi *et al.*, 2018] A. Khodadadi, M. Nakhaee Pishkesh, Behrooz Zaker, and Mehdi Karrari. Parameters Identification and Dynamical Modeling of Excitation System and Generator in a Steam Power Plant. In: *2018 6th International Conference on Control Engineering Information Technology (CEIT)*, 2018 6th International Conference on Control Engineering Information Technology (CEIT), pp. 1–5. Oct. 25-27 2018. (Cited in pages 58, 59, and 61).

[Kim and Lynch, 2012] Junhee Kim and Jerome P. Lynch. Autonomous Decentralized System Identification by Markov Parameter Estimation Using Distributed Smart Wireless Sensor Networks. *Journal of Engineering Mechanics*, vol. 138, no. 5, pp. 478–490, May 2012. (Cited in page 61).

[Kitanidis, 1987] Peter K. Kitanidis. Unbiased minimum-variance linear state estimation. *Automatica*, vol. 23, no. 6, pp. 775–778, November 1987. (Cited in page 18).

[Klema and Laub, 1980] V. Klema and A. Laub. The singular value decomposition: Its computation and some applications. *IEEE Transactions on Automatic Control*, vol. 25, no. 2, pp. 164–176, April 1980. (Cited in page 44).

[Kuppusamy and Joo, 2021] Subramanian Kuppusamy and Young Hoon Joo. Memory-Based Integral Sliding-Mode Control for T–S Fuzzy Systems With PMSM via Disturbance Observer. *IEEE Transactions on Cybernetics*, vol. 51, no. 5, pp. 2457–2465, May 2021. (Cited in page 60).

[Lavenius and Vanfretti, 2018] J. Lavenius and L. Vanfretti. PMU-Based Estimation of Synchronous Machines' Unknown Inputs Using a Nonlinear Extended Recursive Three-Step Smoother. *IEEE Access*, vol. 6, pp. 57123–57136, 2018. (Cited in pages 18, 104, and 105).

[Lee *et al.*, 2020] Yonggu Lee, Seon Hyeog Kim, Gyul Lee, and Yong-June Shin. Dynamic State Estimation of Generator Using PMU Data with Unknown Inputs.

In: *2020 IEEE 29th International Symposium on Industrial Electronics (ISIE)*, International Symposium on Industrial Electronics (ISIE), pp. 839–844. June 17-19 2020. (Cited in page 20).

[Li and Yang, 2021] Liang Li and Ming Yang. Joint Localization Based on Split Covariance Intersection on the Lie Group. *IEEE Transactions on Robotics*, vol. 37, no. 5, pp. 1508–1524, Oct. 2021. (Cited in page 98).

[Li *et al.*, 2019] Yang Li, Jing Li, Junjian Qi, and Liang Chen. Robust Cubature Kalman Filter for Dynamic State Estimation of Synchronous Machines Under Unknown Measurement Noise Statistics. *IEEE Access*, vol. 7, pp. 29139–29148, Feb. 2019. (Cited in pages 20, and 98).

[Lidenholm and Lundin, 2010] J. Lidenholm and U. Lundin. Estimation of Hydropower Generator Parameters Through Field Simulations of Standard Tests. *IEEE Transactions on Energy Conversion*, vol. 25, no. 4, pp. 931–939, Dec. 2010. (Cited in page 58).

[Liu *et al.*, 2018] C. Liu, Y. Wang, D. Zhou, and X. Shen. Minimum-Variance Unbiased Unknown Input and State Estimation for Multi-Agent Systems by Distributed Cooperative Filters. *IEEE Transactions on Automatic Control*, vol. 6, pp. 18128–18141, 2018. (Cited in pages 33, and 45).

[Liu *et al.*, 2020] Xin Liu, Xianqiang Yang, and Shen Yin. Nonlinear System Identification With Robust Multiple Model Approach. *IEEE Transactions on Control Systems Technology*, vol. 28, no. 6, pp. 2728–2735, Nov. 2020. (Cited in page 59).

[Liu *et al.*, 2022] Xinghua Liu, Jianwei Guan, Rui Jiang, Xiang Gao, Badong Chen, and Shuzhi Sam Ge. Robust strong tracking unscented Kalman filter for nonlinear systems with unknown inputs. *IET Signal Processing*, pp. 1–15, January 2022. (Cited in page 102).

[Liu *et al.*, 2014] Yu Liu, Kai Dong, Haipeng Wang, Jun Liu, You He, and Lina Pan. Adaptive Gaussian sum squared-root cubature Kalman filter with split-merge scheme for state estimation. *Chinese Journal of Aeronautics*, vol. 27, no. 5, pp. 1242–1250, October 2014. (Cited in page 20).

[Lu, 2013] Ying Lu. Distributed Information Consensus Filters for Simultaneous Input and State Estimation. *Circuits, Systems, and Signal Processing*, vol. 32, no. 2, pp. 877–888, Apr 2013. (Cited in page 33).

[Ma *et al.*, 2020] Yiming Ma, Libing Zhou, and Jin Wang. Standstill Time-Domain Response Parameter Estimation of the Large Synchronous Condenser in Arbitrary Rotor Position. *IEEE Access*, vol. 8, pp. 166047–166059, Sept. 2020. (Cited in page 58).

[Machowski *et al.*, 2020] Jan Machowski, Zbigniew, Janusz W. Bialek, and James R. Bumby. *Power System Dynamics: Stability and Control*. John Wiley and Sons, 2020. (Cited in page 13).

[Mani *et al.*, 2021] Prakash Mani, Rakkiyappan Rajan, and Young Hoon Joo. Design of Observer-Based Event-Triggered Fuzzy ISMC for T–S Fuzzy Model and its Application to PMSG. *IEEE Transactions on Systems, Man, and Cybernetics: Systems*, vol. 51, no. 4, pp. 2221–2231, April 2021. (Cited in page 60).

[Mejia-Ruiz *et al.*, 2021] Gabriel E. Mejia-Ruiz, Romel Cárdenas-Javier, Mario R. Arrieta Paternina, Juan R. Rodríguez-Rodríguez, Juan M. Ramirez, and Alejandro Zamora-Mendez. Coordinated Optimal Volt/Var Control for Distribution Networks via D-PMUs and EV Chargers by Exploiting the Eigensystem Realization. *IEEE Transactions on Smart Grid*, vol. 12, no. 3, pp. 2425–2438, May 2021. (Cited in page 61).

[Mendes *et al.*, 2020] Jérôme Mendes, Ricardo Maia, Rui Araújo, and Francisco A. A. Souza. Self-Evolving Fuzzy Controller Composed of Univariate Fuzzy Control Rules. *Applied Sciences*, vol. 10, no. 17, p. 5836, August 2020. (Cited in page 60).

[Mendes *et al.*, 2013] Jérôme Mendes, Rui Araújo, and Francisco Souza. Adaptive fuzzy identification and predictive control for industrial processes. *Expert Systems with Applications*, vol. 40, no. 17, pp. 6964–6975, Dec. 2013. (Cited in pages 60, and 66).

[Micev *et al.*, 2021] Mihailo Micev, Martin Ćalasan, and Milovan Radulović. Identification of Synchronous Generator Parameters From Operating Data During

the Short-Circuit From No-Load Operation. In: *2021 20th International Symposium INFOTEH-JAHORINA (INFOTEH)*, 2021 20th International Symposium INFOTEH-JAHORINA (INFOTEH), pp. 1–6. March 17-19 2021. (Cited in page 58).

[Micev *et al.*, 2022] Mihailo Micev, Martin Ćalasan, Shady H. E. Abdel Aleem, Hany M. Hasanien, and Dragan S. Petrović. Two Novel Approaches for Identification of Synchronous Machine Parameters From Short-Circuit Current Waveform. *IEEE Transactions on Industrial Electronics*, vol. 69, no. 6, pp. 5536–5546, June 2022. (Cited in pages 4, 58, and 61).

[Milano, 2002] Federico Milano. PSAT, Matlab-Based Power System Analysis Toolbox. http://faraday1.ucd.ie/psat.html, 2002. URL `http://faraday1.ucd.ie/psat.html`. (Cited in page 108).

[Milano, 2005] Federico Milano. An open source power system analysis toolbox. *IEEE Transactions on Power Systems*, vol. 20, no. 3, pp. 1199–1206, August 2005. (Cited in page 108).

[Millan *et al.*, 2017] P. Millan, A.R. del Nozal, L. Zaccarian, L. Orihuela, and A. Seuret. On stable simultaneous input and state estimation for discrete-time linear systems. *IFAC-PapersOnLine*, vol. 50, no. 1, pp. 6483–6488, July 2017. (Cited in page 33).

[Mitra *et al.*, 2021] Arindam Mitra, Abheejeet Mohapatra, Saikat Chakrabarti, and Subrata Sarkar. Online Measurement Based Joint Parameter Estimation of Synchronous Generator and Exciter. *IEEE Transactions on Energy Conversion*, vol. 36, no. 2, pp. 820–830, June 2021. (Cited in pages 58, 59, and 61).

[Mouni *et al.*, 2008] Emile Mouni, Slim Tnani, and Gérard Champenois. Synchronous generator modelling and parameters estimation using least squares method. *Simulation Modelling Practice and Theory*, vol. 16, no. 6, pp. 678–689, July 2008. (Cited in page 58).

[Müller and Castro, 2016] Heloisa H. Müller and Carlos A. Castro. Genetic algorithm-based phasor measurement unit placement method considering observability and security criteria. *IET Generation, Transmission & Distribution*, vol. 10, no. 1, pp. 270–280, January 2016. (Cited in page 109).

[Netto and Mili, 2018] Marcos Netto and Lamine Mili. A Robust Data-Driven Koopman Kalman Filter for Power Systems Dynamic State Estimation. *IEEE Transactions on Power Systems*, vol. 33, no. 6, pp. 7228–7237, Nov. 2018. (Cited in page 19).

[Netto *et al.*, 2016] Marcos Netto, Junbo Zhao, and Lamine Mili. A robust extended Kalman filter for power system dynamic state estimation using PMU measurements. In: *2016 IEEE Power and Energy Society General Meeting (PESGM)*, 2016 IEEE Power and Energy Society General Meeting (PESGM), pp. 1–5. July 17-21 2016. (Cited in pages 17, and 19).

[Olfati-Saber, 2005] R. Olfati-Saber. Distributed Kalman Filter with Embedded Consensus Filters. In: *44th IEEE Conference on Decision and Control*, CDC 2005, pp. 8179–8184. Dec. 12-15 2005. (Cited in pages 32, and 33).

[Olfati-Saber, 2007a] R. Olfati-Saber. Distributed Kalman filtering for sensor networks. In: *44th IEEE Conference on Decision and Control*, CDC 2007, pp. 5492–5498. Dec. 12-14 2007. (Cited in pages 33, and 35).

[Olfati-Saber, 2007b] Reza Olfati-Saber. Flocking for multi-agent dynamic systems: algorithms and theory. *IEEE Transactions on Automatic Control*, vol. 51, no. 3, pp. 401–420, March 2007. (Cited in page 32).

[Pai and Chatterjee, 2014] M. A. Pai and Dheeman Chatterjee. *Computer techniques in power system analysis*. McGraw-Hill Education (India), 3rd ed., 2014. (Cited in pages xxix, and 108).

[Pan *et al.*, 2010] Shuwen Pan, Hongye Su, Jian Chu, and Hong Wang. Applying a novel extended Kalman filter to missile–target interception with APN guidance law: A benchmark case study. *Control Engineering Practice*, vol. 18, no. 2, pp. 159–167, February 2010. (Cited in page 32).

[Patton *et al.*, 1989] Ron J. Patton, Paul M. Frank, and Robert N. Clarke. *Fault Diagnosis in Dynamic Systems: Theory and Application*. Prentice-Hall, Inc., Upper Saddle River, NJ, USA, 1989. (Cited in page 32).

[Pehlivan and Turksen, 2021] Nimet Yapici Pehlivan and Ismail Burhan Turksen. A novel multiplicative fuzzy regression function with a multiplicative fuzzy clustering

algorithm. *Romanian Journal of Information Science and Technology*, vol. 24, no. 1, pp. 79–98, 2021. (Cited in page 60).

[Pozna *et al.*, 2012] Claudiu Pozna, Nicuşor Minculete, Radu-Emil Precup, László T. Kóczy, and Áron Ballagi. Signatures: Definitions, operators and applications to fuzzy modelling. *Fuzzy Sets and Systems*, vol. 201, pp. 86–104, August 2012. (Cited in page 60).

[Precup *et al.*, 2021] Radu-Emil Precup, Claudia-Adina Bojan-Dragos, Elena-Lorena Hedrea, Raul-Cristian Roman, and Emil M. Petriu. Evolving fuzzy models of shape memory alloy wire actuators. *Romanian Journal of Information Science and Technology*, vol. 24, no. 4, pp. 353–365, 2021. (Cited in page 60).

[Qi *et al.*, 2018] J. Qi, K. Sun, J. Wang, and H. Liu. Dynamic State Estimation for Multi-Machine Power System by Unscented Kalman Filter With Enhanced Numerical Stability. *IEEE Transactions on Smart Grid*, vol. 9, no. 2, pp. 1184–1196, March 2018. (Cited in page 18).

[Qin, 2006] S. Joe Qin. An overview of subspace identification. *Computers & Chemical Engineering*, vol. 30, no. 10, pp. 1502–1513, Sept. 2006. (Cited in page 61).

[Rastegar *et al.*, 2017] Saeid Rastegar, Jérôme Mendes, and Rui Araújo. Online Identification of Takagi-Sugeno Fuzzy Models Based on Self-Adaptive Hierarchical Particle Swarm Optimization Algorithm. *Applied Mathematical Modelling*, vol. 45, pp. 606–620, May 2017. (Cited in page 60).

[Riverso *et al.*, 2013] S. Riverso, M. Farina, R. Scattolini, and G. Ferrari-Trecate. Plug-and-play distributed state estimation for linear systems. In: *52nd IEEE Conference on Decision and Control*, Decision and Control 2013, pp. 4889–4894. Dec. 10-13 2013. (Cited in page 33).

[Rostami and Lotfifard, 2018] Mohammadali Rostami and Saeed Lotfifard. Distributed Dynamic State Estimation of Power Systems. *IEEE Transactions on Industrial Informatics*, vol. 14, no. 8, pp. 3395–3404, September 2018. (Cited in page 16).

[Roy *et al.*, 2012] B.K. Saha Roy, A.K. Sinha, and A.K. Pradhan. An optimal PMU placement technique for power system observability. *International Journal of*

Electrical Power & Energy Systems, vol. 42, no. 1, pp. 71–77, November 2012. (Cited in page 109).

[Schweppe and Wildes, 1970] F. C. Schweppe and J. Wildes. Power System Static-State Estimation, Part I: Exact Model. *IEEE Transactions on Power Apparatus and Systems*, vol. PAS-89, no. 1, pp. 120–125, Jan. 1970. (Cited in page 16).

[Shamsollahi and Malik, 1996] P. Shamsollahi and O. P. Malik. On-line Identification of Synchronous Generator Using Neural Networks. In: *Proceedings of 1996 Canadian Conference on Electrical and Computer Engineering*, Proceedings of 1996 Canadian Conference on Electrical and Computer Engineering, pp. 595–598. May 26-29 1996. (Cited in pages 58, and 59).

[Shariati *et al.*, 2021] O. Shariati, M. R. Aghamohammadi, and B. Potter. On-Line Determination of Salient-Pole Hydro Generator Parameters by Neural Network Estimator Using Operating Data (PEANN). *IEEE Access*, vol. 9, pp. 134638–134648, September 2021. (Cited in pages 58, and 59).

[Sharma *et al.*, 2017] A. Sharma, S. C.Srivastava, and S. Chakrabarti. A Cubature Kalman Filter Based Power System Dynamic State Estimator. *IEEE Transactions on Instrumentation and Measurement*, vol. 66, no. 8, pp. 2036–2045, Aug. 2017. (Cited in page 20).

[Sharma *et al.*, 2015] Ankush Sharma, Suresh Chandra Srivastava, and Saikat Chakrabarti. A multi-agent-based power system hybrid dynamic state estimator. *IEEE Intelligent Systems*, vol. 30, no. 3, pp. 52–59, May 2015. (Cited in page 20).

[Shihabudheen *et al.*, 2018] K.V. Shihabudheen, M. Mahesh, and G.N. Pillai. Particle swarm optimization based extreme learning neuro-fuzzy system for regression and classification. *Expert Systems with Applications*, vol. 92, pp. 474–484, Feb. 2018. (Cited in page 67).

[Simon, 2006] D. Simon. *Optimal State Estimation: Kalman, H Infinity, and Nonlinear Approaches*. John Wiley & Sons, Ltd, 1st ed., 2006. (Cited in pages 23, 24, and 98).

[Sun, 2015] Ye Sun. *A Distributed Local Kalman Consensus Filter for Traffic Estimation: Design, Analysis and Validation.* Master's thesis, University of Illinois at Urbana-Champaign, Urbana, Illinois, January 2015. (Cited in page 35).

[Szedlak-Stinean *et al.*, 2022] Alexandra-Iulia Szedlak-Stinean, Radu-Emil Precup, Emil M. Petriu, Raul-Cristian Roman, Elena-Lorena Hedrea, and Claudia-Adina Bojan-Dragos. Extended Kalman filter and Takagi-Sugeno fuzzy observer for a strip winding system. *Expert Systems with Applications*, vol. 208, p. 118215, Dec. 2022. (Cited in page 65).

[Tebianian and Jeyasurya, 2015] Hamed Tebianian and Benjamin Jeyasurya. Dynamic state estimation in power systems: Modeling, and challenges. *Electric Power Systems Research*, vol. 121, pp. 109–114, April 2015. (Cited in page 17).

[Test and Measurement, 2021] HBM Test and Measurement. RWT310 Torque Transducer. https://www.hbm.com/en/3133/rwt310-torque-transducer.html, 2021. URL `https://www.hbm.com/en/3133/rwt310-torque-transducer.html`. (Cited in page 90).

[Tsai *et al.*, 2007] Jason Sheng-Hong Tsai, Tseng-Hsu Chien, Shu-Mei Guo, Yu-Pin Chang, and Leang-San Shieh. State-Space Self-Tuning Control for Stochastic Fractional-Order Chaotic Systems. *IEEE Transactions on Circuits and Systems I: Regular Papers*, vol. 54, no. 3, pp. 632–642, March 2007. (Cited in page 61).

[Valverde and Terzija, 2011] G. Valverde and V. Terzija. Unscented Kalman filter for power system dynamic state estimation. *IET GENERATION TRANSMISSION & DISTRIBUTION*, vol. 5, no. 1, pp. 29–37, Jan. 2011. (Cited in pages 16, and 18).

[Vandoorn *et al.*, 2010] Tine L. Vandoorn, Frederik M. De Belie, Thomas J. Vyncke, Jan A. Melkebeek, and Philippe Lataire. Generation of Multisinusoidal Test Signals for the Identification of Synchronous-Machine Parameters by Using a Voltage-Source Inverter. *IEEE Transactions on Industrial Electronics*, vol. 57, no. 1, pp. 430–439, Jan. 2010. (Cited in page 58).

[Vilà-Valls *et al.*, 2020] Jordi Vilà-Valls, Damien Vivet, Eric Chaumette, François Vincent, and Pau Closas. Recursive linearly constrained Wiener filter for robust

multi-channel signal processing. *Signal Processing*, vol. 167, p. 107291, February 2020. (Cited in page 98).

[Wamkeue *et al.*, 2011] R. Wamkeue, C. Jolette, A. B. M. Mabwe, and I. Kamwa. Cross-Identification of Synchronous Generator Parameters From RTDR Test Time-Domain Analytical Responses. *IEEE Transactions on Energy Conversion*, vol. 26, no. 3, pp. 776–786, Sept. 2011. (Cited in page 58).

[Wang *et al.*, 2012] Shaobu Wang, Wenzhong Gao, and A. P. Sakis Meliopoulos. An Alternative Method for Power System Dynamic State Estimation Based on Unscented Transform. *IEEE Transactions on Power Systems*, vol. 27, no. 2, pp. 942–950, December 2012. (Cited in pages 18, and 19).

[Wang *et al.*, 2020a] Shaobu Wang, Renke Huang, Zhenyu Huang, and Rui Fan. A Robust Dynamic State Estimation Approach Against Model Errors Caused by Load Changes. *IEEE Transactions on Power Systems*, vol. 35, no. 6, pp. 4518–4527, Nov. 2020. (Cited in page 19).

[Wang *et al.*, 2020b] Wanli Wang, Chi K. Tse, and Shiyuan Wang. Dynamic State Estimation of Power Systems by p -Norm Nonlinear Kalman Filter. *IEEE Transactions on Circuits and Systems I: Regular Papers*, vol. 67, no. 5, pp. 1715–1728, May 2020. (Cited in page 19).

[Wang, 2021] Xin Wang. Power Systems Dynamic State Estimation With the Two-Step Fault Tolerant Extended Kalman Filtering. *IEEE Access*, vol. 9, pp. 137211–137223, October 2021. (Cited in pages 9, 10, 11, 12, and 18).

[Wang *et al.*, 2019] Yi Wang, Yonghui Sun, Venkata Dinavahi, Shiqi Cao, and Dongchen Hou. Adaptive Robust Cubature Kalman Filter for Power System Dynamic State Estimation Against Outliers. *IEEE Access*, vol. 7, pp. 105872–105881, July 2019. (Cited in page 20).

[Wiktorowicz and Krzeszowski, 2019] Krzysztof Wiktorowicz and Tomasz Krzeszowski. Training High-Order Takagi-Sugeno Fuzzy Systems Using Batch Least Squares and Particle Swarm Optimization. *International Journal of Fuzzy Systems*, vol. 22, no. 1, pp. 22–34, November 2019. (Cited in page 60).

[Xu *et al.*, 2019] Yijun Xu, Lamine Mili, and Junbo Zhao. A Novel Polynomial-Chaos-Based Kalman Filter. *IEEE Signal Processing Letters*, vol. 26, no. 1, pp. 9–13, October 2019. (Cited in page 12).

[Yong *et al.*, 2016] Sze Zheng Yong, Minghui Zhu, and Emilio Frazzoli. A unified filter for simultaneous input and state estimation of linear discrete-time stochastic systems. *Automatica*, vol. 63, pp. 321–329, January 2016. (Cited in page 32).

[Yu *et al.*, 2019] Yang Yu, Zhongjie Wang, and Chengchao Lu. A Joint Filter Approach for Reliable Power System State Estimation. *IEEE Transactions on Instrumentation and Measurement*, vol. 68, no. 1, pp. 87–94, Jan. 2019. (Cited in page 19).

[Zaker *et al.*, 2016] Behrooz Zaker, Gevork B. Gharehpetian, Mehdi Karrari, and Naghi Moaddabi. Simultaneous Parameter Identification of Synchronous Generator and Excitation System Using Online Measurements. *IEEE Transactions on Smart Grid*, vol. 7, no. 3, pp. 1230–1238, May 2016. (Cited in pages 58, and 59).

[Zhang *et al.*, 2014a] Guowen Zhang, Jinghua Ma, Zhuo Chen, and Ruirong Wang. Automated eigensystem realisation algorithm for operational modal analysis. *Journal of Sound and Vibration*, vol. 333, no. 15, pp. 3550–3563, July 2014. (Cited in page 61).

[Zhang *et al.*, 2014b] J. Zhang, G. Welch, G. Bishop, and Z. Huang. A Two-Stage Kalman Filter Approach for Robust and Real-Time Power System State Estimation. *IEEE Transactions on Sustainable Energy*, vol. 5, no. 2, pp. 629–636, April 2014. (Cited in page 17).

[Zhao *et al.*, 2019] J. Zhao, A. Gòmez-Expósito, M. Netto, L. Mili, A. Abur, V. Terzija, I. Kamwa, B. Pal, A. K. Singh, J. Qi, Z. Huang, and A. P. S. Meliopoulos. Power System Dynamic State Estimation: Motivations, Definitions, Methodologies, and Future Work. *IEEE Transactions on Power Systems*, vol. 34, no. 4, pp. 3188–3198, July 2019. (Cited in page 16).

[Zhao, 2018] Junbo Zhao. Dynamic State Estimation With Model Uncertainties Using H_∞ Extended Kalman Filter. *IEEE Transactions on Power Systems*, vol. 33, no. 1, pp. 1099–1100, January 2018. (Cited in pages 18, and 19).

[Zhao and Mili, 2018a] Junbo Zhao and Lamine Mili. Power System Robust Decentralized Dynamic State Estimation Based on Multiple Hypothesis Testing. *IEEE Transactions on Power Systems*, vol. 33, no. 4, pp. 4553–4562, July 2018. (Cited in page 19).

[Zhao and Mili, 2018b] Junbo Zhao and Lamine Mili. A Robust Generalized-Maximum Likelihood Unscented Kalman Filter for Power System Dynamic State Estimation. *IEEE Journal of Selected Topics in Signal Processing*, vol. 12, no. 4, pp. 578–592, Aug. 2018. (Cited in page 19).

[Zhao and Mili, 2019] Junbo Zhao and Lamine Mili. A Theoretical Framework of Robust H_∞ Unscented Kalman Filter and Its Application to Power System Dynamic State Estimation. *IEEE Transactions on Signal Processing*, vol. 67, no. 10, pp. 2734–2746, May 2019. (Cited in pages 19, and 98).

[Zhao *et al.*, 2017a] Junbo Zhao, Lamine Mili, and Ahmed Abdelhadi. Robust dynamic state estimator to outliers and cyber attacks. In: *2017 IEEE Power & Energy Society General Meeting*, 2017 IEEE Power & Energy Society General Meeting, pp. 1–5. July 16-20 2017. (Cited in page 18).

[Zhao *et al.*, 2017b] Junbo Zhao, Marcos Netto, and Lamine Mili. A Robust Iterated Extended Kalman Filter for Power System Dynamic State Estimation. *IEEE Transactions on Power Systems*, vol. 32, no. 4, pp. 3205–3216, July 2017. (Cited in pages 17, and 18).

[Zhao *et al.*, 2015] Liqiang Zhao, Jianlin Wang, Tao Yu, Huan Jian, and Tangjiang Liu. Design of adaptive robust square-root cubature Kalman filter with noise statistic estimator. *Chinese Journal of Aeronautics*, vol. 256, pp. 352–367, April 2015. (Cited in page 20).

[Zhou *et al.*, 2015] N. Zhou, D. Meng, Z. Huang, and G. Welch. Dynamic State Estimation of a Synchronous Machine Using PMU Data: A Comparative Study. *IEEE Transactions on Smart Grid*, vol. 6, no. 1, pp. 450–460, Jan. 2015. (Cited in pages 17, and 98).

[Zhou *et al.*, 2017] Ping Zhou, Heda Song, Hong Wang, and Tianyou Chai. Data-Driven Nonlinear Subspace Modeling for Prediction and Control of Molten Iron

Quality Indices in Blast Furnace Ironmaking. *IEEE Transactions on Control Systems Technology*, vol. 25, no. 5, pp. 1761–1774, Sept. 2017. (Cited in page 61).